Ministère de l'Enseignement Supérieur et de la Recherche Scientifique

Université Hassiba Benbouali de Chlef

Faculté de technologie

Département d'électrotechnique

THÈSE

DOCTORAT LMD

Filière : Electrotechnique

Spécialité : Réseaux Electriques et Haute Tension

Par

REGAD MOHAMED SIDI BRAHIM

Thème :

Contribution à la Modélisation et le Contrôle Optimal d'un Micro-réseau Electrique à base d'Energies Renouvelables

(Contribution to Modeling and Optimal Control of Electrical Microgrid based on Renewable Energy)

Soutenue le 29/11/2020, devant le jury composé de :

Mr.BELMADANI Bachir	Professeur	Université de Chlef	Président
Mr.HELAIMI M'hamed	MCA	Université de Chlef	Rapporteur
Mr.TALEB Rachid	Professeur	Université de Chlef	Co-rapporteur
Mr.MANKOUR Mohamed	MCA	Université de Saida	Examinateur
Mr.SEKOUR M'hamed	MCA	Université de Saida	Examinateur
Mr.BOUNADJA Elhadj	MCA	Université de Chlef	Examinateur

Abstract

Contribution to Modeling and Optimal Control of Microgrid based Renewable Energy Generation.

Renewable energy sources based isolated microgrid can be economical and reliable solutions for remote and isolated areas where the main grid is not available. The frequency and voltage fluctuations are major problems in such microgrid due to the intermittent nature of renewable resources like wind speed and solar PV radiation. The frequency and power fluctuations should be kept within small deviations for the stable operation of the microgrid system. This thesis works focused on the frequency and power control of microgrid based wind and photovoltaic (PV) system with storage devices like BESS, FESS, AE, and UC with conventional sources such as Fuel Cell and Diesel Generator based using the investigation of strategies control like PID controller, Fractional Order Controller and Fuzzy-fractional Order controller. Various news optimization methods are investigated to overcome the determination of optimal controllers parameters problems. Among the employed optimization techniques the Krill Herd algorithm is used to optimize the control scheme gains and compared with other classical methods like PSO and GA. A small-signal model of a microgrid is used to analyze the system in the frequency domain and to add a linear control scheme. The detailed analysis of the frequency control is performed by conducting two different case studies under generation and load perturbations. In all the cases, system frequency is maintained within the acceptable range for the stable operation of wind and solar PV based isolated microgrid. Interconnection of two areas Microgrid system is investigated and analysed.

Résumé

Contribution à la Modélisation et le Contrôle Optimal dun Micro-réseau Électrique à base d'Énergies Renouvelables.

Le micro réseau à base de sources d'énergie renouvelables peut être une solution économique et fiable pour les zones éloignées et isolées où le réseau principal n'est pas disponible. La fluctuation de la fréquence et de la tension sont des problèmes majeurs dans tels micro réseaux en raison de la nature intermittente des ressources renouvelables comme la vitesse du vent et le rayonnement solaire PV. Les fluctuations de fréquence et de puissance doivent être maintenues à de petites déviations pour assurer la stabilité du système à micro réseaux. Ce travail concerne l'application de quelques stratégies de commandes au un système Microgrid pour la régulation de fréquence et de puissance. Le système étudié dans cette thèse est constitué d'un système éolien(WTG) et d'un système photovoltaïque (PV) avec des dispositifs de stockage tels que Batterie(BESS),Volant d'inertie(FESS), Electrolyzeur(AE) et Ultra-capaciteur(UC) avec des sources conventionnelles comme les piles à combustible(FC) et les générateurs diesel(DEG). Pour ces raisons, nous avons utilisé trois types de régulateurs comme le régulateur PID, régulateur d'ordre fractionnaire et le régulateur à logique flou. Diverses nouvelles méthodes d'optimisation sont étudiées pour résoudre le problème lié à la détermination les paramètres des régulateurs proposés. Parmi les techniques d'optimisation employées, l'algorithme de Krill Herd est utilisé pour optimiser les gains du schéma de contrôle et comparé à d'autres méthodes classiques comme Optimisation par Swaim de particule (PSO) et Agorithme Génétique(GA). Un modèle à petits signaux d'un micro réseau est utilisé pour analyser le système dans le domaine fréquentiel et pour ajouter un schéma de contrôle linéaire. L'analyse détaillée de la régulation de fréquence est réalisée pour deux configurations de Microgrid avec prise en considération les fluctuations de la puissance générée par l'éolienne et le photovoltaïque, ainsi que les perturbations de charges connectées. Dans tous les cas, la fréquence du système est maintenue dans la gamme acceptable qui assure la stabilité du micro réseau isolé à base de l'énergie renouvelable. Linterconnexion de deux systèmes Microgrids par l'utilisation du modèle Tie-Line est étudiée et analysée. Les

résultats de simulation obtenus par ces régulateurs seront comparés afin de juger les performances de la régulation dans les deux régimes de fonctionnement (transitoire et permanant).

List of Publications

1. Regad Mohamed„ M. Helaimi, R. Taleb, Hossam A. Gabbar, and Ahmed M. Othman. "Frequency control of microgrid system based renewable generation using fractional PID controller." Indonesian Journal of Electrical Engineering and Computer Science 19, no. 2 (2020) : 745-755.
2. Regad Mohamed, M'hamed Helaimi, Rachid Taleb, Ahmed M. Othman, and Hossam A. Gabbar. "Frequency Control of Microgrid with Renewable Generation using PID Controller based Krill Herd." Indonesian Journal of Electrical Engineering and Informatics (IJEEI) 8, no. 1 (2020) : 21-32.
3. Regad Mohamed, M. Helaimi, R. Taleb, H. Gabbar, and A. Othman. "Optimal frequency control in microgrid system using fractional order PID controller using Krill Herd algorithm." Electrical engineering and electromechanics 2 (eng) (2020).
4. Regad Mohamed, M. Helaimi, R. Taleb, Hossam A. Gabbar ,Ahmed M.Othman Control of hybrid power system based renewable energy generations using PID controller International Journal of Power Electronics and Drive Systems (IJPEDS) 11,no.4(2020).

List of Conferences

1. Regad, M., M. Helaimi, R. Taleb, Hossam A. Gabbar, and Ahmed M. Othman. "Fractional Order PID Control of Hybrid Power System with Renewable Generation Using Genetic Algorithm." In 2019 IEEE 7th International Conference on Smart Energy Grid Engineering (SEGE), pp. 139-144. IEEE, 2019.
2. Regad, M., Helaimi, M., Taleb, R., Othman, A. M., & Gabbar, H. A. (2019, November). Frequency Control in Microgrid Power System with Renewable Power

Generation Using PID Controller Based on Particle Swarm Optimization. In International Conference in Artificial Intelligence in Renewable Energetic Systems (pp. 3-13). Springer, Cham.

3. Regad, M., Helaimi, M., Taleb, R., & Maamar, A. T. (2019, November). Optimum Synthesis of the PID Controller Parameters for Frequency Control in Microgrid Based Renewable Generations. In International Conference in Artificial Intelligence in Renewable Energetic Systems (pp. 546-556). Springer, Cham.
4. M. Regad, M. Helaimi, R. Taleb : Contribution to Modeling and Optimal Control of Micro grid-based Renewable energy sources ,The First Doctoral Symposium on Technology : Process, Mechanical and Electrical Engineering DST01-2019 Chlef, Algeria.
5. A.E. Toubal Maamar, M. Helaimi, R. Taleb, M. Regad, A. BELBOULA(2019) : Simulation of a 60 w Solar Panel Model in Matlab/Power Systems, international Conference on Renewable Energy and Energy Conversion-ICREEC2019-USTO-MB Oran, Algeria.
6. M. Regad, M. Helaimi, R. Taleb(2020) : Control of Isolated Microgrid based Renewable Energy Generation using PID Controller The First International Conference on Materials, Energy and Environment, MEE'2020 At El Oued, Algeria.
7. M. Regad, M. Helaimi, R. Taleb(2020) : Analyzed Control of an Autonomous Microgrid System based on Renewable Energy Resources using PIDController La 1ère Conférence Nationale sur la Transition Energétique en Algérie (CNTEA 1 2020) Université Mohamed BOUDIAF de M'sila, le 8-9 Mars 2020, M'sila
8. M. Regad, M. Helaimi, R. Taleb(2020) : Frequency Control of Microgrid based Renewable Generation with a Fuel Cell system,Workshop on Smart Energy Systems 17-Mar-2020 ERC1094 , Oshawa , Canada

Acknowledgments

Dedication

Nomenclature

General

P_s	:Total average power generation.
P_W	:Mechanical power of wind turbines.
P_t	:Net average power of WTGs or PV to the system.
K	:Gain.
T	:Time constant.
Δf	:System frequency deviation.
V_W	:Wind speed (m/s).
Φ	:Solar irradiation ($kW/m2$).

Abbreviations or subscripts

WTG	:Quantities of wind turbine generator.
PV	:Quantities of photovoltaic system.
DEG	:Quantities of diesel engine generator.
AE	:Quantities of aqua electrolyzer.
FC	:Quantities of fuel cells.
BESS	:Quantities of battery energy storage system.
FESS	:Quantities of flywheel energy storage system.
Blade	:Quantities of wind turbine blades.
UC	:Quantities of Ultracapacitor.
MT	:Micro Turbine.
M	:Equivalent inertia constant of the hybrid power system.
D	:Damping constant of the hybrid power system.
MG	:Microgrid.

PID	:Proportional Integral Derivative Controller.
FOPID	:Fractional Order Proportional Integral Derivative Controller.
FL	:Fuzzy Logic.
LFC	:Load Frequency Control.
GA	:Genetic Algorithm.
PSO	:Particle Swarm Optimization.
GOA	:Grasshopper Optimisation Algorithm.
GWO	:Grey Wolf Optimizer.
DE	:Differentiel Evolution.
FPA	:Flower Pollination Algorithm.
SSO	:Small String Optimized.
KH	:Krill Herd.
LV	:Low voltage.
NOCT	:Nominal Operating Cell Temperature.
GNP	:Gross National Product.
PB	:British Petroleum.
MV	:Medium voltage.
AC	:Alternative current .
DC	:Direct current.
PCC	:Point of common coupling.
SS	:Static Switch.
ROM	:Reduced Order Model.
MOR	:Model Order Reduction.
RES	:Renewable Energy Sources.
MPPT	:Maximum Power Point Tracking.
PLL	:Phase Lock Loop.
GP	:Genetic programming.
SA	:Simulated Annealing.
TSO	:Transmission System Operators.
DSO	:Distribution System Operators.
DER	:Distributed Energy Generation.

EMS	:Energy Management System.
Isc	:Short-circuit current.
Voc	:Open-circuit voltage.
a	:Diode idealist factor.
R_s	:Serie resistances.
R_{shunt}	:Parallel resistances .
S_P	:series-parallel.
TCT	:Total Cross-Tied.
BL	:Bridge Link.
STC	:Standard Température Condition.
AGC	:Automatic Generation Control.
PG	:Power generation .
ΔP_m	:Mechanical power change.
ΔP_L	:Load Change.
Δf	:Frequency Deviation.
ΔP	:Power deviation.
ΔU	:Control Signal.
ISTSE	:Integral of Squared Time Squared Error Multiplied.
ISDCO	:Integral of Squared Geviation of the Output Controller.
K_P	:Proportional gain.
K_I	:Integral gain.
K_D	:Derivative gains.
T_I	:Integral time constant.
T_D	:Derivative time constant.
FOC	:Fractional Order Control.
λ	:Derivative Order.
μ	:Differential Order.
C_1 and C_2	:Constant weight factors.
V_i	:Particle velocity in iteration.
X_i	:Particle position.
P_{best}	:Best position achieved so far by particle.
$G_{bes}t$	:Best position found by the neighbors of the particle.
w	:Inertia weight.

N_i	:movement induced by other krill.
F_i	:Poraging movement.
D_i	:Physical diffusion of ith krill.
α^{local}	:Local effect.
α^{target}	:Target direction effect.
V_f	:Foraging speed.
ω_f	:Inertia weight of the foraging motion.
D^{max}	:Maximum diffusion speed.
δ	:Random directional vector.
NV	:the number of variables.
LB_j and UB_j	:the lower and the upper limits of the j^{th} variable.
C_r	:Crossover probability.
IAE	:Integral of Absolute Error.
ISE	:Integral Square Error.
ITAE	:Integral of Time multiplied by the Absolute Error.
ITSE	:Square Error with Time.
ISTSE	:Integral of Squared Time Squared Error Multiplied.
ISDCO	:Integral of Squared Deviation of the Output.

Table of contents

List of figures

List of table

General Introduction

Background and motivation

Electrical consumption is rising according to the growth of world population and technology development. This increase in energy demand accompanied by fossil fuel depletion and climate issues that lead to the research of replacement than the traditional energy sources. Microgrid system based renewable energy generation with storage devices and conventional sources like fuel cell and diesel generator become an important solution to the energy necessity. The increasing need for reducing the greenhouse effect makes the concept of Microgrid system based renewable sources more attractive. The microgrid can reduce emissions compared to conventional utility systems. The energy crisis and climate issues lead many research groups and countries governments to invest and involve in Microgrid projects. Many types of research in the field of microgrid design are accomplished and others in the completion stage around the world [1].
An electrical grid is defined as an interconnection of generating stations, distribution lines and transmission lines, which give power supply to customers. At generating stations, electric power is produced from renewable or non-renewable sources. Secondly, the electric power is carried from one place to another by the transmission lines. Then, electric power is distributed among consumers with the help of distribution feeders [2]. A Microgrid is defined as a low-voltage distribution network with distributed energy

sources altogether with storage devices loads. The Microgrid can be operated in islanding mode and grid-connected [3]. It is the integrated framework for supply a demand-side at the low voltage (LV) distribution grid.

The main role of such Microgridgrid are ; 1) transforming the electrical power system from the centralized system to a decentralized one, 2) increasing the system performance and efficiency, 3) facilitating the interconnection between customers, and electric power producers, and 4) promoting a high integration of renewable generation.

Both component hybrid system and strategy control are usually used to regulate the frequency and power deviation in a linear model of Microgrid. Using renewable generation sources in a hybrid system to produce electricity has been accepted as the most economical and environment-friendly method. The hybrid power system requires a more adequate control design to ensure its ability to reduce the imbalance between generated powers and demand. The produced powers from the renewable sources are stochastic, intermittent, and based on the climate conditions which might cause the unbalance between the power demand and the total power. On the other hand, using storage devices like the battery and flywheel is an efficient tool for improving the performance and stability of the MG systems and demining the unbalance of powers. The method can also enhance the power quality and mitigate the fluctuations of Microgrid frequency. That is making the storage devices one of the most important components of the microgrid. Flywheel Energy Storage device is useful in many industrial systems due to its power density and efficiency to store and release power while short periods.

The proposed stand-alone hybrid power system consists of solar photovoltaic (PV), wind turbine generator (WTG), Fuel-Cell (FC), Diesel Engine Generator (DEG), Aqua Electrolyzer (AE) Battery Energy Storage System and Flywheel Energy Storage System as reported. The existence of the storage devices such as BESS and FESS is vital in the MG for storage the excessive power from renewable sources, if there is still surplus power ; it is absorbed by the aqua electrolyzer for generating hydrogen which is stored in the hydrogen tank for it to be used by Fuel Cells as fuel. When the generated power from these renewable sources increases over the load power, the surplus is stored by the energy Storage System and later discharged to load when it is required. Wind, solar, fuel cells, and diesel generator systems are the most distributed generation resources that are used in the Microgrid system. The FC and DEG are used as second-generation

sources with energy storage systems like the Battery and the Flywheel to compensate for the slower response of DEG and FC. From literature, many simplified models of microgrid using small-signal analysis responses of a microgrid are investigated, where all components are presented by a first-order transfer function which has been considered sufficient for frequency behavior analysis and for also simplifies the simulation process and cntrol implemention. For small-signal analysis, the microgrid components are modeled by a transfer function in the first order forme.
Many research towards designing a control strategy for hybrid energy system control using the standard PID controller, where the genetic algorithm optimizes the PI/PID controller in the hybrid energy system is discussed and robust H^{∞} controller for the hybrid energy system. Some words about the control design of the microgrid energy system have been accomplished. In this thesis PID controller, Fractional Order PID controller and Fractional Order Fuzzy Controller, are used for frequency control in hybrid energy systems.

Scope of Work

The ultimate goal of the work adopted in this thesis is to study different models of a microgrid to show the best configuration suitable for time-domain analysis of frequency control. It also searches to find an optimal controller which can reduce the effect of the intermittent nature of renewable energy sources on the stability and performance of the microgrid system. THE fractional PID controller is proposed to be the best control strategy in this kind of problem. To achieve the optimal controller parameters optimization methods must be applied. Various optimizations techniques are proposed to tuning the FOPID Parameters like Genetic Algorithm, Particle Swarm Optimization and Krill Herd Algorithm. This research study focuses on the frequency control of microgrid. The small-signal analysis model is used for time-domain analysis. The main contributions of this research are outlined as follows :
– Overview on microgrids modeling, control and optimization.
– Modeling of microgrid components embrace TWG,PV, FC, AE, DEG, BESS,FESS and UC.
– Invstigation of different control schemes based PID, FOPID and Fuzzy logic control-

lers which are added to get an improvement of frequency and power fluctuations in microgrid system.

– Appication of various optimization algorithms such as GA, PSO and KH which are investigated to tune the proposed controllers parameters.

– Interconnected of two areas Microgrid using tie-line model.

– The Simulation of diferent configurations of the MG is presented and analyzed.

Thesis Layout

The remainder of this thesis is structured as follows :

Chapter 1 presents the state of the art on electrical microgrid modelling, control and optimization.

Chapter 2 presents the modelling process of microgrid components using in the present thesis such as WTGs, PV, DEG, FC, BESS, AE and FESS. A small-signal model of a microgrid is chosen according to the problem to be studied.

Chapter 3 presents the different control techniques like PID and FOPID investigated to control the frequency deviation and power in proposed microgrid configuration and its parameter optimizations using various optimization techniques such as KH, GA and PSO.

Chapter 4 addresses the hybrid control scheme base on Fractional PID and Fuzzy controller tuning using KH in MG control.

Chapter 5 this chapter presents frequency Control in two areas of microgrid using the Tie-line model.

This thesis achieved by a general conclusion.

CHAPTER 1

Introduction to Microgrid : Modeling, Control and Optimization

1.1 Introduction

This chapter presents an introduction to the Microgrid system. Renewable energy production rises around the world during the few last decades. Worldwide production is presented in this chapter. Also, it discusses the different topologies and structure of microgrid based renewable energy generation and storage devices. An overview of the modelling, control, optimization and protection in the microgrid system is shown in this chapter. Finaly a scope of work, the thesis layout and a conclusion are presented at the end of the chapter.

1.2 Stat of the art review

Energy generation and consumption plays an important role in the economic health of a country that is reflected by the Gross National Product (GNP) [4] .
Due to the depletion of fossil fuels, renewable energy sources have gained interest followed by climate change concerns related to the carbon gaz emissions and high oil prices. In this section an overview on the energy production concept around the word and microgrid system architechture and configurations are illustrated.

1.2.1 Microgrid overview

One of the most advantages of Microgrid systems are of being installed at demands premises that make it to be considered as economical and environment friendly as the electricity is produced by renewables generations units like Wind turbine Generator , Photovoltaic system and fuel cell etc. [5,6]. To design a Microgrid system two or more renewable energy generations always combined with storage devices and convetional sources to deliver electricity to the connected load and ensure the service continuity [7]. The weather conditions based on solar irradiance and wind speed which are the input data to the Photovoltaic system and Wind turbine Generator system respectively ; are stochastic along with the load demand which is intermittent and change over time. The change in both generation powers according to the weather condition and in power demand because of human life conditions affects the stability and continuity of microgrid operation. These issues are discussed by some studies as in [6] [8] which show the utility of the combination of more than one renewables sources along with storage devices and supplementary sources like a Diesel engine and Fuel Cell. Many configurations are shown to be the best configuration of a microgrid that ensures the electrical service continuity with less sensibility to the weather condition change and disturbances of loads. The use of energy storage systems enhances the stability of microgrid by absorbing the surplus of power which can provoke the mismatch between generation and loads and then to release the stored power later when the power load is less than generation during the night or clouded days. On the other hand, they are used to control the frequency and power deviations under the loads change and climate problems. The supplementary sources used to help the primary renewable sources to ensure system reliability [1]. The characteristics of different components model have been described in many works [9, 10].

Such an unbalancing act can be caused by a change in both the consumer loads as well as generating power from renewable sources. It is essential to maintaining the reliable operation of the microgrid system through the integration of energy storage systems and conventional sources. They include Battery, flywheel, Fuel Cell, Aqua electrolyzer and Diesel Generator and so one.

From previous researches, the modern power system requires new microgrid technologies intelligent control strategies and optimization techniques to ensure the generation and load balance which causes serious disturbances. These problems become more important with the increase in microgrid based renewable energy production units that varying naturally. These challenges and uncertainties in power systems make the classical control strategies to be unable to provide better performance stability and reliability over a wide range of operating conditions of the microgrid. The microgrid requires intelligent control to improve the stability and performance operation. To respond to these challenges the present thesis addresses different strategies intelligent controllers like proportional integral derivative PID controller, Fractional Order PID controller and Fuzzy Logic Controller. These controller's robustness is achieved by the optimization of their parameters using meta-heuristics optimization techniques like Genetic Algorithm, Particle Swarm Optimization and Krill Herd.

1.2.2 Worldwide energy production

The government's support on deployment, incentives, commercialization and development of renewable energies are ever-increasing. For example, in March 2007, it is agreed by the European Union members that at least 20% of their nations energy should be produced using renewable energy resources by 2020 [11].

Energy is included in every single human file activities in an industrialized and modern Community and there are various major examples :

– Manufacturing electricity and heat used in humain daly life or industrial products.

– Irrigation and fertilizing in agricultural organizations.

– Household applications such as heating, cooking, air conditioning and lighting.

The worldwide consumption of energy was growing rapidly right after the industrial revolu-tion and it has reached more than 500 EJ. 15 TW of energy has consumed and global energy consumption of 1900 was 0.7 TW. If the hourly consumed power is 3.3 TW, 1 year of consumption corresponds to 29,000 TWh, by 3.3 TW_24 h_365 days. Between 1980 and 2004, the worldwide energy consumption annual growth rate was 2% [11–13].

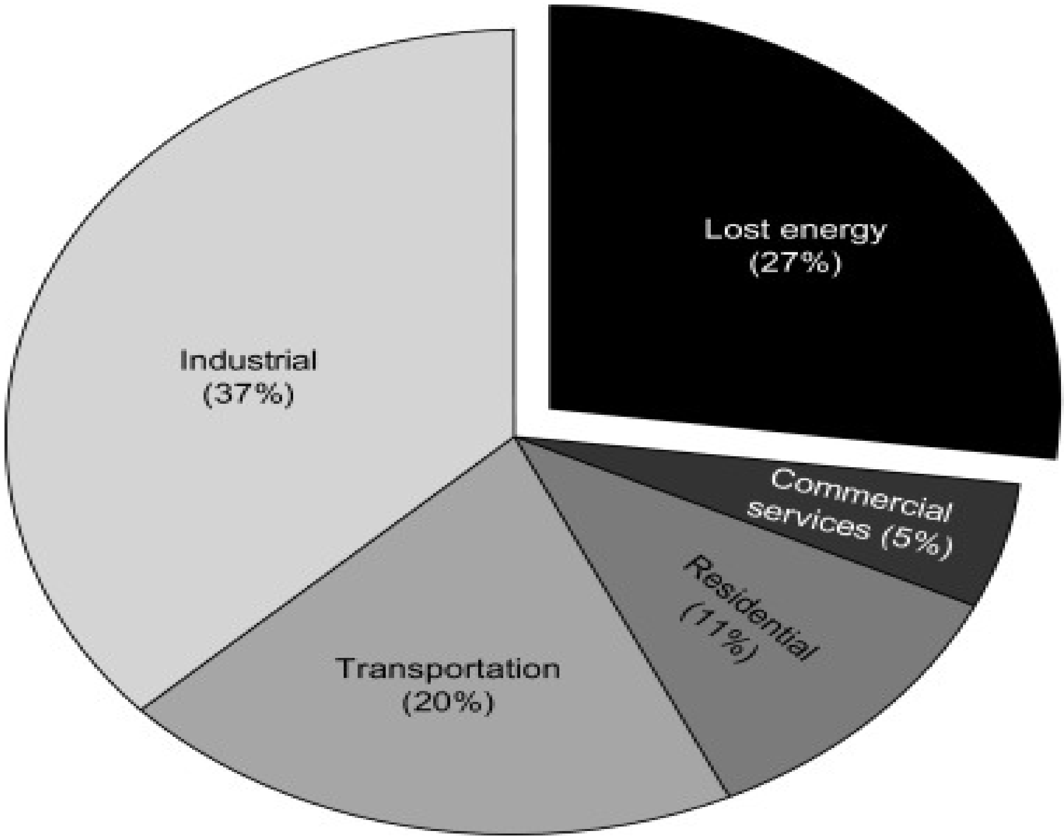

FIGURE 1.1 – Percentage share of sectors on energy consumption .

This figure also imposes that more than a quarter of the produced energy is lost in low efficient conventional energy conversion systems and transmission lines. This problem of energy which lost in low efficient conventional energy conversion systems and transmission lines encourages the increased focus on high efficient renewable energy systems, which may also reduce or eliminate the transmission losses if they are built as distributed energy generation units [11].
There is a high level of uncertainty regarding the future of world coal production that may be influenced by economics, climate stabilization requirements, as well as resource constraints. For the future wind and solar electricity consumption, This report doesnt present a limit for the energy power concemption using solar and wind sources. However, it assumes that the solar and wind annual installation producing capacity will increase at a progressively low rate and eventually approach a certain level of maximum [14]. Figure 1.2 shows that World historical oil, natural gas, and coal consumption from 1950 to 1964 is estimated from carbon dioxide emissions.Solar and wind consumption in electricity around the world was 1.293 terawatt-hours in 2016 (292 million tons of oil

equivalent), 19.2 percent higher than world consumption of wind and solar electricity in 2015.

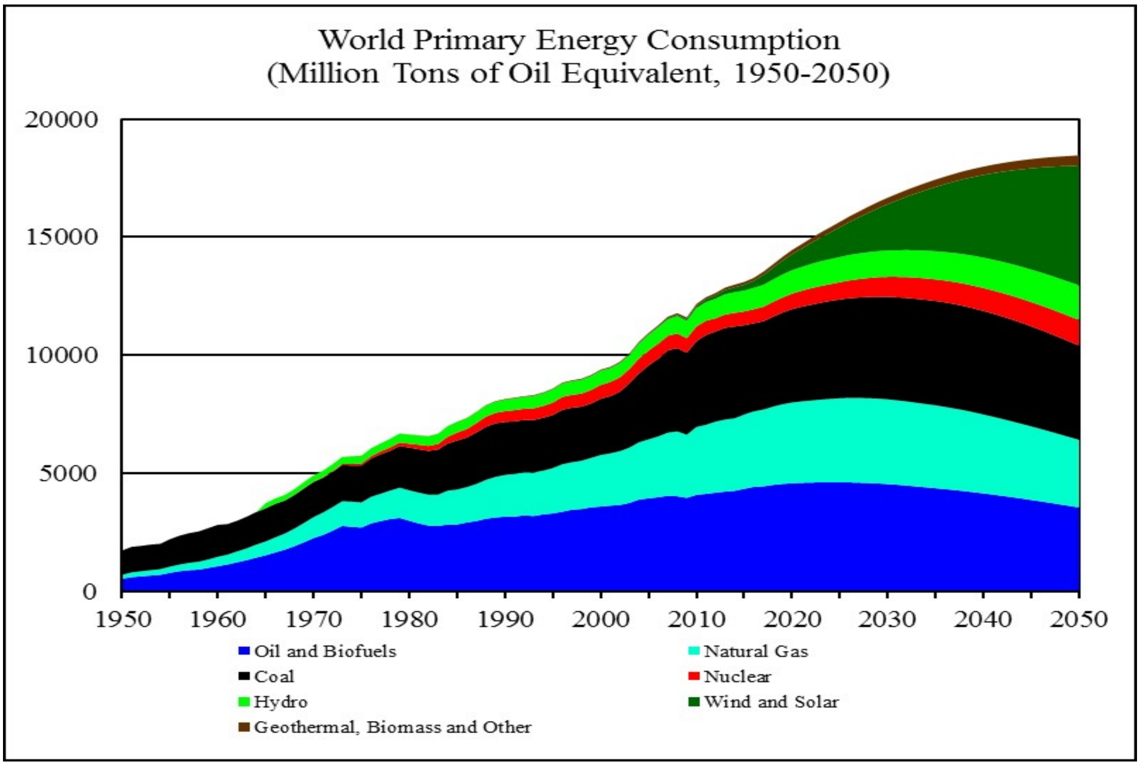

FIGURE 1.2 – World historical Primary energy consumption from 1950 to 2005.

World consumption of wind and solar electricity was 1,293 terawatt-hours in 2016 (292 million tons of oil equivalent), 19.2 percent higher than the world consumption of wind and solar electricity in 2015.

Wind and solar are renewable energy resources. However, wind and solar electricity are intermittent. Incorporation of wind and solar electricity into electric grids requires maintaining a large backup generating capacity and poses challenges to grid reliability. Curtailing of excess wind and solar electricity when surges of wind and solar generation exceed demand may impose limits on how much wind and solar electricity can be absorbed by a given system of electric grids. In the long run, the natural and mineral resources availability limit the solar and wind electricity production [15, 16].

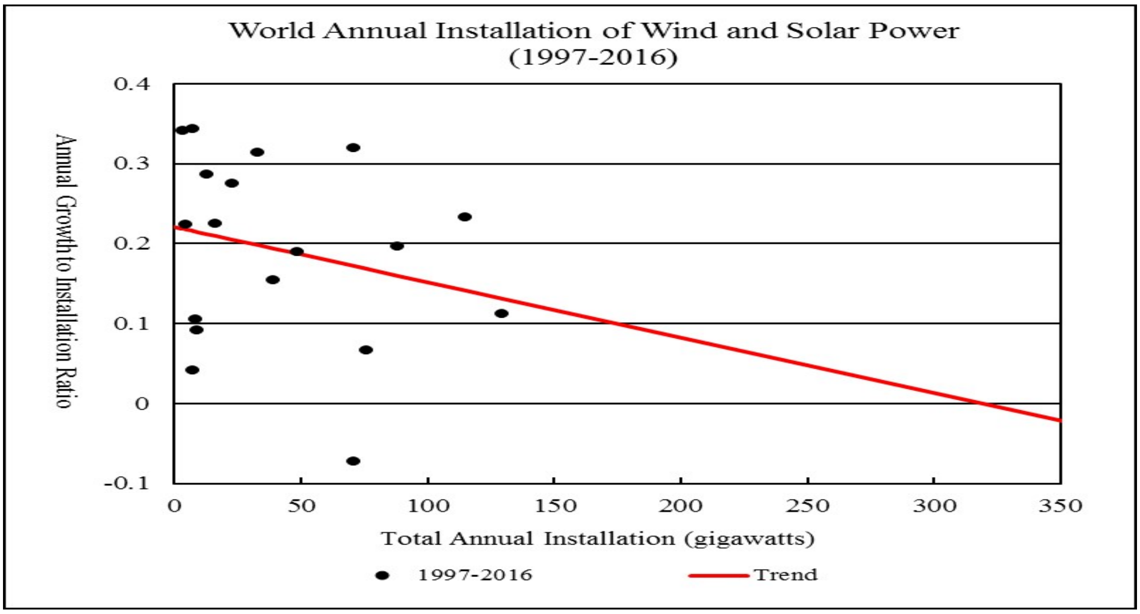

Figure 1.3 – Annual installation of wind and solar generating capacity from 1998 to 2016 is from BP (2017) [16].

The future wind and solar electricity generation can be estimated using the following formula :

$$Electricity\ Generation\ (current\ year) = \frac{Beginning - of - year\ Generating\ Capacity + End - of - year\ Generating\ Capacity}{2 \times 8760\ Hours \times Capacity\ Utilization\ Rate}$$

In comparison with the efficiency of conventional power plants, a new generation of power plants using gas turbines or micro turbines may reach substantially higher efficiency of 55% ; however, they still rely on another fossil fuel, which is natural gas. A new generation of power plants using micro turbines or gas turbines may reach higher efficiency of 55% but they still rely on natural gas. In the eighteenth and nineteenth centuries, coal began to be the main source of energy after the invention of steam engines. In the twentieth century, since automobiles were invented the world moved from Coal to the oil and electricity usage became more popular. The oil becomes too expensive between 1920 and 1970 because it was the main resource fueling the transportation and industry. Over the last 30 years, the use of fossil fuels has continued and their contribution to overall energy production has increased. The coal has large remaining reserves for this it becomes the fastest-growing fossil fuel [17].

1.2.3 Topological microgrid concept and structure

The entities that are located in the remote area or connected to the utility grid which can be worked autonomously are called Microgrids (MGs) [18]. A microgrid (MG) is an interconnection of domestic distributed loads and low-voltage (LV) distributed energy sources, such as micro turbines, wind turbines, photovoltaic (PV), and storage devices. The MGs are attached to the LV/MV substation at a single bus. The Microgrids are placed in the low voltage (LV) and medium voltage (MV) distribution networks. This has important consequences. With numerous micro sources connected at the distributed bus, there are many challenges, like system stability, power quality, and grid operation that must be overcame using an advanced control techniques at LV/MV levels rather than high-voltage levels, which is common in conventional power system control. In other words, distribution networks (demand side) must pass from a passive role to an active one. Figure 1.4 shows the typical structure of the Microgrid [18].

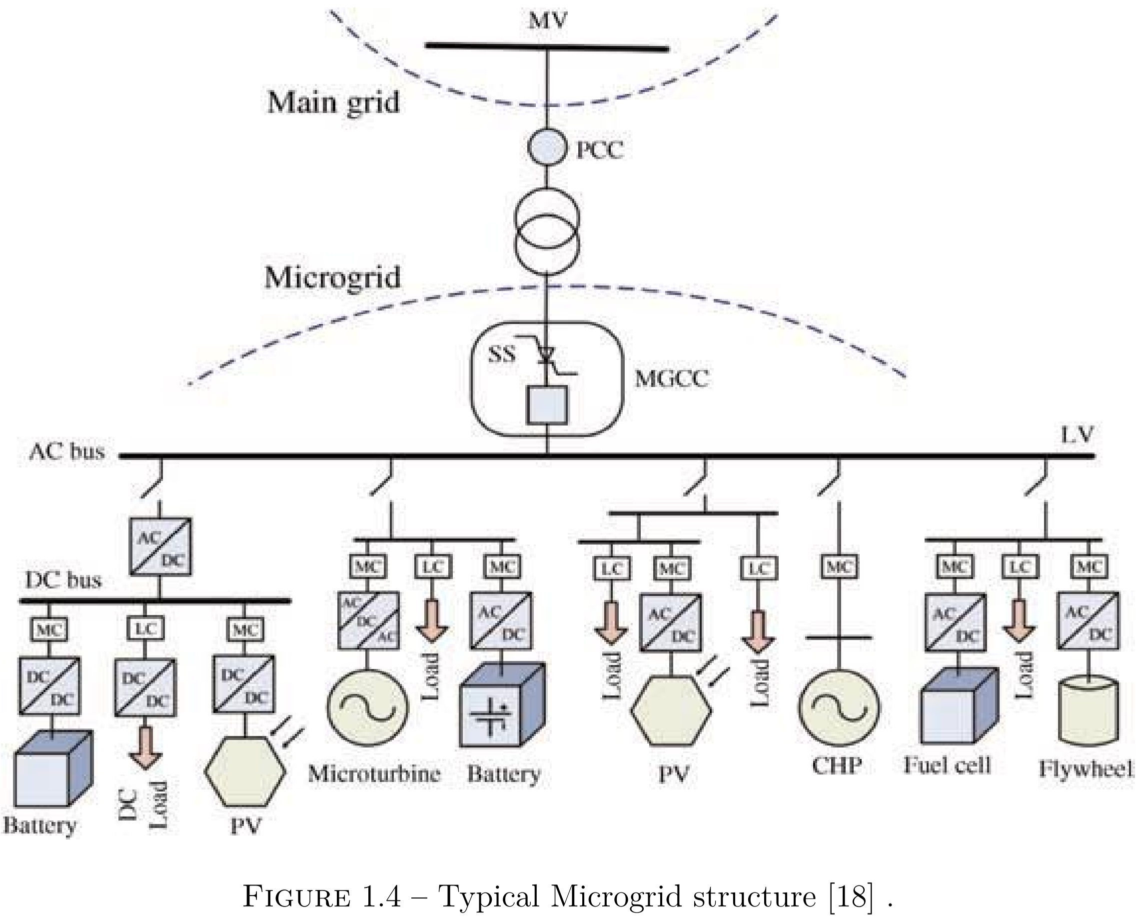

FIGURE 1.4 – Typical Microgrid structure [18] .

The structure of Microgrid which assumes an aggregation of loads and micro sources operating as one system providing heat and power. In the basic Microgrid architecture, there are a cluster of radial feeders and the point of common coupling presents the connection point to the utility grid [19].Most DGs/distributed energy resources (DERs) that can be installed in an MG are not suitable for the direct connection to the electrical network due to the characteristics of the produced energy. One of the important concern in Microgrid is the inverter control which is required for power electronic interface [20]. These systems can be connected to the LV distribution utility, but they can also be operated in islanded mode in case of faults in the main grid. From the customer's point of view, the MGs provide both thermal and electricity supplies, and, also, enhance local reliability, reduce emissions, improve power quality by supporting voltage and reducing voltage dips, and potentially reduce costs of energy supply [18].
According to the utility of AC and DC bus for coupling various elements within the microgrid, there are an AC microgrid, DC microgrid and hybrid AC/DC MicroGrid.

1.2.3.1 AC microgrid

An AC MicroGrid can be defined as an interconnection of distributed energy sources and domestic distributed loads, like wind turbines generator, photovoltaic system, microturbines, storage energy systems. Figure 1.5 presents a simple architecture of an AC MicroGrid, it consists of a group of radial feeders as a part of a distribution system. The domestic load can be divided into sensitive/critical and non-sensitive/noncritical loads via separate feeders. Every unit's feeder has a power flow controller and a circuit breaker commanded by the energy manager or the central controller. A point of common coupling (PCC) connects the AC MicroGrid to the distribution system via a static switch (SS), this latter can island the MG when faults or a contingency occurs or for maintenance purposes [21].

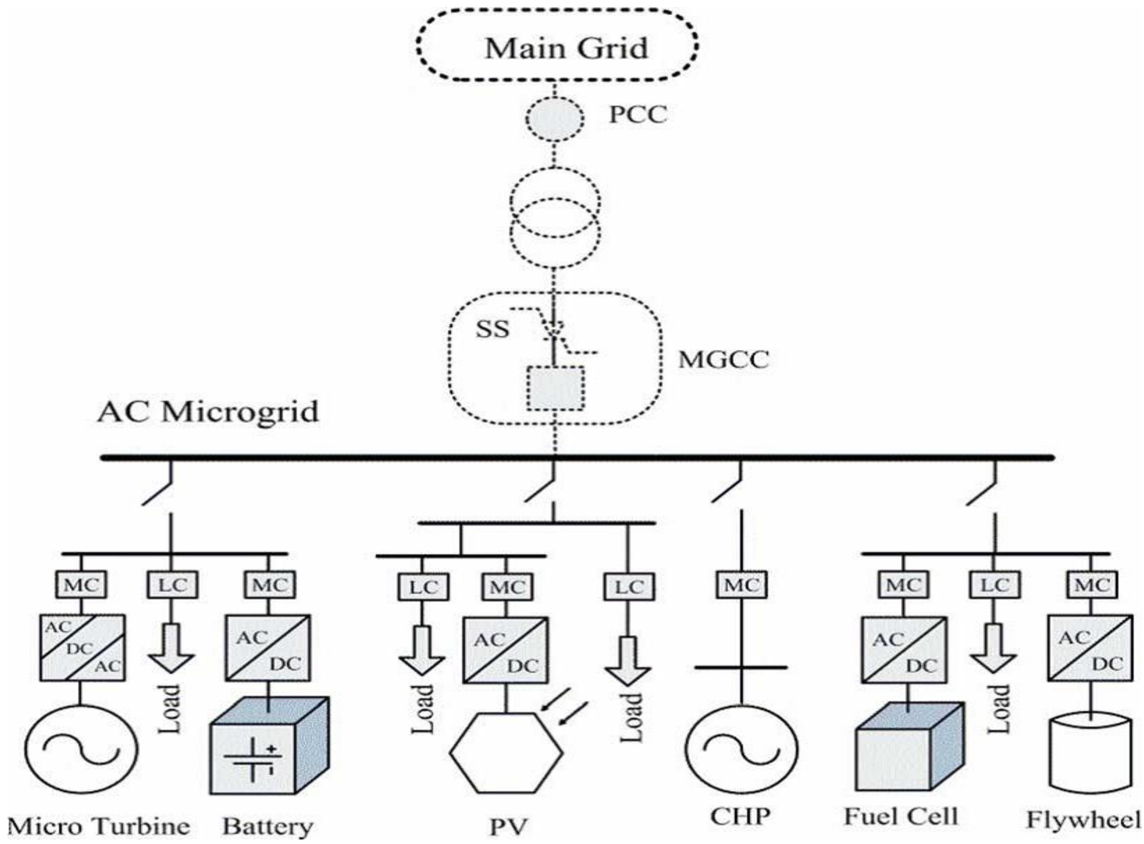

FIGURE 1.5 – AC Microgrid Architecture [21].

The microgrid power system consists of storage devices, a diesel engine, a photovoltaic (PV) system and the public grid all connected to a common DC-link bus through their convenable converters.

1.2.3.2 DC microgrid

Combining contnuie dynamics with directs event dynamics is named as DC Microgrid systems. Next, the behavioural modelling of a global system is proposed utilizing interpreted Petri Net formalism. This work [22] mentioned that the Petri Net is a powerful mathematical and graphical tool for analyzing and describing various hybrid dynamic systems. Figure 1.6 shows the topological architecture of DC Microgrid.

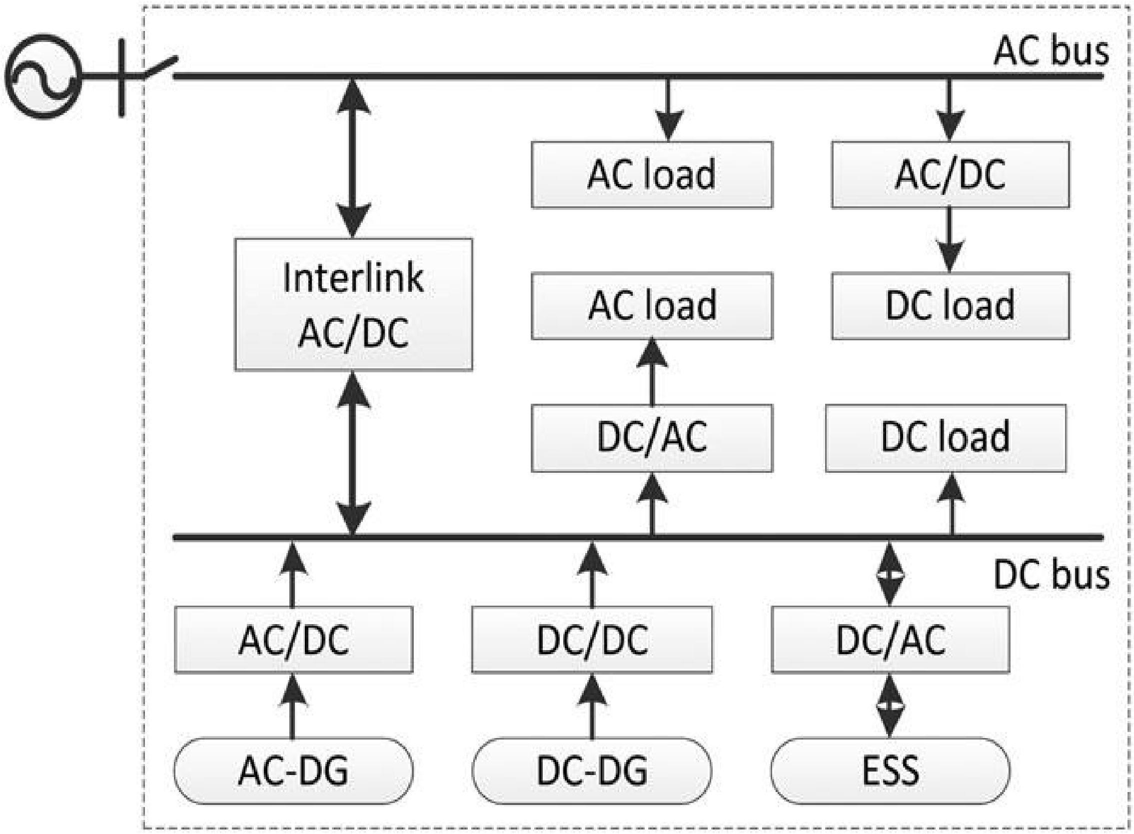

FIGURE 1.6 – Topological Architecture of DC microgrid [22].

The simulation of power system control has a hybrid aspect. The discrete and continuous aspects coexist and interact with each other. The power system components behave with continuous dynamics whereas the control strategy by Petri Net modelling behaves discreetly. State flow and Simulink developments in the MATLAB environment are proposed to perform numerical hybrid simulation tests.
To identify the disrect control model behavior of system and to help the simulinck to modeling the continus system the state flow is used.
State flow devellopement language is depended on the notion of hierarchical automata from State charts and allows design the PN model through the approximation made between places/states and switching/firing transition conditions. AC microgrid refers to the configuration of the coupling AC bus with microgrid elements and connecting to the AC local grid. DC microgrid refers to DC bus coupling and connection to the DC local grid.

1.2.3.3 Hybrid AC/DC microgrid

Hybrid AC/DC microgrid refers to the assistance of both DC and AC coupling. At present, the DC grid is not ubiquitous, but more HVDC transmission lines are being built in MW level, while low voltage DC grid is being adopted, starting with data centers, for the reason of less occupied space, less cost, lower lifetime cost, more efficiency and more reliability.

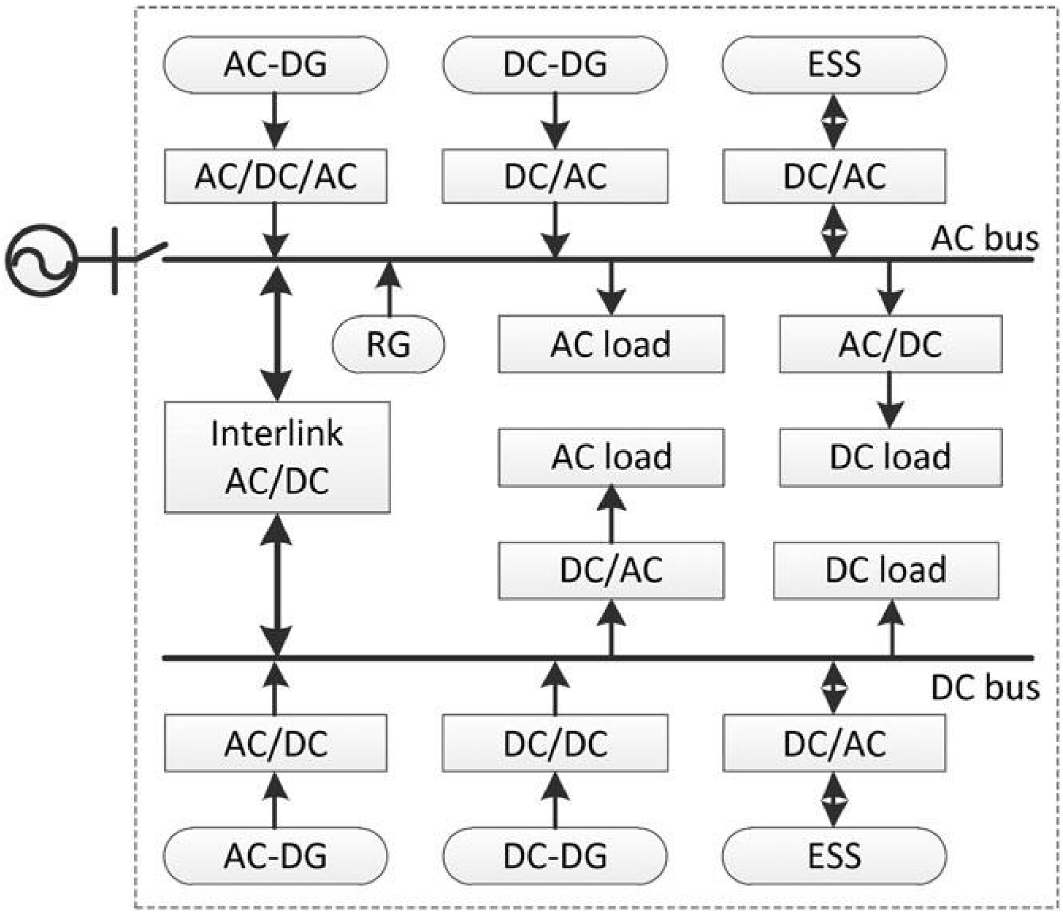

FIGURE 1.7 – Hybrid AC/DC Microgrid structure [22].

1.2.3.4 Comparison between AC and DC micorgird

As a comparison between AC and DC configuration of microgrid, AC systems have more advantages then DC systems in the following points or aspects :
The first point, the AC systems line impedance is much higher than DC systems. Meanwhile, an AC element, such as transformer, can withstand more overloading (As

an example, a 30/40MVA, 138/13.8kV transformer can withstand 160% overload for 30 minutes and 170% during 15 minutes according to transformer factory test [23].
In addition to this, the DC system for which slight overloading for milliseconds over-power electronic device rating could permanently damage the power converter. In case of fault such as short circuit, the AC can be limited and also it rises slowly because of relatively high AC impedance ; thus, the overloading ability provide enough time for protection devices to operate but in DC system, the low DC "impedance" induces high rising rate in the fault current, resulting in more challenges for the design of a fast response DC circuit breaker.
In the second point, the AC circuit breaker is much mature than DC. Forced by AC voltage, AC has nature zero-crossing features but DC is always persisting. Breaking the DC circuit is much more difficult than breaking AC especially in high current rating.
AC voltage can be economically and so easily transformed to another level (increasing or decreasing) by electromagnetic transformers without control strategy but DC transformation requires power electronic devices with complex control and measuring.
Semiconductor applications can be found everywhere, from industrial variable speed motor drive to building lighting, not to mention ubiquitous information technology devices this with technical development.
Appliances based on semiconductors require always the use of DC power. Conversion from AC to DC generally loses 10-25% of energy, depending on various devices and/or their rated power [23]. n addition, DC systems do not experience from skin influence, so the thinner cable can be used with ameliorate material efficiency.
In DC microgrid, AC sources, like diesel generators, wind turbine and MT are integrated to the DC bus through converters. As no reactive power is present in the DC bus, connected AC sources could run with only active power, which increases the power transfer ability and the power efficiency.
Coupling AC microgrid element with AC grid and AC bus obliged all conversion stages to work at the same frequency, while the amplitude and harmonic must also be as consistent as possible to avoid undesired loop current. The DC microgrid, as zero frequency system, only the voltage amplitude should be regulated and there is no need for synchronization when connecting DC bus or DC local grid. Coupling DC bus to AC

local grid needs only one inversion stage.PV sources, the energy storage as batteries and flywheel can be more efficiently and easily integrated with the DC grid without needing inversion stage.
Finally, DC systems would provide an advantage for the end-users in low voltage levels, while AC systems may have more advantages in high power applications and certain high voltage. This work [23] cited that the DC grid is the future trend in both transmission and distribution lines. Now, the main technical obstacle to bring DC grid into reality lies in the aspect of protection, for example, high power rating DC circuit breakers.

1.2.4 Classification of Microgrids

The microgrids are classified into five categories like commercial, community, campus, military, and remote microgrids. The commercial or industrial microgrids are generally designed to work in grid-connected mode to decrease demand and costs. They also provide a backup system to prevent the effects of faulty operating conditions.
The community microgrids are improved to enhance the stability of utility grid while campus microgrids are installed by individual institutions such as colleges, hospitals, and industrial plants due to featured load types and uninterruptible power supply requirements. Military microgrids are implemented in places where physical and cybersecurity are required. These types of microgrids can be remote as others installed in rural places where the utility grid is not available. Most of the remote microgrids are operated in islanded mode and supplied with diesel generators in addition to RESs. Although each microgrid type is improved to meet particular requirements, the grid connection should be performed by following several international standards. Historically, the development of DG took place in the context of electrification of isolated communities and back-up generation for critical loads. The electrification of remote communities in developing countries and geographical islands is a major application of DERs and the development of microgrids. Energy requirements are met by renewable sources (small hydro, solar PV, and wind) in addition to diesel generators. A major characteristic of a remote microgrid is that it is sized to serve the entire load along with an adequate level of reserve capacity to manage contingencies. The power/energy

balancing between variable load and intermittent generation (solar PV and wind) requires strategies to maintain the desired level of reliability. Isolated microgrids could be based on DC distribution to improve efficiency and reduce costs.

1.3 Modeling and Control in Microgrid

Microgrid models with decreased complexity, Microgrid and transmission lines modeling and modeling of loads are presented in [19]. This thesis discussed also the distributed energy sources models that have been simulated in Matlab/Simulink including Fuel Cell, Wind Turbine, Photovoltaic Cell, Diesel Engine, along with the detailed modeling of short term storage (Battery, Aqua Electrilyzer, Ultracapacitor and Flywheel). Then, it mentioned the hybrid sample systems that are built to investigate their transient responses.
Due to the various stability analysis and controller design tasks several models of microgrid have been presented in literature. These modeling techniques can be categorized into four categories which depend upon microgrid configurations and types of its components [5].
In this thesis, the Components wise modelling is selected because it is suitable for frequency analysis. This model interests in obtaining a suitable model with the low order possible of each component. These components including the different micro sources such as WTG, PV, FC, DEG and energy storage systems like BESS, FESS and UC. Along with MS the different types of loads LV network parameters are usually modelled and aggregated to obtain a complete MG model. Finally, the aggregated model can be arranged in one of two standards form i.e. in transfer function or state-space form. The obtained models are of high order around 20th and hence a large-scale system would be reduced. It would be impractical to be used in further applications. Hence these models are required to be simplified to obtain the Reduced Order Model (ROM), mostly by using any available Model Order Reduction (MOR) method. In this proposed model the MG is presented by first Order transfer function for being able to combine these different components and introduce various suitable control strategies. This microgrid can be connected to the grid to enhance the grid to supply the connected loads due to the development of the population. This leads to connected multi

microgrid areas to exchange power and improve power quality and reliability. The tie line model is recently used to interconnected different areas of microgrid [24]. Transmission level is usually considered for multi areas interconnected purposes through the tie lines models. The frequency and tile tine power exchange can vary according to variation in power load and generations. In this thesis, a tie line model for two areas of a microgrid is proposed and simulated.

The energy storage system can work as a backup power system. The principal role is to store or to release electrical power like an energy protector, supporting the operation of distribution loads, generation sources and transmission. Therefore, they are useful to solve the problems of power intermittency and system low inertia in a RES-based power grid. The combination of energy storage devices and RES constitutes a hybrid power generator or a microgrid system that can provide power not only for the local loads but also can supply AS to the main grid-like conventional generators [25].

It is always an advantage if we are using RES to run power system instead of our conventional energy sources. A problem of using RES in power system operation is the fluctuation occurring in the amount of renewable energy obtained. Just for example, we wont be getting a steady flow of wind over a longer period of time. Similar fluctuation is also observed in case of solar energy(on an bright, sunny day one can expect high quantity of solar energy, and on a cloudy day low level of solar energy would be obtained). Our prime objective of using secondary sources is to eliminate load fluctuation or/and principle source fluctuations. So any form of fluctuation in storage devices and loads is undesirable. Hence we cannot directly use RES alone as the sole supply sources. However, we all are aware of the advantage of RES over conventional energy sources. So to accommodate RES in the secondary supply side an alternative method called BESS is used. The power generated from RES is stored inside a battery. This stored power is used to handle the load fluctuation and/or primary source fluctuation situation. From the battery, we can get a constant source of power without any fluctuation and also by this system we can use RES effectively [25, 26].

The distributed energy generation includes renewable sources ; conventional sources and storage devices are generally connected to the microgrid by synchronous generator or power electronic devices. The droop controls determine the steady-state power-sharing in microgrid between different generation units and loads. There are considerable power and frequency swings between generation and loads because of the disturbances in renewable sources and loads profile before such a steady-state is reached. This one of the reason to use conventional sources in microgrid based renewable generations along with storage devices which are interfaced by a converter and give a faster response with small frequency deviations. Moreover in order to guarantee the microgrid frequency control and performance stability many control strategies are addressed in literature such as centralized control, decentralized control and local control [27]. One of The most control issues which are applied by different researchers is Load Frequency control which is the principal role of the Automatic Generation Control system [4] . The main objective of LFC is to keep the frequency and power deviations at limit values and contractual energy exchange between interconnected areas using tie line model. Recently others control strategies for frequency analysis are used, where the others apply PID, FOPID and Fuzzy logic in order to find better performance of microgrid. With the development of optimization these controller get more importance due to the difficulty of tuning their parameters. There are three subcategories of frequency control loops ; primary frequency control, secondary frequency control and supplementary frequency control. The primary frequency control damps the system frequency deviation for few seconds ($\sim$ 30 sec) after occurrence the disturbance. Where, the power requirement is equiliblized by attenuating these deviations (like the governor natural autonomous). While, the secondary frequency control (such as LFC) stabilizes the frequency to its nominal value for a time from few seconds to few minutes after the disturbance [28].

Microgrid power quality problems principally result from grid connection and nonlinear load, both of which introduce harmonic current. Hence, different controllers and control strategies are proposed in the literature. The proportional-Integral-Derivative controller could offer higher harmonic rejection ability at the selected frequency and is widely used for eliminating selective harmonics. The methodology which designs a PID controller is also discussed and studied. Sliding mode control is used for low harmonic and high power factor in grid-connected operation [29]. H cascade current-voltage controller is proposed to introduce equilibrated clean current to the grid while keeping the nonlinear harmonic currents and unbalanced local load currents locally [30].

In case of supplying both single-phase load and three-phase, a three-phase four-wire

configuration must be applied, the authors proposed H current controller to stabilize neutral point voltage for connecting unbalanced load and/or utility grid.
Most of the authors proposed the control strategy based on complex parameters, the classic control theory is used also to avoid complex parameter tuning in MicroGrid control, such as the proportional-integral (PI) controller.
Other control problems are also involved, it's summarized as follows :
– PV maximum power point tracking (MPPT) control algorithm for operation in partial shedding condition.
– The phase lock loop (PLL) for the fast detection of selective individual harmonic.
– New topology of parallel converters for reducing capacity of full power transformed in wind application.
– Smoothing renewable production fluctuations by PID controller fuzzy logic controller and Fraction PID controller with the use of energy storage devices.
– Controlling power transfer at PCC by tap control of a smart transformer [23].
– The Time domain analysis is sufficient for frequency analysis behaviour and gives good results in microgrid frequency control. It also largely employed in the hybrid power system to simplify the model of different components which are presented by the linear model and to introduce a linear control [9, 10].
Among these control concerns in microgrid frequency control strategies and new reserves analysis are considered as a major challenge in microgrid stability and security. For the satisfactory operation of a microgrid system, the frequency and power should be kept nearly constant [4].
There is various new strategies control scheme using in microgrid frequency control among of them PID controller which is widely employed in the industry due to its simplicity and easy implementation. Many important types of research are accomplished in literature interest the use of PID control for frequency control in the hybrid energy system as [9] which shows better performances of this controller in the repression of frequency deviation in the microgrid system. This controller can be extended by adding fractional action that can give more flexibility and robustness to the classical PID controller. The new controller called a fraction order PID controller with derivative and integral. It is well known Fractional Order control is an effective robust control scheme and has the features of fast global convergence and high robustness to external

disturbances and elimination of harmonics [26]. In microgrid control, the fractional control was integrated recently and there is some study about the application of fractional order PID controller in electrical engineering. One of the most nonlinear control schemes used in the large application is the fuzzy logic controller due its robustness and reliability to overshot and eliminate the mismatch between the generation and load which affect the stability of the system. to improve the robustness of the fuzzy logic controller it can be implemented in a hybrid controller with PID or FOPID. The major issue facing the application of these techniques is to determine their optimal parameters.

1.4 Optimization Techniques

The powerful tools for resolving the optimization problems in many fields of researches are metaheuristic algorithms. This thesis addresses the application of various methaheuristiques optimization algorithms, especially those developed in the last few decades, and their applications. Among of these Genetic Algorithms, differential evolution, genetic program, and most useful, swarm-intelligence-based algorithms such as ant and bee algorithms, particle swarm optimization, cuckoo search, firefly algorithm, bat algorithm, and krill herd algorithm.

In metaheuristic algorithms, metasignify beyond or higher level. They almost always present better than simple heuristics. All metaheuristic algorithms use some tradeoff of local search and global exploration. Randomization despite population has always released the variety of solution, in literature, there is no specific definition of heuristic and meta-heuristic. Some researchers use heuristics and metaheuristics interchangeably. To move from local scale search towards global seach space, metaheuristics give a good tool for this chande, howover this lead to name all stochastic randomly techniques metaheuristics optimization methods. For global optimization and nonlinear modeling all metaheuristic algorithms are usefuls and suitable methods [31].

Metaheuristics can be an efficient way to produce acceptable solutions by trial and error of a complex problem in a short practical time. The problem complexity of interest causes the im-possiblity to find possible solution or combination, the aim is to get good feasible solution in an reasonable times. There is no guarantee that the best solutions can be found, and we even do not know whether an algorithm will work and why if it does work [32]. The idea is to have an efficient and practical algorithm that will work most of the time and can produce good quality solutions. Among the found quality solutions , it can be expected that some of them are nearly optimal, though there is no guarantee for such optimality.

The metaheuristic algorithms are composed of exploitation and exploration or intensification and diversification [33]. To generate diverse solutions so as to explore the search space on the global scale is called Diversification, but intensification is to search in a local region by exploiting the information that to find a current best solution in this region. To ensure the convergence to the optimal solutions the section of the best solutions is reauired.

On the other hand, to avoid the solutions being confined at local optimal,and to increases the diversity of the solutions the diversification via randomization is used. The combination of these two components of metaheuristics can usually ensure that the global solutions are found.

Metaheuristic optimization techniques can be categorized in different ways. The trajectory-based and population-based are the best way to classify metaheuristics agorithms [34]. For example, genetic algorithm (GA) and genetic programming (GP) are population-based as they use a set of strings, so is the particle swarm optimization (PSO) which uses multiple agents or particles [35]. On the other hand, simulated annealing (SA) uses a single solution that moves through the design space or search space, while artificial neural networks use a different approach. Modelling and optimization may have a different emphasis, but for solving the real world problems, the optimization and modeling are often used together because modeling is employed to evaluate the objective functions using the mathematical/numerical model of the problem to be resolved , but optimization can determine the optimal settings of parameters. For optimization, the essential part is the optimization algorithms. For this reason, we will focus on the algorithms, especially metaheuristic algorithms [36].

1.5 Research issues on microgrid

Microgrid control problems related to different stages of operation in both the isolated model and connected mode. Although the development and installation of microgrids are still in the evolutionary stage, there are already plans being made to extend the economic operations at the transmission level using transmission system operators (TSOs) to distribution system operators (DSOs) where a DER can function like a generating station in terms of its operation. In principle, DERs can contribute to the provision of all electrical services provided by TSOs. The previous accomplished studies which identified four major regulatory challenges due to DERs : computation of allowed remuneration of distribution networks in the presence of large numbers of DERs, computation of network charges for a diversified ensemble of network users with DERs, an adequate definition of the new role of DSOs with the provision of electricity services, with multiple new actors on suppliers and consumers, and finally managing the new level of complexity in the coordination of DSOs and the TSO.
In this section, the control of the technical issue that affects the operation and stability of microgrids will be discussed as follow.

1.5.1 Load Frequency control

Various utilities which can be connected together using tie-line model to form a modern power system structure. These power systems are subdivided into different regions or/and control areas. The control zone can be constituted of both, renewable energy like the wind, solar, etc and conventional energy sources like thermal gas, diesel, nuclear, etc [37].

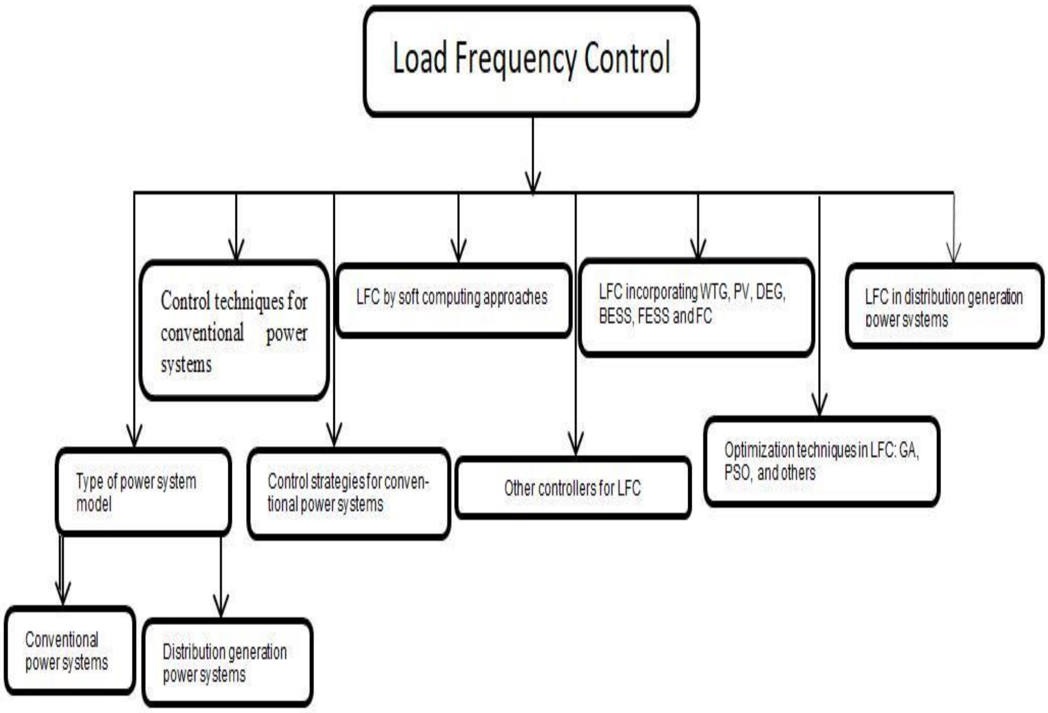

FIGURE 1.8 – Illustration of survey on LFC.

The main obective of this approach was to address an optimised controller parameters using different optimization techniques for resolving the LFC issue. The metaheuristics algorithms that are employed to tune the control schemes were utilized in every area for a two-area pow-er system of microgrid. The investigated optimization methods has been improved the efficiency and performance of the implemented controllers. Additionally, a comparative study was performed among the outcomes that gained from PID and FOPID tuned using KH.In [38] the authors have implemented a hybrid fuzzy logic and PID controller model to resolve the LFC issues of multi-area interconnected microgrid systems with a source hydrothermal power system. The connection between the two control areas was through the tie line. Every area was comprised of diesel generator, renewable energy system like PV and WTG, and storage devices. The primary governor controller and secondary Fuzzy-PID controller has control over the area frequency and power deviations at the time of load variations and generation changes. The gains of the fuzzy PID controller were optimized using GOA, GWO, PSO and DE. Because of the dynamic nature of diverse RES and diverse uncertainties such as dynamics in solar irradiation, wind speed variations, load fluctuations, and system parameters change, in islanded mode the microgrid system has faced by large frequency control issues (Inertia constant and damping coefficient). Owing to these issues, the recent pubished studies has investigated a robust kind of control scheme like fuzzy PID controller for generating the secondary frequency control loop in order to keep power and frequency among their nominal values over diverse uncertainties. The performance analysis has been exploited by comparing the performance of the proposed type-II fuzzy PID controller over type-I fuzzy controller, PI and PID controllers. A meta-heuristic I-SSO algorithm has been developed for exploiting the gain values of aforesaid controllers optimally, and further, the implemented I-SSO approach in terms of performances was differentiated over real PSO, SSO, and GA algorithms. The LFC was adopted for illustrating the outcomes of this research work. The experimental analysis has revealed that the implemented structure based on GA has acted as an attractive and alternative technique for solving the LFC issue from design and performance viewpoint. The examined power system has included three equivalent thermal power systems having a suitable PID controller. The objective function of FPA was assumed with ISE. By comparing the outcomes of the proposed algorithm of optimized PID controller with conventional GA and PSO-based PID controller has revealed the superior performance over the similar examined power system. Additionally, the robustness of the controller was learned by assuming the suitable generate rate constraint having nonlinearity in entire areas. The resultant cumulative comparison on performance has evaluated that the FPA-PID controller has exhibited supremacy while differentiating over the performances of PSO-PID and GA-PID controller-based power systems with and without nonlinearity consequence [39]. In the present thesis, the FOPID and PID controller are employed for load frequency control of two interconnected areas using the Tie-line model, and the controller's gains are optimized by Krill Herd Algorithm as will be discussed in chapter 5.

1.5.2 Frequency and Voltage Stability

The islanded Microgrids faces the challenge of frequency stability where any individual gen-erator power present a part of the total power demand. The frequency stability becomes an issue with DERs that are inverter-based or have low inertias and

damping torques. Under the islanded operation, the use of multiple small DGs can pose problems of synchronization, which is essential for the stable operation of the microgrid. There could also be problems with voltage stability [40].
Conceptually, these problems can be overcame by developing intelligent control schemes, but there are trade-offs. They require a relatively fast communications network that is available to link the various microgrid components. In general, the operation of a power system based on many small components rather than one large generator is a more complex task.

1.5.3 Intermittent Generation

The intermittent generation by renewables (wind and solar, caused by wind gusts or clouds passing overhead) implies that not only the power flow is bidirectional, but the power output from these sources varies randomly. The solution is to use storage devices such as batteries flywheel and supercapacitors.
It would also be desirable to tightly couple the supply to the power demand. Load and generation forecasting can help in the operational management of the microgrid.

1.5.4 Application of Inverters

In a microgrid, inverters are used to convert the DC output of the DG to AC, control the frequency and voltage, monitor power flows in the network, and provide basic fault protection. The parallel operation of inverters without loss of synchronization, prevention of propagation of harmonics, and loss of stability is a challenging task. For large microgrid with numerous inverters, doubts remain regarding the scalability of control techniques proposed for small-scale systems [41].

1.5.5 Microgrid protection

Microgrid protection is considered as one of the important issues that have to be addressed. Generally, a Microgrid can be operated in two principals modes : islanded mode and grid-connected mode. The power static switch (SS) is semiconductor switch which is used to interface the Microgrid system. The Microgrid should be isolated from the grid as possible as fast to avoid the fault on the main grid's side during the connecting operating mode and this is to protect the microgrid loads and to eliminate fault inside the Microgrid, the smallest possible section of the radial feeder should be isolated. It is so important to protect a Microgrid against all types of potential fault for example (overvoltage or under voltage, overcurrent, over frequency and under frequency).

It is still so important to research and develop new fault detection and protection control for the microgrid. It introduces bidirectional current and the flexible "plug and play" feature makes the fault current values varies, conventional relays, breakers and other protection devices may not work anymore, new protection algorithm should respond to the issues [42]. The EMS consisted of two steps : the weather forecasting and hourly load for the day-ahead and the optimal power flow in the Microgrid based on heuristic optimization technique [25].

1.6 Conclusion

This chapter addressed a general overview of electrical microgrid based renewable sources. Firstly the worldwide power production is presented. Secondly different microgrid structures and architecture are studied. Finely literature views on various modeling methods, optimal control strategies optimization techniques in the microgrid are investigated. The next chapter will discuss the modeling of the microgrid in detail.

CHAPTER 2

Modeling of electrical microgrid system

2.1 Introduction

This chapter investigates the modeling of different components of the microgrid system. The proposed microgrid consists of renewable energy sources such as photovoltaic and Wind Turbine Generator. It also includes a Diesel Engine Generator and Fuel Cell as secondary sources to help the system in case of insufficient power from renewable generation power. The energy storage systems such as the Battery energy Storage system, Flywheel Energy Storage System, Aqua Electrolyzer, and ultracapacitor are integrated into the proposed microgrid and modeled in this chapter.

2.2 Modeling of renewable energy sources

In this section, the mathematical model of the output power of the photovoltaic system and wind Turbine Generator is presented in detail.

2.2.1 Model of the photovoltaic system

The PV principle is the conversion of solar irradiance into electricity that is discovered by the Becquerel family and presented to the French Academy of Sciences by the end of 1839. This conversion is realized by the PV cell, the electrical characteristics of which resemble those of the PV source [43].
Figure 2.1 $(a) - (b) - (c)$ are models of the most commonly-used PV cell : a current source parallel with one or two diodes. The model of single diode [44] contents four

elements such as source of current with diode in parallel and resistors series (R_s) en shunt (R_{sh}). Figure 2.1 (b) presents model of two diode : the extra diode is for better curve-fitting [45].

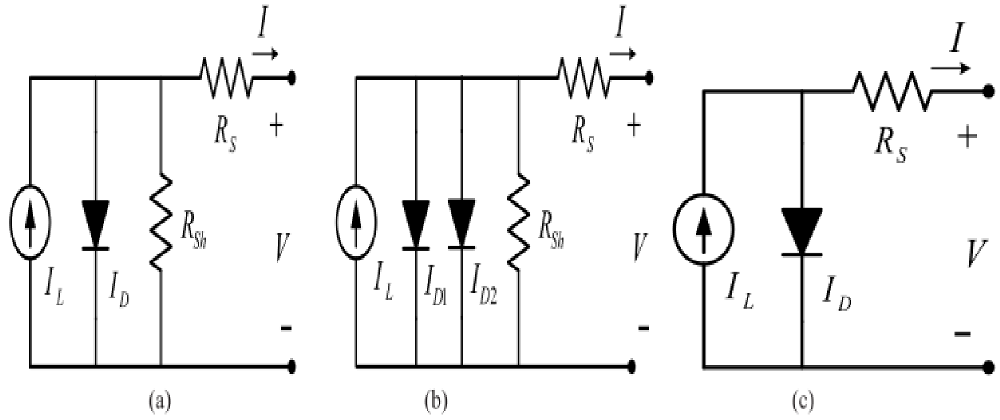

FIGURE 2.1 – Different models of PV.

The photovoltaic system has been considered to become the greatest available potential of all resources of renewable energy around the word in the future, due to its pollution-free and inexhaustible nature. The solar cell is a $p-n$ junction fabricated in a thin layer of semiconductor.

For modeling the photovoltaic system it is necessary to estimate the current- tension and power- tension characteristics to emulate the real function of this system under various conditions.

The most popular method for modeling the PV system is to use the electrical equivalent circuit presented by the diode model. Various models have been shown in the literature [46]. The simple model of a PV system is the model of single-diode that consists of a linear independent current source in parallel with a diode. The three parameters of this model determine the character of the IV curve, namely short-circuit current (I_{sc}), open-circuit voltage (V_{oc}), and diode idealist factor (a). This model is improved by adding two series and parallel resistances respectively R_s and R_{shunt}. The series resistance (R_s) is the internal resistance of the cell and depends mainly on the resistance of the semiconductor used, the contact resistance of the collector grids and the resistivity of these grids and the shunt resistor (R_{shunt} is due to leakage current at the junction ; it depends on how it was done [47].

In literature, it is popularly known as the (R_s)–model. Due to its simplicity and com-

putational efficiency, the (R_s) is by far the most widely used model in PV system simulation. The use of two diode models is used to avoid the effect of modules shading. Several modeling methods are proposed in the literature to determine the PV system parameters as given.
A PV array is the connection of several PV modules, connected in various topologies. Three typical interconnections structures are largely used namely, series-parallel (SP) total cross-tied (TCT) and bridge link (BL). PV system generates dc voltage that is converted into ac using dcac converter. An MPPT technique is largely applied to extract maximum power produced by the PV system. In [47] the other proposes partial modeling of an array system based on an improved two-diode model is proposed. The proposed modeling is interfaced with actual power electronic converters and MPPT algorithms. A PV panel is composed of one or more PV cells, and a PV source consists of one or several PV panels [48].

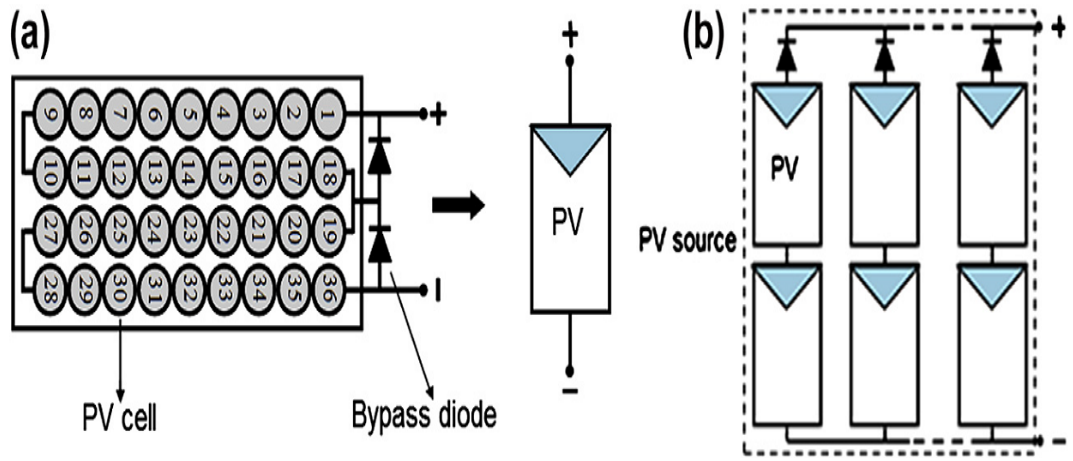

FIGURE 2.2 – Photovoltaic system modules.

The STC relates to the IEC 60904 standards, short-circuit current Isc, open-circuit voltage Voc, and maximum-point power (Pmpp) that are specified for PV modules to ±10% tolerance. Realistically, these conditions occur very rarely; however, if the sun shines with the specified intensity, then, cell temperature will be higher than 25°C. $I-V$ curves and $P-V$ curves were simulated for various irradiances and temperatures by using MATLAB. The $PV - AE125MF5N$ module was chosen as it is one of the types to be used in the experiment [49].

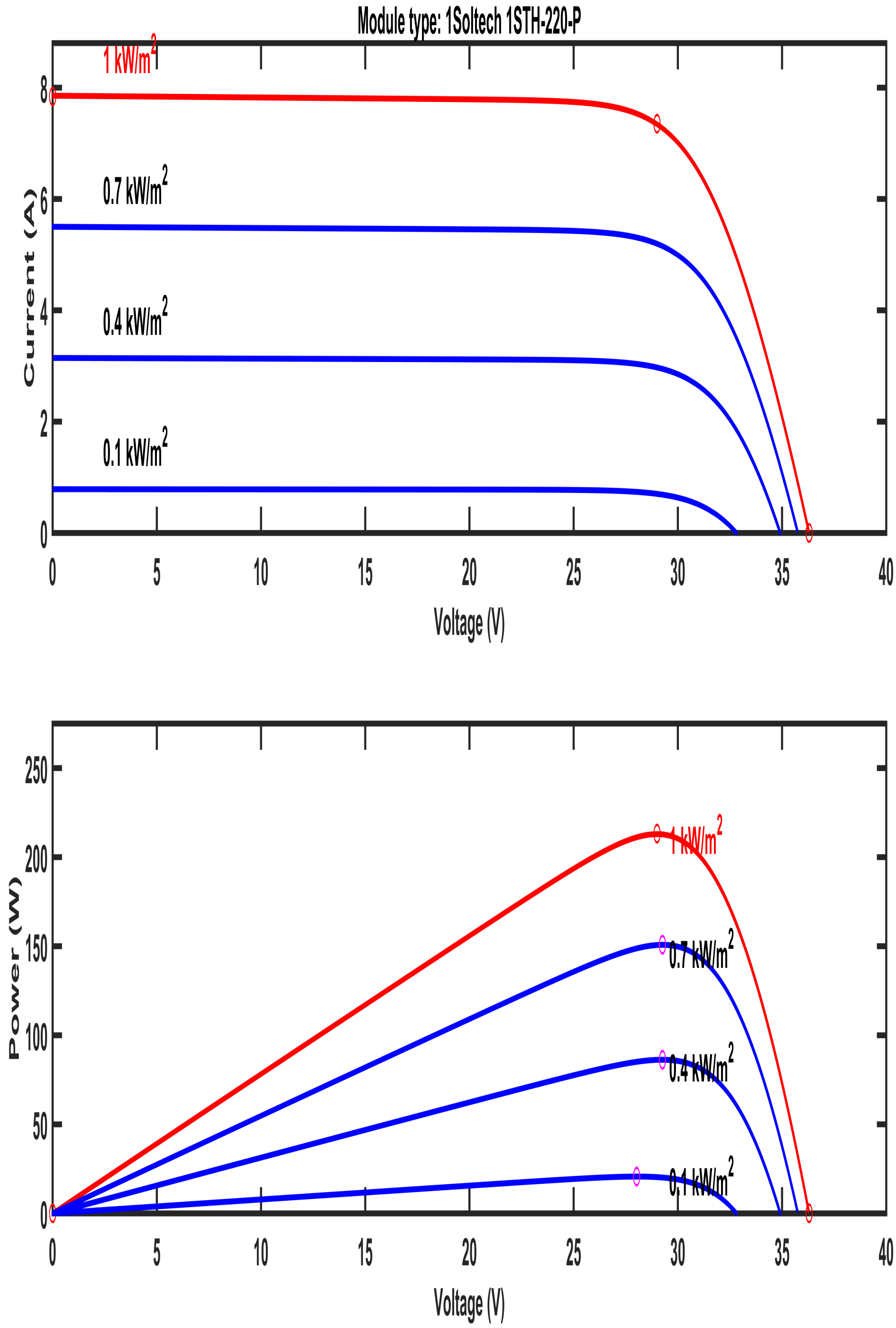

FIGURE 2.3 – Characteristic of PV cell for different value of irradiation and constant value of temperature.

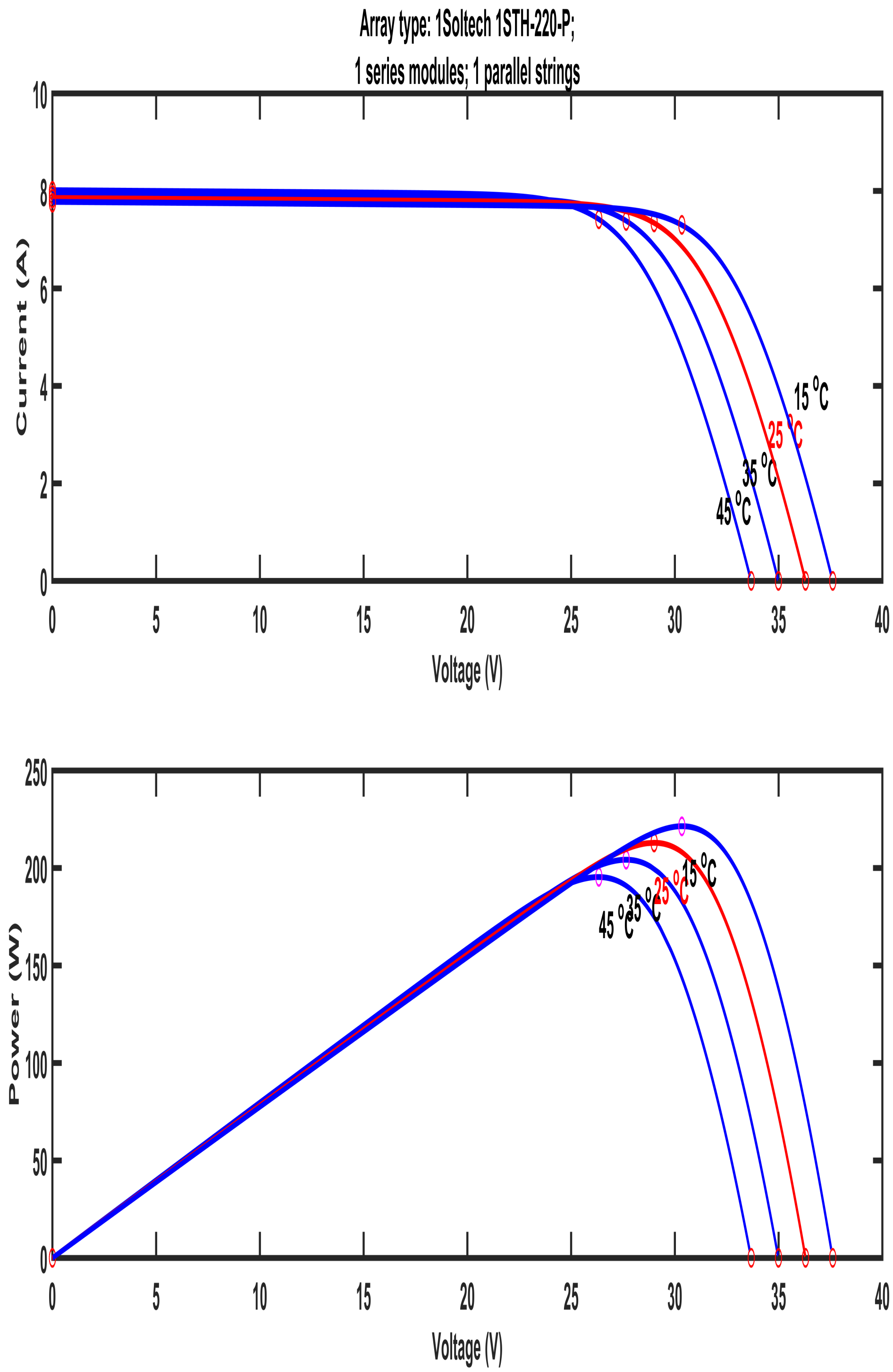

FIGURE 2.4 – Characteristic of PV cell for different values of temperature and constant value of radiations.

2.2.2 Modeling of solar cell

The simplest equivalent electrical model of the solar cell system is considered as a current source connected in parallel with a diode.The current output is proportional to the light falling on the cell area. A current source in parallel with a diode presents the simplest equivalent circuit of a solar cell. The current source output is directly proportional to the light falling on the cell (photocurrent I_{ph}). During darkness, the solar cell is not an active device ; it works as a diode, i.e. a $p-n$ junction. It generates neither a current nor a voltage. However, if it is connected to an external supply (large voltage) it produces a current ID, called diode (D) current or dark current. The diode proves the $I-V$ characteristics of the cell [50].

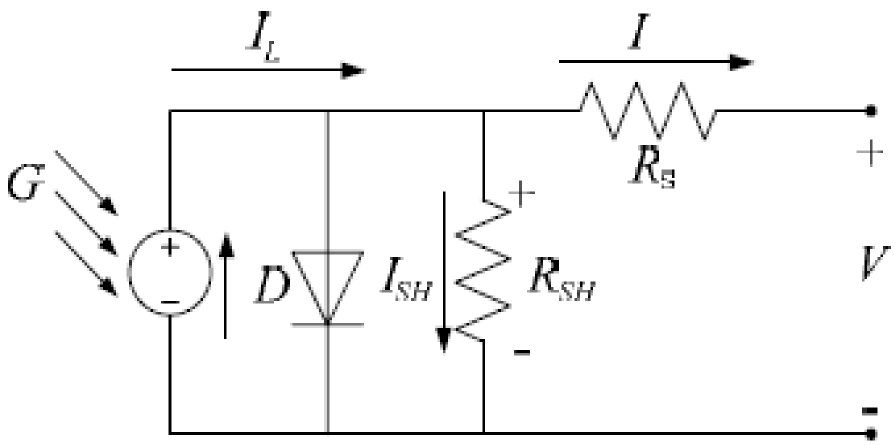

FIGURE 2.5 – Model of solar cell.

In an ideal model of cell $R_s = R_{sh} = 0$, that is a relatively common appropriation [51]. For this thesis, a model of moderate complexity was used(suprmimé). The net current of the cell is calculated by the difference between the photocurrent, I_L and the normal diode current I_0 :

$$I = I_L - I_0 \left(e^{\frac{q(V+RI)}{nkT}} - 1 \right) \tag{2.1}$$

The model included temperature dependence of the photocurrent I_L and the saturation current of the diode I_0.

2.2.3 Mathematical Modeling of PV Generator

For design and installing of PV generator performances under natural irradiation is a key issue to deal with the integration of PV power generation in microgrid and uncertainty. The per unit area PV power output from a PV generator (PVP) with a fixed orientation is represented by : [52]

$$P_{PV} = \eta_{PV}(t).A_{PV}.I_r(t) \tag{2.2}$$

where, η_{PV} is the power conversion efficiency of the module (power output from the system divided by power input from the sun) ; A_{PV} (m^2), is the surface area of PV panels ; Ir (W/m^2), is the solar irradiations. The PV generator efficiency is given by :

$$\eta_{PV} = \eta_r.\eta_{Pc}(1 - \beta(T_C - NOCT)) \tag{2.3}$$

η_r is the reference module efficiency ; it depends on the cell material. Polycrystalline silicon technology has been used with a 13% efficiency. β is the generator efficiency temperature coefficient, ranging from 0.004 to $0.006/°C$. T_C is the cell temperature $(°C)$. A PV module of polycrystalline silicon solar cells can be estimated from the ambient temperature $T(°C)$ and the solar irradiation I_r as follows.

$$T_C = 30 + 0.017(I_r(t) - 300) + 1.14(T(t) - 25) \tag{2.4}$$

The photovoltaic output model can be expressed using the previous definition as

$$P_{PV} = \eta_{PV}(t).A_{PV}.I_r(t)(1 - 0.0035(T(t) - 25)) \tag{2.5}$$

The output power of the photovoltaic generator can be expressed by another formula as follow without the time

$$P_{PV} = \eta.S.\Phi(1 - 0.0035(T_a - 25)) \tag{2.6}$$

where η ranging from 9% to 12% is the conversion efficiency of the PV array, $S(= 4084m^2)$ is the measured area of the PV array, $\Phi(= 1kW/m^2)$ is the solar radiation, and T_a is the ambient temperature in degree Celsius. Among the factors which affect its power output, the intensity of solar radiation and the atmospheric temperature changes must be considered when the equation is applied for PV power forecasting. These variations of solar radiation and temperature vary with seasons and different weather types. The value of P_{PV} depends on T_a and Φ because η and S are constant. In this thesis, T_a is kept at $25°C$ and P_{PV} is linearly varied with Φ only. Linear, small-signal models of the photovoltaic system and their converters are required to perform power system stability and eigenvalue analyses. For the frequency domain analysis, the PV system is presented by a first-order lag transfer function. The nature of solar power is fluctuating in nature, so to following the solar model [53] as shown in Figure 2.4 has been taken to realize the effect of microgrid integration solar plant. The PV output power determined by the first-order transfer function (TF) model of PV by neglecting nonlinearities can be expressed as [54, 55]

$$G_{PV} = \frac{\Delta P_{PV}}{\Delta \Phi} = \frac{K_{PV}}{1 + s.T_{PV}} \tag{2.7}$$

Where $\Delta\Phi$ indicates a change in the irradiation ; K_{PV} indicates the gain of the PV array ; T_{PV} indicates the time constant of PV array including converter time delay also.

2.2.4 Characteristics of Wind Turbine

The level detail of modeling renewable energy sources depends on the power phenomena to be analyzed. The wind turbine can be studied in two different ways. The first is its behavior analysis in a stationary state. The second corresponds to the dynamic analysis of the system. Generally, the study of the wind turbine in a steady-state is done when it is required to determine the generated power of the turbine under certain conditions of wind speed [56].

2.2.5 Wind speed model

The generated power of the WTG depends on wind speed V_W. The wind is modeled as the algebraic sum of base wind speed, gust wind speed, ramp wind speed, and noise wind speed. The associated equations for different wind-speed components are given next [57].
The base wind-speed component can be expressed by [57] :

$$V_{WB} = K_B \tag{2.8}$$

where K_B is a constant and it is always assumed to be present in the study when the WTG is operating. The gust wind-speed component can be expressed by :

$$V_{WG} = \begin{cases} 0, \quad t < T_{1G} \\ V_{cos}, \quad T_{1G} < t < T_{1G} + T_G \\ 0, \quad T_{1G} + T_G < t \end{cases} \tag{2.9}$$

$$V_{cos} = (MAXG/2)\left[1 - \left[\cos 2\pi(t/T_G) - (T_{1G}/T_G)\right]\right] \tag{2.10}$$

T_G is the gust period, T_{1G} the gust starting time, and MAXG gust used in wind studies. the gust peak. The gust wind speed is the usual $(1cosine)$ The ramp wind-speed component can be expressed by :

$$V_{WR} = \begin{cases} 0, \quad t < T_{1R} \\ V_{ramp}, \quad T_{1R} < t < T_{2R} \\ 0, \quad T_{2R} < t \end{cases} \tag{2.11}$$

Where

$$V_{ramp} = (MAXR)\left[1 - (t - T_{2R})/(T_{1R} - T_{2R})\right] \tag{2.12}$$

$MAXR$ is the ramp maximum, T_{1R} the ramp start time, T_{2R} the ramp maximum time. The values of MAXR are, respectively, selected to be 3 and 7.5 when $200s < t < 201s$ and $250s < t < 251s$ during the simulations. The noise wind-speed component can be expressed by :

$$V_{WN} = 2\sum_{i=1}^{N} \sqrt{S_V(w_i)\Delta w}\cos(w_i t + \varphi_i) \tag{2.13}$$

probability density on the interval $[0 - 2\pi]$, and where $w_1 = (i - 1/2)\Delta w$, φ_i a random variable with uniform

$$S_V(w_i) = \frac{2K_N F^2 |w_i|}{\pi^2 \left[1 + (Fw_i/\mu\pi)^2\right]^{4/3}} \tag{2.14}$$

is the spectral density function, $K_N(= 0.004)$ the surface drag coefficient, $F(= 2000)$ the turbulence scale, and μ the mean wind speed at reference height of $7.5, 4.5$ and $15m$, respectively. Various studies use $N = 50$ and $\Delta w = 0.5 - 2.0\ rad/s$ to obtain excellent results. According to the aforementioned four wind-speed components, the employed wind-speed model is defined by :

$$V_W = V_{WB} + V_{WG} + V_{WR} + V_{WN} \tag{2.15}$$

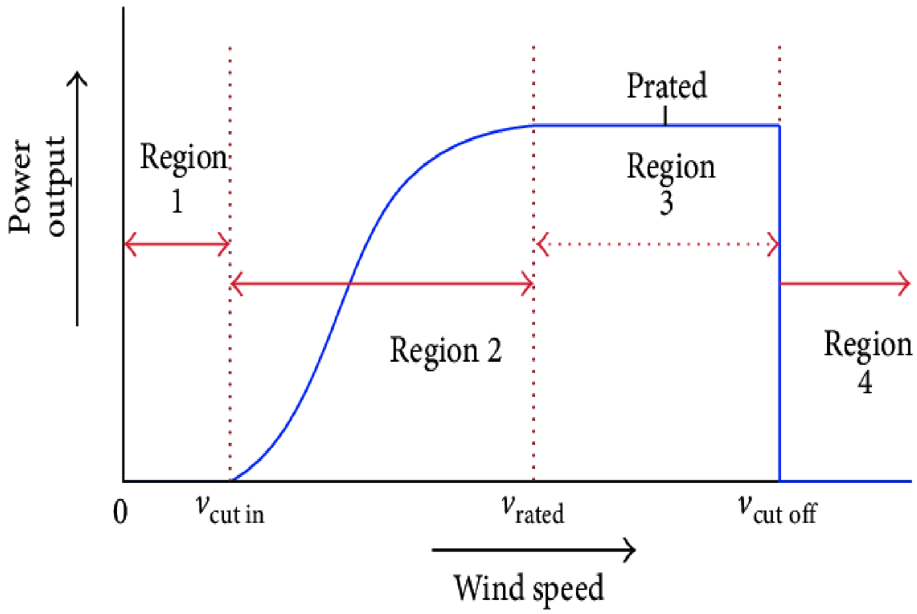

FIGURE 2.6 – The characteristic curve of output mechanical power versus wind speed of the studied WTGs.

2.2.6 Model Wind Turbine Generator 's Output

The turbine is composed of a directly coupled with a squirrel cage induction generator through a gearbox. The turbine rotor model provides the aerodynamic power extracted from the wind by the following equation Due to uncertainty in wind speed, the output of WTG is highly fluctuating in nature. The output power of the wind turbine generators is dependent on wind speed. The mechanical power of the wind turbine was provided in Eq 2.16 [58].

$$P_W = \frac{1}{2}.\rho.A_r.C_p.V_W^3 \tag{2.16}$$

Where ρ , A_r and C_P represent air density, the effective surface area of the blades, and power coefficient respectively as a function of the tip speed ratio of a blade. ρ and A_r parameters in Eq 2.16 were considered to be $1/25Kgm^3$ and $1735m^2$ respectively. The value of C_P in Eq 2.16 can be obtained by Eq 2.17 [57]

$$C_p = (0.44 - 0.0167\beta)\left[\frac{\pi(\lambda-3)}{15-0.3\beta}\right] - 0.0184(\lambda-3)\beta \tag{2.17}$$

The value of λ in Eq 2.17 can be obtained

$$\lambda = \frac{R_{blade}w_{blade}}{V_W} \tag{2.18}$$

The value of R_{blade} is the blade radius and w_{blade} is the blade rotational speed in Eq 2.18 which were considered $23.5m$ and $3.14rads$ respectively. The comparison between the output power of wind turbine generators and wind speed has been illustrated in Figure 2.6. This figure shows while wind speed was more than a certain limit, the output power will remain the same. In this study, when wind speed was more than $25m/s$ the system will fail because of the security of its initial tools. Also when wind speed was more than $15m/s$ output power of wind turbine generators was fixed at the peak. When wind speed was less than $4m/s$, the output power of wind turbine generators was fixed to zero. generators was fixed to zero.
The transfer function of wind turbine generators which was shown in Figure 2.6 is stated in Eq 2.19 [59]

$$G_{WTGk}(s) = \frac{\Delta P_{WTGk}}{\Delta P_W} = \frac{K_{WTG}}{1 + s.T_{WTG}}, \qquad \text{k=1,2,3} \tag{2.19}$$

Where K_{WTG} indicates the gain of the WTG array ; T_{WTG} indicates the time constant of WTG array including converter time delay also.

2.3 Modeling of conventional sources

In this section, the conventional sources like Diesel Engine Generator and Fuel Cell are modeled in frequency domain analysis by a first transfer function.

2.3.1 Modeling of Fuel Cell System

A fuel cell is a static electrochemical device that converts chemical energy into electrical energy through an electrochemical reaction. Fuel cells utilize hydrogen as fuel and oxygen as the oxidant in the reaction and its by-products are water and heat. As fuel cells do not have any moving parts, their efficiency is high when compared to conventional combustion engines [60].
For frequency analysis, the fuel cell is considered as one of the suitable energy generations. It can be modeled by a transfer function in first-order.
The fuel cell has recently highlighted as it maintains to provide an efficiency performance of the power generation system by reducing the greenhouse. It comes with many advantages such as a more efficient, simple structure and negligible emission

which make it a suitable distributed generation system in microgrid applications [61]. Power is produced in a fuel cell with the help of an electrochemical reaction between hydrogen and oxygen. The benefits of using fuel cells over conventional generators (like diesel generators) are that the energy produced is very pure and free from pollution. Usually, a fuel cell generates a very small voltage which is not sufficient to meet our needs. To create large enough voltage, the cells are arranged in a series-parallel combination to make a fuel cell stack. Hydrogen, which helps in power generation in the fuel cell, is an expensive source as compared to other conventional energy sources. This is the only drawback of the fuel cell. Normally a fuel cell generator has a higher-order model and also non-linearity. However, during low-frequency domain analysis, we can consider it to have a first-order lag transfer function model given [62] and implemented in the DGS model as a fellow.

$$G_{FCk}(s) = \frac{\Delta P_{FCk}}{\Delta P_{AE}} = \frac{K_{FC}}{1 + s.T_{FC}}, \qquad \text{k=1,2} \tag{2.20}$$

2.3.2 Modeling of Diesel Engine Generator

A standby generator consists of an engine-driven generator that is used to provide auxiliary power during solar blackouts or when the battery power discharge reaches a minimum level. The output of the diesel generator is connected to the auxiliary input of the inverter and engines that drive the motors to operate with gasoline, diesel, natural gas, propane, or any type of fuel. Because of the intermittent nature of renewable sources, the use of DEG in the hybrid system becomes more required to produce the demand power. It works as a secondary source. The diesel engine generator can be presented by a first-order transfer function. Load demand can be followed by the Diesel generator using its governor control and speed droop. The governor maintains the fuel input to an engine through a valve mechanism. The engine works like a turbine and moves the synchronous generator. The governor of the diesel generator can be modeled with a first-order transfer function [63, 64], as depicted.

$$G_{DEG}(s) = \frac{\Delta P_{DEG}}{\Delta f} = \frac{K_{DEG}}{1 + s.T_{DEG}} \tag{2.21}$$

2.4 Energy storage system modeling

This section presents different models of energy storage systems used in this thesis like Battery, Flywheel, Ultracapacitor, and Aqua electrolyzer which is modeled in the first-order model for the frequency analysis and control implementation.

2.4.1 Battery Energy Storage model

The big challenge faces energy is the storage operation. The energy storage devices are widely used to store the surplus of power from renewable sources to release it later when there is an imbalance between the demand and the generation. These are of benefit in any power system but in an islanded system where very high penetration levels may be required, an ES becomes more critical. The most energy storage components are Battery, which presents a more efficient and suitable component in microgrid applications. The energy storage is ready to assume a key part in the incorporation of renewable energy (RE) based power generation into the electricity grid. Exceptionally compelling is the utilization of energy storage to help with the successful and dependable reconciliation of RE-based generation whose yield is variable, essentially wind and sun-powered and conceivably including sea wave and tidal energy generation. A few main key terms include [65].
1– Output variability.
2– A transient (time-related) befuddle among generation and power requirement and
3– Undesirable electrical impacts created by RE-based generation.
The solar radiation and wind speed are fluctuating intermittently and in order to provide the stability of power system supplementary energy sources are required. Energy storage systems are usually used as supporting or backup power system. The energy storage system (ESS) can provide a big advantages to the electrical system, to power end-clients, and society overall [66]. There are five wide application/use classifications can summarise the variety of ESS such as :

- Charging and discharging cycle based on time.
- Worked with grid connexion.
- Grid infrastructure Reduction.

- Benefits to clients.
- Integration with renewable energy generation, and others.

There is often a limited need for electricity at night and there is usually more supply than there is a need. At those times, the cost to produce electricity and the price for that electricity is relatively low. Conversely, during weekdays, especially summer weekdays, there is high use of electric energy and as are the cost to generate and the price to acquire the electric energy. The second electric supply benefitelectric supply capacityis related to a reduced need for electricity generation equipment. Quite simply, if storage use limits the need to install new generation capacity then the benefit from storage is the avoided or reduced cost associated with building and owning that generation equipment. In the evening, there is normally a restricted requirement for power and there is regularly more supply than need. At those times, the expense to produce power and the generation cost are generally low. On the other hand, during weekdays, particularly summer weekdays, the utilization of electrical energy is high and the generation cost and the cost to buy the electric energy are high. This battery can be modeled by a first-order transfer function.

$$G_{BESS}(s) = \frac{K_{BESS}}{1 + s.T_{BESS}} = \frac{\Delta P_{BESS}}{\Delta f} \tag{2.22}$$

2.4.2 Flywheel energy storage system model

In flywheels (FES) or kinetic energy storage systems (KESS) the electric power is stored as kinetic energy. The maximum stored energy is limited by the tensile strength of the flywheel material. High-speed flywheels can be operated up to about $40,000 rpm$ and low-speed flywheels around $7000 rpm$. By adopting superconducting magnetic bearings very high overall efficiency, exceeding 90% is obtained. The flywheel can be modeled by a first-order transfer function [67].

$$G_{FESS}(s) = \frac{K_{FESS}}{1 + s.T_{FESS}} = \frac{\Delta P_{FESS}}{\Delta f} \tag{2.23}$$

2.4.3 Ultra capacitor system modeling

The ultra-capacitor system is made up of two conducting electrodes, an aqueous electrolyte solution, and a porous membrane separator [67]. This structure is responsible for imparting characteristics of both conventional capacitors and electrochemical-based battery to the ultra-capacitor. Long cycle duration, reaching approximately 105 cycles with a high efficiency ranging between 84 and 97%, are some of its features. The major drawback associated with this storage technology is the high capital cost and high discharge rate varying from 5 to 40% [68]. This technology is suited for applications that require high bursts of power for the short term. Large-scale power systems do not prefer employing this technology. Recent developments and active research in this field have vastly improved this technology [67].

$$G_{UC}(s) = \frac{K_{UC}}{1 + s.T_{UC}} = \frac{\Delta P_{UC}}{\Delta f} \tag{2.24}$$

2.4.4 Modeling of Aqua Electrolyzer

To solve this problem we use an aqua electrolyzer that produces hydrogen. Hydrogen is produced in the aqua electrolyzer by the method of electrolysis of water for which electric current is obtained from the power system. The transfer function model of the aqua electrolyzer is presented by the transfer function shown bellow [69].

$$G_{AE}(s) = \frac{K_{AE}}{1 + s.T_{AE}} = \frac{\Delta P_{AE}}{P_{WTG}(1 - K_n)} \text{or} \frac{\Delta P_{PV}}{P_{WTG}(1 - K_n)} \tag{2.25}$$

2.5 Frequency Response Model and AGC Characteristics

In an interconnected power system, the control area concept needs to be used for the sake of synthesis and analysis of the AGC system. The control area is a sound area composing of a group of generators and loads, where all the generators respond to changes in wind speed, solar radiation and in load simultaneously. The frequency deviation is required to be the same in all points of each control area. A multi area power system comprises areas that are interconnected by high-voltage transmission lines or tie-lines. The AGC system in an interconnected power system should control the area frequency as well as the interchange power with the other control areas [70,71]. An appropriate frequency response model for a control area in a multi area power system is shown. In AGC practice, to clear the fast changes and probably added noises, system frequency gradient and ACE signals must be filtered before being used.

If the ACE signal exceeds a threshold at interval TW, it will be introduced to the controller block. The controller can be operated to send higher/lower pulses to the participant generation units if its input ACE signal exceeds standard limits. Delays ramping rate, and range limits are different for various generation units. Concerning the limit on generation, governor dead-band, and time delays, the AGC model becomes highly nonlinear ; hence, it will be difficult to use the conventional linear techniques for performance optimization and conňtrol design [72].

2.5.1 Droop Characteristic

The ratio of speed (frequency) change Δf to change in output-generated power ΔP_g is known as droop or speed regulation and can be expressed as

$$R\,(Hz/pu.MW) = \frac{\Delta f}{\Delta P_g} \tag{2.26}$$

For example, a 5% drop means that a 5% deviation in nominal frequency (from 60 to 57 Hz) causes a 100% change in output power. The interconnected generating units with dierent droop characteristics can jointly track the load change to restore the nominal system frequency. The change in the network load causes the units to decrease their speed, and the governors increase the outputs until they reach a new common operating frequency. As expressed in Eq 2.26, the amount of produced power by each generating unit to compensate the network load change depends on the units droop characteristic [73]

$$\Delta P_{gi} = \frac{\Delta f}{R_i} \tag{2.27}$$

2.5.2 Generation-Load Model

For AGC synthesis and analysis in the presence of load disturbances, a simple, low-order linearized model is commonly used. The overall generation-load dynamic relationship between the incremenňtal mismatch power ($\Delta P_m \Delta P_L$) and the frequency deviation (Δf) can be expressed as Eq 2.28 [22]

$$\Delta P_m(t)\Delta P_L(t) = 2H\frac{\Delta f(t)}{dt} + D\Delta f(t) \tag{2.28}$$

where (ΔP_m) is the mechanical power change, (ΔP_L) is the load change, H is the inertia constant, and D is the load damping coefficient. Using the Laplace transform, Equation can be written as [74]

$$\Delta P_m(s)\Delta P_L(s) = 2Hs\Delta f(s) + D\Delta f(s) \tag{2.29}$$

Eq 2.29 is represented on the right-hand side of the frequency response model.

2.5.3 Fundamental Frequency Control Loops

The frequency of a power system is depended on real power balance. A change in real power demand of the microgrid system is reflected throughout the system by a fluctuation in frequency. Therefore, system frequency provides a useful tool to indicate microgrid system generation and load imbalance. The control of microgrid based on the frequency regulation. Any short term energy imbalance causes by renewable intermittent nature and loads disturbances will result in instantaneous deviations in microgrid system frequency. A significant sudden change in generation power without adequate control can provoke extreme fluctuation in microgrid frequency which results in important problems such as instability and security issues. Therefore these are the major challenges to integrate renewable energy sources in microgrid design. The control of frequency and power generation is commonly indicated as loadfrequency control (LFC) which is one of the major functions of automatic generation control (AGC) systems. It is used in system control based on conventional generation units. With the microgrid based renewable generation units, anothers controlling strategies are necessary to be employed [75].

2.5.4 Power and Frequency Responses Modelling

Power systems have a highly non-linear and time-varying nature. However, for frequency control synthesis and analysis in the presence of renewable sources and loads disturbances, a simple low-order linearized model is used and sufficient in the time-domain analysis. In comparison with voltage and rotor angle dynamics, the dynamics affecting frequency response are relatively slow, in the range of seconds to minutes what justified by the use of a small-signal model for frequency response analysis.
In a power system comprising of a synchronous generator, if the balance between the generation and load demand is not maintained, the frequency deviates based on the domination of generation or load [76,77]. The power deviation is the difference between

the power generation PG and the power demand P_L. To maintain a stable operation of the autonomous system, the power-frequency balance must be maintained. It can be achieved by the proper control of various components in the hybrid system. The power mismatch is given by [44]

$$\Delta P_l = \Delta P_g^* - \Delta P_g \tag{2.30}$$

$$P_g = P_{WTC} + P_{DEG} + P_{FC} - P_{FC} \pm P_{FESS} \pm P_{BESS} \tag{2.31}$$

$$P_g = P_{PV} + P_{DEG} + P_{FC} - P_{FC} \pm P_{FESS} \pm P_{BESS} \tag{2.32}$$

$$P_g = \left(\sum_{i=1}^{3} P_{WTGi} \right) + P_{DEG} \pm P_{FESS} \qquad \text{when} \qquad t \geq t_i \tag{2.33}$$

$$P_g = P_t + P_{DEG} + P_{FC} \pm P_{FESS} \pm P_{BESS} \tag{2.34}$$

$$P_t = P_{WTG} - P_{AE} = \sum_{i=1}^{3} P_{WTGi} - P_{AE} = K_n P_{WTG} \tag{2.35}$$

$$P_t = P_{PV} - P_{AE} = K_n P_{PV} \tag{2.36}$$

$$\Delta f = \frac{\Delta P_l}{K_{sys}} \tag{2.37}$$

$$G_{sys} = \frac{\Delta f}{\Delta P_l} = \frac{1}{K_{sys}(1 + s.T_{sys})} = \frac{1}{D + M.s} \tag{2.38}$$

Where M and D are, respectively, the equivalent inertia constant and damping constant of the hybrid power system.

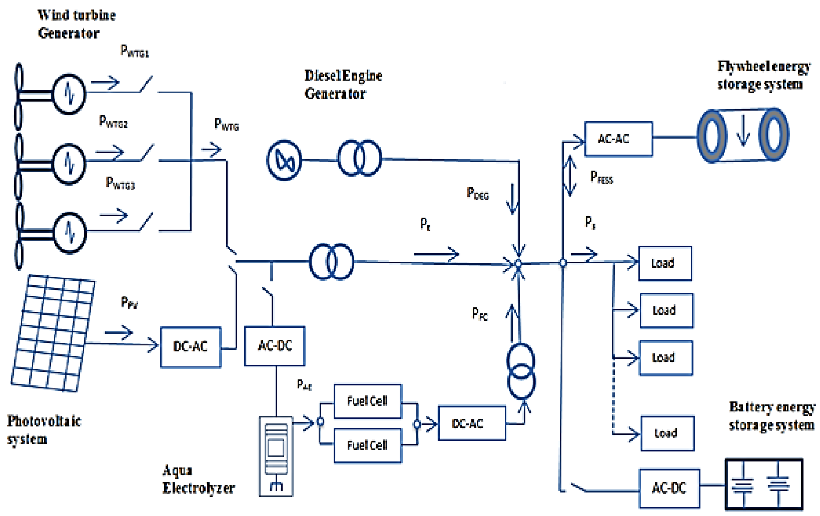

FIGURE 2.7 – Schematic of microgrid generation with storage devices.

TABLE 2.1 – Parameters of the proposed Microgrid system.

Component	**Gain (K)**	**Time constant (T)**
Wind Turbine Generator	$K_{WTG} = 1$	$T_{WTG} = 1.5$
Photovoltaic Generator	$K_{SPV} = 1$	$T_{PV} = 1.8$
Fuel Cell (FC)	$K_{FC} = 0.01$	$T_{FC} = 4$
Diesel Engine Generator	$K_{DEG} = 0.003$	$T_{DEG} = 2$
Battery Energy Storage System	$K_{BESS} = -0.003$	$T_{BESS} = 0.1$
Flywheel Energy Storage System	$K_{FESS} = -0.01$	$T_{FESS} = 0.1$
Aqua Electrolyser (AE)	$K_{AE} = 0.002$ $T_{AE} = 0.5$	$K_n = 0.6$

2.5.5 Primary Frequency Control

The primary frequency control is a local automatic control aiming to match the balance of the active power to counteract the frequency deviations. It operates both on the active power supplied by rotating generators and on the consumption of controllable loads. Its role is crucial for the stability of the power system to stabilize the frequency in case of load outage or a large generation. All the generators that are located in a synchronous zone are fitted with a speed governor which performs this control automatically. The demand side also participates in this control by the self-regulating effect of frequency-sensitive loads such as induction motors [48,49] or connecting/disconnecting some load by the action of frequency-sensitive relays set-up with a given frequency threshold. The action of the primary frequency control is subject to some constraints. First of all, an increase of the delivered energy to face the frequency drop can be maintained only for a relatively short time and must be replaced before it runs out. Secondly, this increase of power should be distributed across the network to minimize the power transit and to enhance the security of the system in particular for a large generation outage. Finally, the uniform repartition helps the stability of islanded systems in case of a power system separation [77].

2.5.6 Secondary Frequency Control

The secondary frequency control aims to bring the frequency back to the target value. It is a centralized automatic control as well. Whereas the primary frequency control limits the frequency deviations, the secondary frequency control adjusts the power production of the generating units located in the area of imbalance. Usually, the loads do not participate in this control. The secondary frequency control is not indispensable ; some power systems prefer to regulate the frequency by the primary frequency control and the manual tertiary frequency control. Anyway, it is adopted in all large interconnected systems since the manual action could be not sufficient to quickly remove overloads [44].

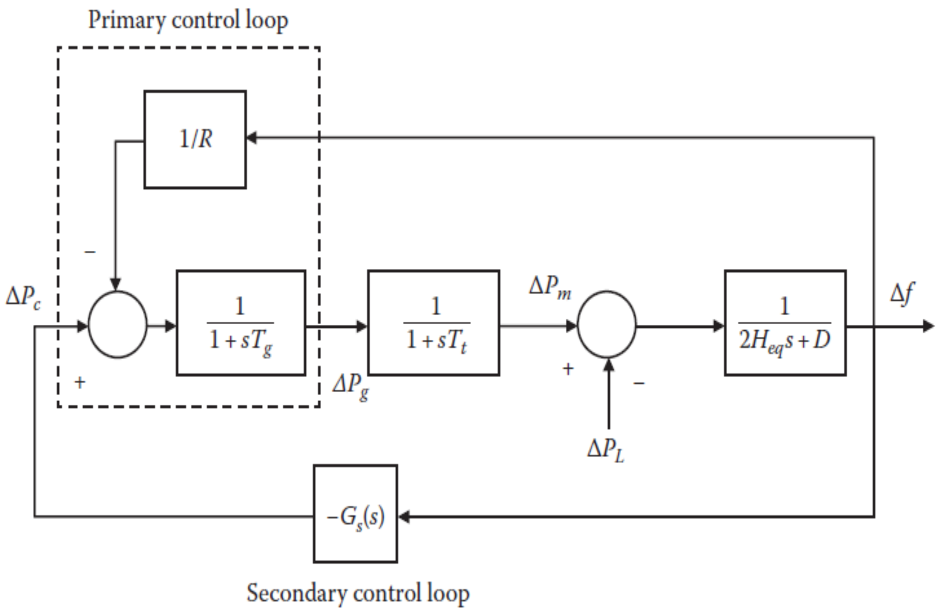

FIGURE 2.8 – Block diagram of an isolated area equipped with primary and secondary controls.

2.6 Conclusion

This chapter summarizes the different models of all microgrid components mostly used. The microgrid is composed of renewable sources like PV system and wind turbine generator with conventional sources such as Fuel cell and diesel engine generator along with storage devices such as the battery, Flywheel, and ultracapacitor energy storage devices and Aqua electrolyzer for storing the hydrogen used by fuel cell as a fossil. All the components are presented by first-order transfer function to facilitate the frequency analysis in the small-signal model and implement different control strategies.

CHAPTER 3 Performance improvements of microgrid system using fractional controllers

3.1 Introduction

In this chapter, we will define some important notions of the PID and Fractional order PID controllers used for microgrid control improvement. It also discusses various optimization methods applied for the controller parameter tuning. The metaheuristics algorithm like genetic algorithm, Particle Swarm Algorithm and Krill Herd Algorithm are presented its principal, concepts, characteristics and application. An overview of these three optimization techniques is surmised in this chapter. These techniques are used to tune the parameters of the two proposed controllers. The results of microgrid frequency control using a PID controller and FOPID controller based PSO, GA and KH are shown and analyzed in this chapter.

3.2 Proposed microgrid concept

The schematic of the proposed microgrid system using various renewable energy generation and storage units is displayed in Figure 2.7 For small-signal analysis, the transfer functions of energy generation and storage devices are presented by first-order transfer functions with the associated gains and time constants shown in the table. The model is considered for analysis and demonstration of frequency behavior which requires an effective control scheme to improve the system performances and stability [53–57].

3.3 Problem formulation

To obtain good performance monitoring frequency of a microgrid, the variation of frequency f and the change of the control signal (Δu) to the output of the PID and FOPID controllers should be minimized. Proportional-integral-Derivative (PID) plays an important role in industrial processes that have since been introduced. Many control systems use the PID controller for its simplicity and it is proved satisfactory. He still has a wide application in industrial control [78]. The proposed FOPID controller is a generation of the classical PID controller and have has five parameters ($KP, KI, KD, \lambda \quad and \quad \mu$) that must now be optimized to adjust system control laws while maintaining some control objectives incorporated as performance indices in the time domain. In this study, the integral performance index (J) to minimize by appropriate genetic algorithms is the weighted sum of ISTSE (Integral of Squared Time Squared Error Multiplied) And ISDCO (Integral of Squared Deviation of the Output Controller) Given as follows [55].

$$J_{opt} = \int_{T_{min}}^{T_{max}} \left[w\left(\Delta f\right)^2 + \left(\frac{1-w}{Kn}\right)\left(\Delta u\right)^2 \right] dt \tag{3.1}$$

Where w represents the importance of Integral square error (ISE) of frequency deviation and the Integral of Squared Deviation of Control Signal, it is taken as 0.7. $Kn = 10^4$ is the normalizing constant of the proposed objective function.

3.4 PID controller structure

A proportional-integral-derivative controller (PID controller) is considered as a control loop feedback mechanism scheme largely employed in industrial control systems. A PID controller calculates an error value as the difference between a measured process variable and the desired set point. The controller attempts to minimize the error by adjusting the process through the use of a manipulated variable [78].

The PID controller consists of three separate constant parameters, and is accordingly sometimes called three-term control : the proportional, the integral, and derivative values, designated P, I, and D. Simply put, these values can be explained in terms of time : P depends on the present error, I on the accumulation of past errors, and D is

a prediction of future errors, depended on the current rate of change. The weighted sum of these three actions is used to adapt the process via a control element such as the position of a control valve, a damper, or the power supplied to a heating element. In the absence of knowledge about the underlying process, a PID controller has historically been considered to be the most useful controller. By tuning the three parameters of the PID, the controller can assign control action designed for specific process requirements. The response of the controller can be described in terms of the responsiveness of the controller to an error, the degree to which the controller overshoots the set point, and the degree of system oscillation. Note that the use of the PID algorithm for control does not guarantee optimal control of the system or system stability.
Some applications may require using only one or two actions to provide the appropriate system control. This is achieved by setting the other parameters to zero. A PID controller will be called a PI, PD, P, or I controller in the absence of the respective control actions. PI controllers are fairly common, since derivative action is sensitive to measurement noise, whereas the absence of an integral term may prevent the system from reaching its target value due to the control action.
A standard PID (Proportional Integral Derivative) control is the most simple often type used today in the industry. PID controllers are being extensively used by industries today due to their simplicity. Many control systems using PID control have proved satisfactory. It has a wide range of applications in industrial control. PID controller still has been found possible to set satisfactory controller parameters for the stability of the industrial system. Whose transfer function is generally written in the parallel form given by Eq 3.2 or the ideal form given by Eq 3.2 [10], [67], [79, 80] :

$$G(S) = K_p + K_I \frac{1}{S} + K_D S \tag{3.2}$$

$$= K_p \left(1 + \frac{1}{T_I S} + T_D S \right) \tag{3.3}$$

Where K_p is the proportional gain, K_I the integral gain, K_D the derivative gains, K_I the integral time constant and, T_D is the derivative time constant.
PID control consists of three types of control, Proportional, Integral, and Derivative control.

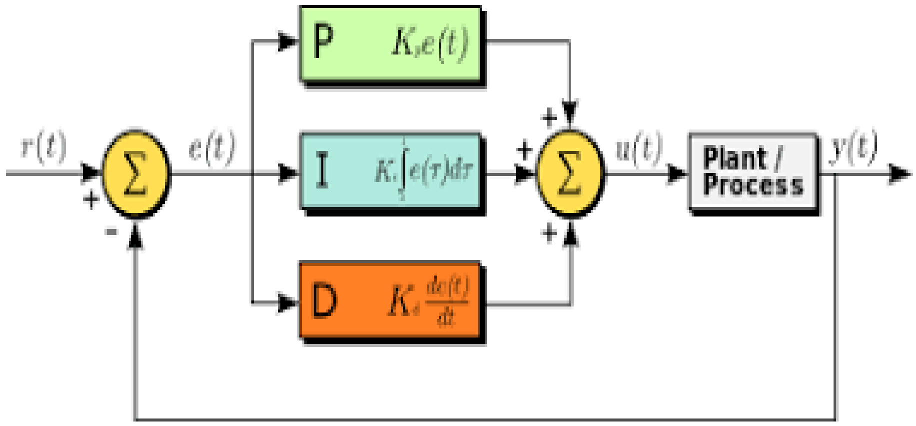

Figure 3.1 – Block of PID controller model.

– The proportional term providing an overall control action proportional to the error signal through the all-pass gain factor.

– The integral term reducing steady-state errors through low-frequency compensation by an integrator.

– The derivative term improving transient response through high-frequency compensation by a differentiator.

3.5 Fractional Order PID Controller

Maybe the first sign of the potential of FOC, though without using the term fractional, emerged with Bode [80,81]. A key problem in the design of a feedback amplifier was to devise a feedback loop so that the performance of the closed-loop is invariant to changes in the amplifier gain. Bode presented an elegant solution to this robust design problem, which he called the ideal cut-off characteristic, nowadays known as Bodes ideal loop transfer function, whose Nyquist plot is a straight line through the origin giving a phase margin invariant to gain changes. This ideal system is, from our point of view, a fractional-order integrator with transfer function $G(s) = (cg/s)\alpha$ known as Bodes ideal transfer function, where cg is the gain crossover frequency and the constant phase margin is $\phi_m = \pi - \alpha\frac{\pi}{2}$. This frequency characteristic is very interesting in terms of the robustness of the system to parameter changes or uncertainties and several design methods have made use of it. In fact, fractional-order integrators can be designed as an alternative reference system for control [55].

This first step towards the application of fractional calculus in controlled to the adaptation of the FC concepts to frequency-based methods.
The frequency response and the transient response of the non-integer-order integral (in fact Bodes loop ideal transfer function) and its application to control systems were introduced by Manabe [59] and more recently.

3.5.1 Fractional Order Calculus

In fractional Order calculus the fundamental differ-integration operator (where a and t are the limit of the operation) is defined as :

$$ {}_aD_t^{\lambda} = \begin{cases} \frac{d^{\lambda}}{dt^{\lambda}} & \lambda > 0 \\ 1 & \lambda = 0 \\ \int_a^t (d\tau)^{\lambda} & \lambda < 0 \end{cases} \tag{3.4} $$

Where λ is the order of the operation generally $\lambda \in R$ but λ could also a complex number.
Some popular definitions of fractional differ-integration in fractional order calculus are :
Definition 1*(Grunwald Letnikov)*

$$ {}_aD_t^{\lambda} = \lim_{h \to 0} \frac{1}{h\lambda} \sum_{j=0}^{\left[\frac{t-a}{h}\right]} (-1)^j \binom{\lambda}{j} f(t - jh) \tag{3.5} $$

$\left[\frac{t-a}{h}\right]$ truncates $(t-a)/h$ to an integer
Definition 2*(Rieman Liouville)*

$$ {}_aD_t^{\lambda} = \frac{1}{\Gamma(h-\lambda)} \left(\frac{d}{dt}\right)^n \int_a^t \frac{f(\tau)}{(t-\tau)^{\lambda-n+1}} d\tau \tag{3.6} $$

$n - 1 \leq \lambda < n$ where n is an integer and a is a real number.
Definition 3*(Caputo)*

$$ {}_aD_t^{\lambda} f(t) = \frac{1}{\Gamma(h-\lambda)} \int_a^t \frac{f(\tau)^{(n)}}{(t-\tau)^{\lambda-n+1}} d\tau \tag{3.7} $$

3.5.2 The fractional Order transfer function

A linear time-invariant fractional model of a system with input u and output y takes the following form :

$$a_n D^{\lambda_n} y(t) + a_{n-1} D^{\lambda_{n-1}} y(t) + ... + a_0 D^{\lambda_0} y(t) = b_n D^{\mu_m} u(t) + b_{m-1} D^{\mu_{m-1}} u(t) + ... + b_0 D^{\mu_0} u(t) \quad (3.8)$$

Where $a_i(i = 0......n), \lambda_i(i = 0.......n), b_k(k = 0.......m), u_k(k = 0.......m)$. The Laplace transform of the fractional-order operator for zero initial conditions is

$$L({}_aD_t^{\lambda} f(t)) = S^{\lambda} F(s) \quad (3.9)$$

Therefore, the Laplace transform on both sides of Eq 3.8 for zero initial conditions leads to the following transfer function :

$$\frac{Y(s)}{U(s)} = \frac{b_n S^{\mu_m} + b_{m-1} S^{\mu_{m-1}} + ... + b_0 S^{\mu_0}}{a_n S^{\lambda_n} + a_{n-1} S^{\lambda_{n-1}} + ... + a_0 S^{\lambda_0}} \quad (3.10)$$

3.5.3 Approximation of Fractional-Order Operators

The Oustaloup recursive filter, gives a very good approximation of fractional operators in a specified frequency range. It is a well-established method and is often used for practical implementation of fractional-order systems and controllers. It is summarized next.

In order to approximate a fractional differentiator of order α or a fractional integrator of order (λ) by a conventional transfer function one may compute the zeros and poles of the latter using the following equations :

$$s^{\alpha} \approx K \prod_{k=1}^{N} \frac{s + w'_k}{s + w_k} \quad (3.11)$$

where

$$w'_k = w_b . w_u^{(2k-1-\alpha)/N}$$

$$w_k = w_b . w_u^{(2k-1+\alpha)/N}$$

$$K = w_h^{\alpha} \quad , w_u = \sqrt{w_h / w_b}$$

and N is the order of approximation in the valid frequency range $(w_b; w_h)$.

3.5.4 Fractional-order controllers

From the control engineering point of view, the application of fractional order calculus can be in either system modeling or control design. The typical fractional order controller (C(s)) found in the literature [60].

1– Fractional order proportional-integral- controller

PI^{λ}

$$C(s) = K_p\left(1 + \frac{K_i}{s^{\lambda}}\right) \tag{3.12}$$

$[PI]^{\lambda}$

$$C(s) = K_p\left(1 + \frac{Ks}{s}\right)^{\lambda} \tag{3.13}$$

2– Fractional order proportional- derivative

PD^{μ}

$$C(s) = K_p\left(1 + Ks^{\mu}\right) \tag{3.14}$$

$[PD]^{\mu}$

$$C(s) = K_p\left(1 + Ks\right)^{\mu} \tag{3.15}$$

3.5.5 Fractional Order Proportional- Integral- Derivative controller

PID controller is a specific control loop feedback technic generally used in the industrial control system [80] , [82]. The PID controller consists to correct the error between a measured process variable and the desired set point. The PID controller can be explained that the classical PID controller is improved by adding fractional action to the derivative and integral actions. Two additional parameters with more specifications can be met, thus can enhance the performance of the system and could lead to more robust control performances, more adequate modeling and adds more flexibility to controller design. We can control our real-world processes more accurately [9]. The FOPID controller has three parameters similar to the PID controller along with the two additional parameters namely; the integral order λ, and the differential order μ. In the past decades, some fractional-order controllers have been studied, such as PI^{λ} , PD^{μ} and $PI^{\lambda}D^{\mu}$. The most common form of a fractional-order PID controller is the $PI^{\lambda}D^{\mu}$ controller, which includes an integrator of order λ and a differentiator of order μ, where $\lambda \in (0,2)$ and $\mu \in (0,2)$. Not only the PID controller can be used to control fractional-order systems, but it can also be applied to the control of integer-order systems. A block diagram of the fractional-order $PI^{\lambda}D^{\mu}$ control system is given in Figure 3.2 [54–56].The model in the Laplace domain of $PI^{\lambda}D^{\mu}$ the controller is given by :

$$C(s) = K_p + K_I s^{-\lambda} + K_D s^{\mu} \qquad \lambda, \mu \in R^{+} \tag{3.16}$$

Where C(S) is controller output, K_p is proportional constant gain, K_I is integration constant gain, K_D is derivative constant gain, λ is Order of integration μ is the Order of differentiators.When taking $\lambda = \mu = 1$ the result is the classical PID controller.

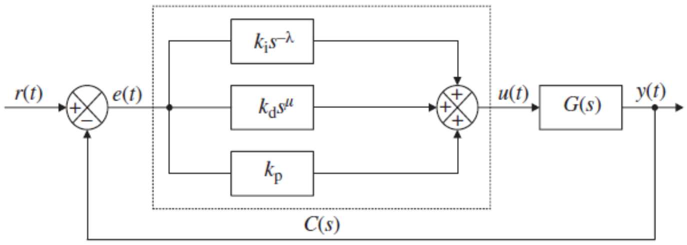

FIGURE 3.2 – Fractional order PID controller.

Applying Laplace transform to this equation with null initial conditions, the transfer function of the controller can be expressed by :

$$C(s) = K_p + K_I s^{-\lambda} + K_D s^{\mu} = K \frac{(\frac{s}{w_f})^{\lambda+\mu} + \frac{s\delta_f}{w_f} + 1}{s^{\lambda}} \tag{3.17}$$

Figure 3.2 Shows the frequency response of this controller for $k = 1$,$w_f = 1$, $\delta_f = 1$, and $\lambda = \mu = 0.5$

Frequency response of the fractional-order PID controller with $k = 1$,$w_f = 1$, $\delta_f = 1$, and $\lambda = \mu = 0.5$

As can be observed, this fractional-order controller allows us to select both the slope of the magnitude curve and the phase contributions at both high and low frequencies. Graphically, the control possibilities using a fractional-order PID controller are shown in Figure 3.3 , extending the four control points of the classical PID to the range of control points of the quarter-plane defined by selecting the values of λ and μ.

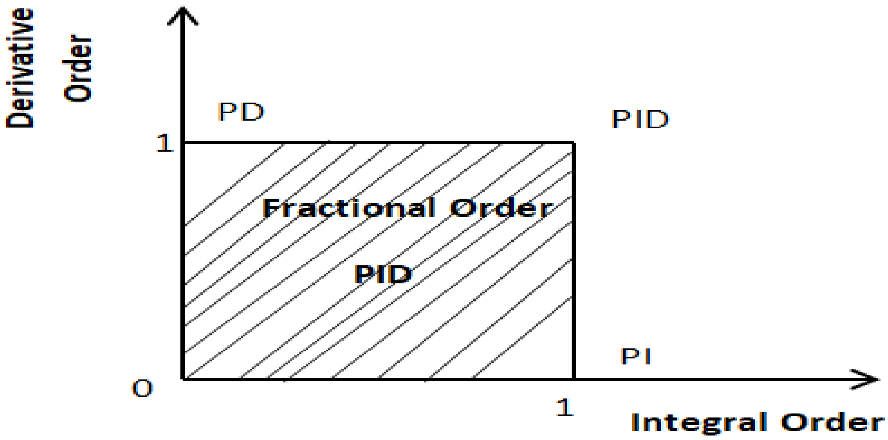

FIGURE 3.3 – Expanding from Point to Plane.

3.6 Overview of Metaheuristics Algorithm

In metaheuristics algorithms, meta- means higher level or beyond. Generally, they perform better than simple heuristics. All metaheuristics algorithms use some global exploration and tradeoff of local search. The variety of solutions is often found via randomization [32–35].

Metaheuristics algorithms can be classified in many ways. One way is to classify them as trajectory-based and population-based. For example, genetic programming (GP) and genetic algorithm (GA) are population-based as they use a set of strings, so in the particle swarm optimization (PSO) that multiple agents or particles are used. Then, simulated annealing (SA) uses a single solution that moves through the search space or design space, while artificial neural networks use a different approach.

Optimization and modeling may have a different emphasis, but for solving the real-world problems, we often have to use both optimization and modeling because optimization can achieve the optimal settings of design parameters while modeling makes the objective functions are evaluated using the correct numerical /mathematical model of the problem of interest. For optimization, optimization algorithms are the important part.......

Metaheuristics algorithms have become powerful methods for modeling and optimization. An overview has provided of nature-inspired metaheuristics algorithms and their applications. many algorithms such as genetic programming, genetic algorithms, fuzzy logic, differential evolution and the most important one are swarm-intelligence-based algorithms such as bee algorithms and ant, cuckoo search, particle swarm optimization, firefly algorithm, bat algorithm, and krill herd algorithm are introduced with their characteristics and some outline recent applications.

3.6.1 Genetic Algorithm

A genetic algorithm (GA) is a powerful and simple algorithm. It has been used successfully in the field of science, technology, and sociology, but it has some limitations. GA may require long processing time to get a near-optimum solution.Moreover, when it is applied to highly epistemic objective functions, there is a regression efficiency, the crossover and mutation operations cannot guarantee better fitness of offspring because chromosomes in the population have a similar structure and their average fitness are high toward the end of the evolutionary process. The scope is to compare the competence of GA with the conventional one [83–86].
Concept of the genetic algorithm can be described as a fellow [37]
Step1 : Creation of a population of initial parameters solutions. Each parameter called a nuisance. A chromosome consists of genes and thus each chromosome has a solution to the problem.
Step 2 : Evaluate the objective function (fitness) for each solution of individuals.
Step 3 : Remember the best solution for stopping rule verification. If so, finish.
Step 4 : Generation "offspring" : Offspring is a new chromosome obtained through the selection steps, crossover and mutation.
Step 5 : Putting people's products in the new population.
Step 6 : Replace the old population of individuals by the news.
Step 7 : Terminate the program when the termination criterion is reached ; otherwise go to step 2.
Figure 3.4 shows the flowchart of Genetic Algorithm :

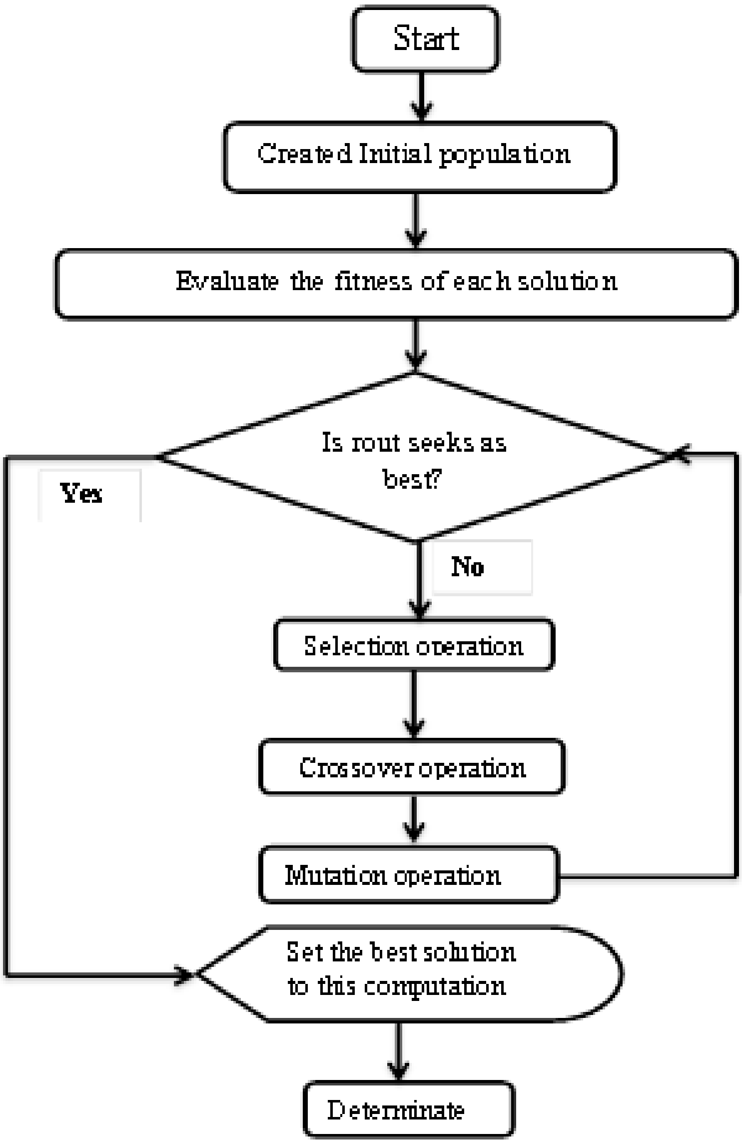

FIGURE 3.4 – Flowchart of Genetic Algorithm.

The parameters of Genetic Algorithms used in this thesis are as presented in Table 3.1.

TABLE 3.1 – Parameters of Genetic Algorithms (GA)

Parameters	**Values**
Population size	40
Number of variables	3 and 5
Mutation Probability	0.05
binary number Length	30
Iteration Number	100

3.6.2 Particule Swarn Optimisation Algorithm

Particle Swarm Optimization (PSO) is a technique used to explore the search space of certain problems to find the parameters or settings demanded to maximize a particular objective function. This latter, first described by James Kennedy and Russell C. Eberhart in 1995 arises from two separate theories [87] :
–The theory of swarm intelligence depended to the observation of swarming habits by certain kinds of animals (such as birds and fish)
– and the field of evolutionary computation.
Many problems have not an exact solution that gives the results in a reasonable time. For overcoming these problems some metaheuristics methods offer an approached solution after much iteration are recently proposed. Among these methods, the Particle Swarm Optimization algorithm has a general principle to be applied in many fields of optimization problems. PSO is a stochastic optimization algorithm developed by Eberhart and Kennedy, inspired by the social behaviour and fish schooling of bird flocking.Each particle in the swarm is a possible group of the unknown variables of the objective function to be optimized. The swarm consists of N particles moving around in a D-dimensional search space. Each particle is initialized with a random position and a random velocity [9]. The new velocity can be calculated by the fellow formula [62], [69].

$$V_{i+1} = w.V_i + C_1.r_1(P_{best} - X_i) + C_2.r_2(G_{best} - X_i) \tag{3.18}$$

$$X_{i+1} = X_i + V_{i+1} \tag{3.19}$$

Where V_i is the component in the dimension of the particle velocity in iteration, X_i is the component in the dimension of the particle position in iteration,C_1 and C_2 are constant weight factors, P_{best} is the best position achieved so far by particle, G_{best} is the best position found by the neighbours of the particle, and are random factors in between 0 and 1 interval, and w is inertia weight which is started from a positive initial value (w_0) and decreases during the iterations by $W_{(k+1)} = \beta.W_k$.
The first term . is called the inertia component ; it is responsible for keeping the particles search in the same direction. The low value of the inertia constant w accelerates the swarms convergence toward the optimum position, while the high value discovers the entire search space.

The second term $C_1.r_1(P_{best} - X_i)$ is called the cognitive component ; it represents the particles memory. The particle tends to return to the field of search space in which it has high individual fitness and the cognitive coefficient C_1 affects the step size of the particle to move toward its local best position P_{best}.
The third term $C_2.r_2(G_{best} - X_i)$ is called the social component ; it is responsible to move the particle toward the best region found by the swarm so far. The social coefficient C_2 affects the step size of the particle to find the global best position G_{best}.
According to Eq 3.19 , the position of each particle updates itself by using the new velocity and its previous position. In this case, a new search process starts over the updated search space to find the global optimum solution.
The algorithms of PSO can be described as follows :
Step1 : Initialize a population of particles with random positions and velocities on D-dimensions in the problem space.
Step2 : Evaluation of desired optimization fitness function in D variables for each particle.
Step3 : Comparison of particles fitness evaluated with its best previous position. If the present value is better, then place the best previous position equal to the current value, and pi equals to the current location xi in D dimensional space.
Step4 : Identifying the particle in the neighbourhood with the best fitness so far, and assign its index to the variable g.
Step5 : Change velocity and position of the particle according to Eq 3.18 and Eq 3.19.
Step6 : Return to step 2 until a criterion is met or end of iterations.
The flowchart of this algorithm is presented by Figure 3.6 as fellow :

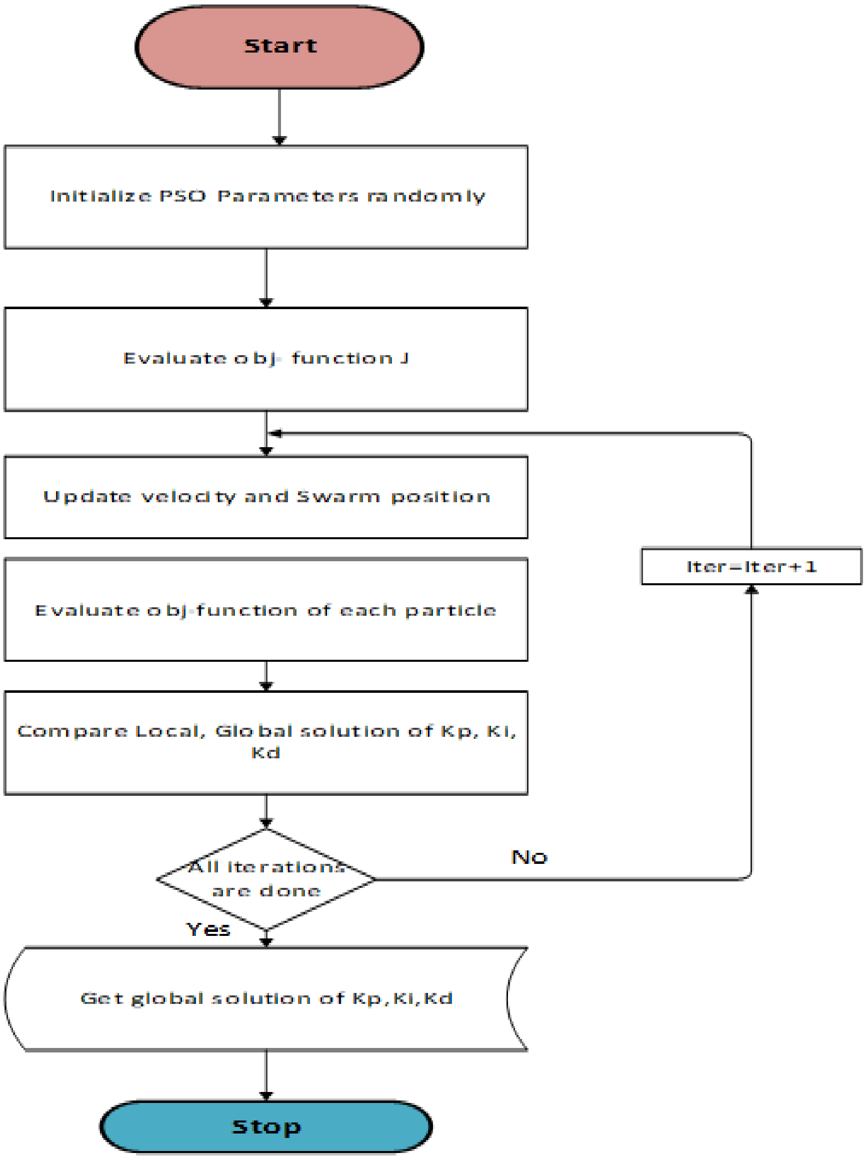

FIGURE 3.5 – Flowchart of PSO algorithm.

TABLE 3.2 – Parameters of Particle Swarm Optimization (PSO)

Parameter	**Values**
Population size	40
Number of variables	3 and 5
inertia weight	0.4
acceleration factors	2
Lower and upper bounds of variables	0 and 10
Iteration Number	100

The PSO is easy to be implemented with fewer parameters for tuning.
The PSO memory capability is more effective than the GA because each particle can remember its own previous best position and the neighborhood best too.
To maintain the diversity of the swarm The PSO is more efficient. This is because most successful information is used by the swarm to move toward the best which is similar to the community social behavior.

3.6.3 Krill Herd Algorithm

In this section, we discuss the definition, principle, and concept of the KH Algorithm.

3.6.3.1 Definition and principal of KH

Krill Herd (KH) algorithm is new bio-inspired swarm intelligence, it is based on herding conduct of krill and formulating their swarm movement [88].
The herding of the krill individuals is a multi-objective process including two main goals :
1– Increasing krill density.
2– Reaching food.
In krill herd, this process is taken into consideration to suggest a new metaheuristics algorithm for solving global optimization problems. The density-dependent attraction of finding food (areas of high food concentration) and krill (increasing density) are used as objectives that can finally lead the krill to herd around the global minima. In this process, an individual krill moves toward the best solution when it searches for the highest density and food [89].
The position of a krill in a 2D surface is determined by the following three actions :
1– Movement induced by other krill individuals.
2– Foraging activity.
3– Random diffusion.
Therefore, the following Lagrangian model is generalized to an n-dimensional decision space :

$$\frac{dX_i}{dt} = N_i + F_i + D_i \tag{3.20}$$

Where ; N_i is the movement induced by other krill. , F_i the is foraging movement. and D_i is the physical diffusion of ith krill. The direction of N_i which is called i is affected by local density and position of the best krill.
N_i is calculated with the following formula :

$$N_i^{new} = N^{max}\alpha_i + w_n N^{old} \tag{3.21}$$

Where N^{max} the maximum is induced speed, and α_i is defined as :

$$\alpha_i = \alpha^{local} + \alpha^{target} \tag{3.22}$$

w_n is the inertia weight of the motion induced in the range $[0, 1]$, N^{old} is the last motion-induced, α^{local} is the local effect provided by the neighbors and α^{target} is the target direction effect provided by the best krill individuals.
and Nmax is the maximum induced speed, $_n$ is the inertia weight of the motion induced in the range $[0, 1]$, Niold is the last motion-induced, (α^{ilocal}) is the local effect provided by the neighbors and itarget is the target direction effect provided by the best krill individual.
According to the measurements of the maximum induced speed, it is taken 0.01 $(ms-1)$. In KH algorithm, the effect of neighbours (α^{ilocal}) is formulated as follows : [90]

$$\alpha_i^{target} = \sum_{j=1}^{NN} \widehat{K}_{i,j}\widehat{X}_{i,j} \tag{3.23}$$

$$\widehat{X}_{i,j} = \frac{X_i - X_j}{\|X_i - X_j\| + \varepsilon} \tag{3.24}$$

$$\widehat{K}_{i,j} = \frac{K_i - K_j}{K_{worst} - K_{bestj}} \tag{3.25}$$

where K_{best} and K_{worst} are the best and the worst fitness values of the krill individuals so far ; K_i represents the fitness or the objective function value of the ith krill individual ; K_j is th fitness of j^{th} $(j = 1, 2, ..., NN)$ neighbor ; X represents the related positions ; and NN is the number of the neighbors.
For choosing neighbours on the first hand, the sensing distance of each krill are calculated with the following equation :

$$d_{s,i} = \frac{1}{5N}\sum_{j=1}^{N} \|X_i - X_j\| \tag{3.26}$$

If the distance of two krill individuals is less than the defined sensing distance, then they are neighbours. The best krill effects on others by α_i^{target} which is given by :

$$\alpha^{target} = C^{best}\widehat{K}_{i,best}\widehat{X}_{i,best} \tag{3.27}$$

And

$$C^{best} = 2\left(rand + \frac{I}{I_{max}}\right) \tag{3.28}$$

3.6.3.2 Foraging motion

The foraging motion (Fi) is estimated by the two main components. One is the food location and the other is the prior knowledge about the food location. For the i^{th} krill individual, this motion can be approximately formulated as follows :

$$F_i = V_f\beta_i + w_f F_i^{old} \tag{3.29}$$

Where

$$\beta_i = \beta_i^{food} + \beta_i^{best} \tag{3.30}$$

V_f is the foraging speed, w_f is the inertia weight of the foraging motion and it is a number in the range $[0, 1]$, Fiold is the last foraging motion. In this paper, we set V_f to 0.02.

3.6.3.3 Physical diffusion

The physical diffusion of krill individuals is considered to be a random process. It can be formulated as follows : [91]

$$D_i = D^{max}\delta \tag{3.31}$$

where D^{max} is the maximum diffusion speed, and δ is the random directional vector, and its arrays are random values in the range of $[-1, 1]$. The better position of krill leads to less random motion. Furthermore, another term is added to the physical diffusion formula to consider this effect.

$$D_i = D^{max}\left(1 - \frac{I}{I_{max}}\right)\delta \tag{3.32}$$

3.6.3.4 Motion process of the KH algorithm

This term linearly decreases the random speed with the time (iterations) According to three main actions mentioned above ; the velocity of each krill can be calculated. The new position of each krill from t to $t + dt$ is formulated as below : [92]

$$X_i(t + \Delta t) = X_i(\tau) + \Delta t \frac{dX_i}{dt} \tag{3.33}$$

Δt is a very important parameter which determines the effect of velocity on the new position of krill. This parameter is extremely affected by search space, so that it can be as the following equation :

$$\Delta t = C_t \sum_{j=1}^{NV} (U\,B_j - L\,B_j) \tag{3.34}$$

Where NV is the number of variables and LB_j and UB_j are the lower and the upper limits of the j^{th} variable. C_t is varied in the range $[0, 2]$. It is obvious that small values of C_t result precisely search in the search space.

3.6.3.5 Crossover

As it is evaluated in the first KH, the crossover is an effective evolutionary mechanism in the KH algorithm. By generating a random vector with values in the range [01], the m^{th} component of x_i, $x_{i,m}$, is manipulated as : [93]

$$x_{i,m} = \begin{cases} x_{r,m} & rand_{i,m} < C_{r,i} \\ x_{i,m} & else \end{cases} \tag{3.35}$$

$$C_{r,i} = 0.02\widehat{K}_{i,best}$$

Where C_r is a crossover probability. The Krill Herd Algorithm can be simplified in the following flowchart [15].

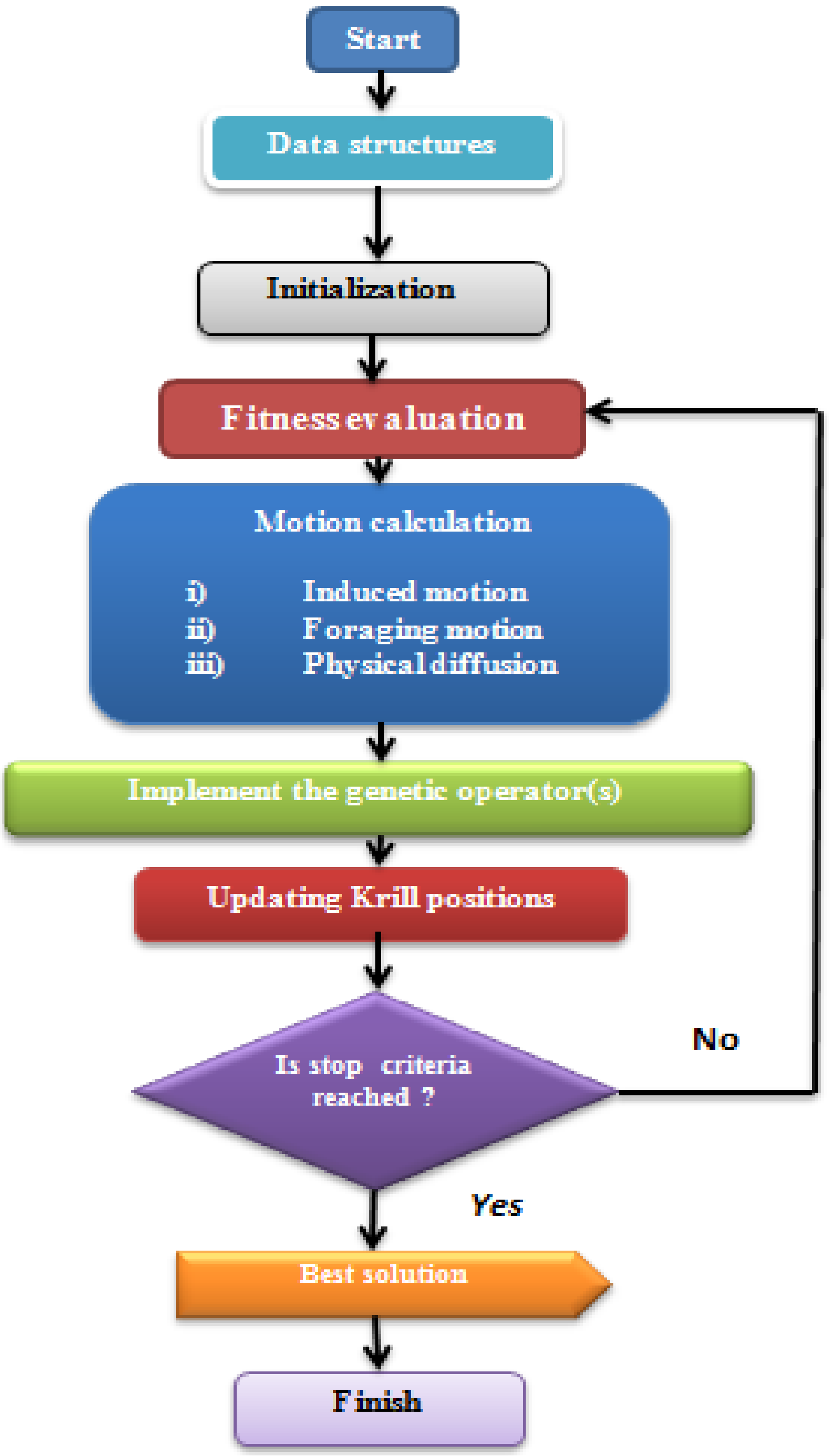

FIGURE 3.6 – Simplified flowchart of the krill herd algorithm.

Table 3.3 – Parameters of Krill Herd

Parameters	**Values**
Number of Runs	10
Number of variables	3 and 5
Number of Krills	25
Crossover flag	1
Lower and upper bounds of variables	0 and 5
Maximum Iteration Number	100

The Krill Herd algorithm is a bio-inspired and swarm-based algorithm which can be solving many complex optimization problems, give efficiency performance of hybrid energy system and outperform other metaheuristics algorithm.

3.7 Results and Discussion of the simulation test system

The proposed configuration of the microgrid is simulated under a nominal condition during 100s and 120s using Matlab/ Simulink enviroment. A PID controller and FOPID controller are introduced to eliminate the frequency and power fluctuations provoked by the integration of renewable power generation such as PV and wind which have intermittent nature and stochastic changes during the simulation time. The simulation results are showed in followed figures.

Table 3.4 – The best parameters of PID controller using KH, GA, and PSO

Method/controller		K_P	K_I	K_D	λ	μ
GA	FOPID	4.8275	4.236	0.790	0.8183	0.7526
	PID	4.6867	4.9998	0.4880	-	-
PSO	FOPID	4.454	6.687	9.62	0.203	2.320
	PID	4.9342	2.4297	2.5018	-	-
KH	FOPID	4.81	3.0959	1.4917	0.79865	0.953
	PID	6.3937	3.7218	6.4380	-	-

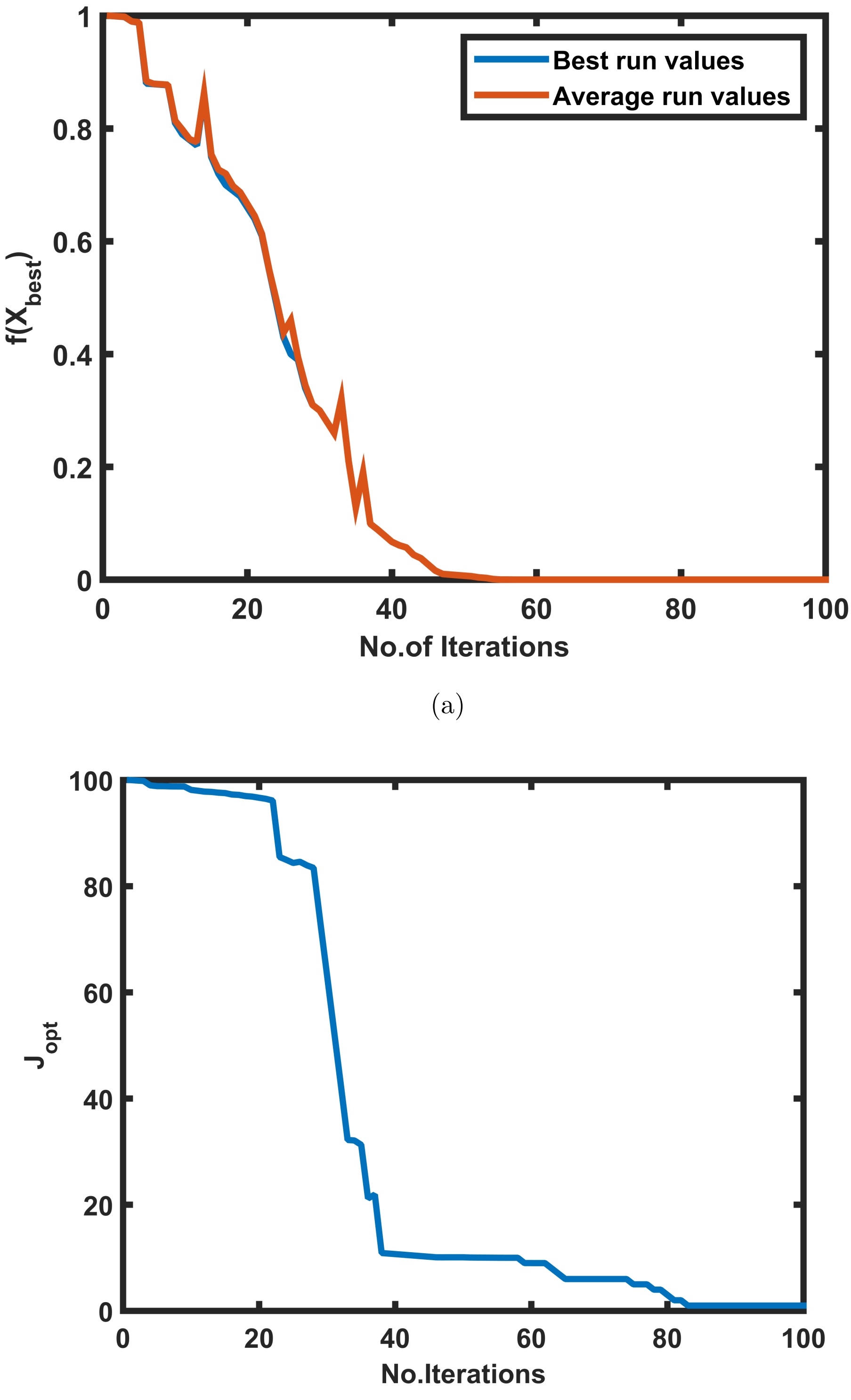
Best run values
Average run values
f(X$_{best}$)
No.of Iterations
0
20
40
60
80
100
0
0.2
0.4
0.6
0.8
1
J$_{opt}$
No.Iterations
0
20
40
60
80
100

(a)

(b)

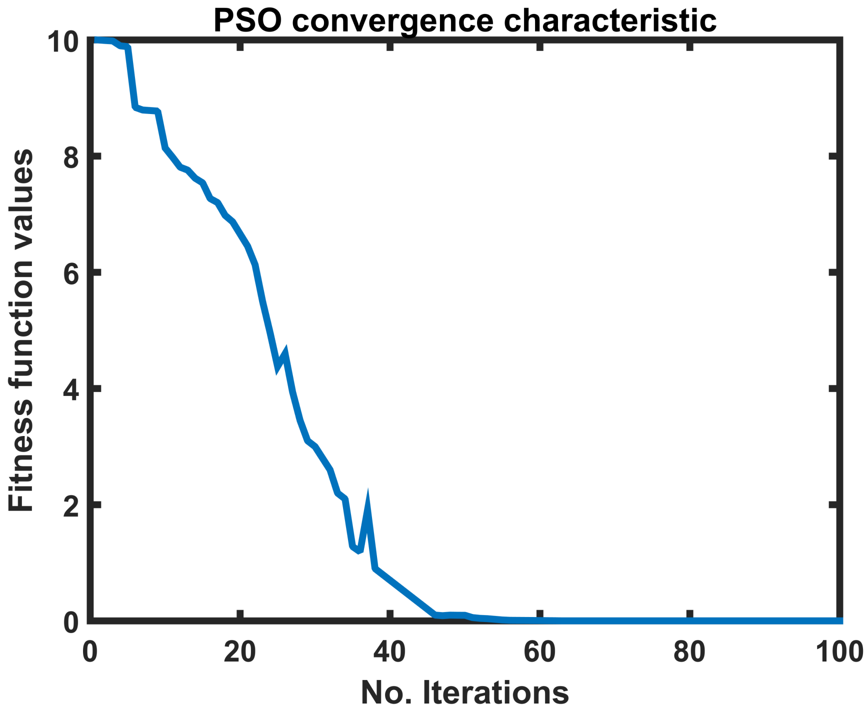

(c)

Figure 3.7 – Convergence characteristic of KH(a), GA(b) and PSO(c) respectively

Power generation with different compounds of microgrid

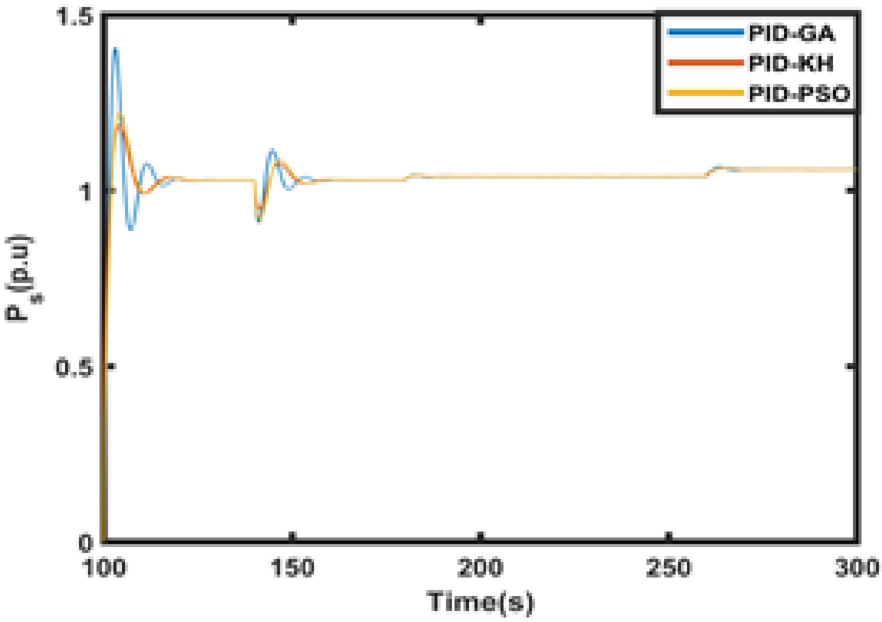

(a)

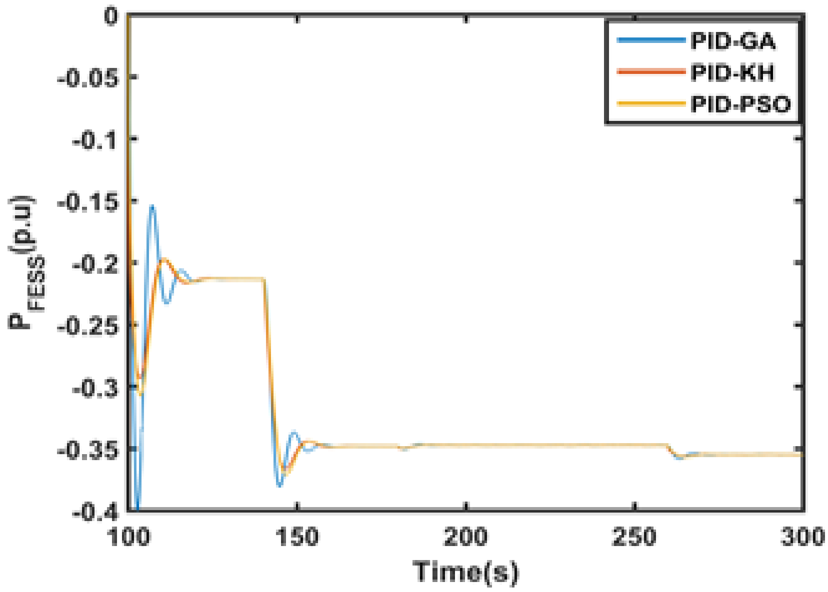

(b)

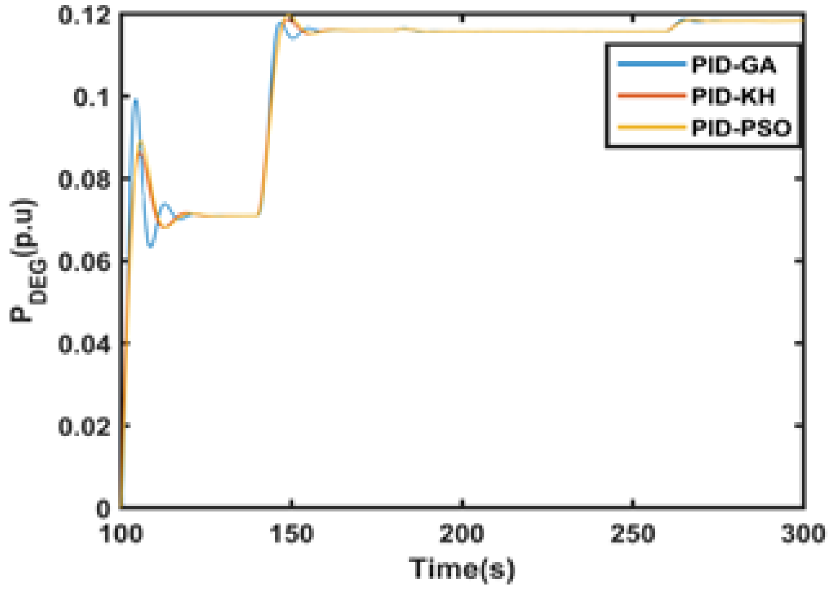

(c)

FIGURE 3.8 – Output powers of the different components of the Microgrid system PS(a), PFESS(b) and PDEG(c) .

It can be noted that the diesel generator and fuel-cell system used to supply the load power. This shows that the oscillations are greatly reduced using the proposed PID controller based KH algorithm. Then the particle Swarm Optimization technique reduces the fluctuation better in comparison to the Genetic Algorithm. However, it enhances the damping characteristics of the power system and shows the best performances of the proposed system.

This bellow figure presents the power and frequency deviation using three optimization techniques like GA, PSO, and KH with the best PID controller parameter.

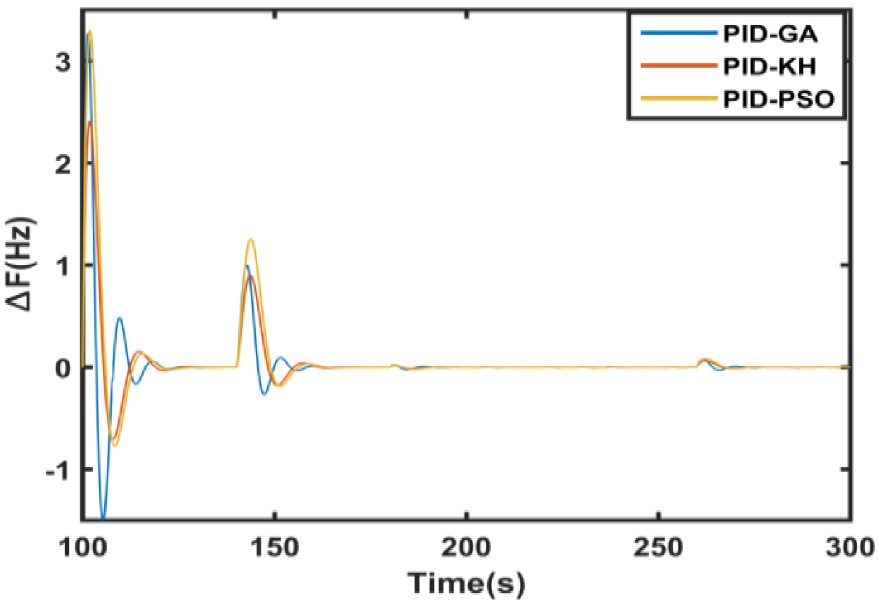

(a)

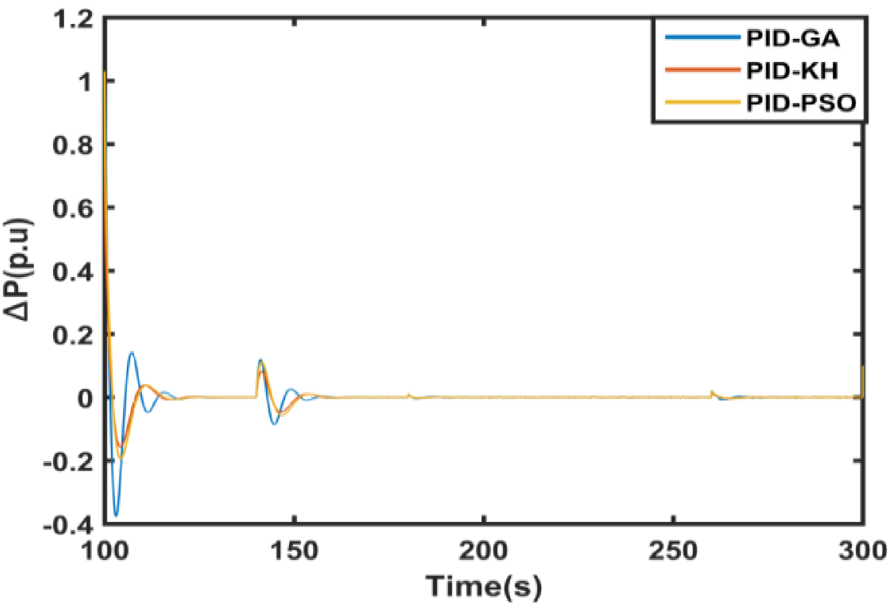

(b)

FIGURE 3.9 – Frequency deviation(a) and power deviation(b) of the investigated system with best obtained PID controllers.

The frequency deviation (Δf) and power variation (ΔP) corresponding to the best-obtained parameters of the proposed controller are displayed in Figure 3.9. These simulation results show that the frequency and power deviations change according to the sudden change in both generate power and load. It is necessary to note that the controller works to meet the equality between the load and generation with the impact of the weather conditions on the generated power from wind and photovoltaic systems. The fluctuation of frequency and power seriously influences the microgrid stability. Hence compared to the PID controller optimized using GA, PSO, and KH ; it shows that KH based PID controller greatly enhances the system stability and damping performance for frequency and power deviation compared to GA and PSO tuning PID controller. It is also proved from the shown result that the Particle Swarm Optimization algorithm gives better performances of the system frequency and power control compared to the Genetic Algorithm.

The change in power demand and generation causes fluctuations in frequency and power deviations which are settled down after a few seconds due to the coordination with generation sources and storage devices through the controller. With a thorough analysis of results, it can be observed that a small deviation of frequency and power is achieved by using of PID controller based PSO compared to the results given using GA based PID controller. The proposed controller-based PSO appeared better than the controller based GA in performances and stability of the system.

3.7.1 Comparison between GA and KH based FOPID under the nominal operating conditions of the microgrid

This subsection presents different results of the comparison between the Genetic Algorithm and Krill herd based Fractional Order PID controller for frequency and power deviations. The corresponding power and frequency deviations are reported in Figure 3.10 It can be observed that there are fewer power fluctuations with the FOPID controller-based Krill Herd is better than for GA. Thus it would be a better optimization tool in this case study of the microgrid. These sets of data are obtained by substituting the values of the controller parameters in the power system model. It can be observed that there are fewer power fluctuations with the FOPID-KH than FOPID-GA.

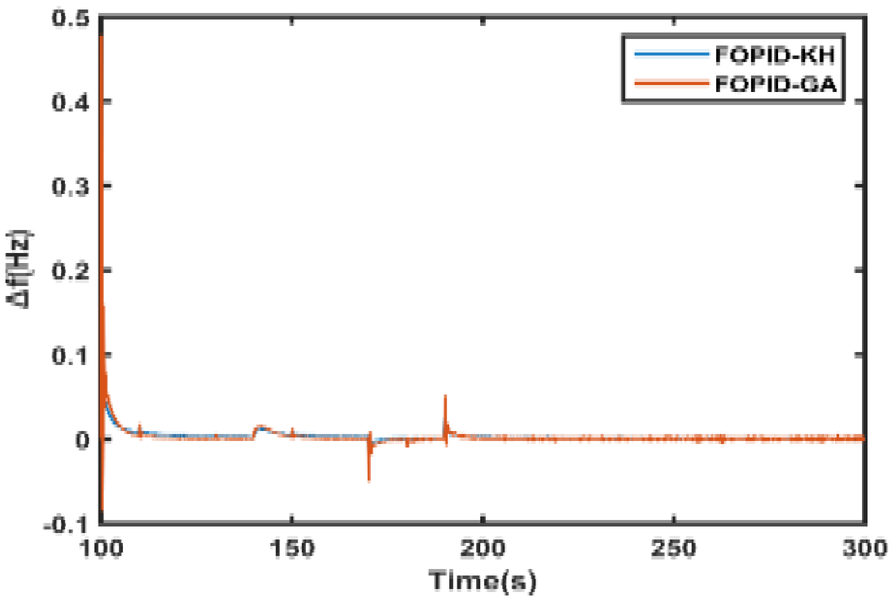

(a)

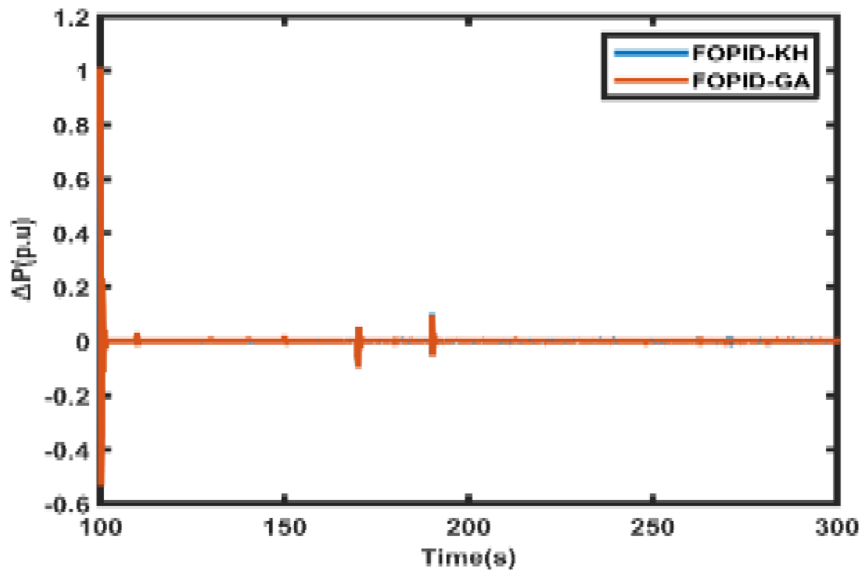

(b)

FIGURE 3.10 – Frequency deviations(a) and power deviation(b) of microgrid with best obtained /FOPID controllers.

3.7.2 Robustness against disconnecting the UC using FOPID based KH

Due to the presence of stochastic terms in generation and load, the optimization of the parameters controller leads to eliminate the frequency and power deviation. The system is simulated with and without UC using the Krill Herd based FOPID to display the advantages of the fractional-order controllers, impact of these devices and suitability of optimization techniques. This focuses on the section of an objective function as in Eq 3.1 to be resolved using KH while its variables are the gains of the controller. Figure 3.11 shows the corresponding powers generated by different components of microgrid with and without ultra-capacitor. The results show that this device has an important impact on the microgrid operation and state of power. This implies that the sizing of these energy generation and storage devices can be shown smaller than if the FOPID controller is employed.

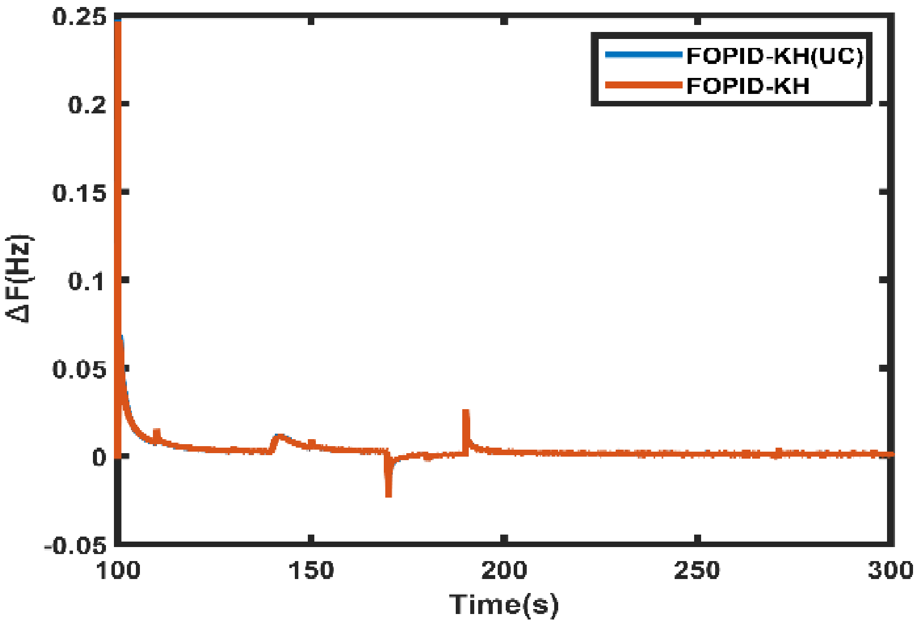

(a)

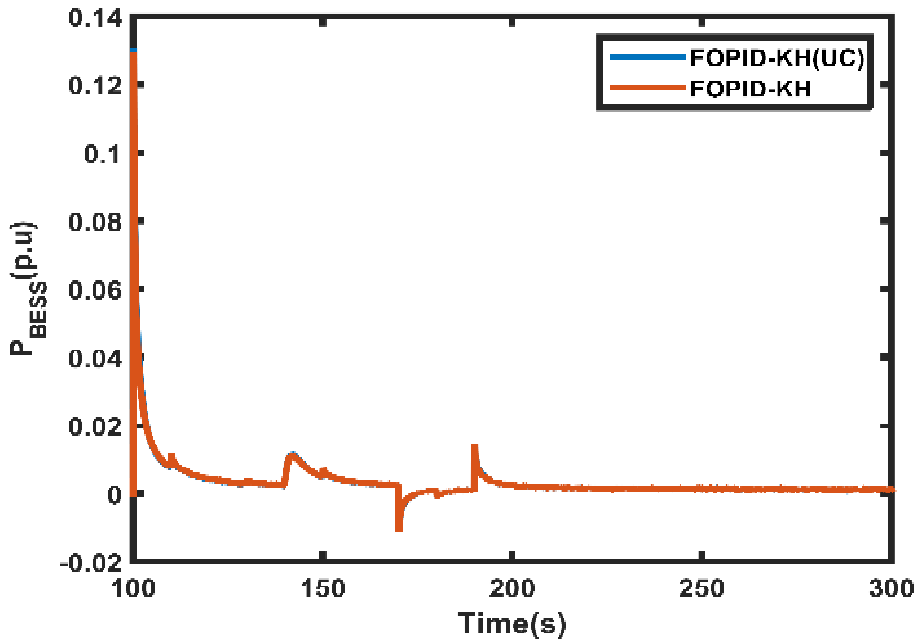

FOPID-KH(UC)
FOPID-KH
0.14
0.12
0.1
0.08
0.06
0.04
0.02
0
-0.02
P_{BESS}(p.u)
100
150
200
250
300
Time(s)

(b)

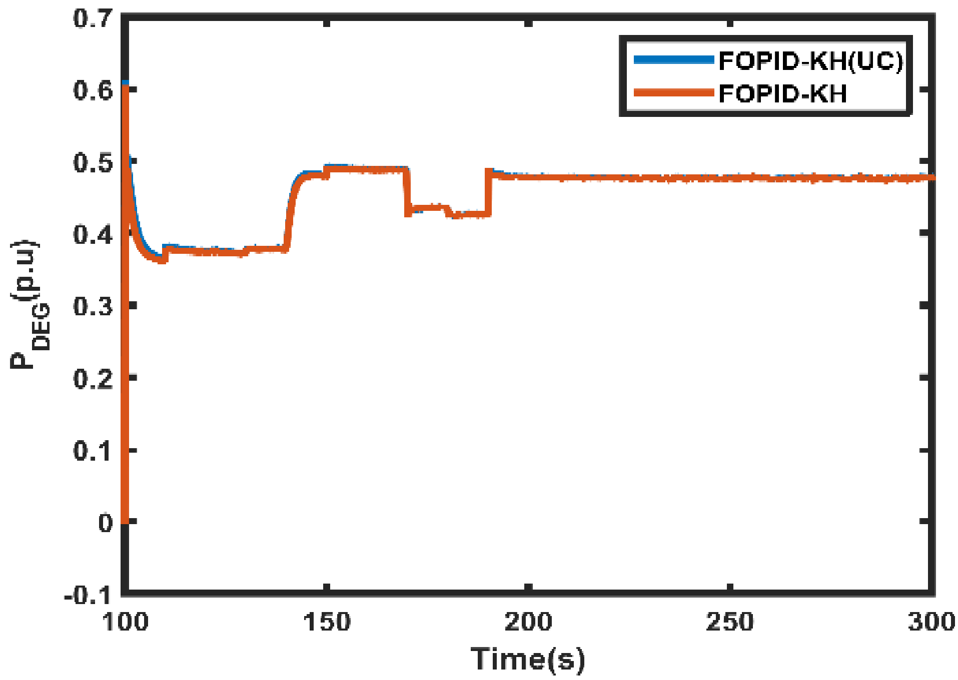

FOPID-KH(UC)
FOPID-KH
0.7
0.6
0.5
0.4
0.3
0.2
0.1
0
-0.1
P_{DEG}(p.u)
100
150
200
250
300
Time(s)

(c)

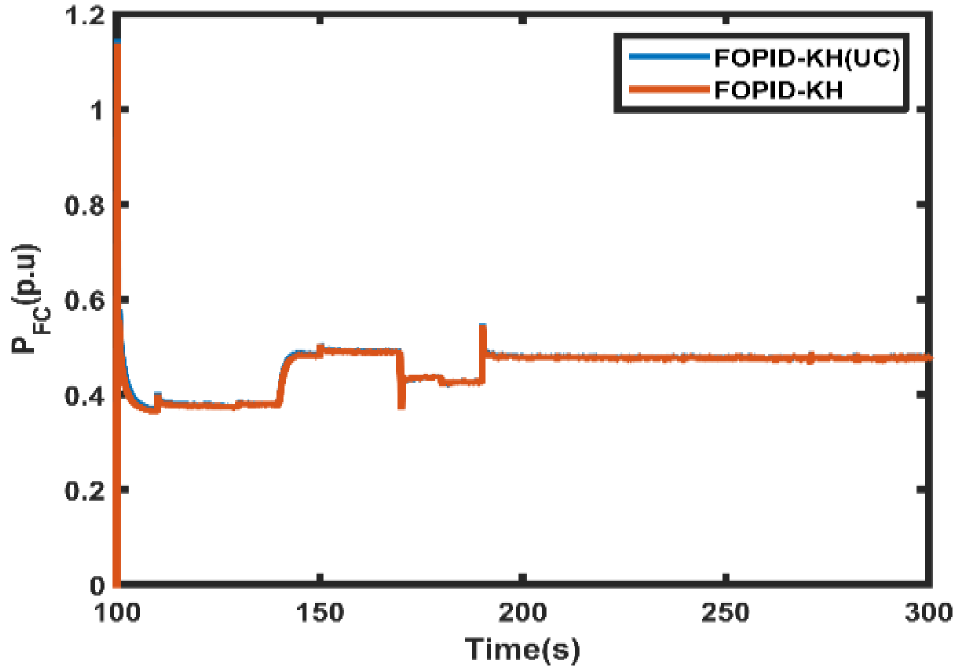

(d)

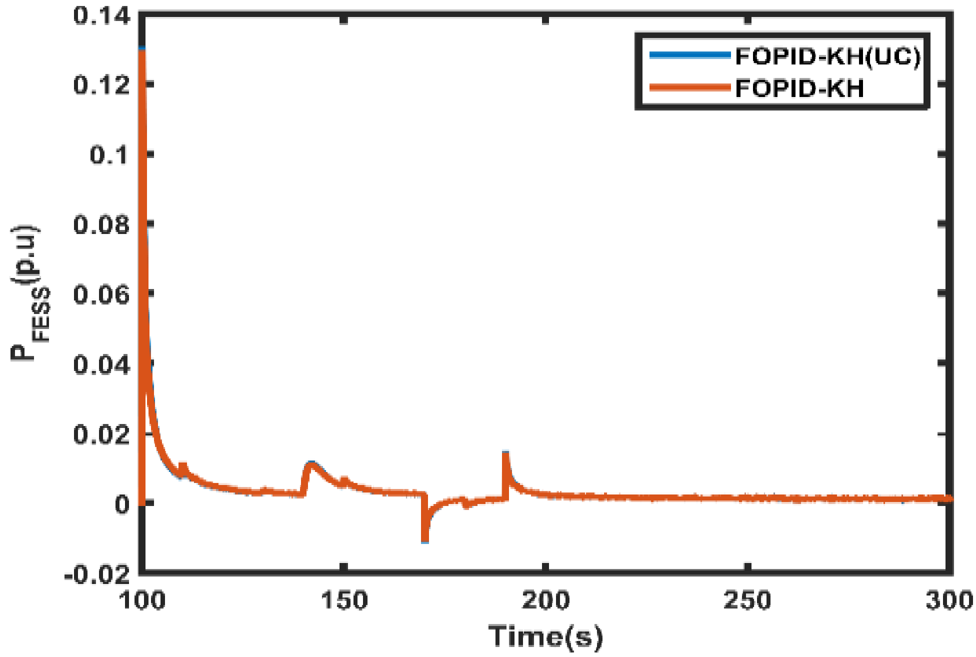

(e)

FIGURE 3.11 – Frequency deviation(a) and Generated power by different Microgrid components like $P_{BESS}(b)$, $P_{DEG}(c)$,$P_{FC}(d)$ and $P_{FESS}(e)$ respectively .

3.7.3 Robustness against the microgrid parameters variations using FOPID based KH and GA

The system is simulated under perturbations in parameters for testing the robustness of the proposed fractional PID controller based Krill Herd and Genetic Algorithm against the parameters increase and decrease and the objective function values are reported in the followed Table. The obtained results are shown in the bellow figures.

TABLE 3.5 – Robustness against perturbation in microgrid parameters

Microgrid parameters	*Perturbations* ±	*Controllers FOPID*	*J increase*	*J decrease*
		KH	0.0393	0.0392
D	70%	GA	0.05093	0.05091
		KH	0.03931	0.03929
T_{FC}	20%	GA	0.05093	0.05092
		KH	0.03931	0.03928
T_g	20%	GA	0.05093	0.05091
		KH	0.03931	0.03927
T_t	70%	GA	0.05094	0.05091
		KH	0.0393	0.0393
T_{IC}	70%	GA	0.05093	0.05093
		KH	0.03932	0.03928
T_{IN}	0.5%	GA	0.05092	0.0509
		KH	0.03929	0.03992
R	70%	GA	0.05092	0.05099
		KH	0.03929	0.03935
2H	50%	GA	0.05089	0.0511

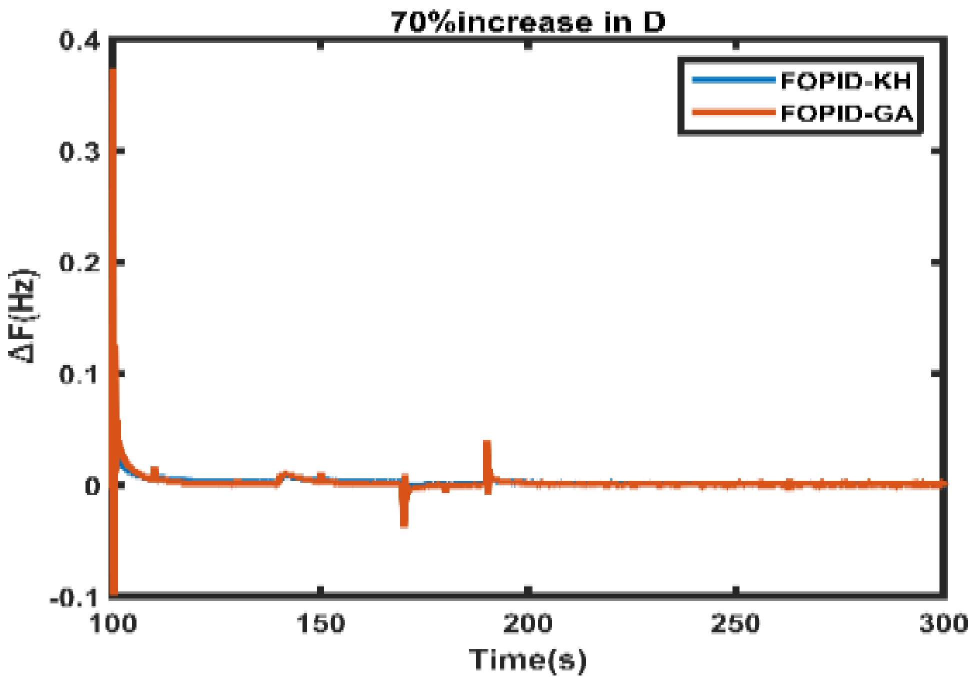
70%increase in D
FOPID-KH
FOPID-GA
ΔF(Hz)
Time(s)
0.4
0.3
0.2
0.1
0
-0.1
100
150
200
250
300

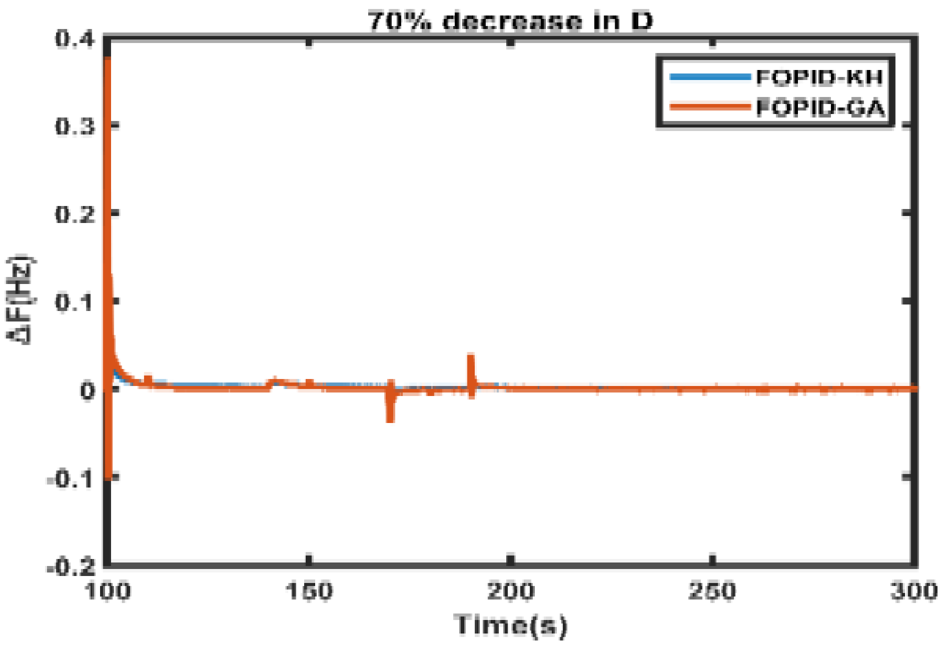
70% decrease in D
FOPID-KH
FOPID-GA
ΔF(Hz)
Time(s)
0.4
0.3
0.2
0.1
0
-0.1
-0.2
100
150
200
250
300

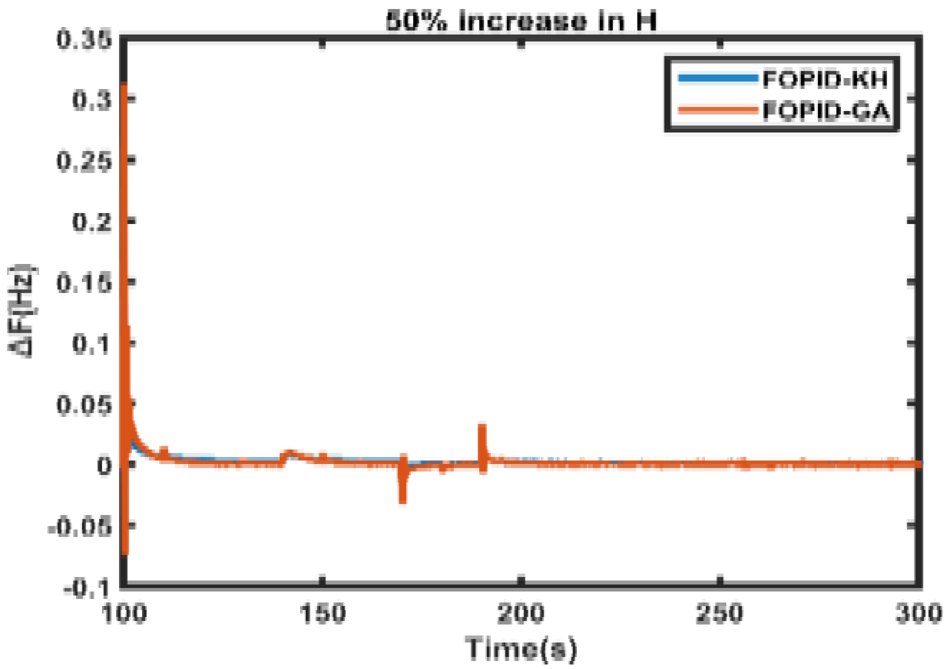
50% increase in H
FOPID-KH
FOPID-GA
ΔF[Hz]
Time(s)

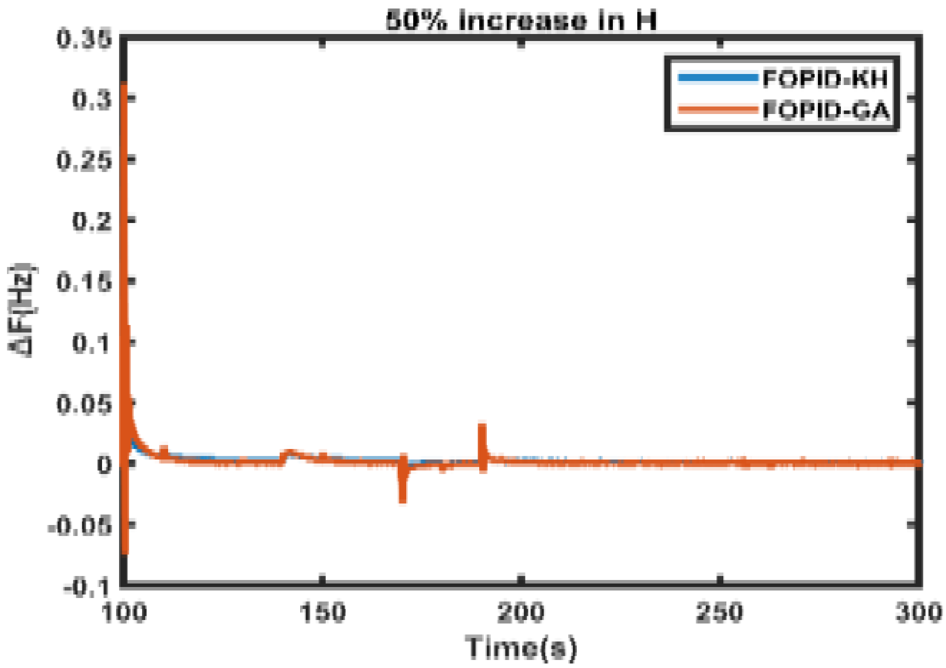
50% increase in H
FOPID-KH
FOPID-GA
ΔF[Hz]
Time(s)

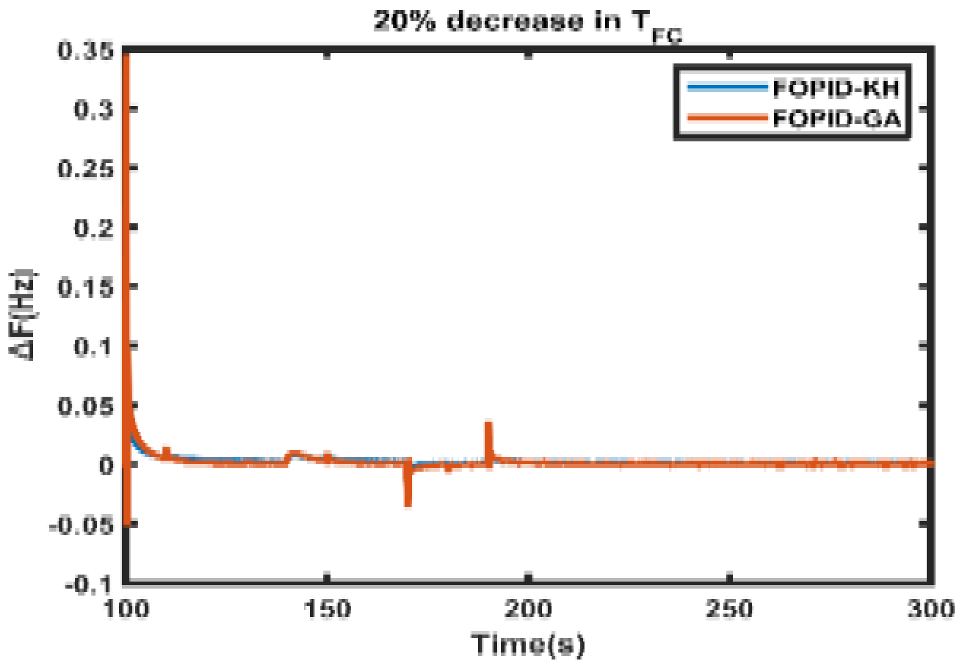
20% decrease in T_{FC}
FOPID-KH
FOPID-GA
ΔF(Hz)
0.35
0.3
0.25
0.2
0.15
0.1
0.05
0
-0.05
-0.1
100
150
200
250
300
Time(s)

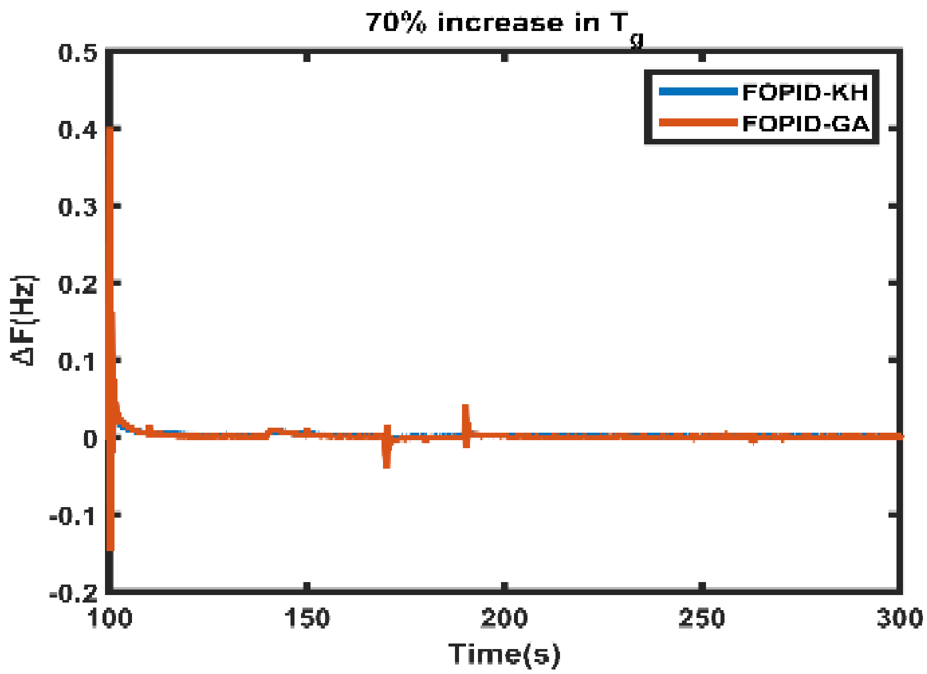
70% increase in T_g
FOPID-KH
FOPID-GA
ΔF(Hz)
0.5
0.4
0.3
0.2
0.1
0
-0.1
-0.2
100
150
200
250
300
Time(s)

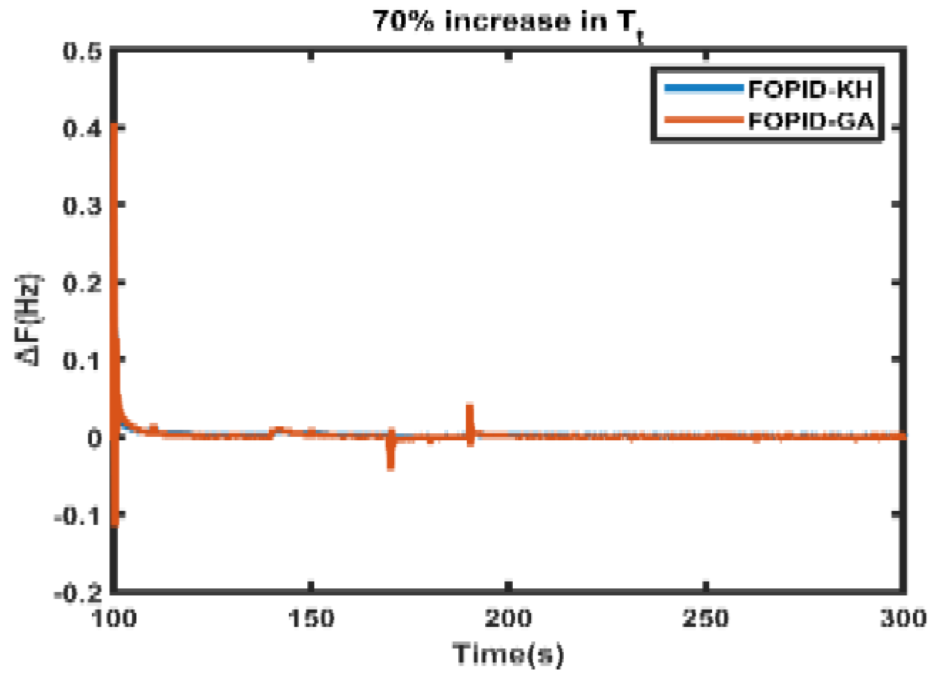
70% increase in T
FOPID-KH
FOPID-GA
ΔF(Hz)
0.5
0.4
0.3
0.2
0.1
0
-0.1
-0.2
100
150
200
250
300
Time(s)

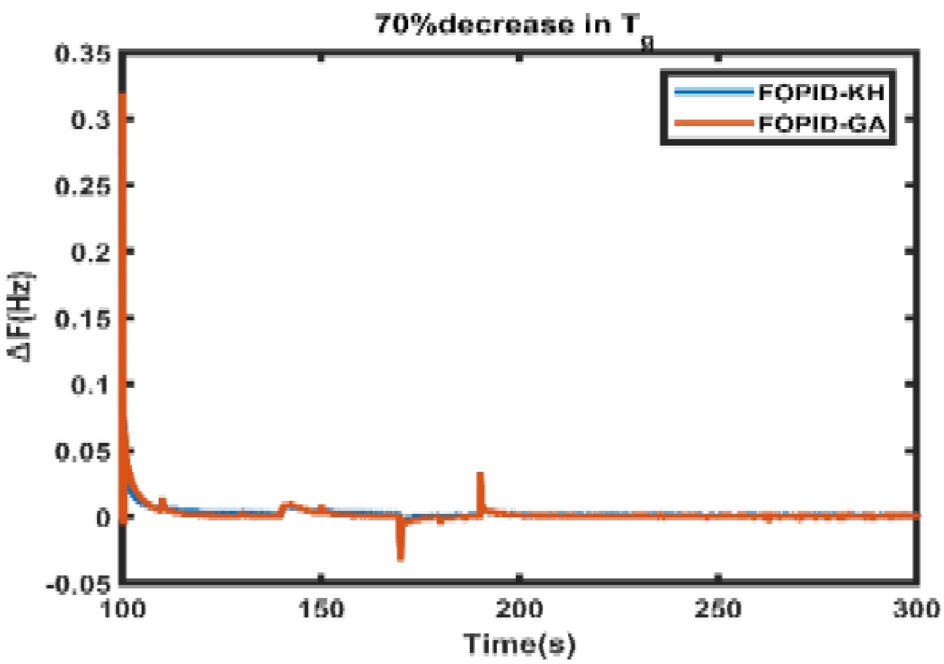
70%decrease in T
FOPID-KH
FOPID-GA
ΔF(Hz)
0.35
0.3
0.25
0.2
0.15
0.1
0.05
0
-0.05
100
150
200
250
300
Time(s)

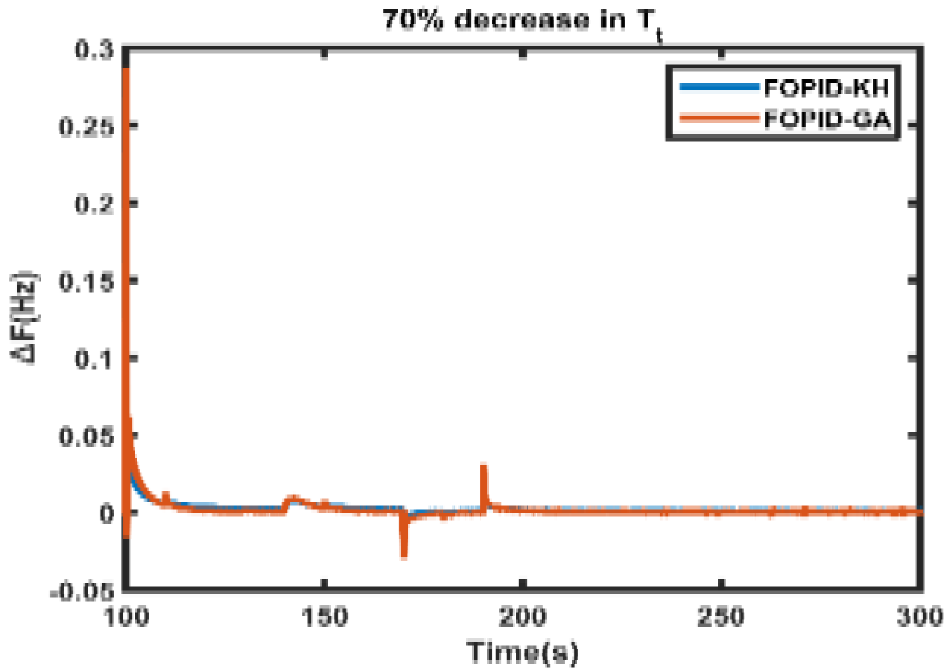
70% decrease in T_t
FOPID-KH
FOPID-GA
ΔF(Hz)
Time(s)
0.3
0.25
0.2
0.15
0.1
0.05
0
-0.05
100
150
200
250
300

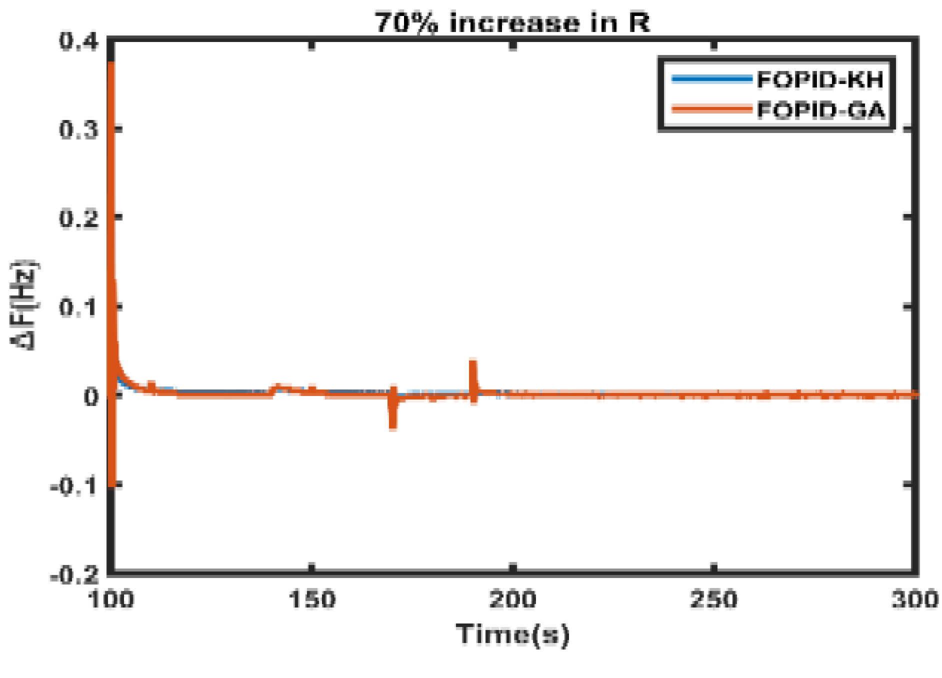
70% increase in R
FOPID-KH
FOPID-GA
ΔF(Hz)
Time(s)
0.4
0.3
0.2
0.1
0
-0.1
-0.2
100
150
200
250
300

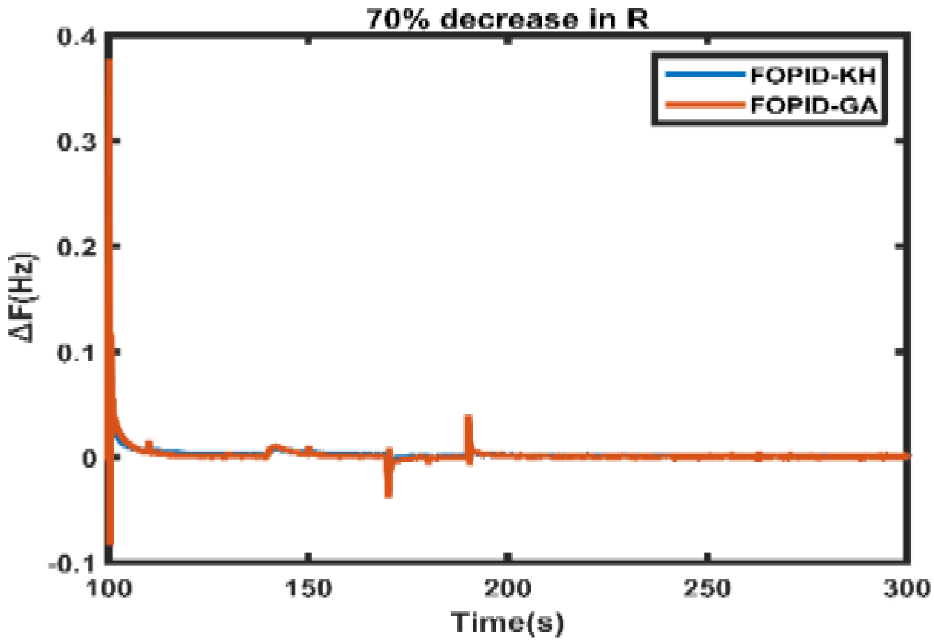
70% decrease in R
FOPID-KH
FOPID-GA
ΔF(Hz)
Time(s)
0.4
0.3
0.2
0.1
0
-0.1
100
150
200
250
300

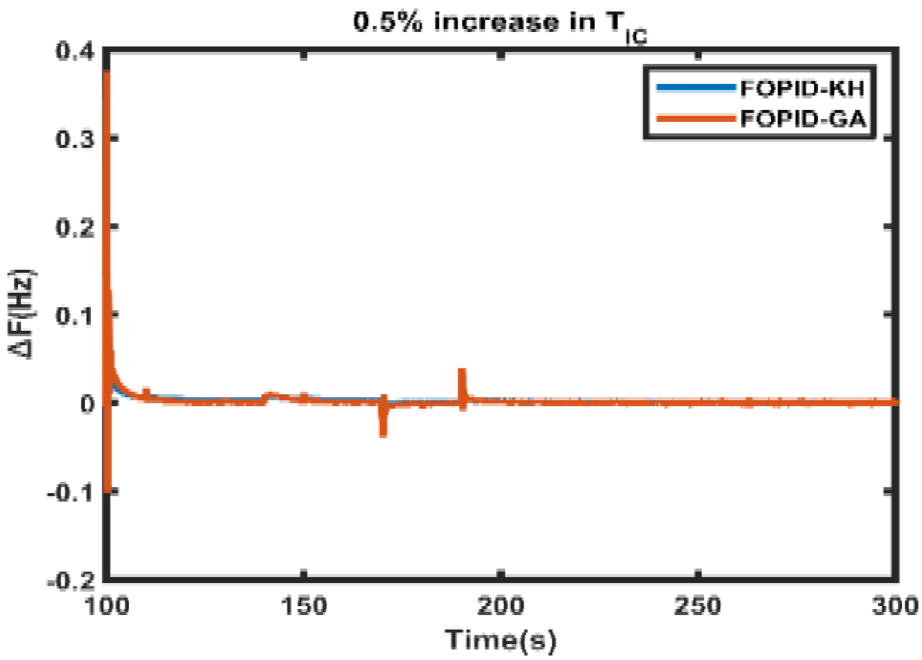
0.5% increase in T_{IC}
FOPID-KH
FOPID-GA
ΔF(Hz)
Time(s)
0.4
0.3
0.2
0.1
0
-0.1
-0.2
100
150
200
250
300

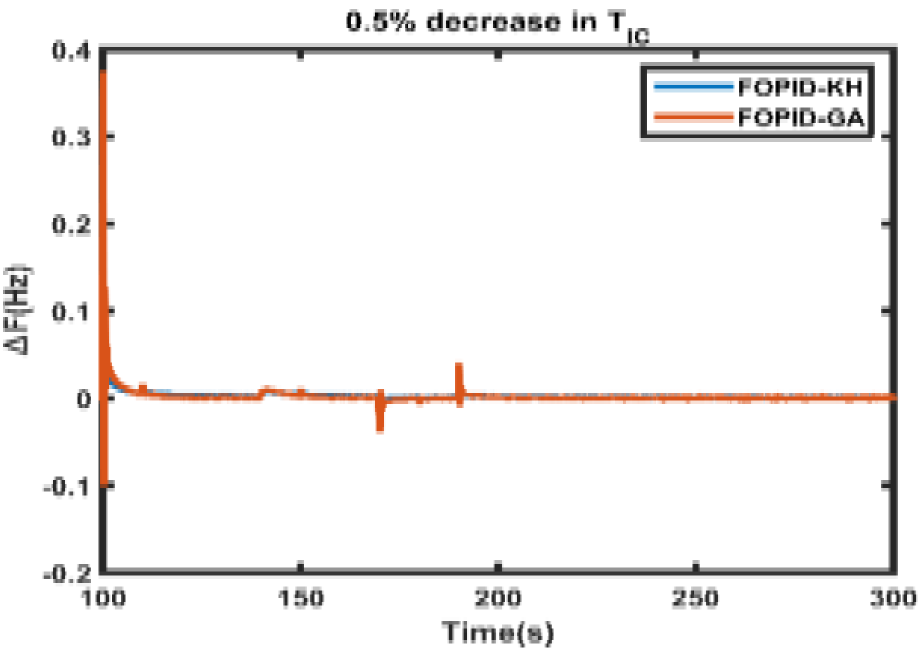
0.5% decrease in T_{IC}
FOPID-KH
FOPID-GA
ΔF(Hz)
Time(s)
0.4
0.3
0.2
0.1
0
-0.1
-0.2
100
150
200
250
300

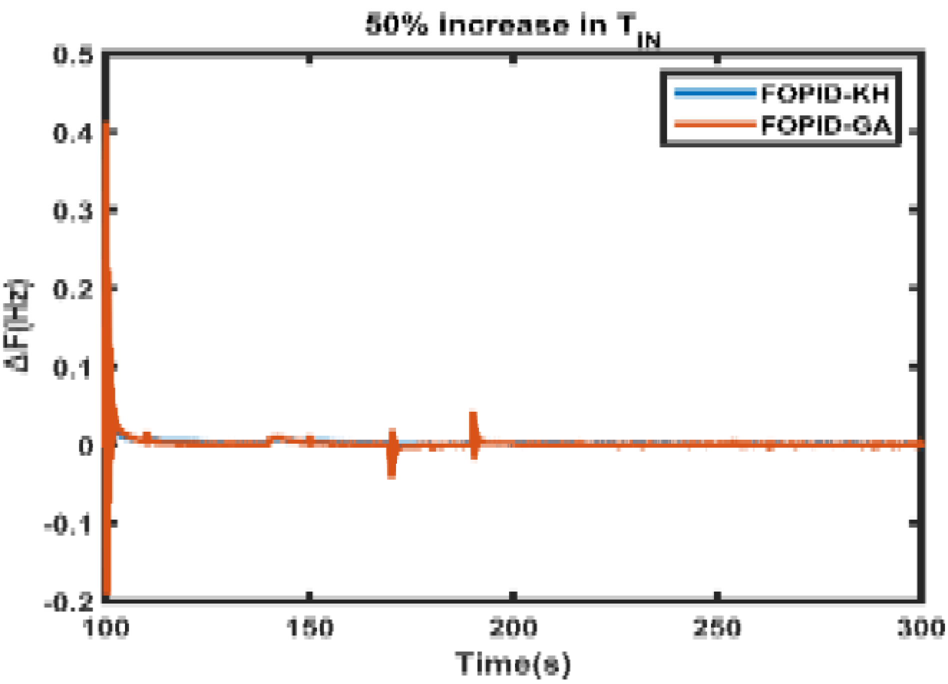
50% increase in T_{IN}
FOPID-KH
FOPID-GA
ΔF(Hz)
Time(s)
0.5
0.4
0.3
0.2
0.1
0
-0.1
-0.2
100
150
200
250
300

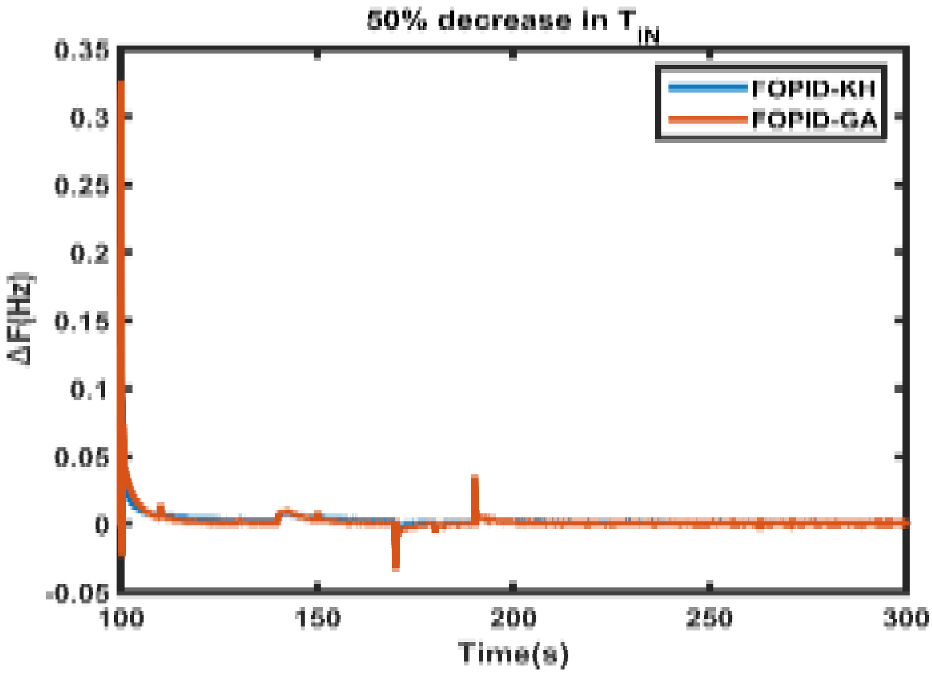

FIGURE 3.12 – Output power of different component of Microgrid using best FOPID.

3.7.4 Robustness of FOPID using KH and PSO under nominal conditions

In this subsection, the system is simulated under the nominal condition with the application of FOPID optimized using PSO and KH. A comparison between the two optimization techniques is achieved.

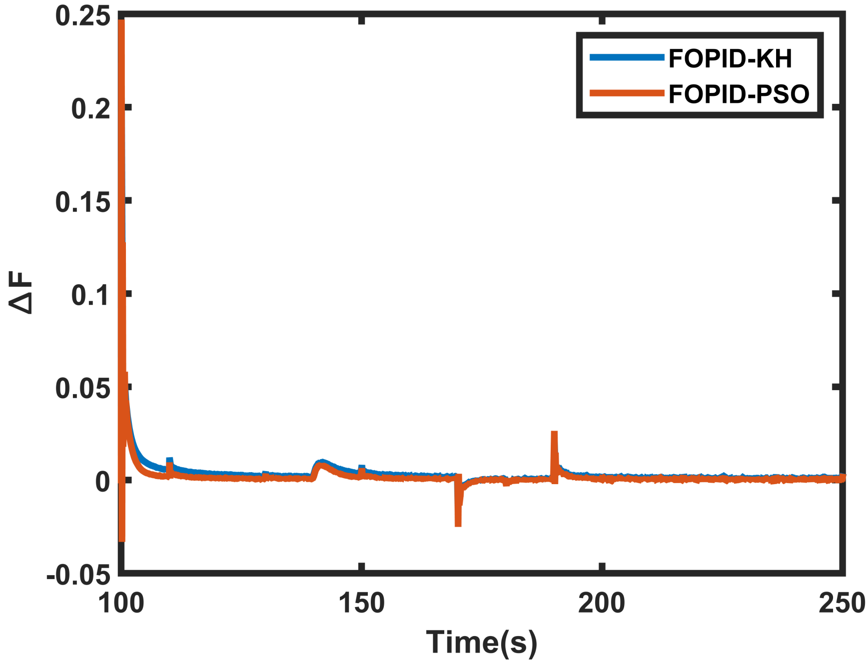

(a)

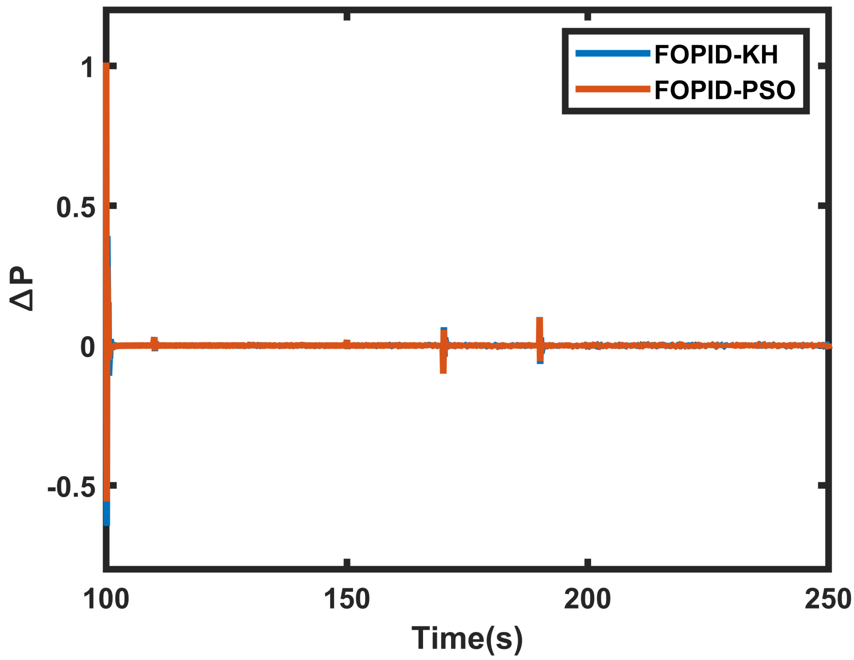

(b)

FIGURE 3.13 – Frequency (a) and power(b) deviations using best FOPID based KH and PSO

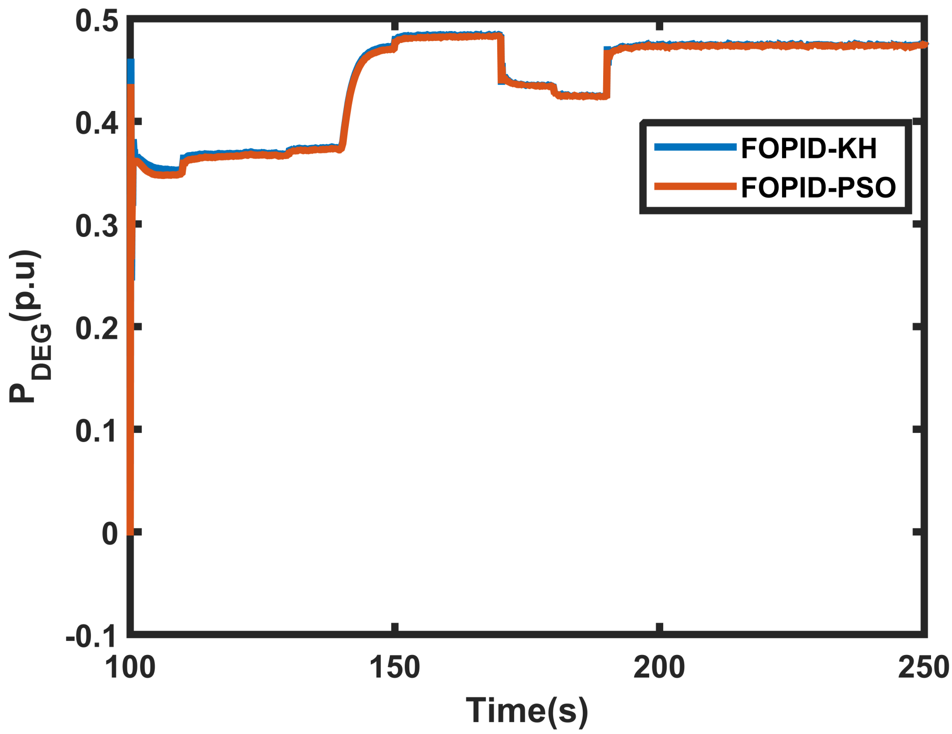
0.5
0.4
0.3
0.2
0.1
0
-0.1
100
150
200
250
Time(s)
P_DEG(p.u)
FOPID-KH
FOPID-PSO

(a)

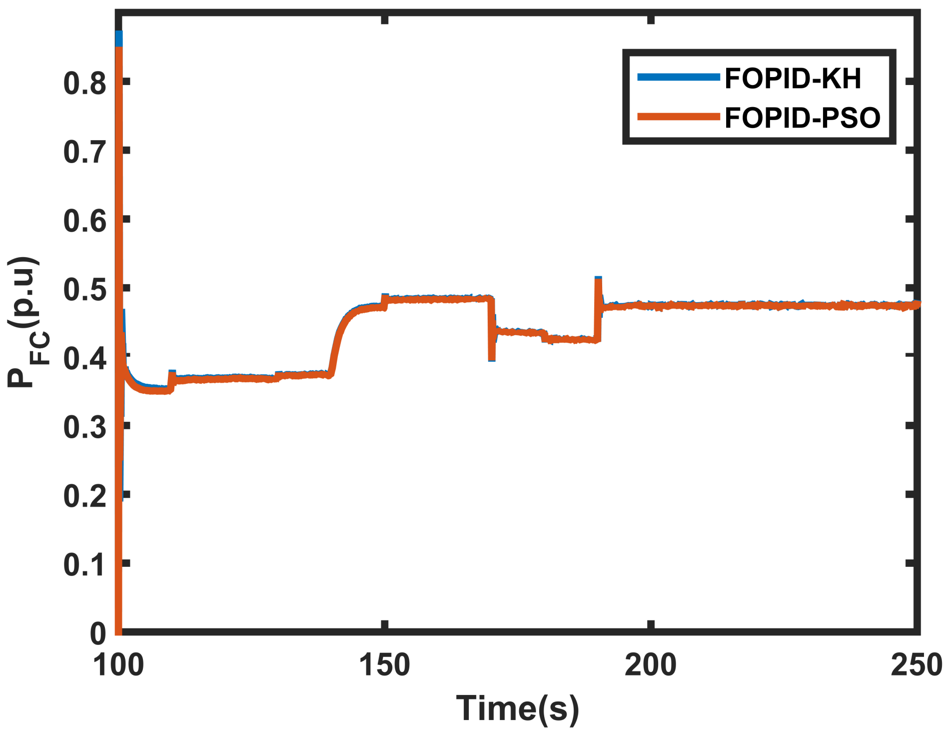
0.8
0.7
0.6
0.5
0.4
0.3
0.2
0.1
0
100
150
200
250
Time(s)
P_FC(p.u)
FOPID-KH
FOPID-PSO

(b)

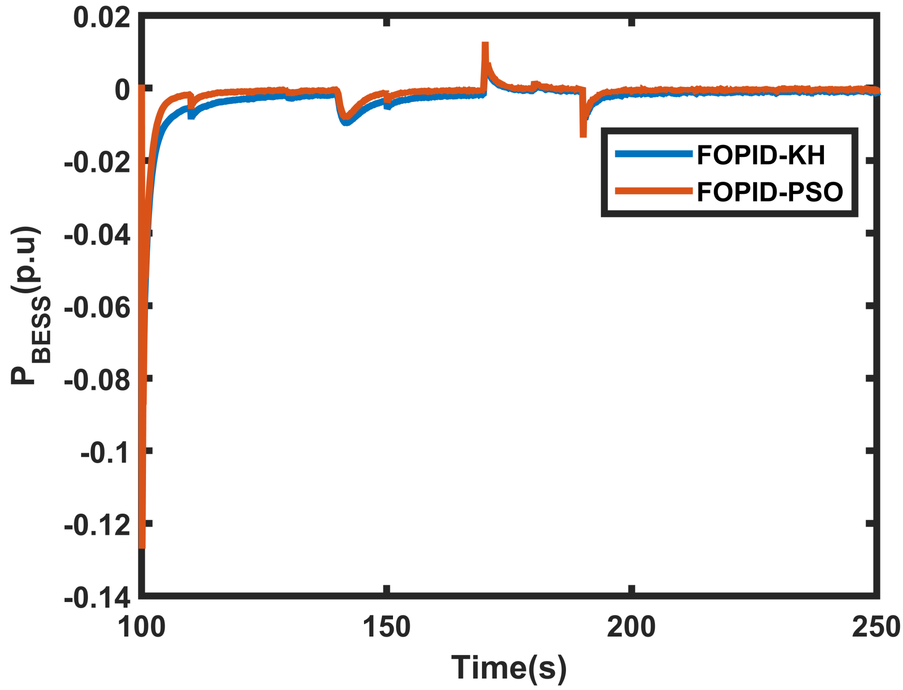

(c)

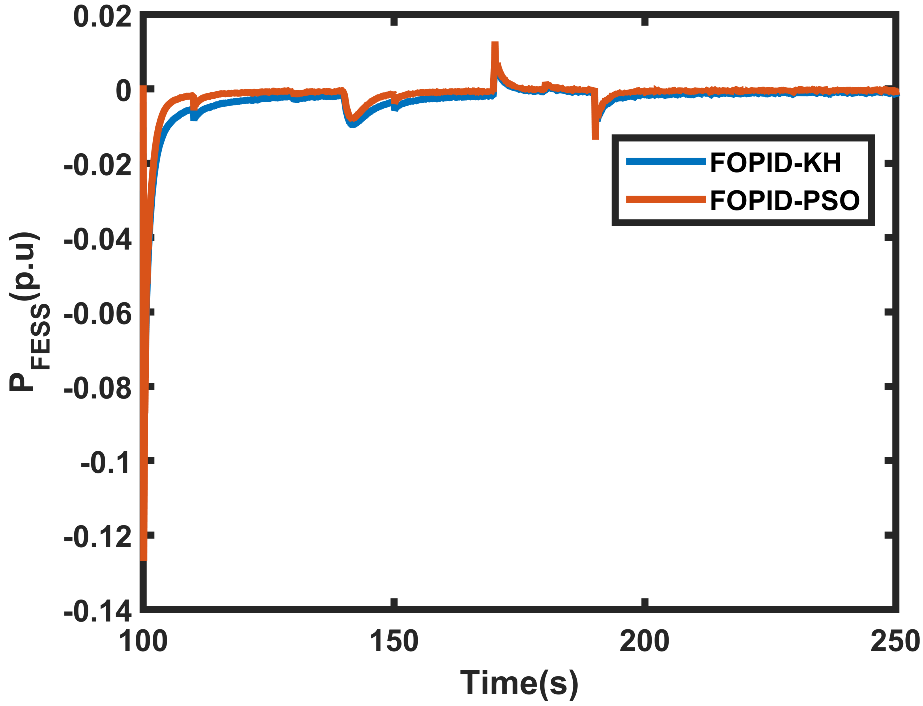

(d)

FIGURE 3.14 – The output power of different component of Microgrid $P_{DEG}(a)$, $P_{FC}(b)$, $P_{BESS}(c)$ and $P_{FESS}(d)$ using the best FOPID

The simulation results showed that the Krill Herd based- FOPID controller scheme is favourable to send away the frequency and power deviations under perturbation operation conditions in comparison with PSO based FOPID controller because the frequency deviation is small with FOPID-KH (around 0.218) than for FOPID-PSO (around 0.235) and the power deviation varies from $1p.u$ to $-0.5p.u$ with FOPID-KH and from $1p.u$ to $-0.6p.u$ with FOPID-PSO which signify the best performances with FOPID-KH. Furthermore, the proposed controller is suitable to control the perturbation string along with renewable energy sources intermittences and sudden variation in power load. The generated power from DEG is enhanced using the FOPID-KH than by FOPID-PSO as shown (P-DEG equal to 0.41p.u for FOPID-KH and 0.426p.u for FOPID-PSO.

Form the presented results it can be easily observed that the Krill Herd is considered as the best optimization technique in terms of rapid response, good robustness to tuning the controller parameters and to improve the proposed system performance. In conclusion, the selected control strategy based optimization technique gives high suitability in microgrid frequency control.

3.7.5 Robustness against Disconnecting of BESS and FESS using FOPID based KH

The system is simulated with and without FESS using the FOPID controller which optimized by KH. The obtained results are compared and shown the marked effect of the disconnecting flywheel energy storage system that required adequate control. This control necessity is achieved by applying FOPID. Figure 3.15 shows the frequency response of the system under FESS and BESS disconnecting.

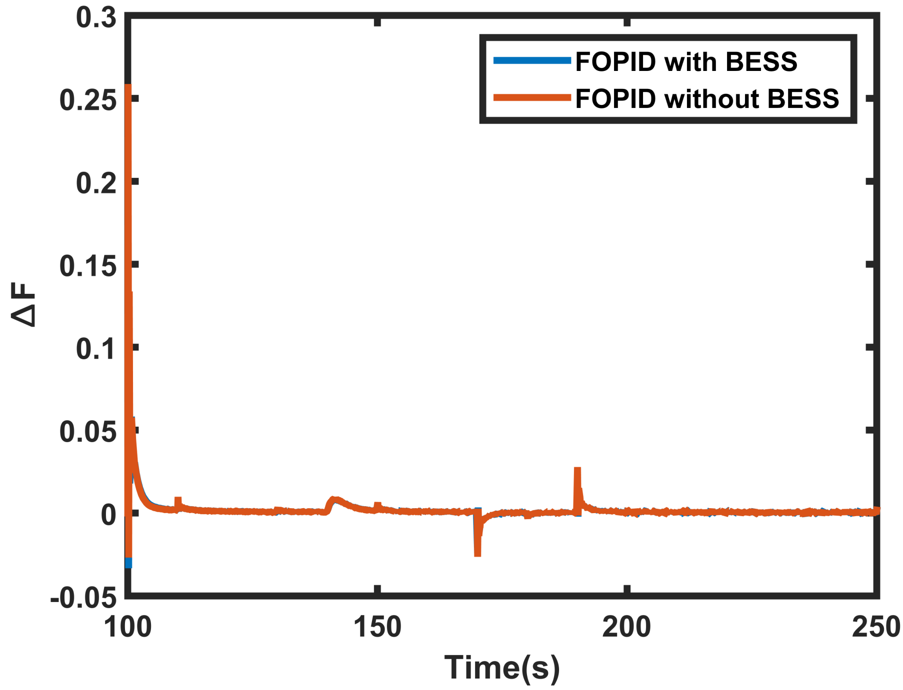
FOPID with BESS
FOPID without BESS
ΔF
Time(s)
0.3
0.25
0.2
0.15
0.1
0.05
0
-0.05
100
150
200
250

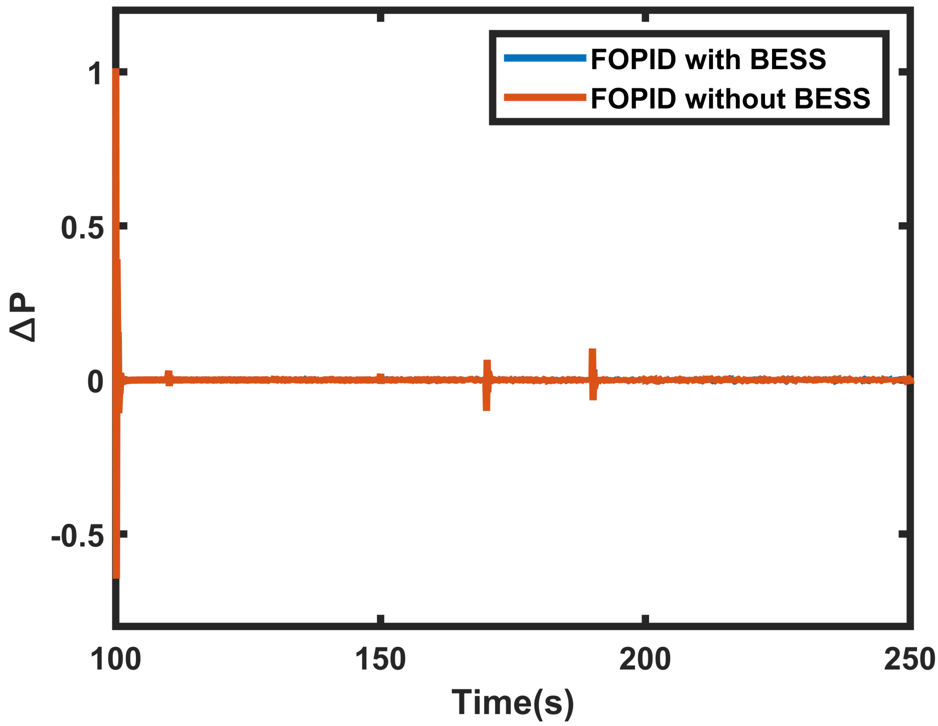
FOPID with BESS
FOPID without BESS
ΔP
Time(s)
1
0.5
0
-0.5
100
150
200
250

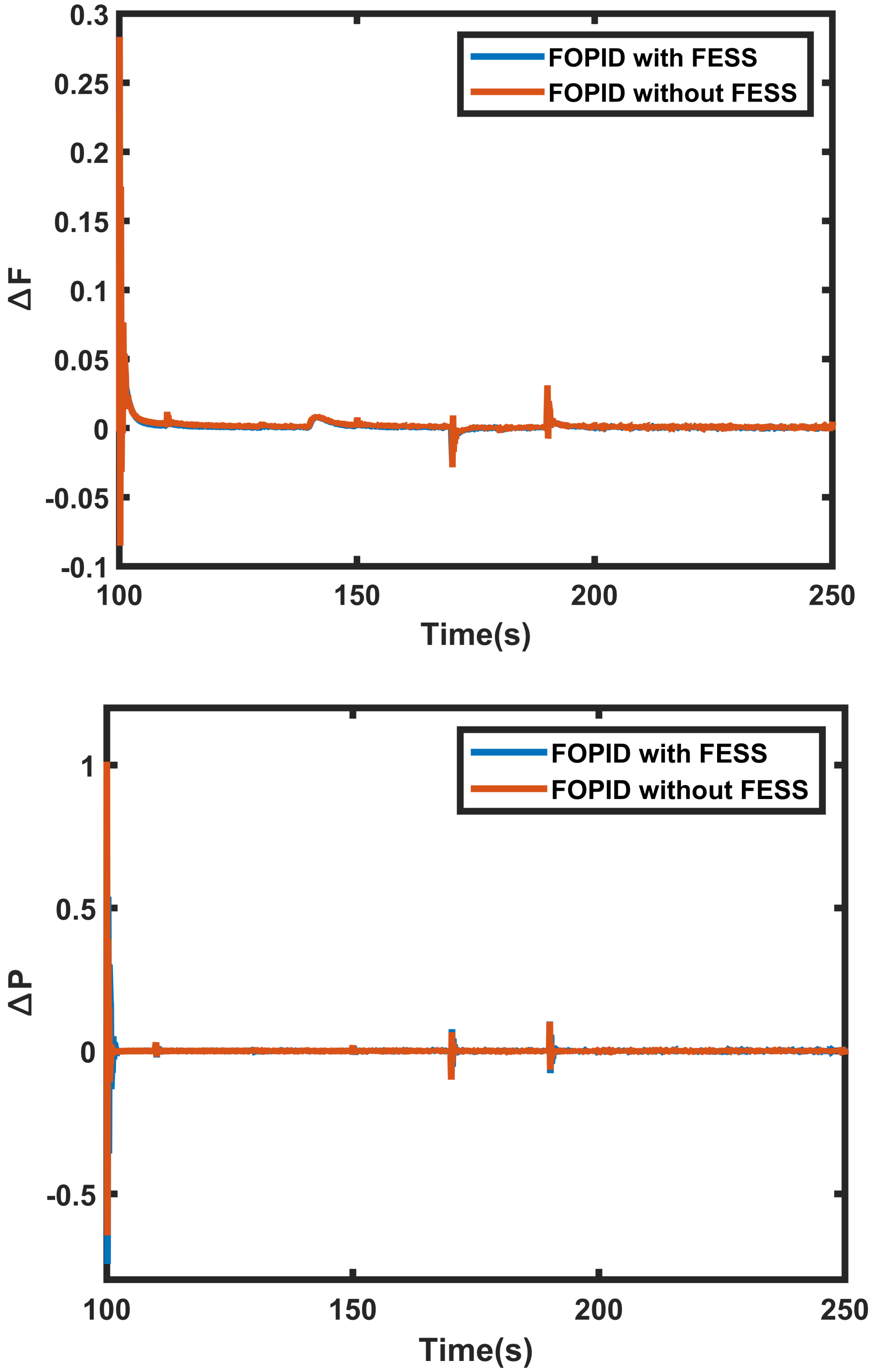

FIGURE 3.15 – Impact of BESS and FESS absence using KH with best FOPID

3.8 Conclusion

In this chapter, the fundamentals of fractional-order control have been introduced and designed for microgrid control. Three optimization methods like GA, PSO and Krill Herd algorithm have been investigated to determining the optimal parameters of the proposed controller. After a review of fractional-order control strategies in control systems and Krill Herd algorithm, a study of the frequency regulation for microgrid system using the fractional-order PID controller based krill Herd algorithm has been given and compared with GA and PSO. Finally, the generalized PID controller is discussed in the frequency domain. This chapter aims to be an introduction and application to the fractional-order controller in the microgrid system, taking the very well-known PID controller as the starting point. The results are compared using the classical PID controller using different optimization techniques. The followed chapter will discuss the hybridization of the fractional controller and fuzzy logic controller.

CHAPTER 4

Fractional Order Fuzzy Controller in Microgrid Frequency regulation

4.1 Introduction

This chapter present the use of hybrid control scheme using Fractional Order fuzzy controller in microgrid frequency control. An overview of fuzzy logic control is shown in details and structure of proposed controller. Optimization of control investigation is achieved using Krill herd algorithm. The results of microgrid frequency control using fractional order fuzzy controller is displayed and analyzed.

4.2 Microgrid concept

This study focuses on the use of isolated microgrid including renewable sources like PV and Wind generators with conventional source like DEG used as secondary sources that can regulate the frequency when imbalance between generation and load occurs through secondary loop control [94]. As shown in Figure 4.1distributed sources are interfaced by electronic devices in order to facilitate the exchange of power between different components like charge and discharge of storages devices. When the load decreases the surplus power from wind and or photovoltaic, the storage devices start to charges and as well as the power in DEG decreases. From literature many simplified model of microgrid using small signal analysis response of microgrid are investigated, where all components are presented by first order transfer function which has been considered sufficient for frequency behaviour analysis and for also simplifies the simulation process. The model of proposed microgrid is presented in Figure 4.1

and its parameters are shown in table 4.1 [95–97].

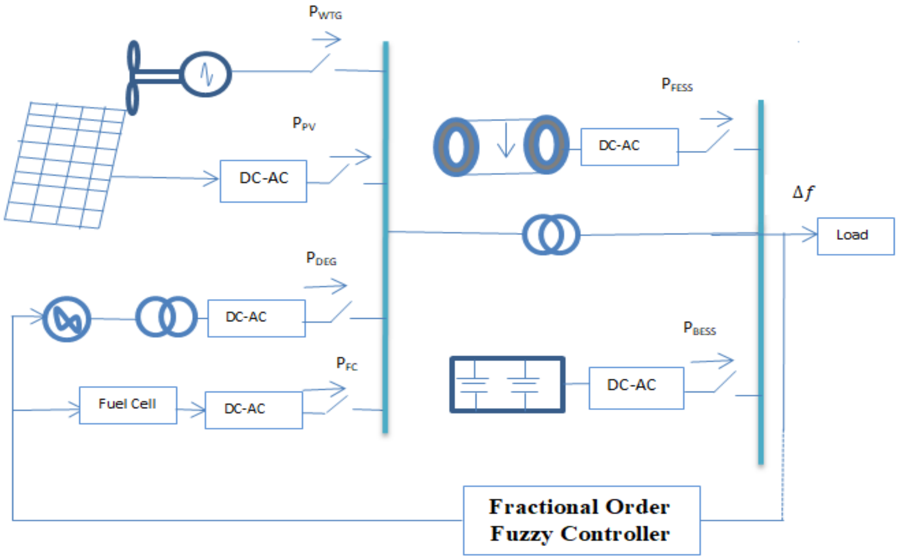

FIGURE 4.1 – Microgrid system with renewable generation and storage devices.

TABLE 4.1 – Microgrid components parameters

Component	**Gain (K)**	**Time constant (s)**
WTG	$K_{WTG} = 1$	$T_{WTG} = 1.5$
PV	$K_{PV} = 1$	$T_{1N} = 0.04$ $T_{1/C} = 0.004$
FC	$K_{FC} = 0.01$	$T_{FC} = 4$
DEG	$K_{DEG} = 0.003$	$T_{DEG} = 2$
BESS	$K_{BESS} = 1$	$T_{BESS} = 0.1$
FESS	$K_{FESS} = 1$	$T_{FESS} = 0.1$

4.3 Hybrid fractional Fuzzy controller

4.3.1 Generality on Fuzzy logic controller

As conventional on-off controller is based on the binary inputs and output, this may cause transition from one state to another state with hard boundaries between transition states which is not suitable to represent the real-world applications. Therefore, it is more convenient to use a control type which has a decision-making algorithm closer to human nature [98].

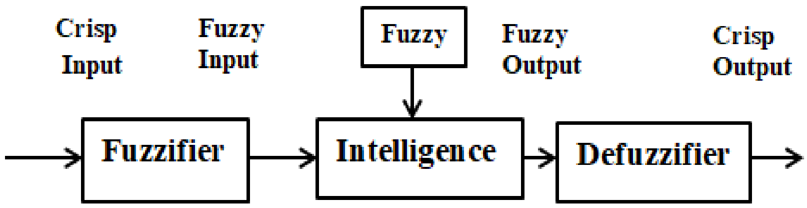

FIGURE 4.2 – The general structure of Fuzzy.

In such scenario, FLC brings quantitative expression between zero and one for the particular parameter. Mathematical expression used here is implied to the rule based if- then statements so that simplicity is brought to the model with more complex input output scenarios.
MacVicar-Whelan [98] constructed the linguistic control protocol forest FLC algorithm. Since, design requires expertise and experience knowledge application would be limited of this type of FLC though they were successful compared to classical controllers [99]. The general structure of Fuzzy consists of three steps named as fuzzication, fuzzy inference process and defuzzication as shown in Figure 4.2.
In the rest step, the degree of crisp inputs is based on each fuzzy set is decided. These fuzzed inputs are then fed to the inference engine in order to evaluate the fuzzy rules stored in the fuzzy rule base. Set of membership functions are used for this transform based on the suitability of the application [100] . Inference engine based on the fuzzy rules generates the Fuzzy output values. Defuzzier transforms the fuzzy set obtained by the inference engine into a crisp value.

Defuzzier achieves output signals based on the output fuzzy sets obtained. Furthermore, FLC performed exceptional character in evolving conventional PI, PID controllers by providing certain advancements in adaptive nature [101].
The applications of FL can be found in many engineering and scientific works.
FL has been successfully used in numerous applications, such as control systems engineering, image processing, power system engineering, industrial automation, robotics, consumer electronics, optimisation, medical diagnosis and treatment plans, as well as stock trading [102]. Regarding the power system, FL has also been useful in the application of parameter identification. A fuzzy identifier has been used to track the parameters of the power system and update the adaptive controller. Based on the knowledge of the plant, the input signals to the fuzzy system are fuzzified : a rule table is constructed and the output signals are finally defuzzified. Parameters of the fuzzy identifier are updated in real time by minimising a defined cost function using the gradient descent method.
It can be seen that in order to design an FL system, four steps are required to be considered : [103]
1– Fuzzification : Fuzzification is the process of mapping the input data into corresponding universes of discourses and converting the input into suitable linguistic values. The task of the fuzzification process can be summarised as follows :
– Measure the values of input variables map the values of input variables to a corresponding universe of discourse convert the input data into appropriate linguist values.

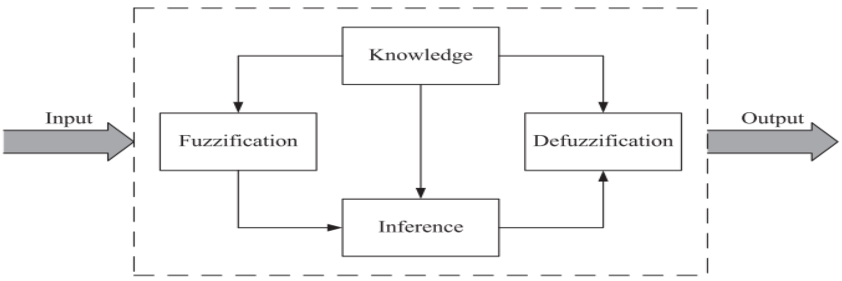

FIGURE 4.3 – Structure of a fuzzy system.

2– Knowledge base : The purpose of the knowledge base or rule base step is to provide definitions that express the relation between the input and output fuzzy variables. It defines the control goals by means of a set of linguistic control rules. The rule base is

often expressed in the form of IFTHEN rules.
3–Fuzzy inference : The fuzzy inference is considered the core of any FL system. The fuzzy inference mechanism is a process by which the input values for each of the fuzzy variables in the antecedent are matched with all rules in the fuzzy rule base and an inferred fuzzy set is obtained. The membership values obtained in the fuzzification step are combined through a specific fuzzy operator to obtain the firing strength of each rule. Based on the firing strength, the consequent part of each qualified rule is produced.

4.3.2 Fractional order PID

A general approach is desired for optimizing performance of a FOPID control loop regardless of the plant type. However, there is a vast array of well-established tuning approximated by a simple model to a certain degree of validity ; it may be used to obtain initial conventional PID controller parameters. These parameters can then be further optimized to achieve better performance using techniques for common model types. So if a fractional-order model can be approximated by a simple model to a certain degree of validity, it may be used to obtain initial conventional PID controller parameters [104].
A block diagram of the fractional-order $PI^{\lambda}D^{\mu}$ control system and a model in the Laplace domain of $PI^{\lambda}D^{\mu}$ the controller is discussed and reported in chapter4.

4.3.3 Fractional order Fuzzy Controller

The design of fractional order fuzzy controller has been presented with The input of controller are considered the gain Ke,kd and the output are known as $\{K_{pi}, K_{pd}\}$ of scaling factors (SFs) [105–107]. The frequency deviation ΔF is the input of the hybrid controller and the output is the control signal ΔU. The diagram scheme of the proposed controller is displayed by the Figure 4.4 as bellow.
The corresponding membership function of hybrid fractional order fuzzy logic controller is shown in Figure 4.5. The fuzzy linguistic $NL, NM, NS, ZR, PS, PM, PL$ represent Negative Large, Negative Medium, Negative Small, Zero, Positive Small, Positive Medium and Positive Large Respectively as reported in table 4.2 . The crisp output of fuzzy Logic controller is determined by using center of gravity method of

defuzzification The Fractional Order PID Fuzzy controller SFs and integral-differential orders$\{K_e, K_d, K_{PI}, K_{PD}, \mu, \lambda\}$ optimized using KH for fixed rule based membership function type [108–110].

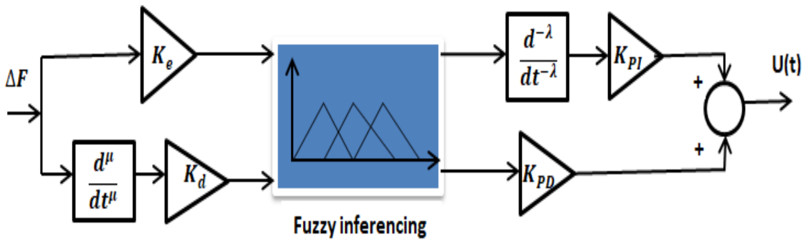

FIGURE 4.4 – Schematic of the fractional order fuzzy PID controller.

TABLE 4.2 – Rule-base table with 49 rules

$\frac{d^{\mu}e}{dt^{\mu}}$ \ e	NB	NM	NS	ZR	PS	PM	PL
PL	ZR	PS	PM	PL	PL	PL	PL
PM	NS	ZR	PS	PM	PL	PL	PL
PS	NM	NS	ZR	PS	PM	PL	PL
ZR	NB	NM	NS	ZR	PS	PM	PL
NS	NB	NB	NM	NS	ZR	PS	PM
NM	NB	NB	NB	NM	NS	ZR	PS
NB	NB	NB	NB	NB	NM	NS	ZR

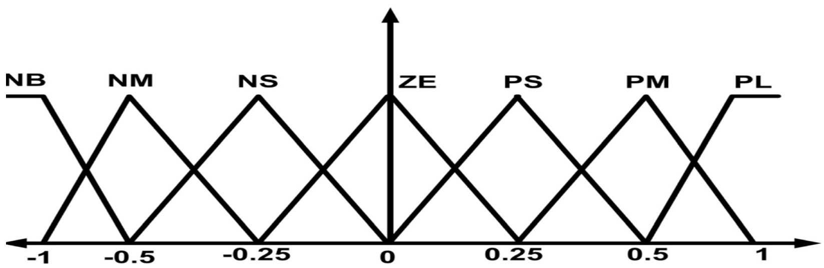

FIGURE 4.5 – Rule base for error, fractional rate of error and FLC output.

4.4 Objective function and optimization strategy

The objective function (J) for optimization has been considered as an integral performance index over the simulation period of Tmax 120s, using the weighted sum of squared frequency deviation and the deviation of control signal u from its expected steady state values as given as follow :

$$ISE = \int_{T_{min}}^{T_{max}} \left[w_1 \left(\Delta f\right)^2 + w_2 \left(u - u_{ss}\right)^2 \right] dt \tag{4.1}$$

In Eq 4.1 the first term represents the Integral of Squared Error (ISE) of grid frequency deviation and the second term is known as the Integral of Squared Deviation of Controller Output ($ISDCO$) for a disturbance rejection task of the controller. since it is placed in the feedback path. In Eq 4.1, the weights w_1 and w_2 govern the relative importance of each term in the objective function. They are taken as $w_1 = w_2 = 1$ to give equal importance to both. Here, the steady state control signals Uss changes after each switching in the generation and load. For the present simulation study [111, 112].

$$T_{max} = 120s \quad and \quad u_{ss} = 0.81H(t) + 0.17H(t-40) + 1.12H(t-80) \tag{4.2}$$

In this chapter KH algorithm is employed to optimize the proposed controllers parameters. A literature view on Krill Herd Algorithm has been presented in the previous chapter 3, which address details about this methods and application in frequency microgrid system [88], [113, 114].

4.5 Results and Discussion

This section focuses on analyzing the stability and improving of frequency and power deviations in a MG using the proposed control method. In order to enhance the system stability two controllers like Fuzzy FOPID and FOPID are employed tuned using KH algorithm. The robustness against the variation in system parameters as well as with disconnecting storage system like UC is verified.

4.5.1 System performances in nominal condition of the Microgrid system

The proposed microgrid configuration is simulated with different controller structures and tuned using KH as in section 4, where all the components of system are presented by a linear transfer function. The total simulation time is considered as 100 seconds.

The corresponding power from renewable sources with the load demand are considered independently of controller structure and used as disturbances components as in Figure 4.6.

It has been found from previous study like in [54] that the Fractional PID controller tuned with GA overcome the classical PID controller in convergence and frequency regulation.

Similar analysis of system with the fuzzy PID and FOPID controllers are shown in figure reporting the corresponding frequency and power deviations with the best controllers parameters along with the generated power from different components of system.

The convergence characteristics for different KH algorithms for each of the controllers are presented in Figure 4.6.

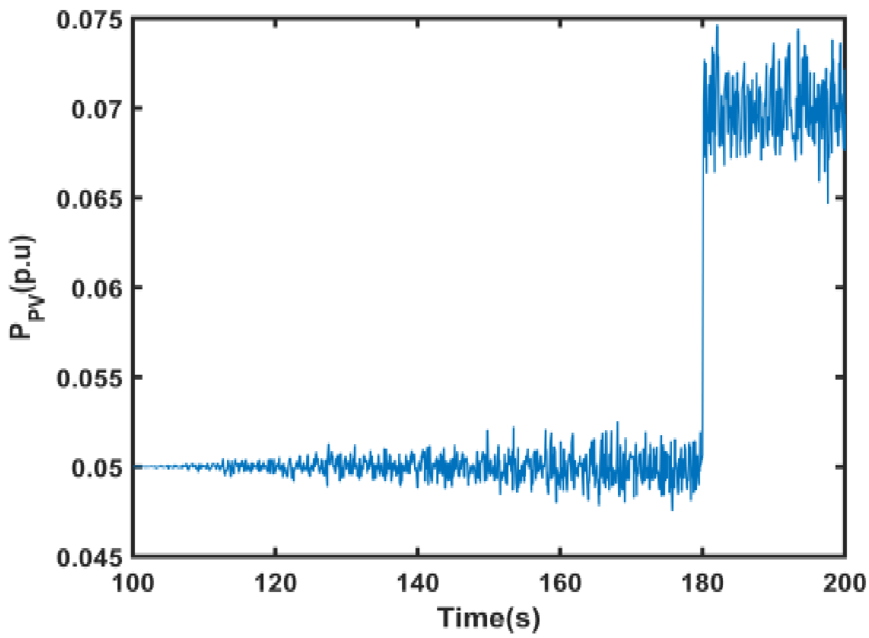

(a)

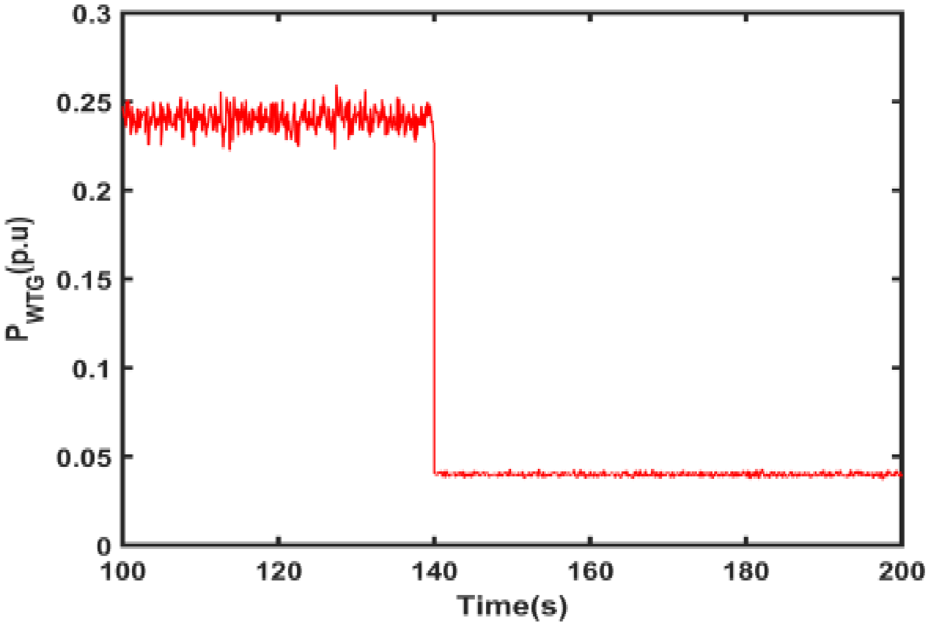
0.3
0.25
0.2
0.15
0.1
0.05
0
P_{WTG}(p.u)
100
120
140
160
180
200
Time(s)

(b)

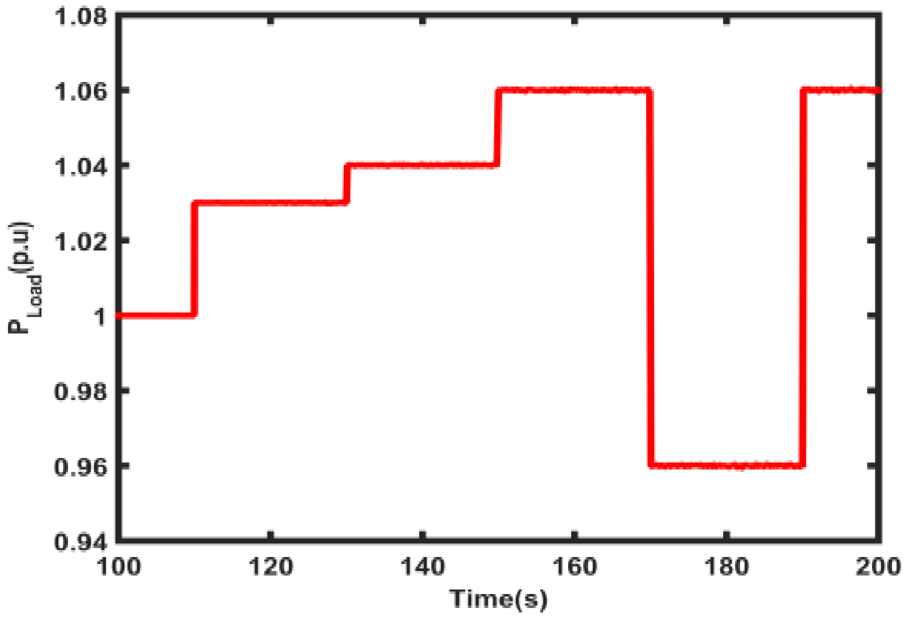
1.08
1.06
1.04
1.02
1
0.98
0.96
0.94
P_{Load}(p.u)
100
120
140
160
180
200
Time(s)

(c)

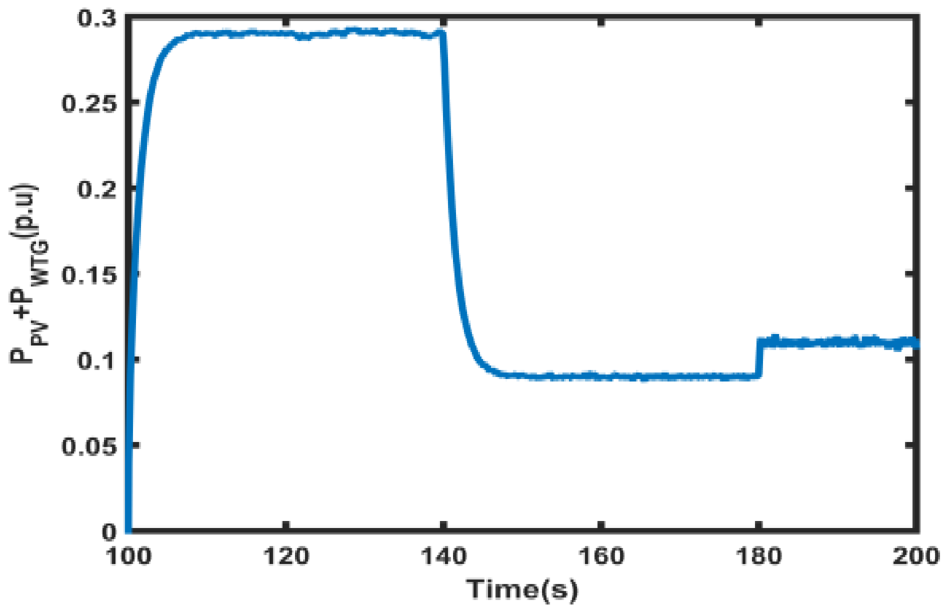

(d)

FIGURE 4.6 – Generated Power from PV(a),WTG(b) and Power Demand PL(c) with (PV^+,WTG)(d).

Figure 4.6 shows the corresponding of stochastic nature of power generation from renewable sources and load demand. A sudden fluctuation is occurred in both wind and solar power which automatically appear in steady state deviation of system frequency and power.

The controllers are designed to take in consideration the high change in generation power depending on weather condition along with load power perturbations. Thence, the controllers are anticipated to work with a large variability in generation and load.

4.5.2 Frequency and power deviations $(\Delta F, \Delta P)$ with signal control signal for FOPID and FLC-FOPID

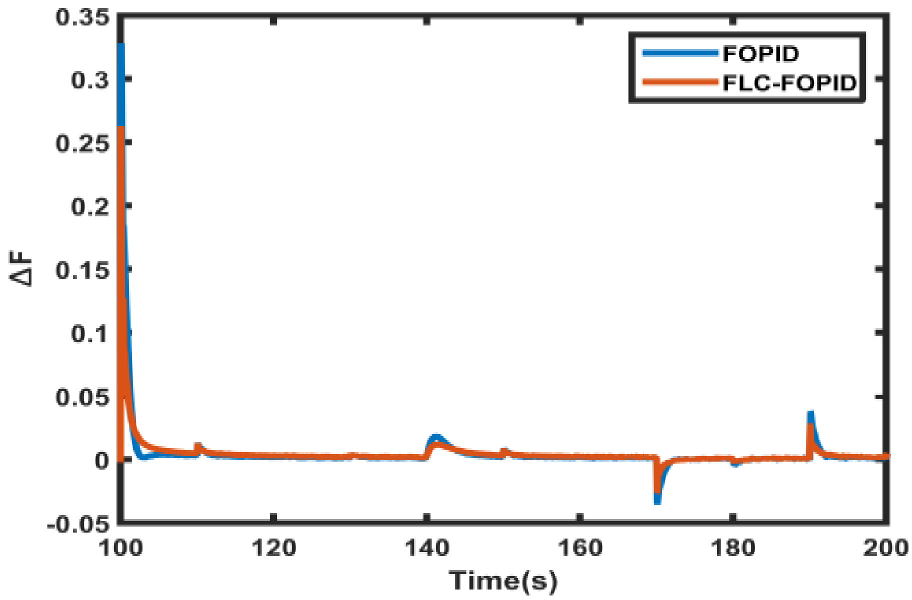

(a)

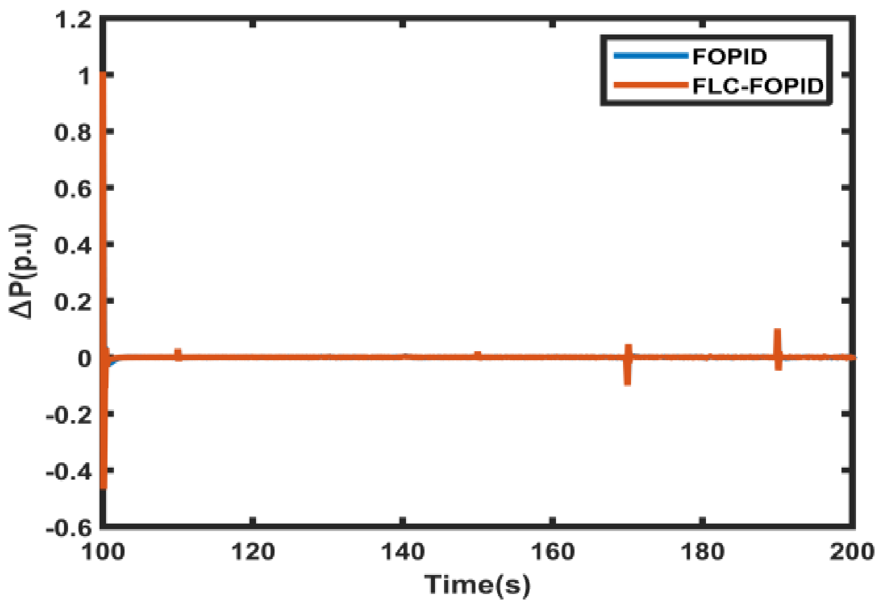

(b)

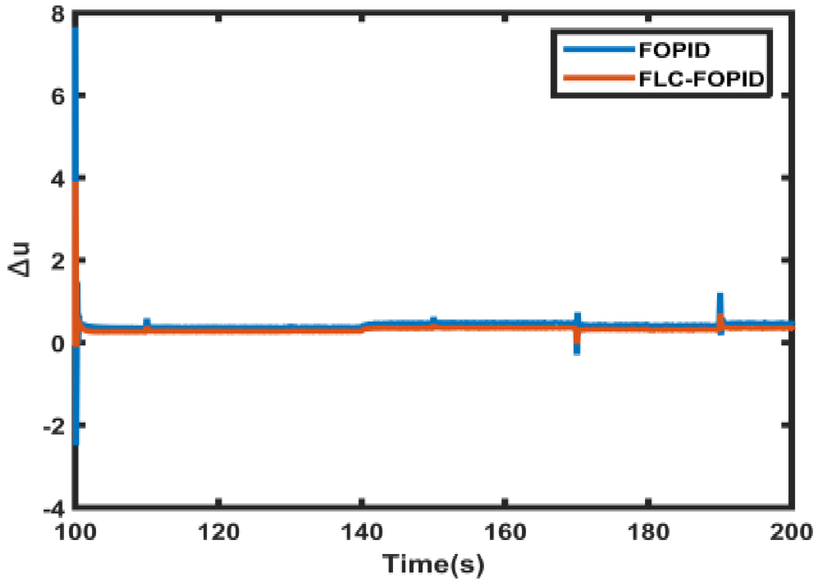

(c)

FIGURE 4.7 – Frequency (a) and Power(b) deviations with signal control(c) for FOPID and Fuzzy-FOPID.

4.5.3 Generated power of different components of Microgrid for FOPID and FLC-FOPID

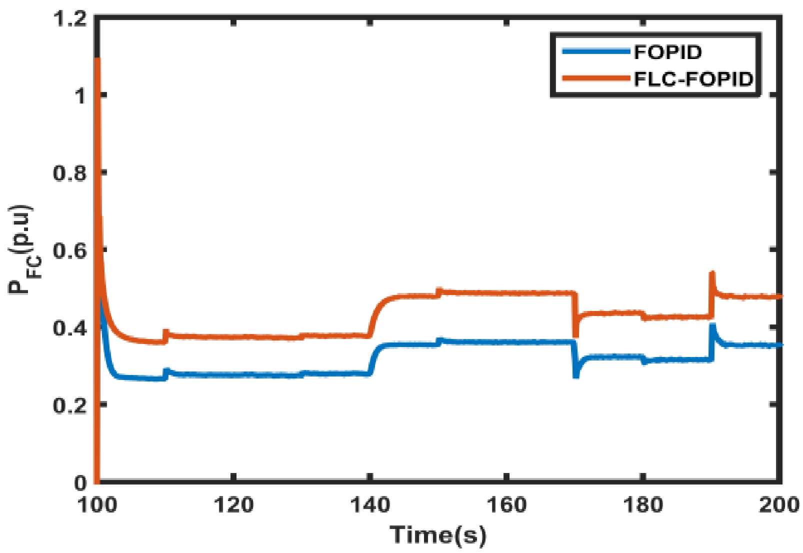

(a)

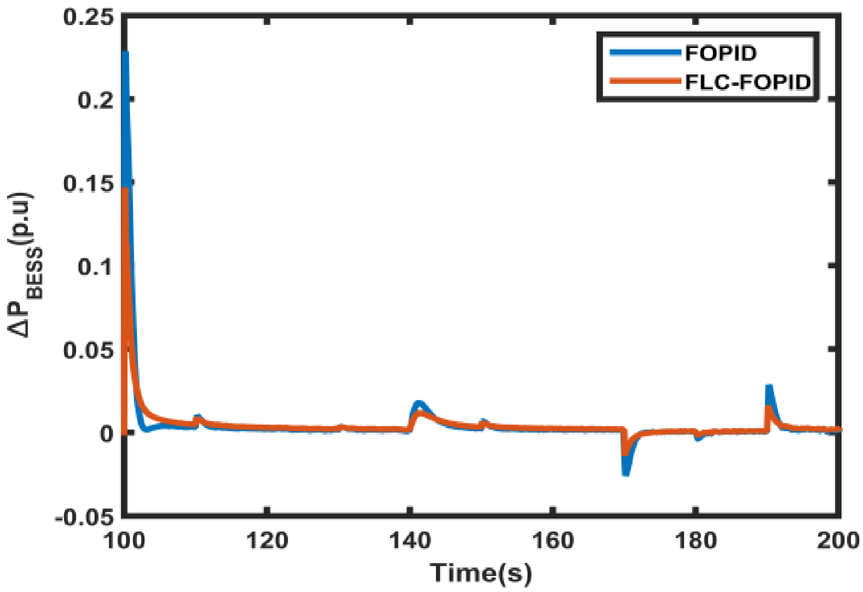

(b)

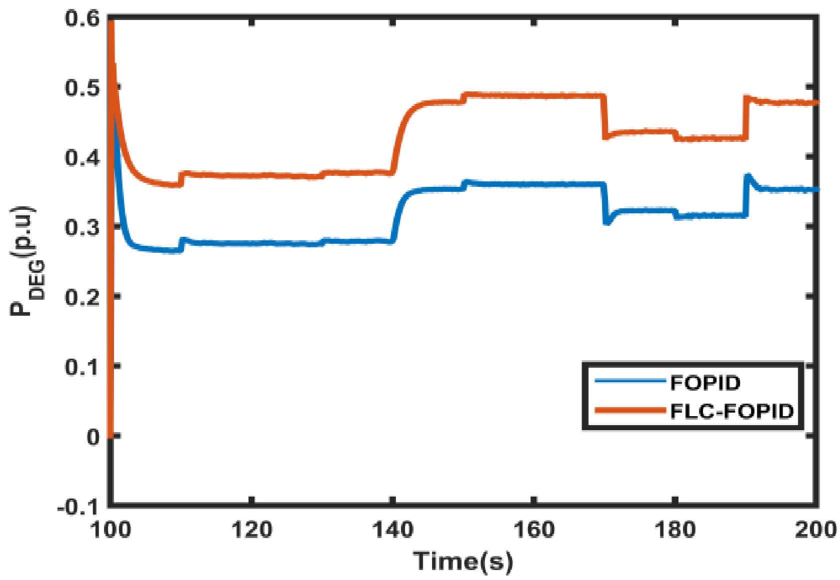

(c)

FIGURE 4.8 – Microgrid components power $P_FC(a)$, $P_BESS(b)$ and P_DEG(c) with FOPID and FLC-FOPID.

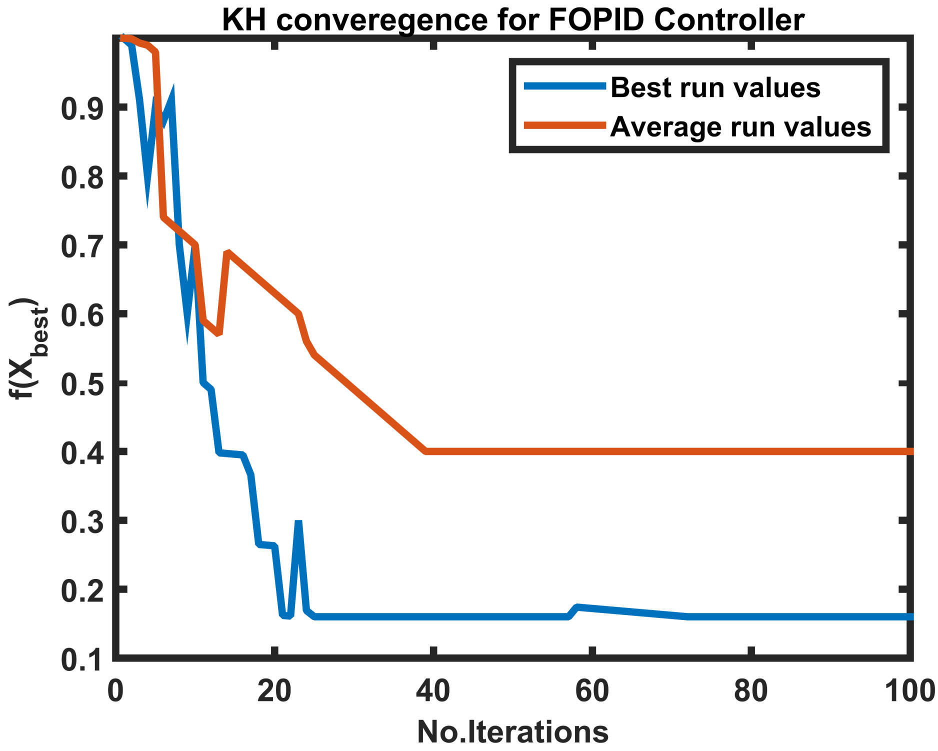

(a)

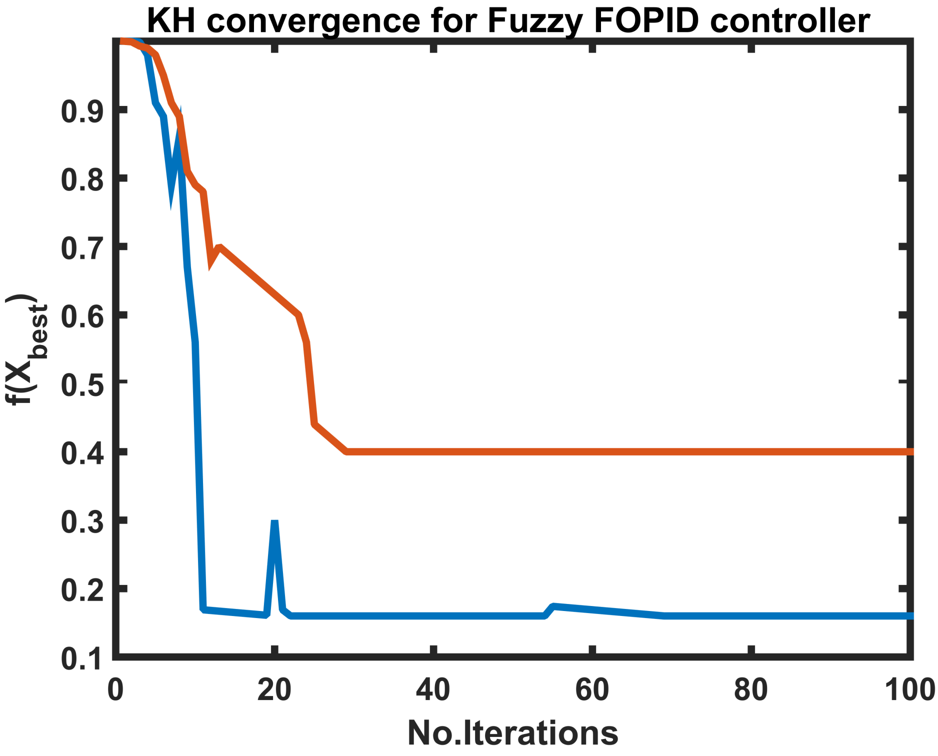

(b)

FIGURE 4.9 – Convergence characteristics of KH algorithm for the two controllers FOPID(a) and FL-FOPID(b).

It is previously shown that for the case of the FOPID overcoming the PID controller in term of performances system and stable. However from Figure 4.7, it is proved that with the best parameters of Fuzzy FOPID and FOPID obtained by the KH algorithm the frequency and power deviations are improved with Fuzzy FOPID in comparison with FOPID.
Also the convergence characteristics for these two controllers as shown in Figure 4.9 indicate that the Fuzzy FOPID-KH converges to the solution quickly as compared to the FOPID- KH. The results indicate towards a general trend that the KH algorithm is better in the two kinds of controllers. From the frequency and power deviations curves, it is easy to distinguish that the fuzzy FOPID controller works better than the FOPID controller.
The corresponding individual powers of the different components of the proposed microgrid system for these cases are shown in Figure 4.8.
However, from the control signal curve in Figure 4.7 , it can be observed that the band of oscillations for the fuzzy FOPID controller is less than that with the FOPID controller. This is especially important from the practical implementation point of view because the control signal actuates mechanical components like the FESS, BESS, and DEG etc.
Also, in Figure 4.8 positive powers in FC, DEG indicates that they are power producing and positive and negative powers in FESS and BESS signify that they are energy storing elements in the microgrid system.

4.5.4 Microgrid Parametric Robustness for optimum solutions of FLC-FOPID

The system is simulated under parameters increase and decrease using the optimal value of the two proposed controllers. The corresponding performance measures (J) are reported in table4.3 The performance is better with fuzzy FOPID controller than with FOPID controller. Also, the severity of the performance deterioration is the minimum for fuzzy FOPID as shown Figure 4.10.

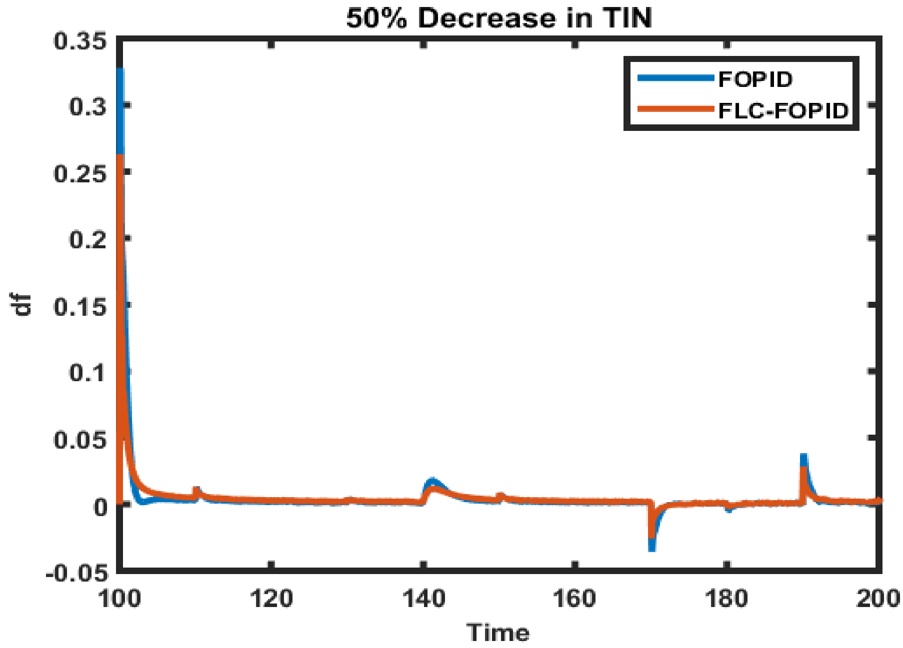
50% Decrease in TIN
FOPID
FLC-FOPID
0.35
0.3
0.25
0.2
0.15
0.1
0.05
0
-0.05
df
100
120
140
160
180
200
Time

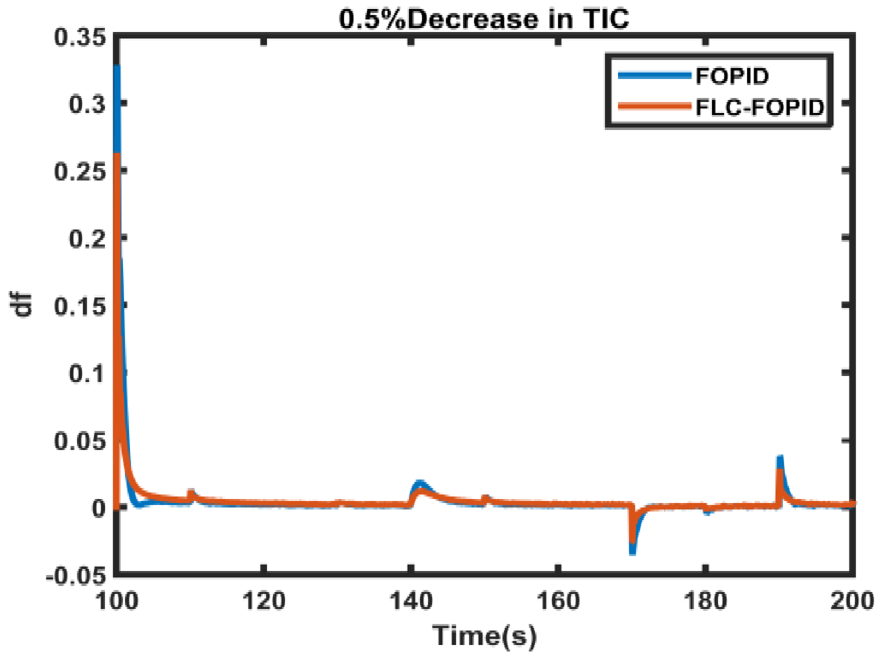
0.5%Decrease in TIC
FOPID
FLC-FOPID
0.35
0.3
0.25
0.2
0.15
0.1
0.05
0
-0.05
df
100
120
140
160
180
200
Time(s)

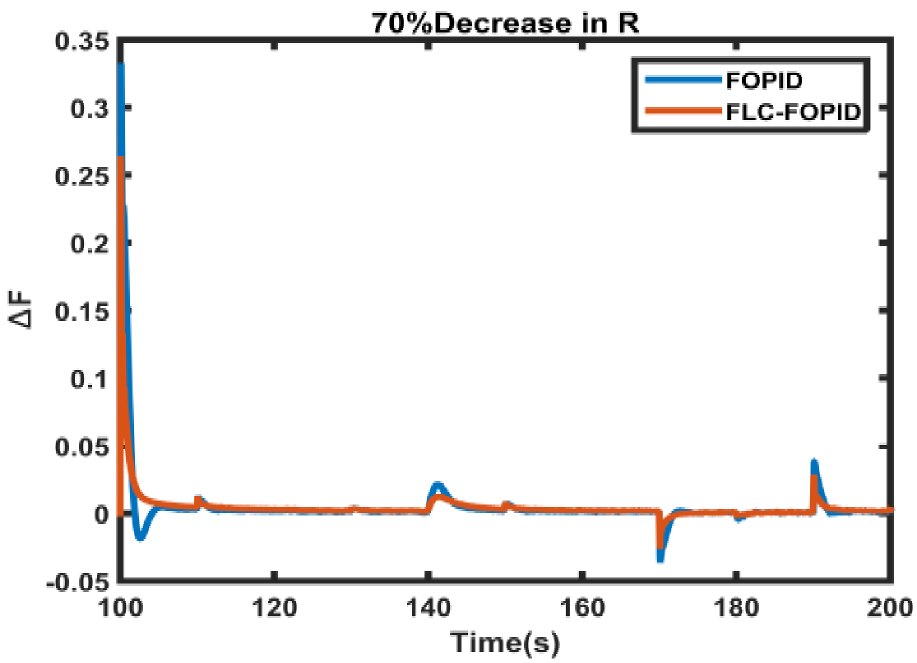
70%Decrease in R
FOPID
FLC-FOPID
ΔF
Time(s)
0.35
0.3
0.25
0.2
0.15
0.1
0.05
0
-0.05
100
120
140
160
180
200

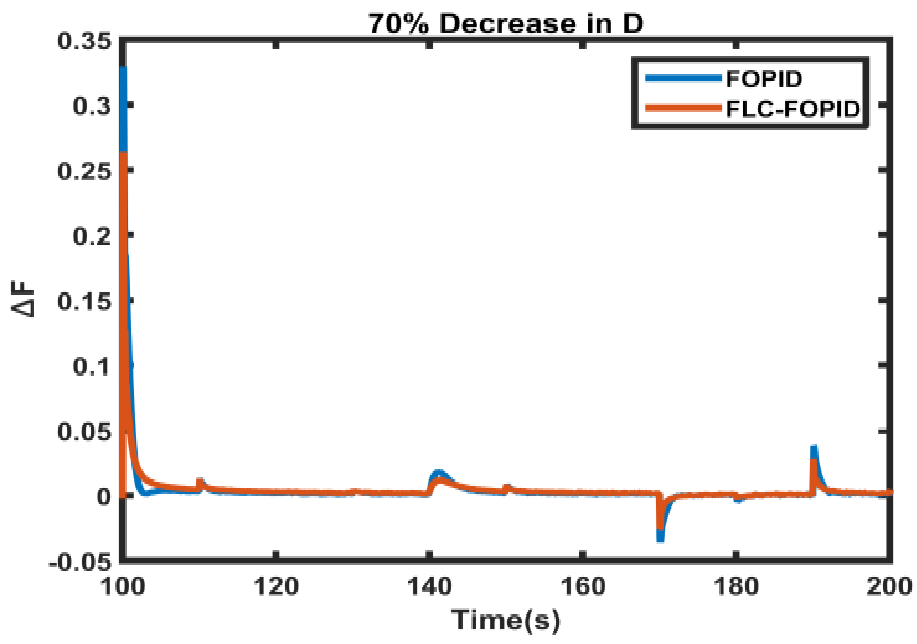
70% Decrease in D
FOPID
FLC-FOPID
ΔF
Time(s)
0.35
0.3
0.25
0.2
0.15
0.1
0.05
0
-0.05
100
120
140
160
180
200

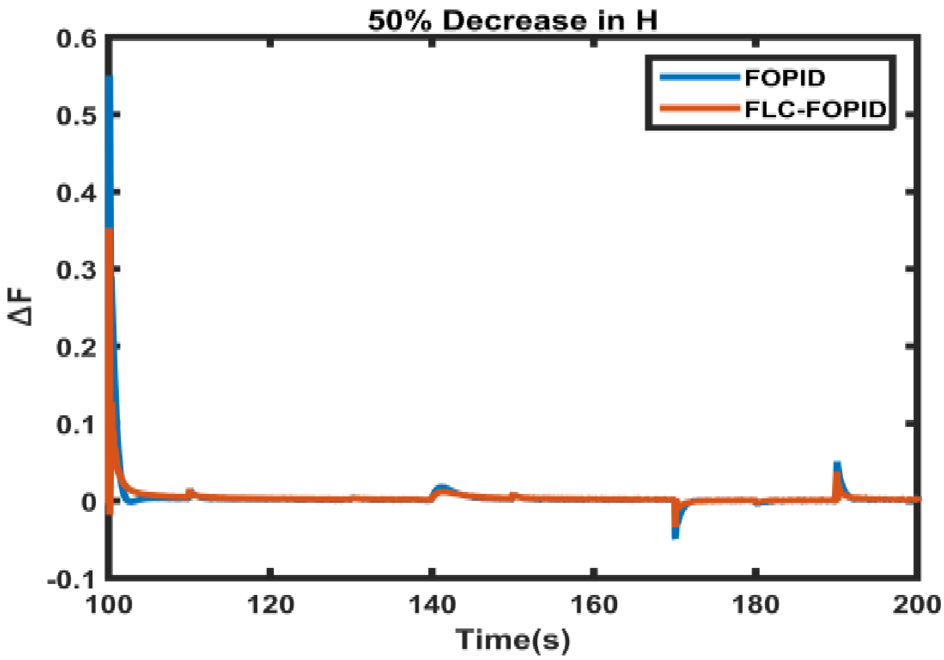
50% Decrease in H
FOPID
FLC-FOPID
ΔF
0.6
0.5
0.4
0.3
0.2
0.1
0
-0.1
100
120
140
160
180
200
Time(s)

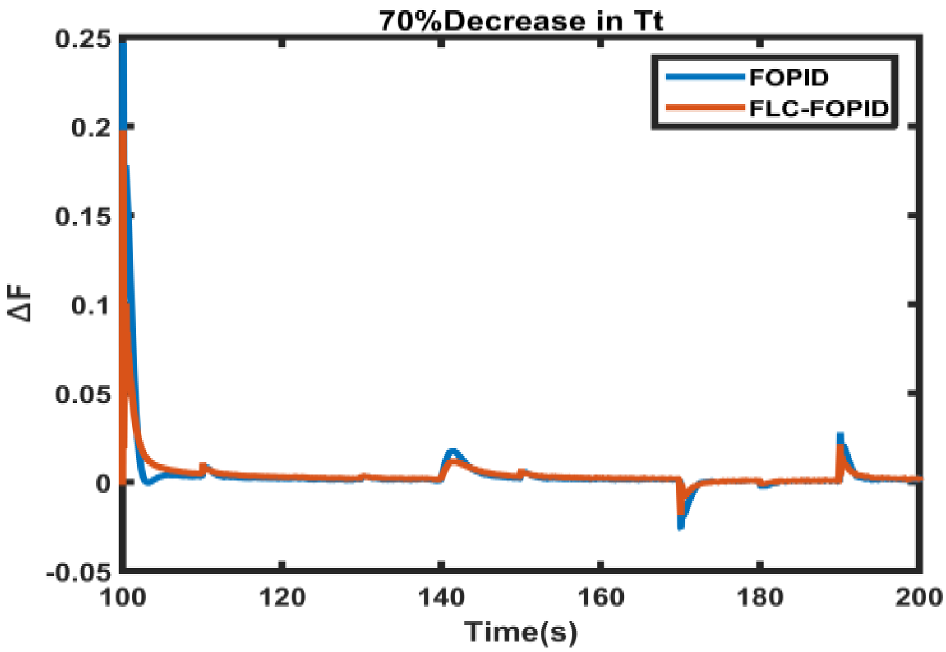
70%Decrease in Tt
FOPID
FLC-FOPID
ΔF
0.25
0.2
0.15
0.1
0.05
0
-0.05
100
120
140
160
180
200
Time(s)

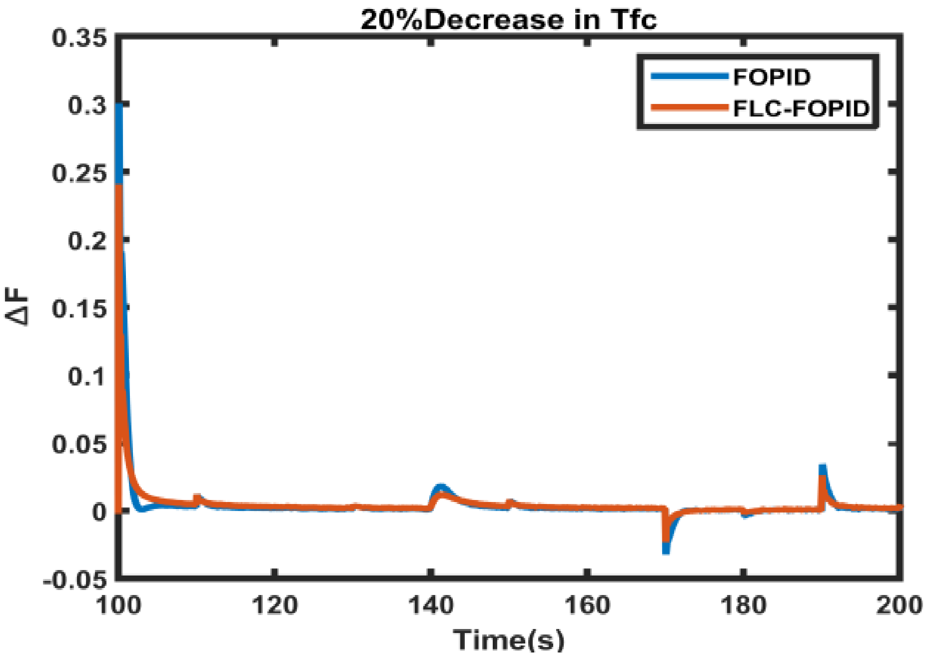
20%Decrease in Tfc
FOPID
FLC-FOPID
ΔF
Time(s)
0.35
0.3
0.25
0.2
0.15
0.1
0.05
0
-0.05
100
120
140
160
180
200

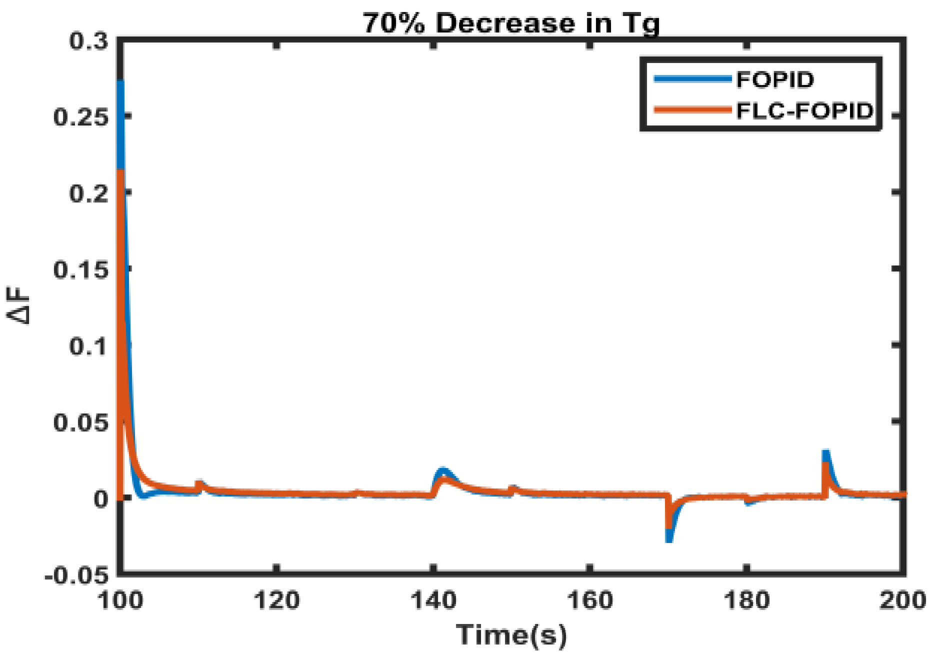
70% Decrease in Tg
FOPID
FLC-FOPID
ΔF
Time(s)
0.3
0.25
0.2
0.15
0.1
0.05
0
-0.05
100
120
140
160
180
200

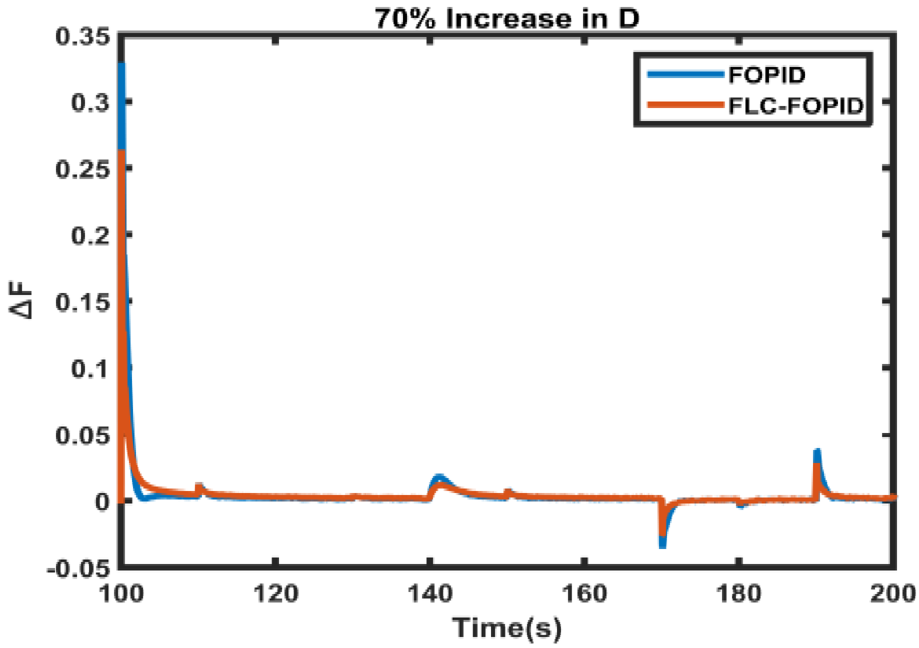
70% Increase in D
FOPID
FLC-FOPID
ΔF
0.35
0.3
0.25
0.2
0.15
0.1
0.05
0
-0.05
100
120
140
160
180
200
Time(s)

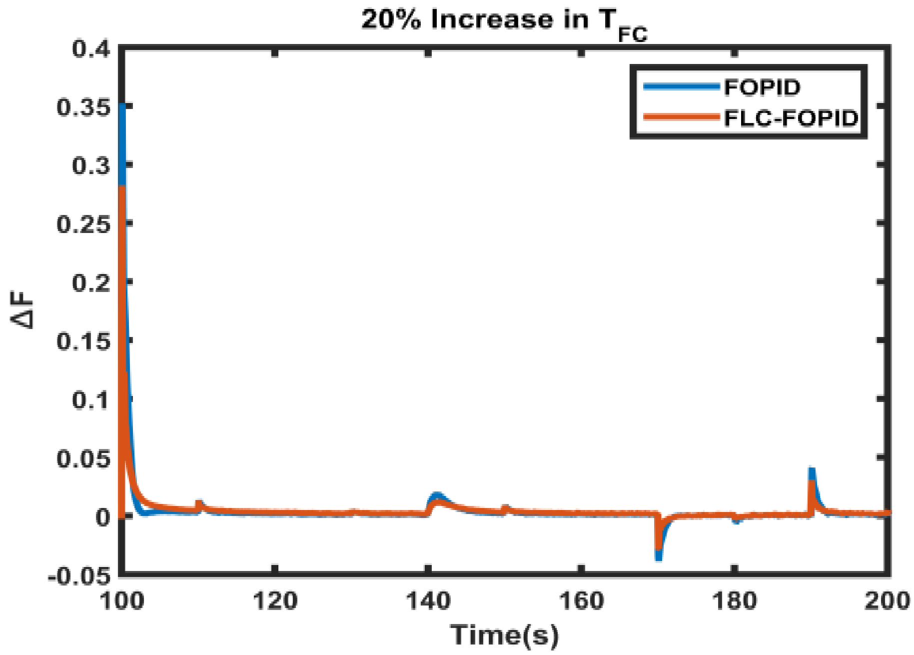
20% Increase in T_{FC}
FOPID
FLC-FOPID
ΔF
0.4
0.35
0.3
0.25
0.2
0.15
0.1
0.05
0
-0.05
100
120
140
160
180
200
Time(s)

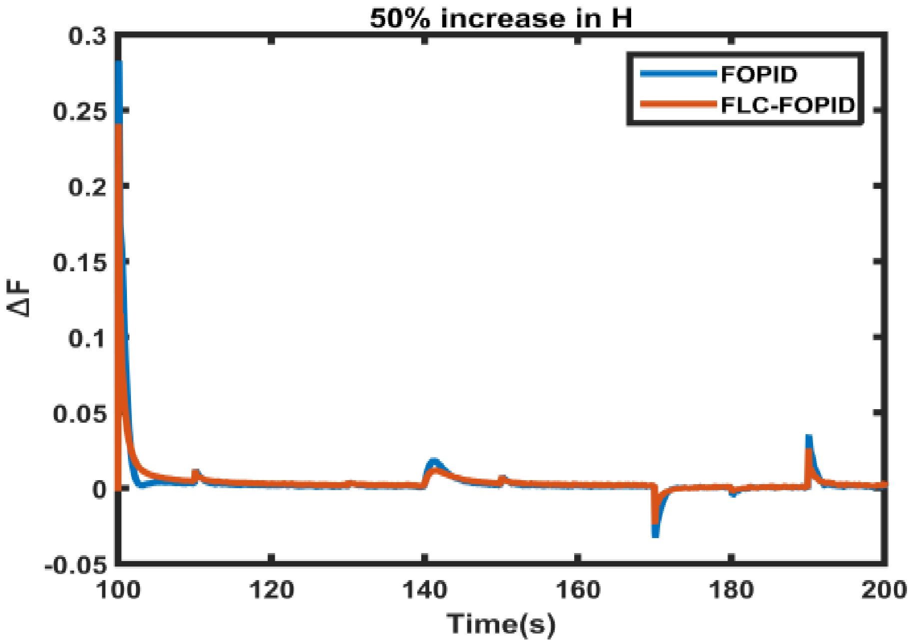
50% increase in H
FOPID
FLC-FOPID
ΔF
Time(s)

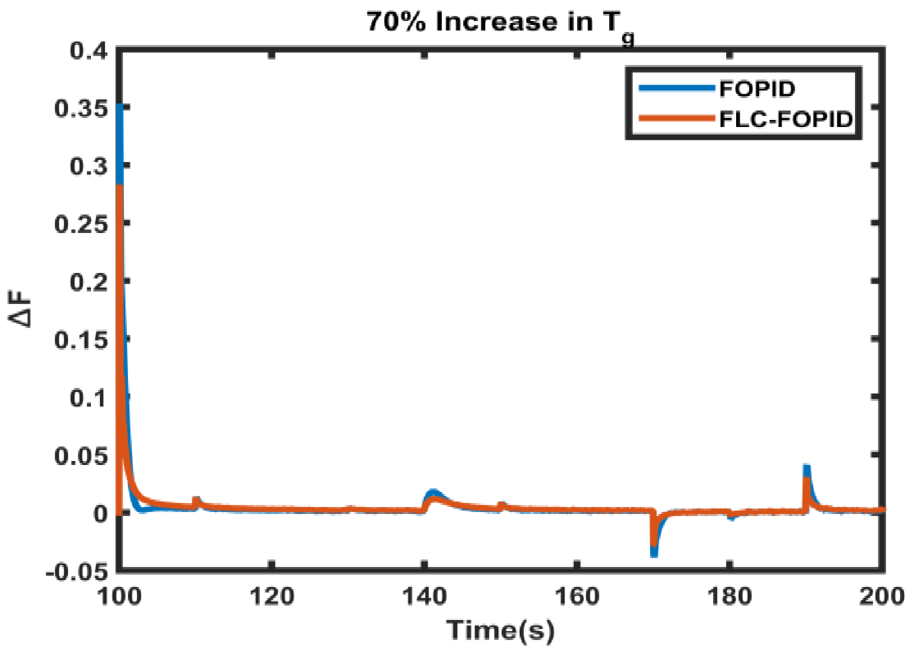
70% Increase in T g
FOPID
FLC-FOPID
ΔF
Time(s)

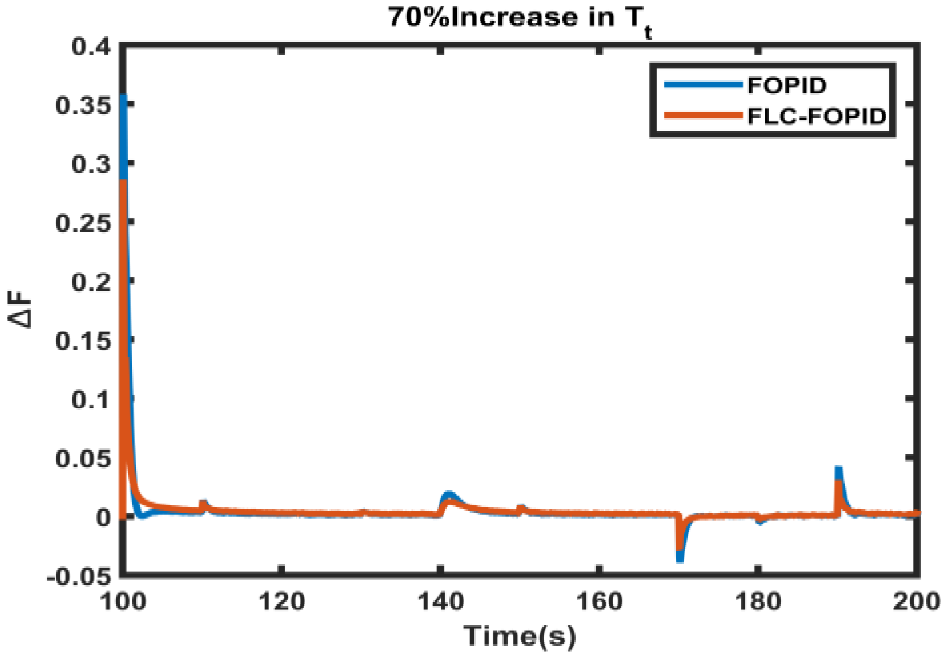
70%Increase in T_t
FOPID
FLC-FOPID
ΔF
Time(s)
0.4
0.35
0.3
0.25
0.2
0.15
0.1
0.05
0
-0.05
100
120
140
160
180
200

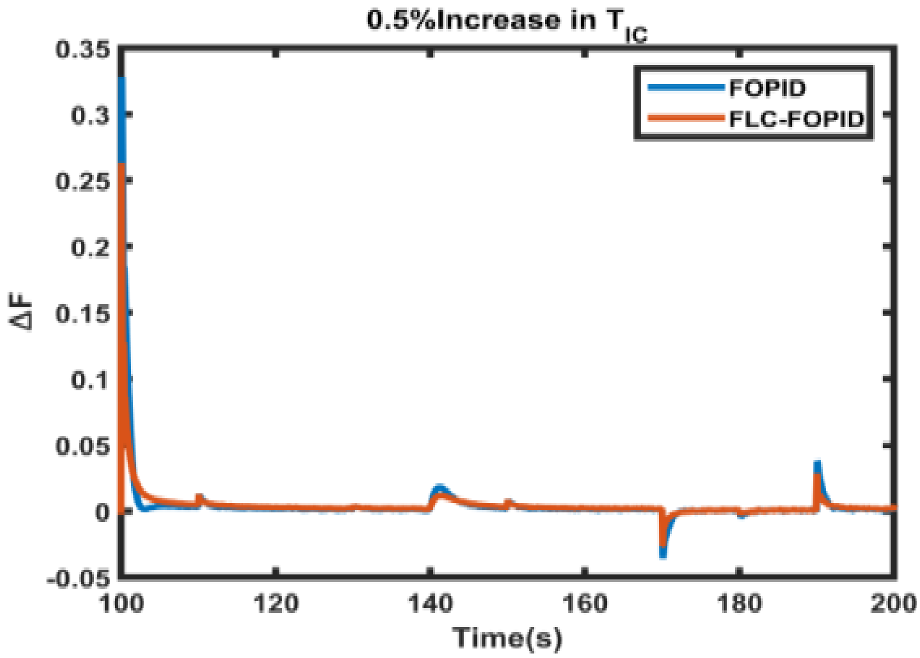
0.5%Increase in T_{IC}
FOPID
FLC-FOPID
ΔF
Time(s)
0.35
0.3
0.25
0.2
0.15
0.1
0.05
0
-0.05
100
120
140
160
180
200

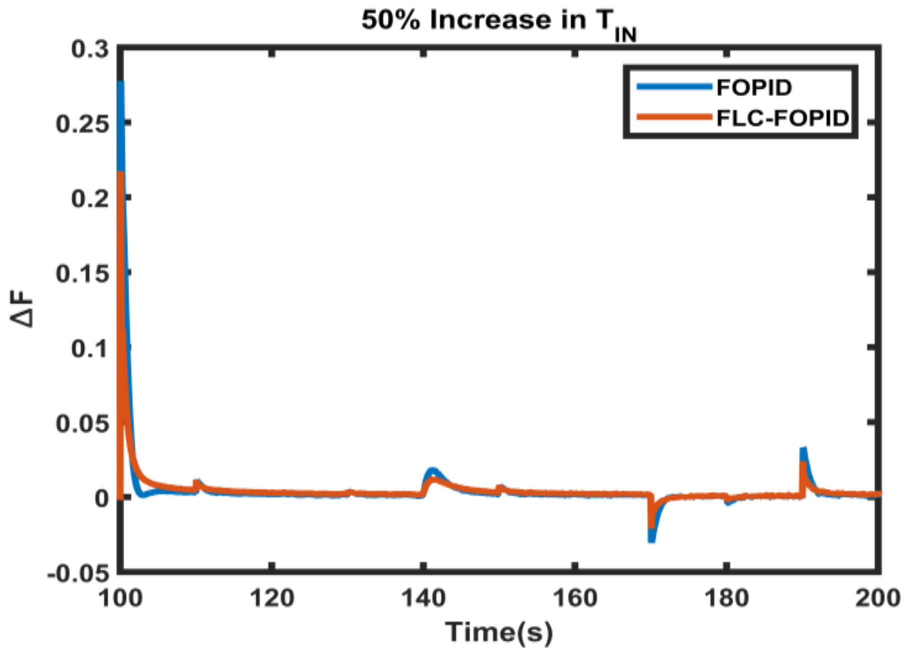

FIGURE 4.10 – Robustness against parametric change of Microgrid

TABLE 4.3 – Robustness for perturbation in microgrid parameters

Microgrid parameters	Perturbations ±	*Controllers*	*J increase*	*J decrease*
D	70%	FOPID	0.2989	0.2985
		FLC-FOPID	0.01042	0.01047
2H	50%	User B	0.2872	0.2915
		FLC-FOPID	0.009917	0.01017
R	70%	FOPID	0.2974	0.3058
		FLC-FOPID	0.01034	0.01112
T_{FC}	20%	FOPID	0.2978	0.2987
		FLC-FOPID	0.01119	0.09665
T_g	70%	FOPID	0.2979	0.2996
		FLC-FOPID	0.01119	0.009275
T_t	70%	FOPID	0.3003	0.296
		FLC-FOPID	0.01233	0.08356

Microgrid parameters	Perturbations ±	*Controllers*	*J increase*	*J decrease*
T_{IC}	0.5%	FOPID	0.2984	0.2974
		FLC-FOPID	0.01045	0.01035
T_{IN}	50%	FOPID	0.2993	0.299
		FLC-FOPID	0.009981	0.009615

4.5.5 Robustness against disconnecting of UC

Robustness of the obtained solutions is verified next by disconnecting Ultracapacitor. The Figure 4.11 reports the corresponding response of frequency and power deviations with and without the UC using Fuzzy FOPID controller.

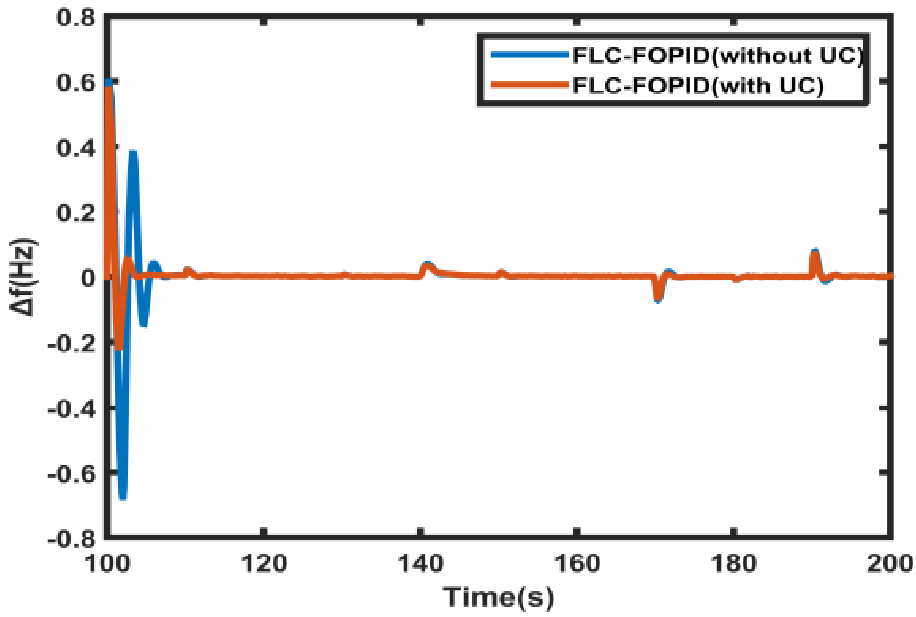

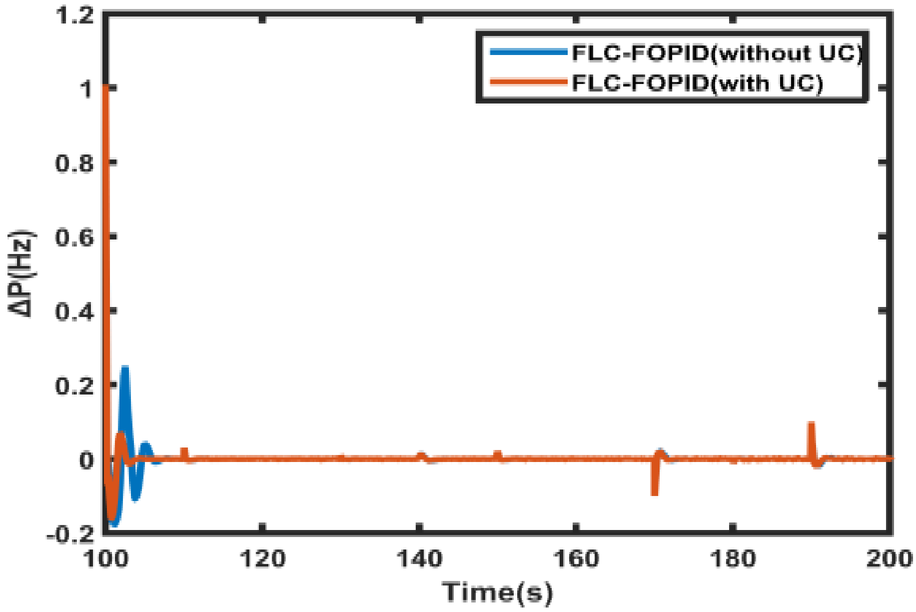
FLC-FOPID(without UC)
FLC-FOPID(with UC)
ΔP(Hz)
Time(s)
1.2
1
0.8
0.6
0.4
0.2
0
-0.2
100
120
140
160
180
200

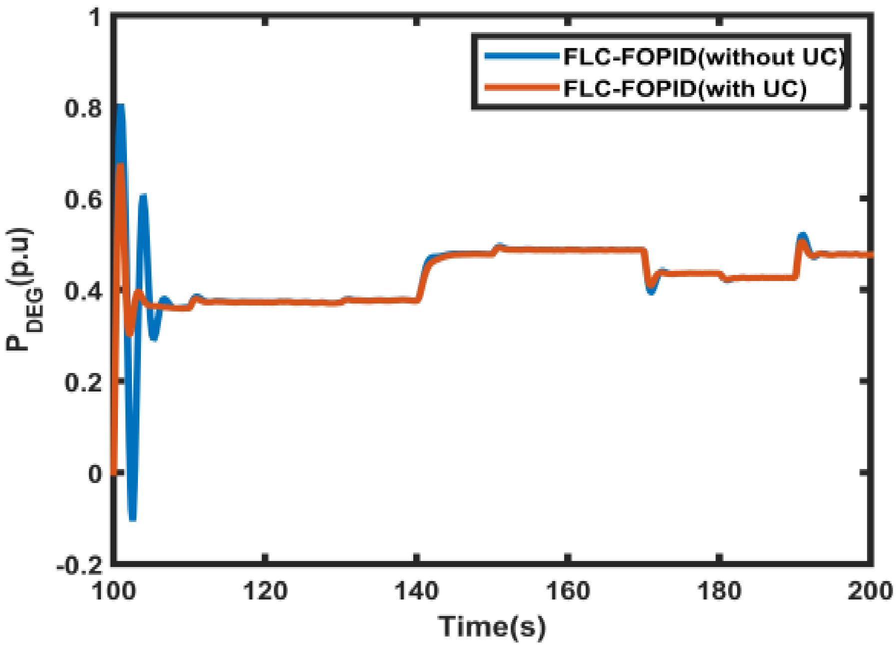
FLC-FOPID(without UC)
FLC-FOPID(with UC)
P_{DEG}(p.u)
Time(s)
1
0.8
0.6
0.4
0.2
0
-0.2
100
120
140
160
180
200

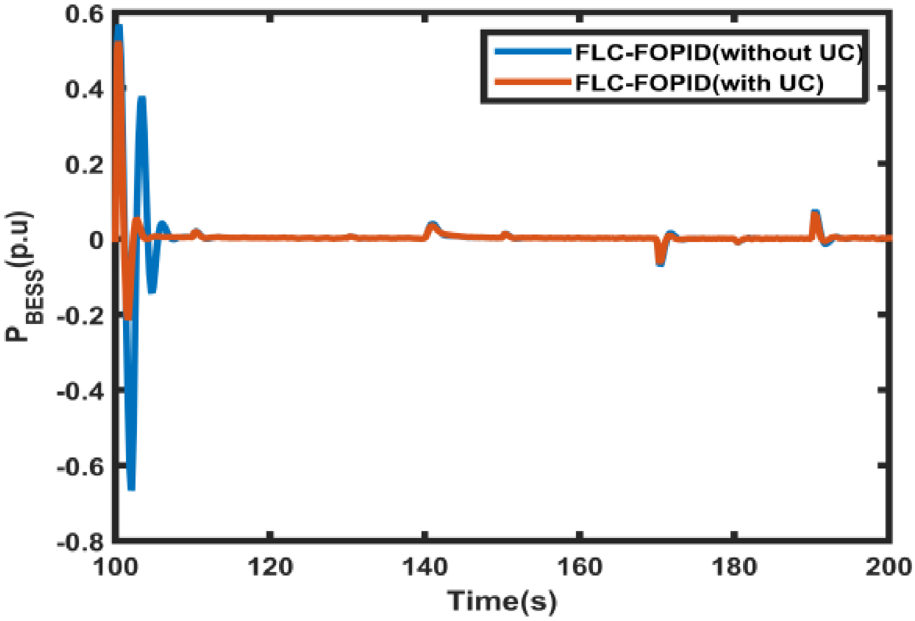

FLC-FOPID(without UC)
FLC-FOPID(with UC)
0.6
0.4
0.2
0
-0.2
-0.4
-0.6
-0.8
P_{BESS}(p.u)
100
120
140
160
180
200
Time(s)

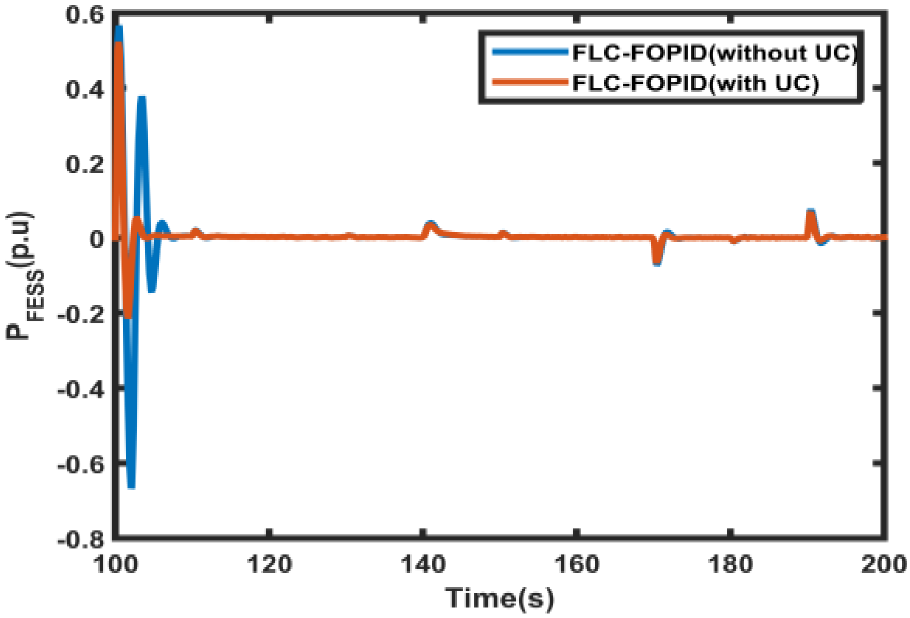

FLC-FOPID(without UC)
FLC-FOPID(with UC)
0.6
0.4
0.2
0
-0.2
-0.4
-0.6
-0.8
P_{FESS}(p.u)
100
120
140
160
180
200
Time(s)

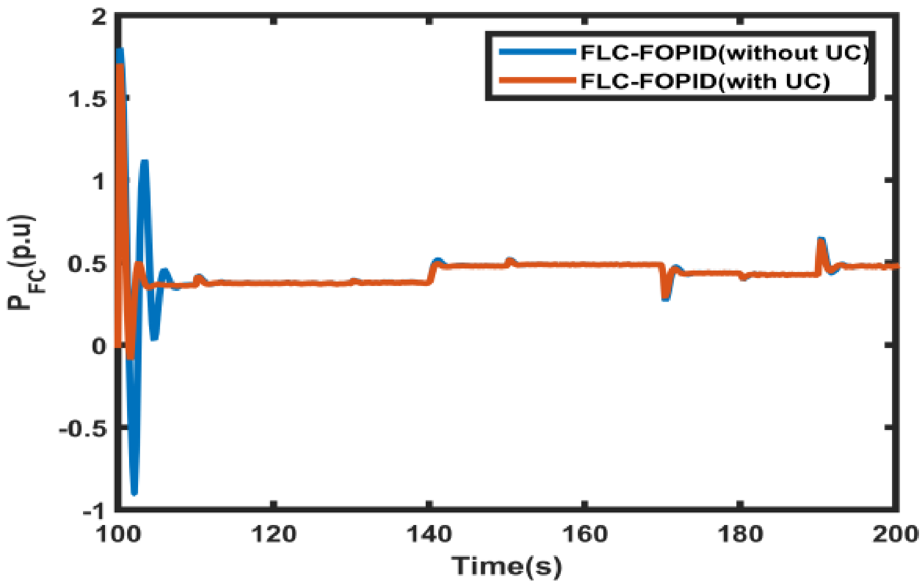

FIGURE 4.11 – Effect of disconnecting UC with the best FLC-FOPID.

4.5.6 Discussion

We have initially tuned the two controllers with linear models of the microgrid system components. Then, we have tested the performance of the controllers under nominal operation of the microgrid components. Since our optimization methodology is stochastic in nature. The fractional order fuzzy controllers also have high robustness properties as demonstrated in previous figures. This is important since the control design can take into account the effects of different modelled dynamics which are neglected while modelling the different power system components. Therefore in spite of the consideration of small signal linear models in the initial power system components, the other advantages of robustness like parametric uncertainties, and robustness against disconnection of Ultracapacitor, due to the presence of fuzzy logic in the FO controller. Therefore the objective of introducing the simulation results with the PID controller is solely to serve as a benchmark of traditionally accepted industrial practices. The focus of the present study is to make a comparison between the integer order fuzzy PID controller and the fractional order fuzzy PID controller. Naturally these are more complicated control system designs and would require more expensive hardware to implement. The system designer can look at the relative improvement in performance as obtained by these fuzzy strategies over the simple PID controller and decide whether it is worthwhile for his specific application to obtain this improvement in control system performance.

4.6 Conclusion

This chapter investigates the application fuzzy fractional PID controller for frequency regulation in microgrid system. The proposed microgrid includes renewable system as principle generation units which depend on the weather conditions and disturbances loads. The frequency and power deviations are affected by the intermittent nature of these renewable sources that requires the use of storage devices and conventional sources which improve the microgrid operation. The fluctuation in frequency and power requires to be controlled using a flexible and robust control strategy , the hybridation of fuzzy and fractional order control is considered as suitable solution of this problem due to it and overcome others controllers structure. The frequency and power deviation are limited within small variation by the use of the controllers. Good performance of the system in term of small perturbations and more stable are accomplished with FLC-FOPID in comparison with the FOPID. The obtained results show better performance and robustness of fuzzy-FOPID in comparison with FOPID. The table 4.3 shows different values of objective function in both decrease and increase of system parameters. The robustness against disconnecting of UC is achieved and the results show that Fuzzy FOPID is better than FOPID.

CHAPTER 5

Load frequency control of two area power systems using tie line model

5.1 Introduction

In this chapter, control of two interconnected systems using tie line model is used. Under it, the power input has also to vary. If the input/output balance is not maintained, a change in frequency will occur. The control of frequency is achieved primarily through speed governor mechanism aided by supplementary means for precise control. At the outset, the speed governor mechanism and its operation will be presented. Governor : The power system is basically dependent upon the synchronous generator and its satisfactory performance. The important control loops in the system are [115,116] :
1– Frequency control.
2– Automatic voltage control.
In this chapter, the frequency control will be discussed. Frequency control is achieved through the generator control mechanism. The governing systems for thermal and hydro-generating plants are different since the inertia of water that flows into the turbine presents additional constraints that are not present with the steam flow in a thermal plant. However, the basic principle is still the same ; such as the speed of the shaft is sensed and compared with a reference, and the feedback signal is utilized to increase or decrease the power generated by controlling frequency and deviations.

5.2 Proposed System Configuration

In the present study, two areas interconnected power system is used for the analysis of load frequency control. Both the areas (Area 1 and Area 2) are of the same ratings. Each area is comprised of a thermal generating unit with a reheat turbine and a hydro generating unit. The mathematical model of the system proposed for simulation and the time domain analysis of its performance is presented in Figure 5.1. The different blocks are shown in Figure 5.1 represents the electro-mechanical components of each of thermal-hydro generating units. Switch S shown in Figure 5.1 indicates that the two area systems can be simulated with and without considering the tie line [117–120].

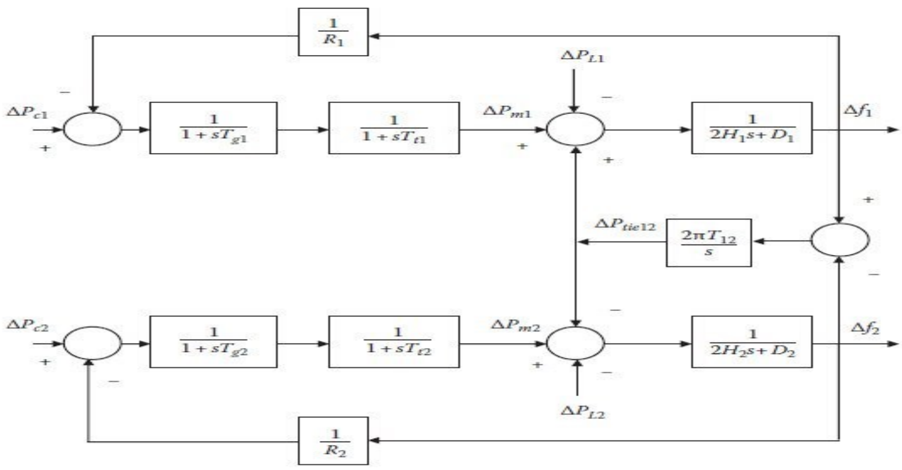

FIGURE 5.1 – Block diagram of a two-area power system under the primary control actions.

5.3 Load frequency control

In Tie-line Load-bias control all the power systems in the interconnection aid in regulating frequency regardless of where the frequency change originates. The equipment consists of a master load frequency controller and a tie line recorder measuring the power input on the tie as for the selective frequency control. The error signal like Δf and ΔP_{tie} tie are amplified, mixed, and transformed to real power command signal PV which is sent to the prime mover to call for an increase in the torque.

The prime mover shall bring about a change in the generator output by an amount PG which will change the values of Δf and ΔP_{tie} within the specified tolerance. The first step to the analysis of the control system is the mathematical modeling of the systems various components and control system techniques [121, 122].

5.4 Automatic Generation Control

Automatic generation control (AGC) is a significant control process that operates constantly to balance the generation and load in power systems at a minimum cost. The AGC system is responsible for frequency control and power interchange, as well as economic dispatch.

The role of the AGC system in connection with the power system monitoring/ control master stations, and remote site control centers to manage the electric energy, is emphasized. Power system operations and frequency control in different ranges of frequency deviation are briefly explained. A frequency response model is described, and its usefulness for simulation and AGC dynamic analysis is examined [123].

5.4.1 AGC in a single area

With the primary LFC loop, a change in the system load will result in a steady-state frequency deviation, depending on the governor's speed regulation. To reduce the frequency deviation to zero we must provide a reset action by introducing an integral controller to act on the load reference setting to change the speed setpoint. The integral controller increases the system type by 1 which forces the final frequency deviation to zero. The integral controller gain must be adjusted for a satisfactory transient response [124–126].

The fundamental objective of secondary control is to reestablish the balance between the area load and its generation. This can be achieved when the control action keeps the frequency deviation close to zero and the net interchange power with neighboring areas at scheduled levels. A control signal of the secondary control loop known as the area control error (ACE) is used to realize the desired objectives. In the literature, there are many forms of ACE. The most commonly used form of ACE consists of two terms, one is the tie-line power flow deviation ΔP_{tie12} added to a second term, which is proportional to the frequency deviation f. Thus, the ACE signals for a two-area system are given by [127, 128]

$$ACE_1 = \Delta P_{tie12} + B_1 \Delta f_1 \tag{5.1}$$

$$ACE_2 = \Delta P_{tie21} + B_2 \Delta f_2 \tag{5.2}$$

$$ACE_1 = \Delta P_{tie12} + B_1 \Delta f_1 = -\frac{\Delta P_{L1}}{2} - B_1 \frac{\Delta P_{L1}}{2\beta} \tag{5.3}$$

$$ACE_2 = \Delta P_{tie21} + B_2 \Delta f_2 = \frac{\Delta P_{L1}}{2} - B_2 \frac{\Delta P_{L1}}{2\beta} \tag{5.4}$$

5.4.2 AGC in multi-area system

In many cases, a group of generators are closely coupled internally and swing in unison. Furthermore, the generator turbines tend to have the same response characteristics. Such a group of generators is said to be coherent. Then it is possible to let the LFC loop represent the whole system and the group is called the control group. For a two-area system, during normal operation, the real power transferred over the tie line is given by [121], [129]

$$R\,(Hz/pu.MW) = \frac{\Delta f}{\Delta P_g} \tag{5.5}$$

$$ACE_i = \Delta P_{tie,i} + \beta_i \Delta f_i \tag{5.6}$$

$$\beta_i = \frac{1}{R_i} + D_i \tag{5.7}$$

$$\Delta P_{tie,i} = \sum_{\substack{j=1 \\ j \neq i}}^{N} \Delta P_{tie,ij} = \frac{2\pi}{s} \left[\sum_{\substack{j=1 \\ j \neq i}}^{N} T_{ij} \Delta f_i - \sum_{\substack{j=1 \\ j \neq i}}^{N} T_{ij} \Delta f_j \right] \tag{5.8}$$

5.5 Problem formulation

The typical unity feedback closed-loop system is shown in the figure. For our exploration, we select the $PI^{\lambda}PD^{\mu}$ controller as given in Eq 5.8.

Various time-domain integral performance indices like IAE, ISE, and ITAE are considered in this thesis as in literature . Every integral performance index has certain advantages in control system design. The $ITAE$ performance tries to reduce time multiplied absolute error in the control system. The multiplication by the time penalizes the error more at the later stages at the beginning and hence effectively reduces the settling time which cannot be achieved with IAE or ISE based tuning. The various performance indices and their significance are as follows

–IAE index

$$J = \int_{T_{min}}^{T_{max}} |\Delta F(t)|\, dt \tag{5.9}$$

–ISE index

$$J = \int_{T_{min}}^{T_{max}} |\Delta F(t)|^2\, dt \tag{5.10}$$

–ITAE index

$$J = \int_{T_{min}}^{T_{max}} t\,|\Delta F(t)|\, dt \tag{5.11}$$

–ITSE index

$$J = \int_{T_{min}}^{T_{max}} t\,|\Delta F(t)|^2\, dt \tag{5.12}$$

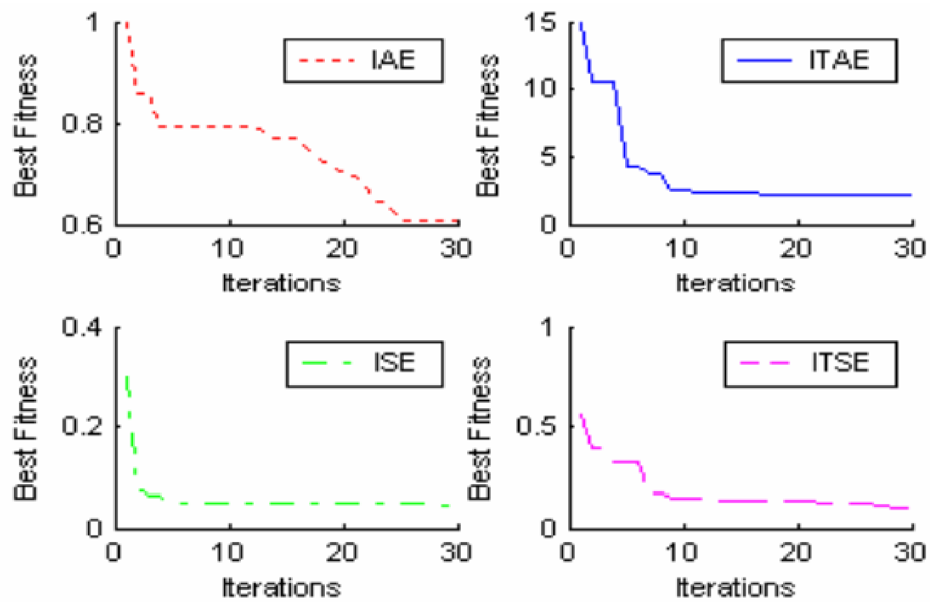

FIGURE 5.2 – Best fitness convergence based on KH.

TABLE 5.1 – Comparaison between various INDEXS

INDEX	IAE	ITAE	ISE	ITSE
Best fitness	0.6	2.56	0.0812	0.12

Let $\Delta F\left(T\right)$ the sampled value of the error $\Delta F\left(t\right)$ at an instant T where T is the sampling interval.
The $ITSE$ penalizes the error more than $ITAE$ and due to the time multiplication term, the oscillaton damps out faster. However for a sudden change in set point the ITSE based controller produces larger controller output than the ITAE based controllers, which is not desirable from an actuator design point of view. Other integral performance indices like ISTES and ISTSE both have higher powers of time and error terms. These result in faster rise time and selling time while also ensuring the minimization of the peak overshoot. These, however, might lead to the very high value of control signal and are only are used in acute cases where the time-domain performance is of critical importance and not a large control signal. To obtain good performance monitoring frequency of a microgrid, the variation of frequency (Δf) and the change of the control signal (Δu) to the output of the fractional order PID controller should be minimized. In this study, the integral performance index (J) to minimize by appropriate KRILL HERD is the weighted sum of $ISTSE$ (Integral of Squared Time Squared Error Multiplied) and $ISDCO$ (Integral of Squared Deviation of the Output Controller) given as follows.

$$J = \int\limits_{T_0}^{T_{sim}} \left(\Delta {F_1}^2 + \Delta {F_2}^2 + \Delta {P_{tie-line}}^2\right) dt \tag{5.13}$$

Where ΔF is the system frequency deviation of the Microgrid. The T_{sim} is the time simulation.

5.6 Proposed controller

This objective function will be resolved using the Krill Herd optimization algorithm to determine the optimal parameters of the Fractional Order PID controller [81, 130–134]. The optimization problem expressed by, minimize J.
Subjected to,

$$\begin{cases} K_P^{min} \leq K_P \leq K_P^{max} \\ K_I^{min} \leq K_I \leq K_I^{max} \\ K_D^{min} \leq K_D \leq K_D^{max} \\ \lambda^{min} \leq \lambda \leq \lambda^{max} \\ \mu^{min} \leq \mu \leq \mu^{max} \end{cases} \tag{5.14}$$

Where w presents the efficiency relation of two objectives function (ISE and ISDCO) and it takes the value of $0.5.Kn$ is the constant of normalization in ISE and ISDCO. The conception problem of fractional order PID controller is the challenge to tune its five parameters. This problem can be overcome using optimization methods. In this chapter, a new bio-inspired optimization technique called Krill Herd is investigated in chapter 3 to determine the proposed controller parameters which are considered as the input variable of the objective function described above.

5.7 Results and Discussion

In two areas interconnected power system load change in one area will affect the generation in all other interconnected areas. Tie line power flow should also be taken into account other than the change in frequency. In this chapter, two area interconnected systems considering different types of units as shown in Figure 5.1 are considered for designing the proposed controller. An area is interconnected with each other by a tie line which is used for economy and continuity of power supply. There are different cases considered for analysis.

5.7.1 Generated power and load demand independently of the controller

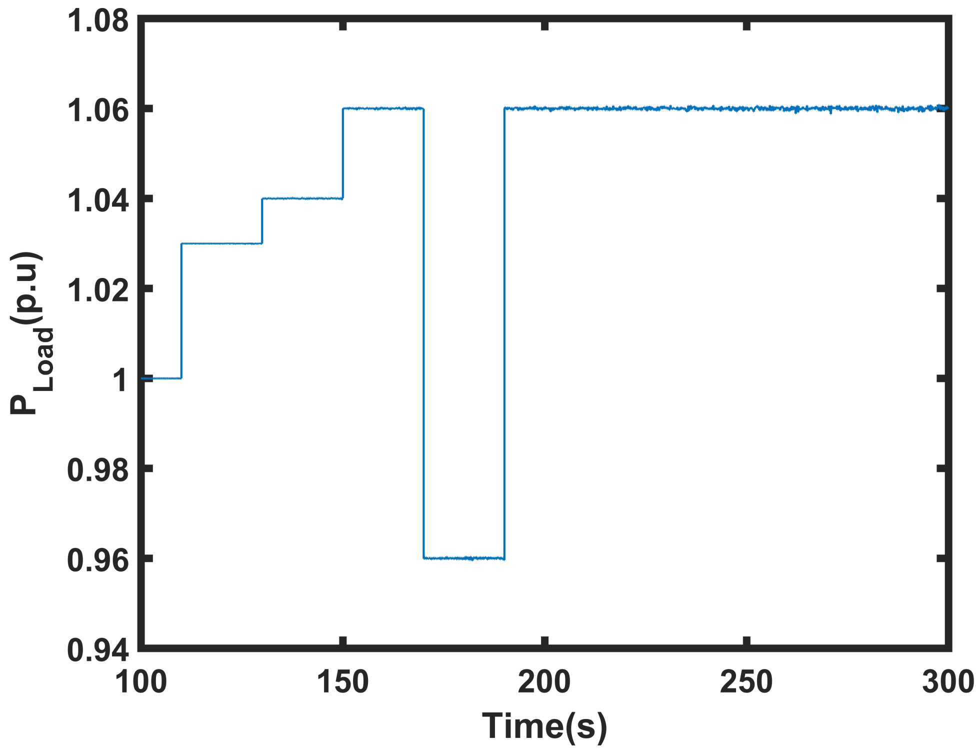

(a)

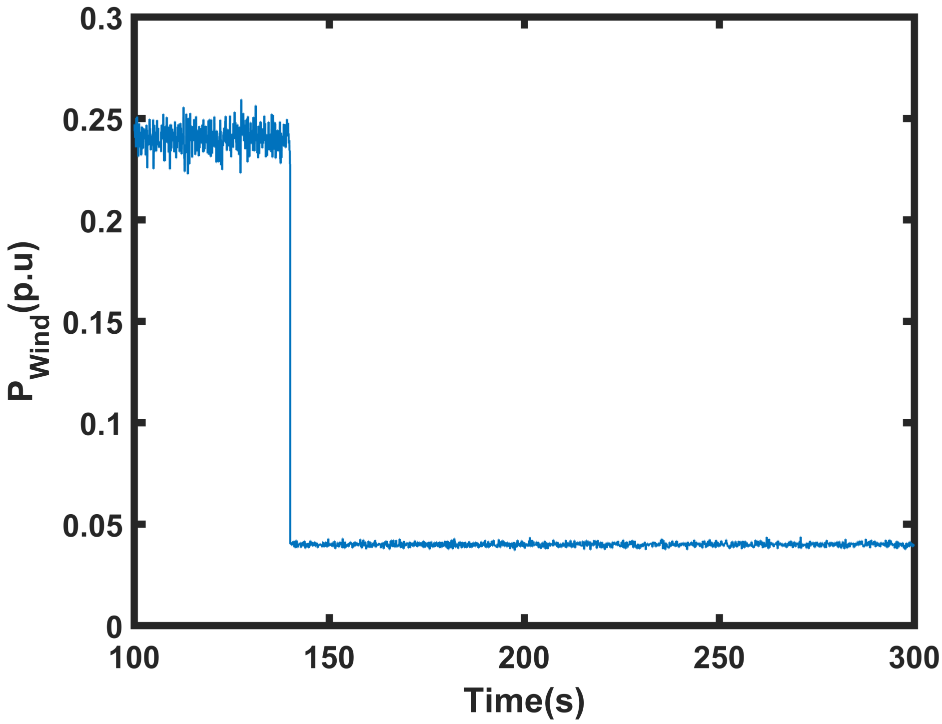

(b)

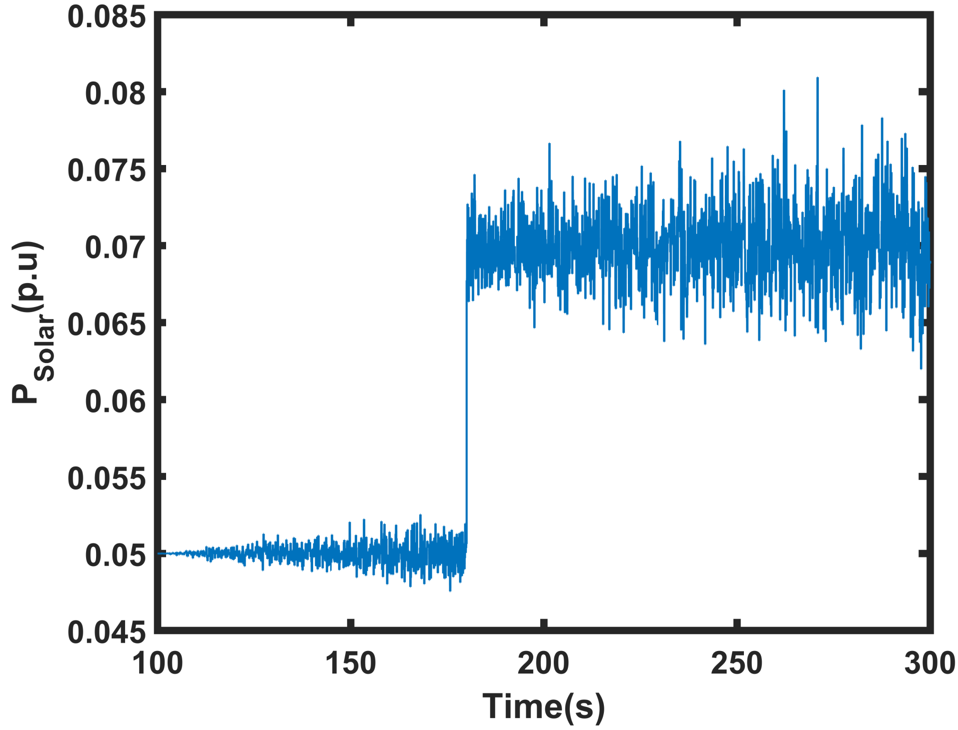

(c)

FIGURE 5.3 – Realization of demand powers (a), the stochastic generated from WTG(b) and PV(c).

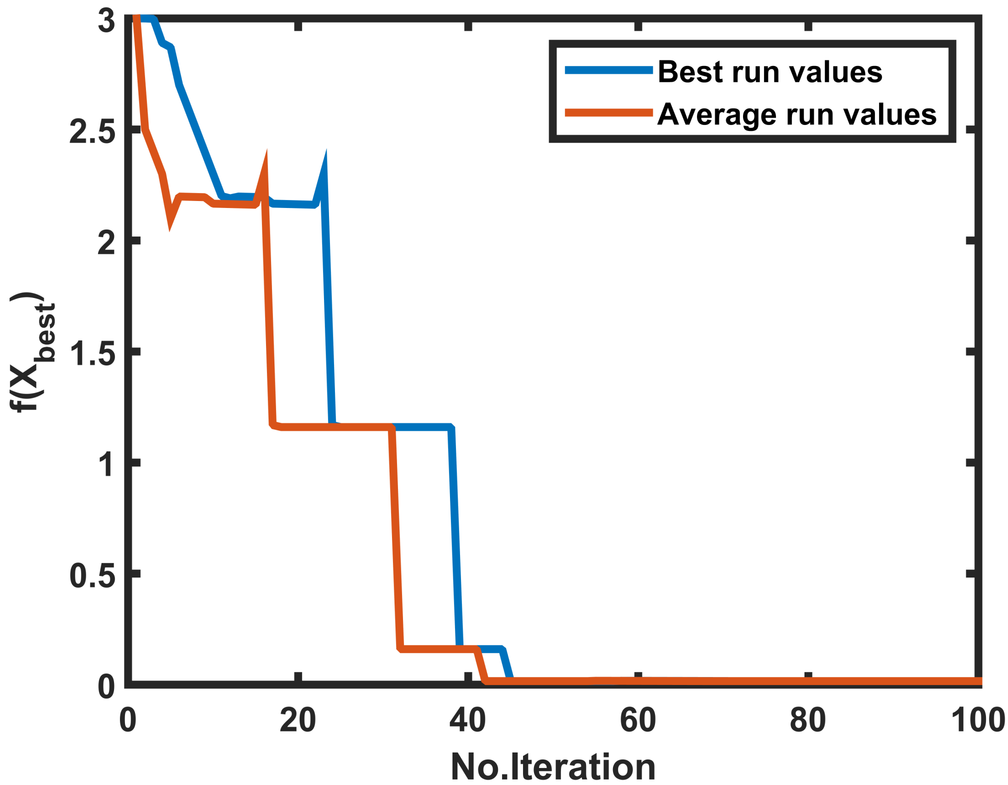

FIGURE 5.4 – Characteristic convergence of KH.

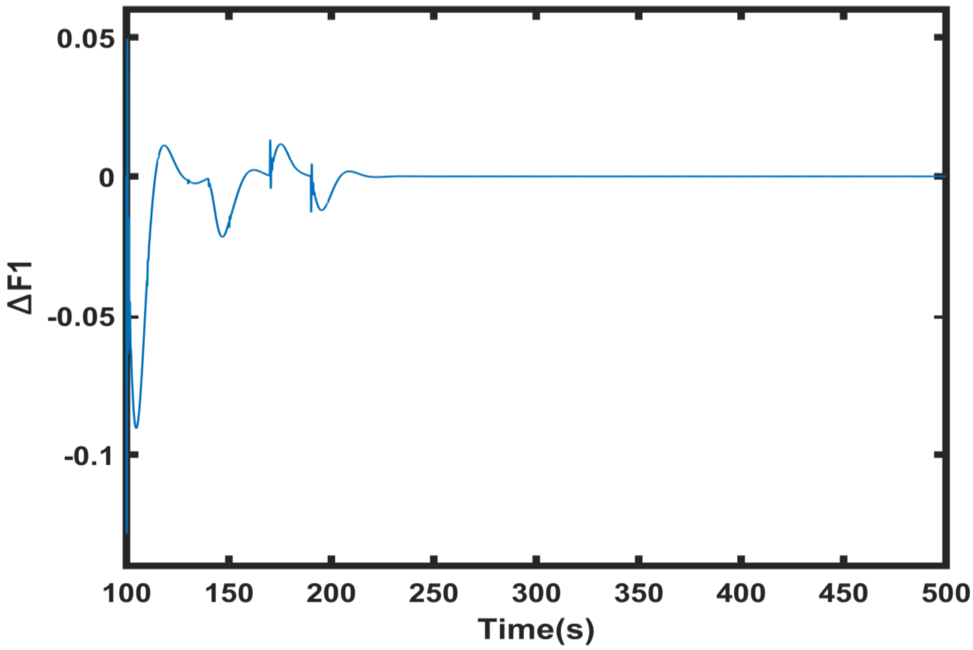
0.05
0
-0.05
-0.1
ΔF1
100
150
200
250
300
350
400
450
500
Time(s)

(a)

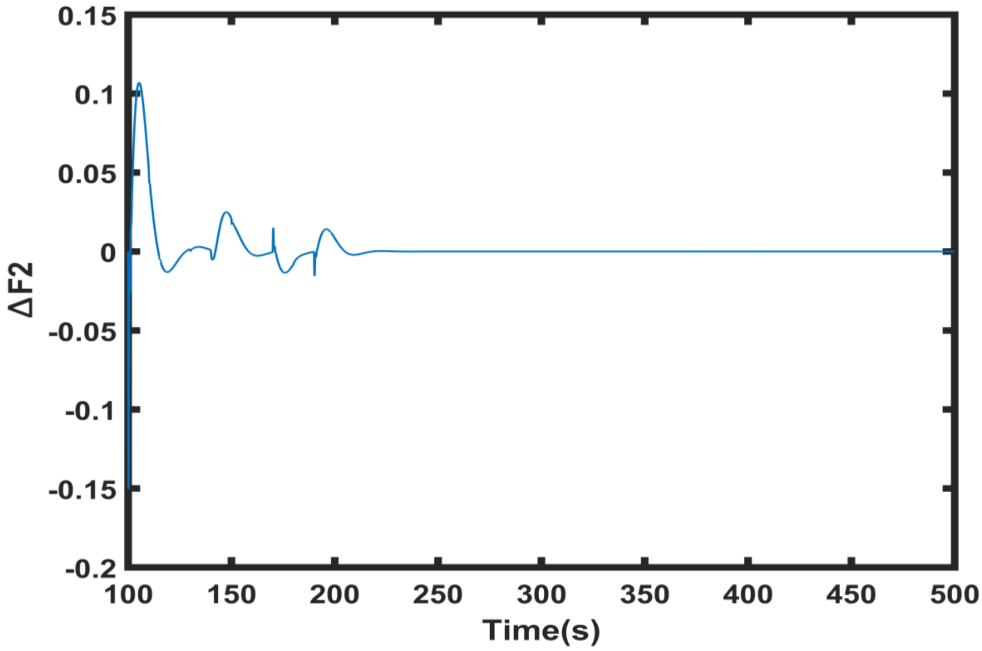
0.15
0.1
0.05
0
-0.05
-0.1
-0.15
-0.2
ΔF2
100
150
200
250
300
350
400
450
500
Time(s)

(b)

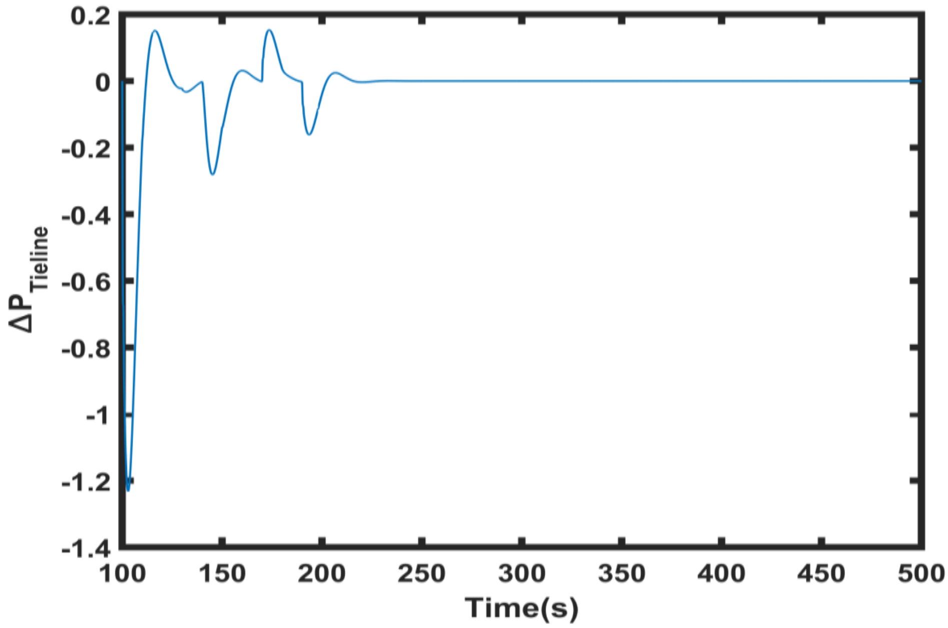

(c)

FIGURE 5.5 – Frequency deviation of two systems ΔF_1(a) , ΔF_2(b) and Tie line power deviations ΔP_{tie}(c) .

5.7.2 Performance analysis of PID controller using Krill Herd Algorithm

The considered system is provided with the PID controller using KH and PSO one at a time. These techniques are used for optimizing the controller parameters in each control area. The same types of two controllers are used in a control area. The system dynamics are obtained by considering the penetration of wind and solar powers in each area as disturbances with load power variation. Using these optimum values the dynamic responses are obtained for the proposed controller and compared as shown in the figure. From the dynamic responses, the characteristics of the responses such as settling time, peak overshoot, and undershoot are shown in the figure. From Figure 5.6, it is clear that the performance of PID controller based KH is better than using PSO from peak overshoot, undershoot, and settling time. Hence, further studies are carried out by using a PID controller.

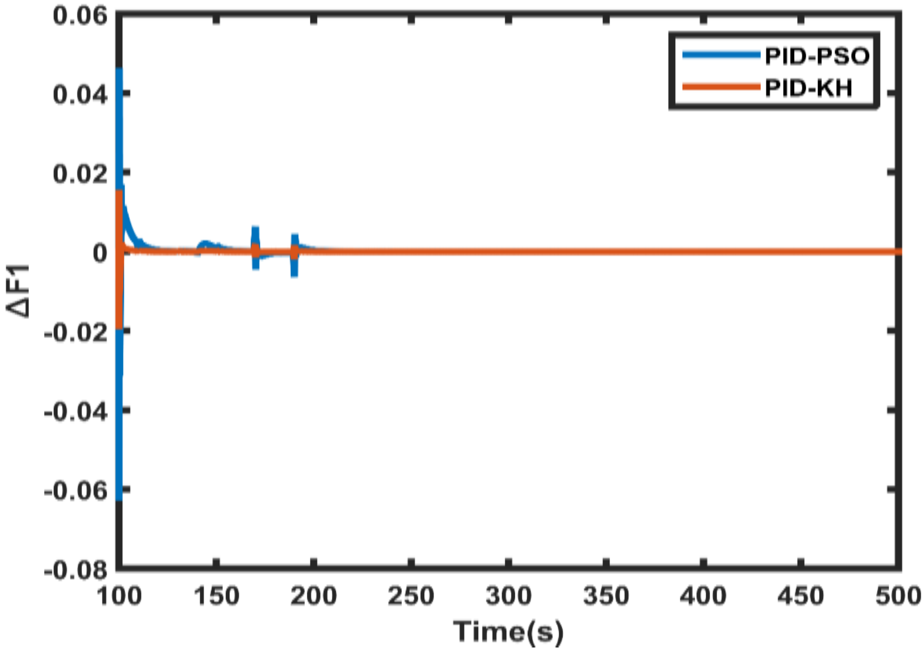
0.06
0.04
0.02
0
-0.02
-0.04
-0.06
-0.08
ΔF1
100
150
200
250
300
350
400
450
500
Time(s)
PID-PSO
PID-KH

(a)

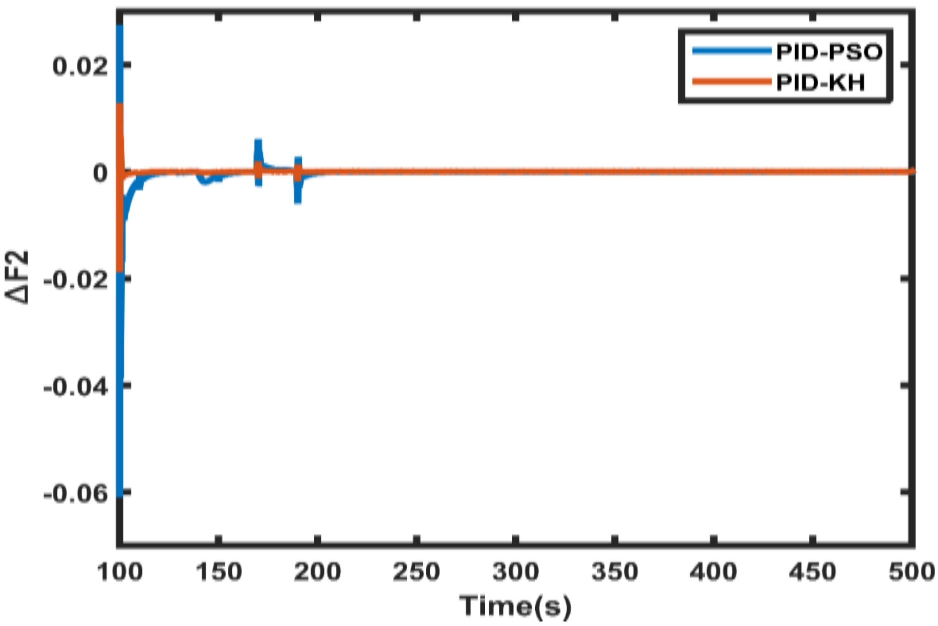
0.02
0
-0.02
-0.04
-0.06
ΔF2
100
150
200
250
300
350
400
450
500
Time(s)
PID-PSO
PID-KH

(b)

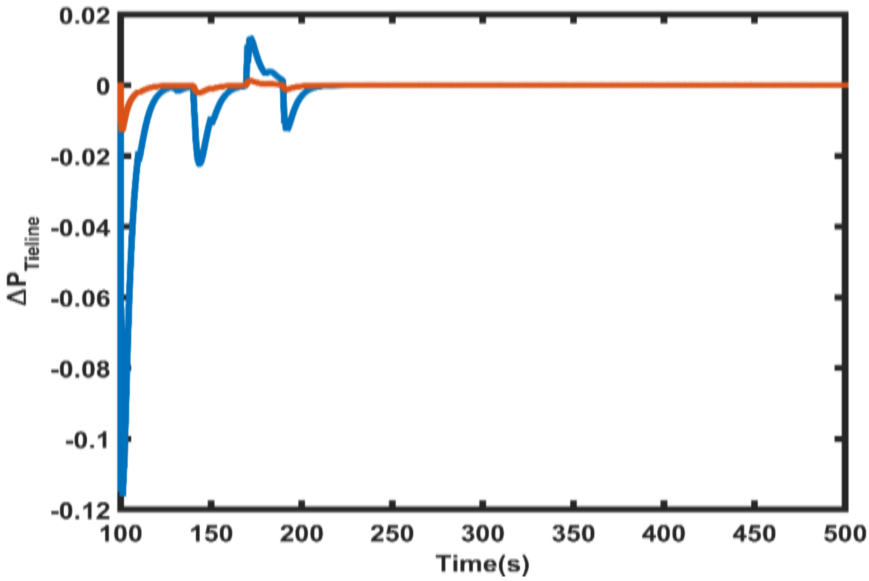

(c)

FIGURE 5.6 – Frequency deviation of two systems $\Delta F_1(a)$, $\Delta F_2(b)$ and Tie line power deviations $\Delta P_{tie}(c)$ with the best PID based KH and PSO.

5.7.3 Comparison between PID controller and Fractional Order PID controller

The performance of the PID controller was compared with the Fractional Order PID controller with disturbances in both load and generation in each area. Both controllers are applied to a two area non- reheat power plant. Frequency responses of area 1 and area 2 with tie-line power deviation are shown in Figure 5.7 respectively.

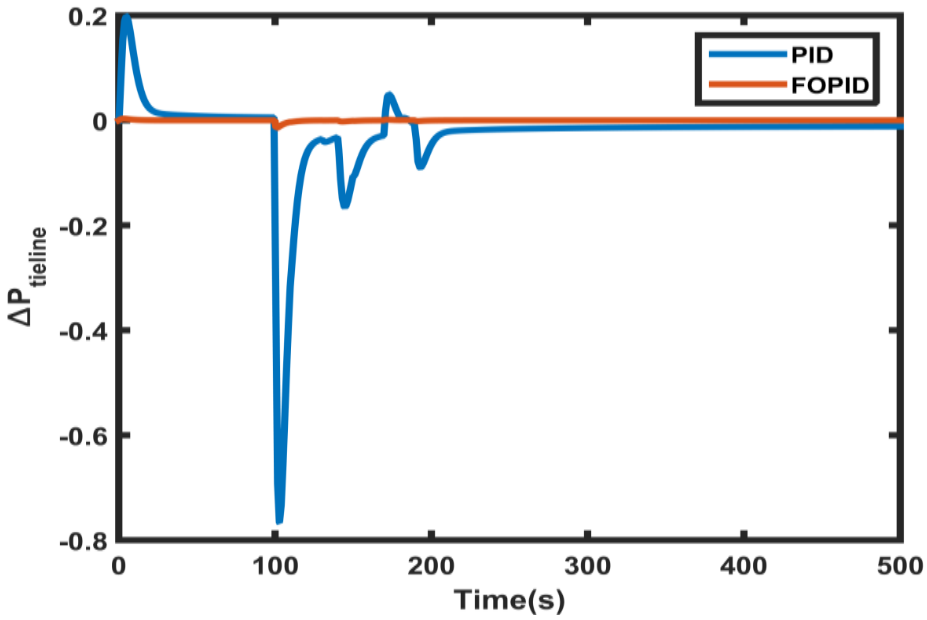
0.2
0
-0.2
-0.4
-0.6
-0.8
$\Delta P_{tieline}$
0
100
200
300
400
500
Time(s)
PID
FOPID

(a)

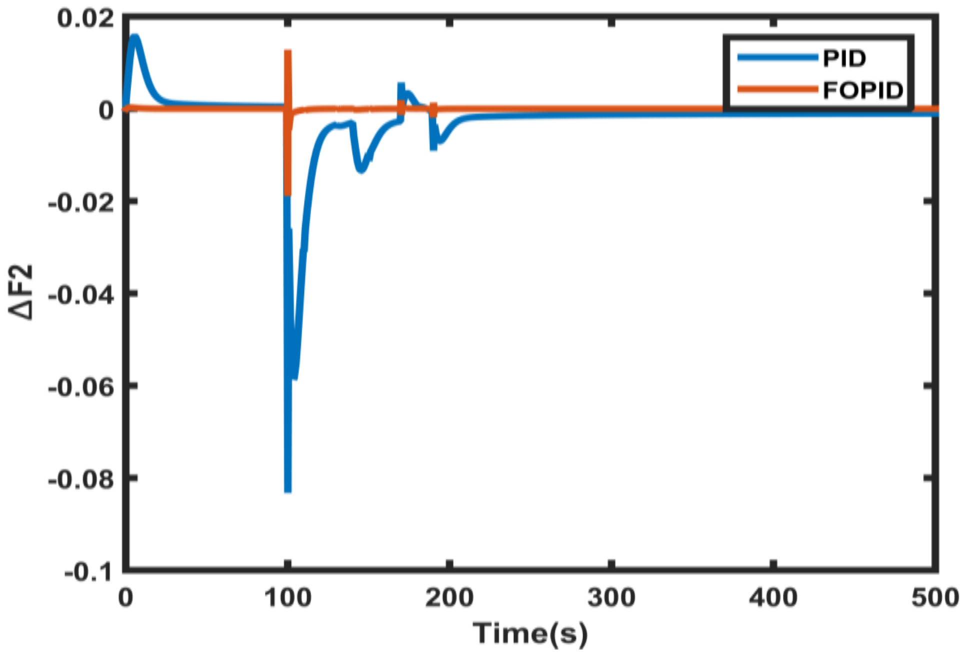
0.02
0
-0.02
-0.04
-0.06
-0.08
-0.1
ΔF2
0
100
200
300
400
500
Time(s)
PID
FOPID

(b)

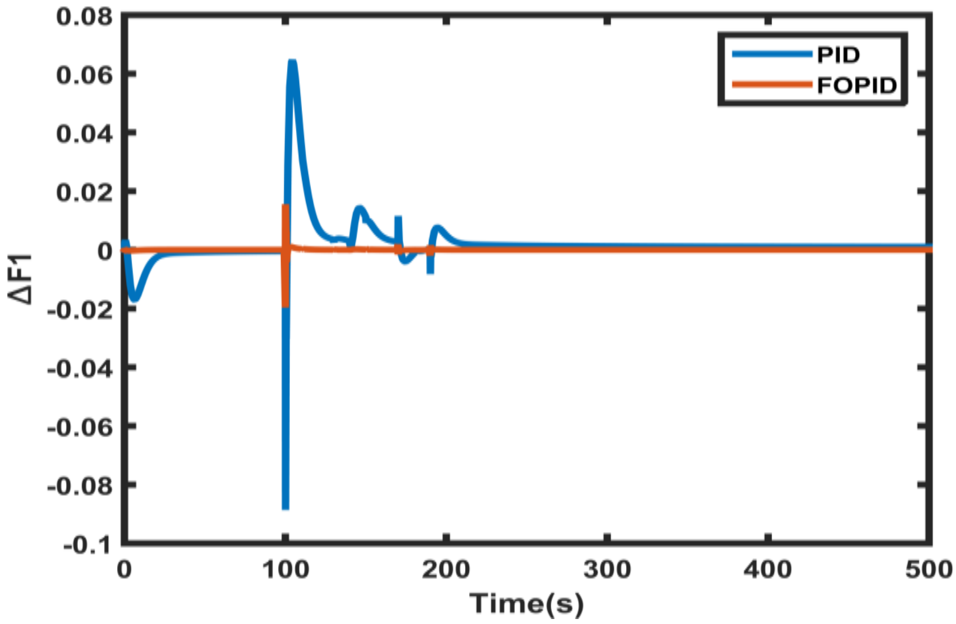

(c)

FIGURE 5.7 – Frequency deviation of two systems $\Delta F_1(a)$, $\Delta F_2(b)$ and Tie line power deviations $\Delta P_{tie}(c)$ with the best PID and FOPID.

5.7.4 Time-domain responses of Case1

In the present case, during the first part of time $0 < t \leq 40s$ the solar thermal power and wind power are kept in $0.36pu$ and $0.5pu$ respectively. During $0 < t \leq 80s$ the load is 1pu. In the $40s$ the wind speed and solar radiation are decreased to $0.36pu$ and $0.18pu$ respectively and at $80s$ the load increases to $1.1pu$. The fluctuations in generation and load are reduced by the system components like BESS, FC, AE, and DEG by the controller in feedback. The controller is worked to reduce the frequency deviations and kept it within small deviations. The best PID controller based KH give better performances of system in term of less transient fluctuations in frequency deviation in comparison with the PID based PSO. The figure shows the generated power from WTG and STPS with load power.

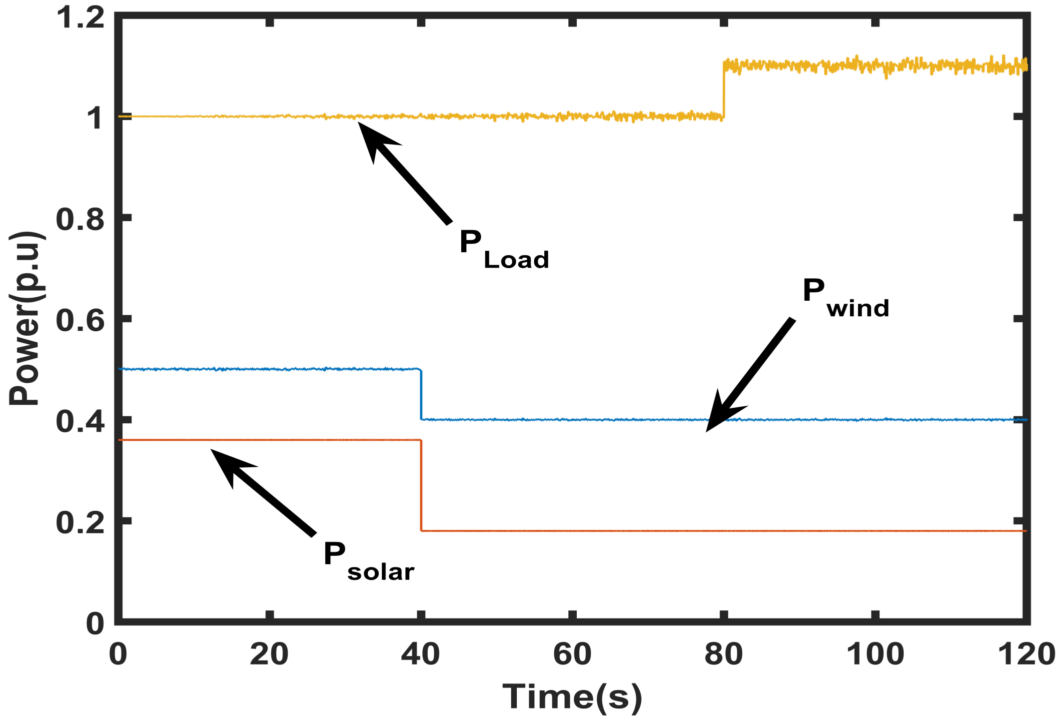

FIGURE 5.8 – Generated power from WTG and STPS with load demand.

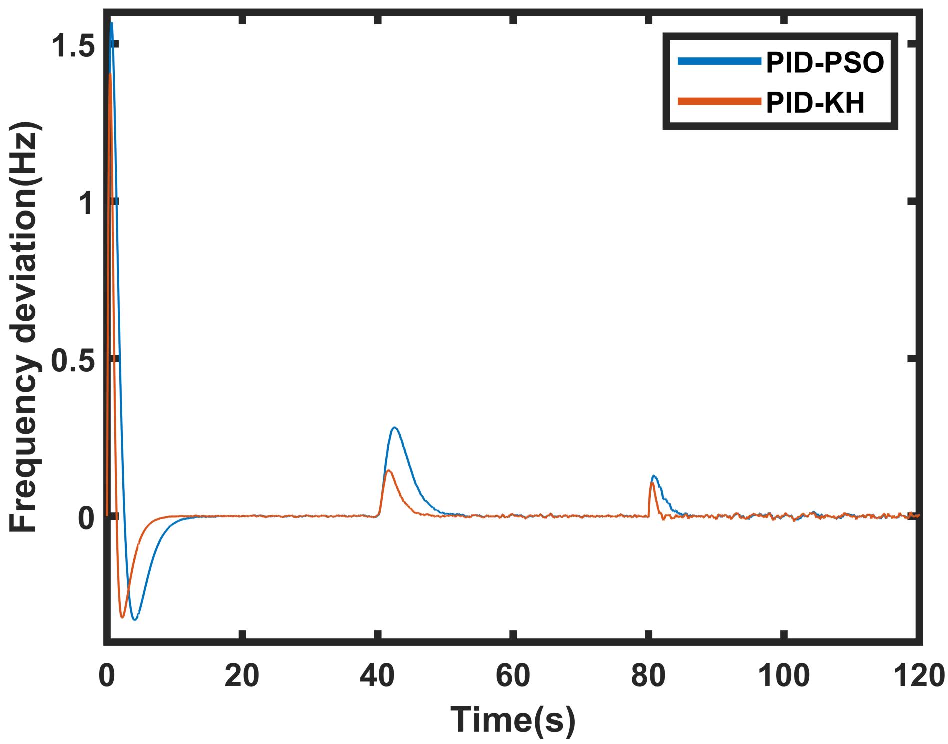

(a)

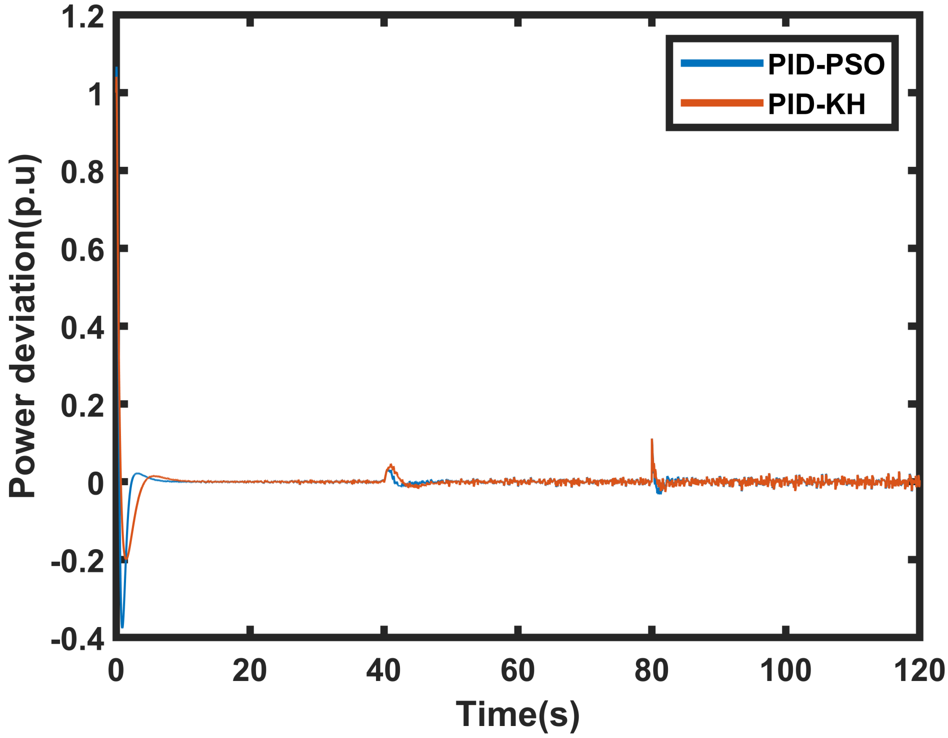

(b)

FIGURE 5.9 – Frequency(a) and power(b) deviations.

5.7.5 The time-domain response of Case2

In this case, the proposed configuration is simulated under the random variation in the generated power and loads demand. The time simulation is taken to equal 120s. During the first time interval between 0s and 10s, there is a sudden change in power which affects the frequency and power deviation before that the system attainted the state of stability. This perturbation is occurring also in the generated power by various components of the microgrid.

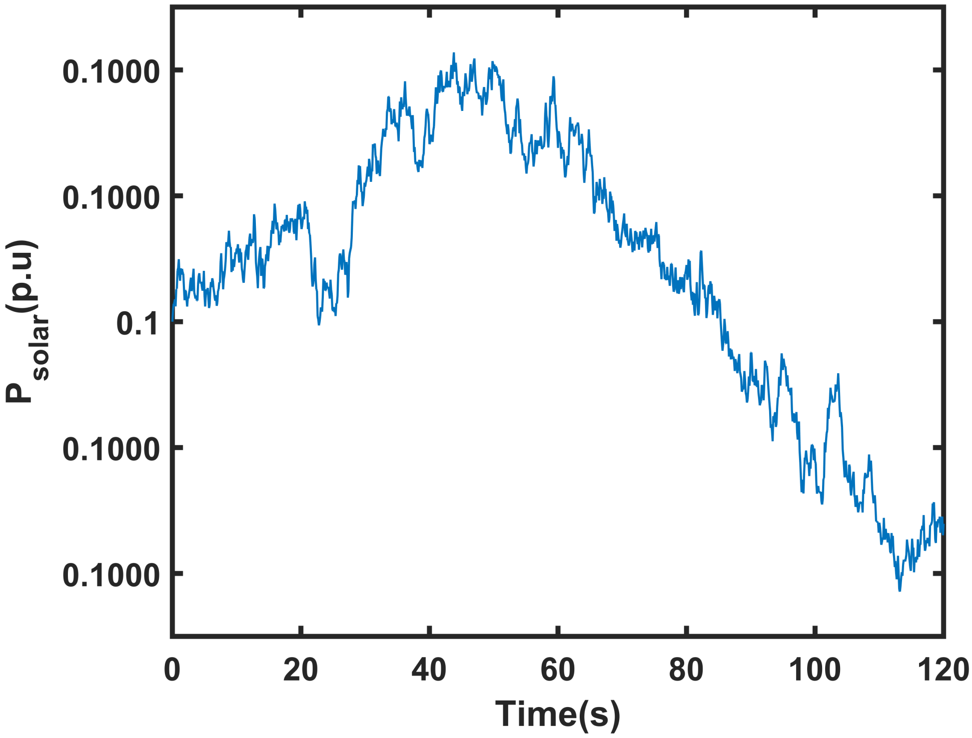
0.1000
0.1000
0.1
0.1000
0.1000
P_{solar}(p.u)
0
20
40
60
80
100
120
Time(s)

(a)

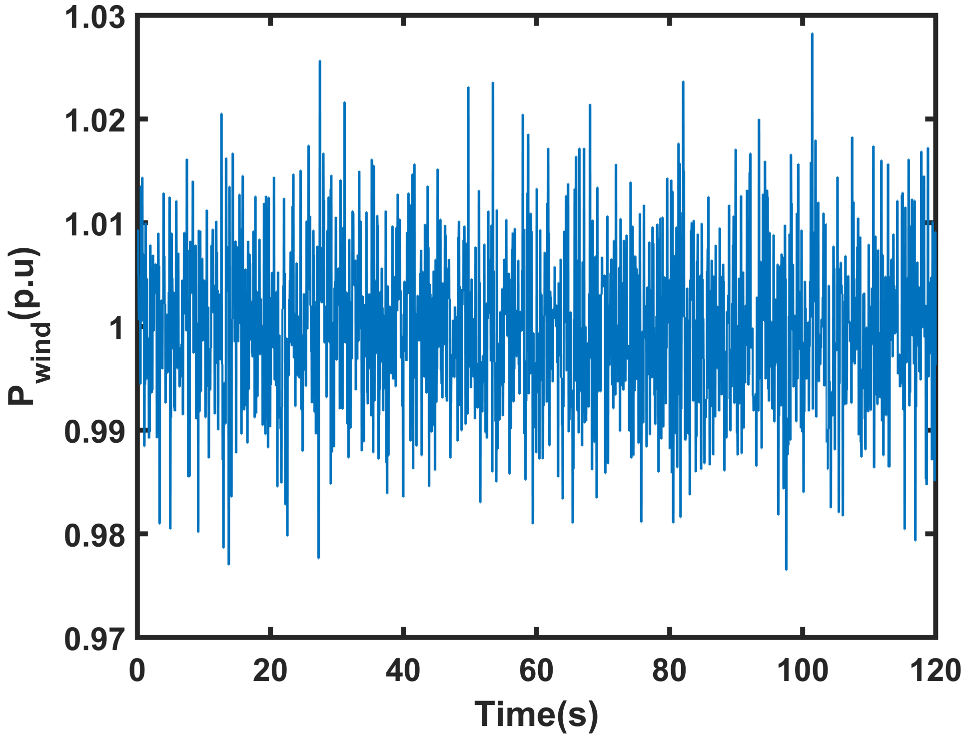
1.03
1.02
1.01
1
0.99
0.98
0.97
P_{wind}(p.u)
0
20
40
60
80
100
120
Time(s)

(b)

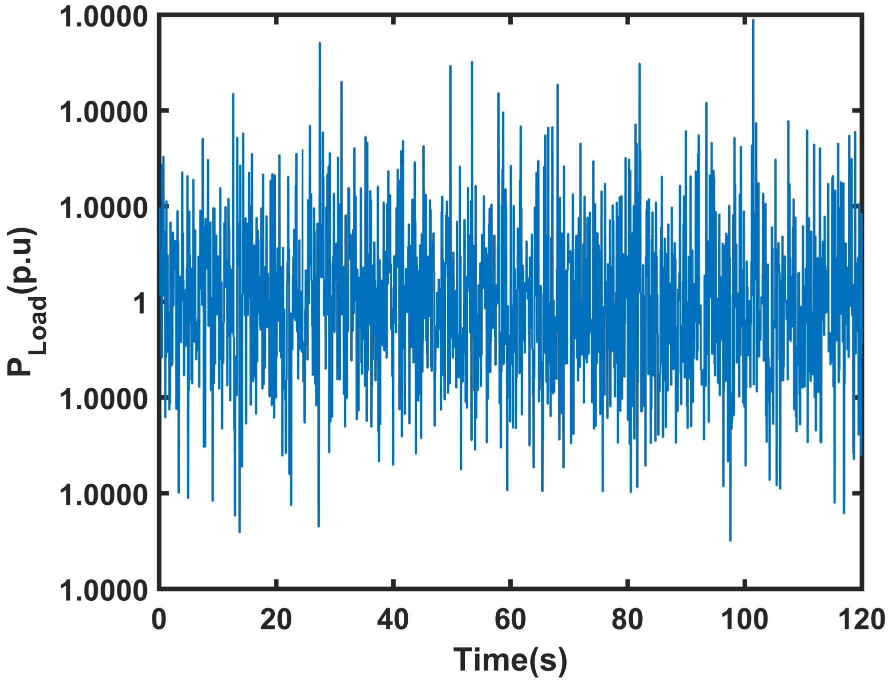

(c)

FIGURE 5.10 – Generated from STPS(a) , and WTG(b) with load power demand (c) under random conditions.

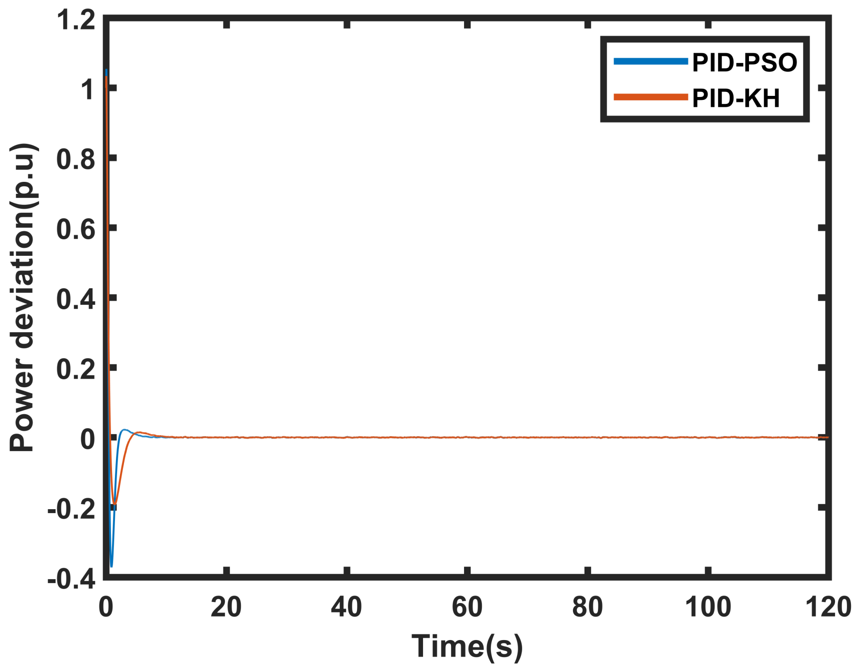

(a)

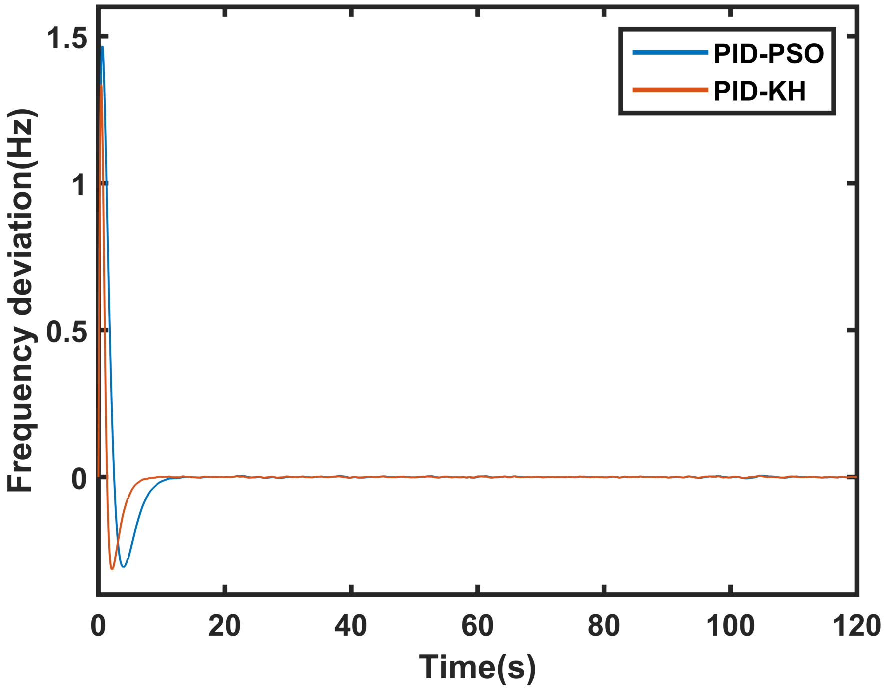

(b)

FIGURE 5.11 – Power(a) and frequency(b) deviations for the second case.

5.7.6 Domain analysis of Case3

In this case, the proposed configuration composed of a Photovoltaic system, wind Turbine Generator, Diesel Engine Generator, Fuel cell, Aqua electrolyzer, and Energy Storage components like such as Battery and Flywheel. The combination of two renewable sources with conventional sources and energy storage system enhances the reliability and operation of a microgrid in islanded mode. The frequency and power deviations fluctuated because of the sudden variations in solar radiation, wind speed, and load demand power. It is controlled using a PID controller implanted in the output of all system components which its values parameters are optimized as well as the frequency and power deviations are minimal.

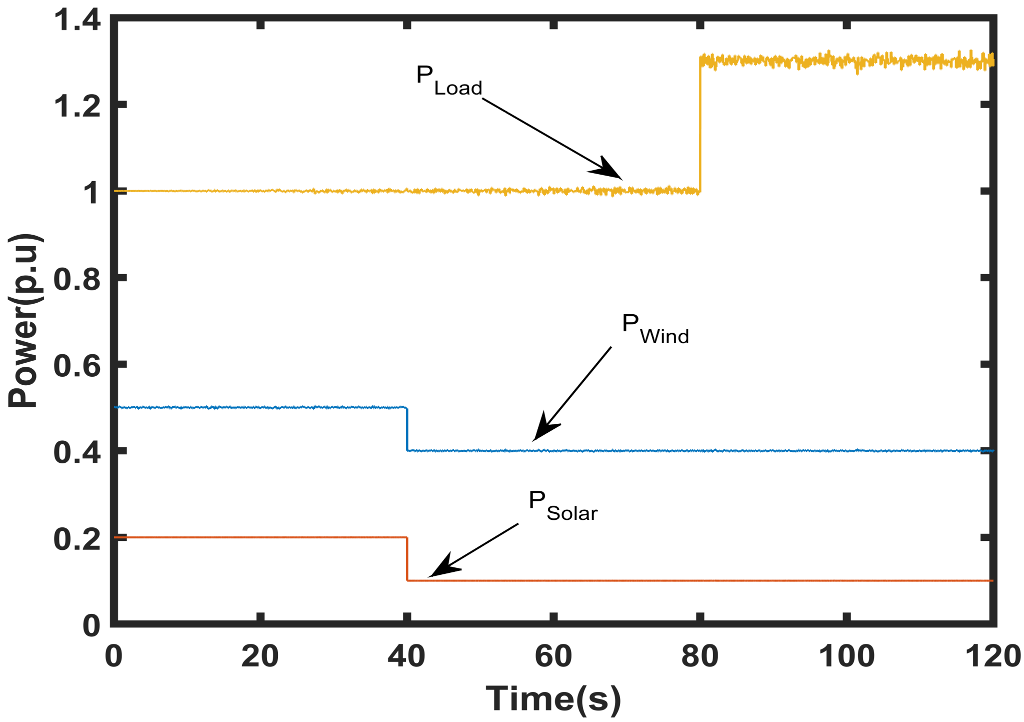

FIGURE 5.12 – Load demand outputs a power of PV and WTG.

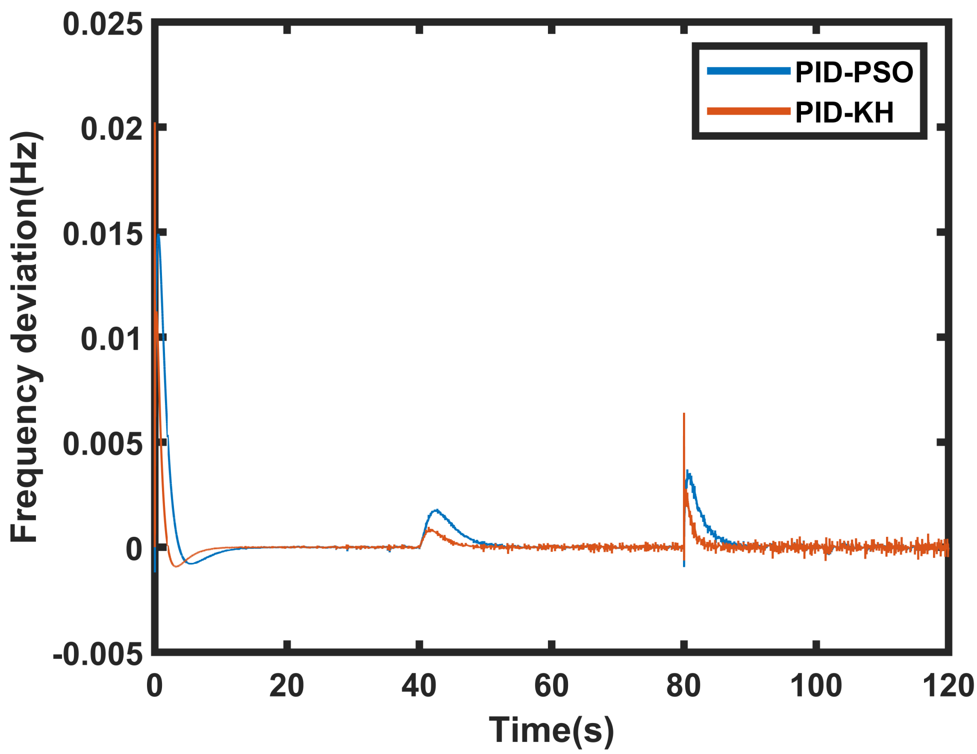

(a)

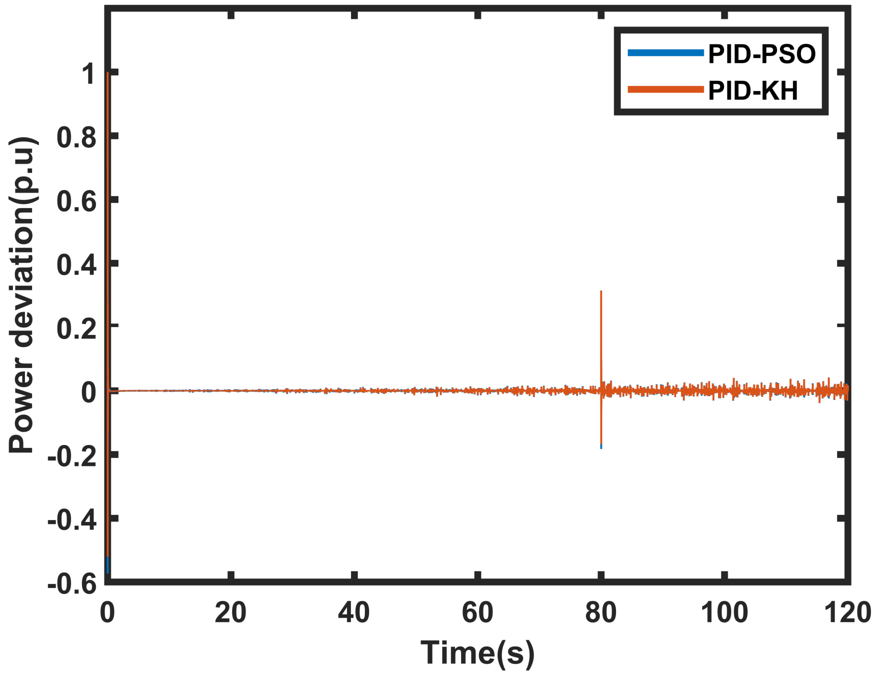

(b)

FIGURE 5.13 – Frequency(a) and power(b) deviations with the best PID-PSO and PID-KH.

5.7.7 Time-domain responses of Case04

This case considers WTG, PV, AE, FC, DEG, BESS, UC, and the load connected in the system. This system is simulated under variation in generated power and load during 120s as shown in Figure 5.14. The PID controller is connected in the input of different components like AE, FC, DEG, BESS, and UC to regulate the frequency deviation. The PID parameters are tuned using PSO and KH and the results are compared and reported in the following figures.

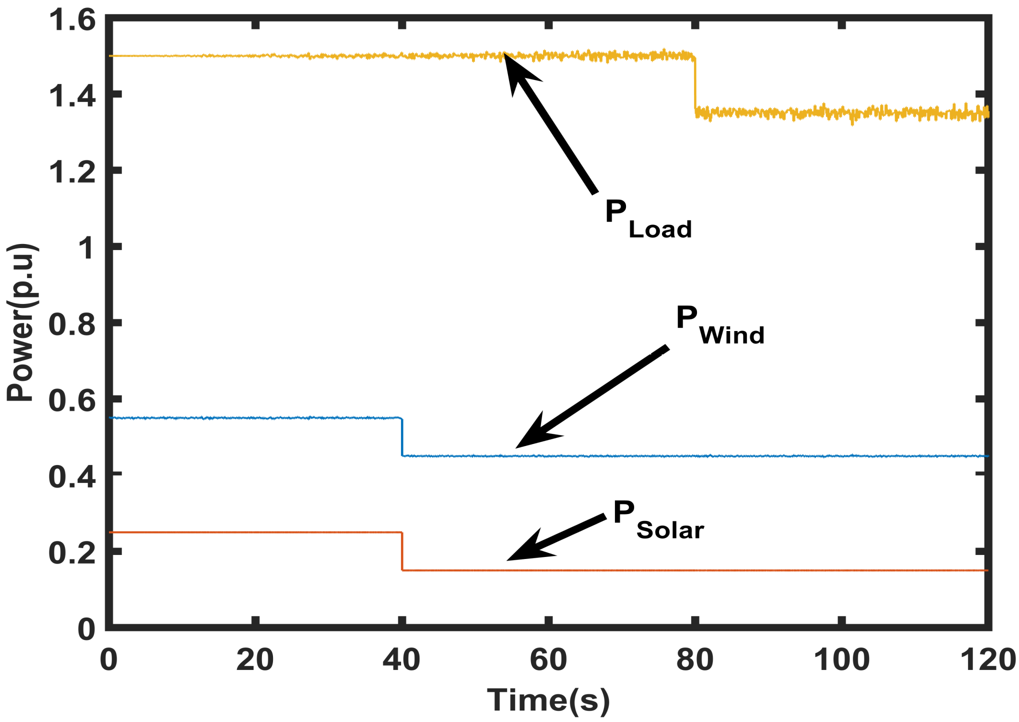

FIGURE 5.14 – Power Load demand and generated power from WTG and PV.

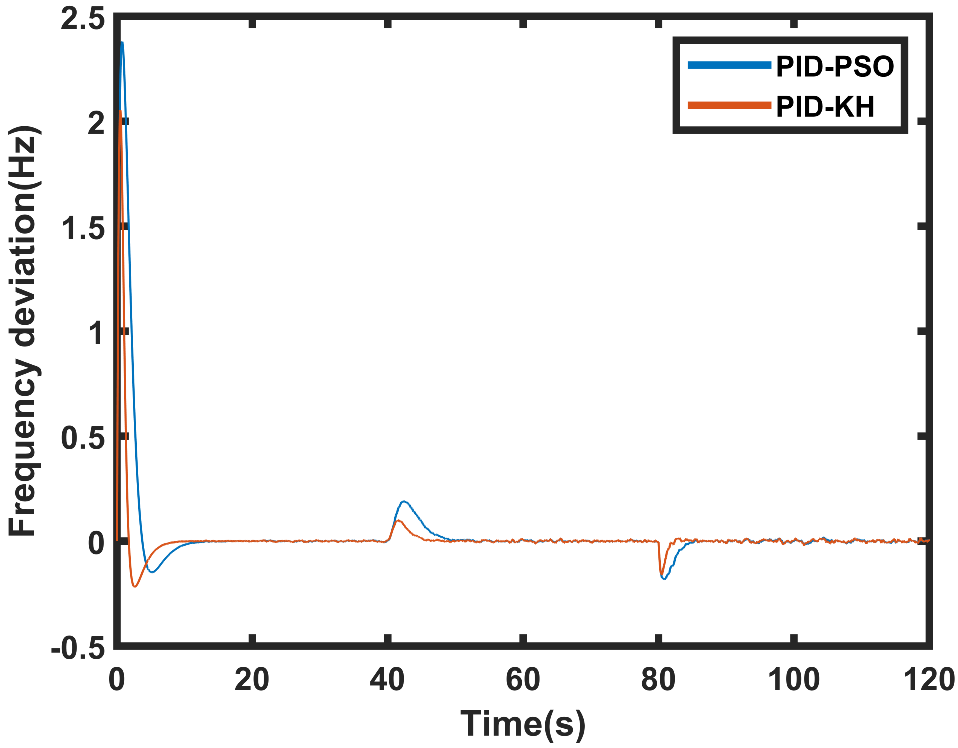

(a)

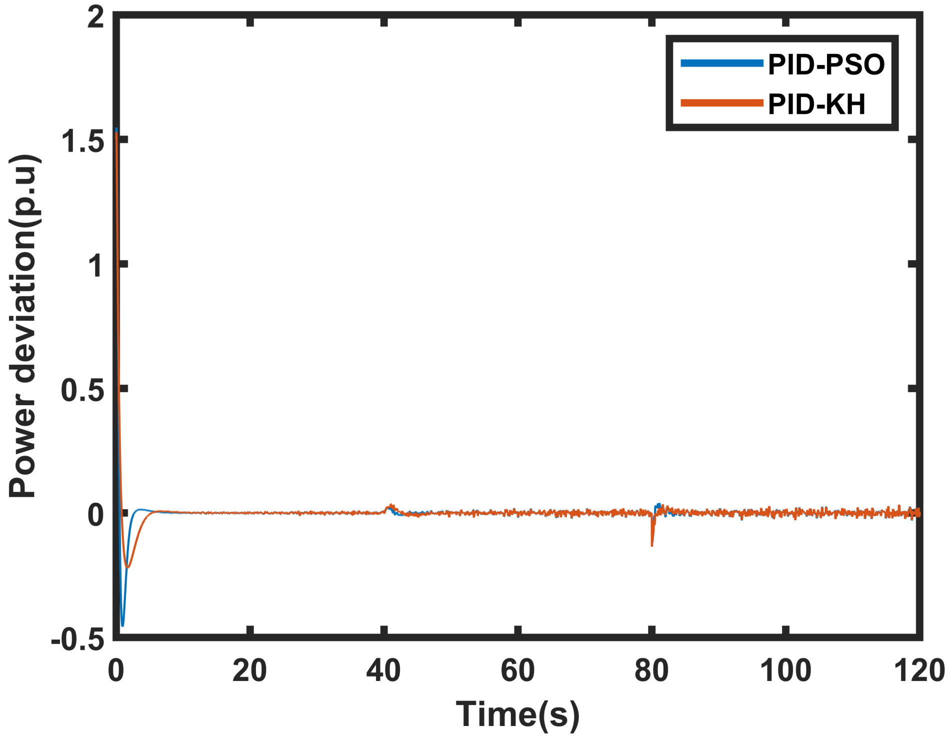

(b)

FIGURE 5.15 – Frequency(a) and power(b) deviations for four case.

The above figures show the frequency control in time domain analysis of microgrid. The results show the fast convergence of the Krill herd to find the optimal controller parameters. The best obtained PID controller parameters reduce the frequency and power fluctuation against the stochastic variations in produced power from the renewable sources and loads demand perturbations. The sudden change in generation and load affect the frequency and power stability and the controller work to reduce this effect by the feedback signal to the storage devices and secondary sources like the FC and DEG.

5.8 Conclusion

In this chapter, KH and PSO optimized PID and FOPID controllers are investigated for frequency control of two areas interconnected microgrid systems. A comparison between the two optimization techniques is done and certifies that KH provides better performance robustness of the controller compared to PSO. Simulation of different scenarios of operation under various load and generation conditions is achieved and a comparison is accomplished. The simulation results verify the best dynamics responses of the system using FOPID compared to the PID controller using the KH algorithm.

General Conclusion and Future Works

General Conclusion

The microgrid concept is faced by many challenges that make its operation, control and security difficult like the intermittent nature of renewable sources which affect the frequency and voltage stability. To overcome these aforementioned problems this thesis contributed to modeling and optimal control of a microgrid based renewable energy sources like wind and photovoltaic system with storage devices. The system frequency deviation can be changed according to the load change and change in renewable power generations. However, the frequency can be maintained within the normal range of operation by setting the appropriate controllers parameters using optimizations techniques. The robustness of setting the parameters values was analysed and compared in the design of adequate control strategies.

One of the important studies addressed in this thesis was about the frequency control scheme using a PID controller for eliminating the Microgrid frequency fluctuation caused by the disturbances in power generation and load. This proposed controller offers the advantage of reducing the power fluctuation and gives the best performance to the microgrid system. Parameters of the PID controller are tuned using Particle Swarm Optimization, Genetic Algorithm, and Krill Herd algorithms. The Krill Herd technique is better than the PSO and GA in the quality of the solution and giving faster convergence. Simulation results show that the KH algorithm optimizes the PID

controller parameters is robust in operation and improves the damping performance of frequency and power deviation system compared to GA and PSO tuning PID controller. Using a PID controller based optimization techniques in the system leading to the enhancement of system stability and robustness as aforementioned.
This thesis also investigated the application fuzzy fractional PID controller for frequency regulation in the microgrid system. The proposed microgrid includes the renewable system as principle generation units which depend on the weather conditions and disturbances loads. The frequency and power deviations are affected by the intermittent nature of these renewable sources that require the use of storage devices and conventional sources that improve the microgrid operation. The fluctuation in frequency and power requires to be controlled using a flexible and robust control strategy, the hybridization of fuzzy and fractional order control is considered as a suitable solution to this problem due to it and overcome others controllers structure. The frequency and power deviation are limits within small variation by the use of the controllers. Good performance of the system in terms of small perturbations and more stability is accomplished with FLC-FOPID in comparison with the FOPID. The obtained results show better performance and robustness of fuzzy-FOPID in comparison with FOPID. The results show different values of the objective function in both decrease and increase of system parameters. The robustness against the disconnecting of UC is achieved and the results show that Fuzzy FOPID is better than FOPID.
Another contribution reached in this thesis was the simulation and control of two area of microgrid system using tie line model. In this study, KH and PSO optimized PID and FOPID controllers are implemented for frequency control of two areas interconnected microgrid systems. A comparison between the two optimization techniques is done and certifies that KH provides better performance robustness of the controller compared to PSO. Simulation of different scenarios of operation under various load and generation conditions is accomplished and a compared. The simulation results verify the best dynamics responses of the system using FOPID compared to the PID controller using the KH algorithm.
In this Thesis, the microgrid modeling and control based renewable energy sources and impact of intermittent nature of wind seed, solar radiations and load change on microgrid frequency and power stability are studied in detail.

There are some main contributions drawn from the study as follows ;

1– Modeling of microgrid configurations using small signal model presented first order transfer function.

2– Design of control Scheme based classical PID controller, Fractional order PID controller and hybrid Fuzzy Fractional order controller for frequency microgrid control.

3– Investigation of new optimization techniques called Krill Herd Algorithm.

4– Simulation and control of two area microgrid system using Tie-line model.

5– Reduce the greenhouse gas emissions and this investigate RES rising.

- ✓ The use of various generation systems enhance the energy efficiency.
- ✓ The helping up of the electricity market enables to subedit the producers emergence.
- ✓ Faceplate the construction with short periods and lower investments, compared to the conventional power units.
- ✓ A power production close to the consumption leads to a transportation costs reduction.

Future work

Hybrid optimization techniques can be a solution to enhance the frequency stability and kept it within small deviations in comparison to the use of single optimization technique.

One of the future works would be the coordination and control of multiple isolated microgrids. Hierarchical control strategy could be developed for coordination and control of multiple microgrids. Running a microgrid and validates the developed models in real area and collected real data. Extensive experimental test by using various load profiles, storage technologies, weather conditions and other real world considerations.

Annex

Validations of results by comaprisons with previous works

Table 2 – PID parameters using KH and KA

Algorithm	K_p	K_i	K_d
KH [135]	3.188	3.92	1.53
GA [55]	3.124	1.08	0.324

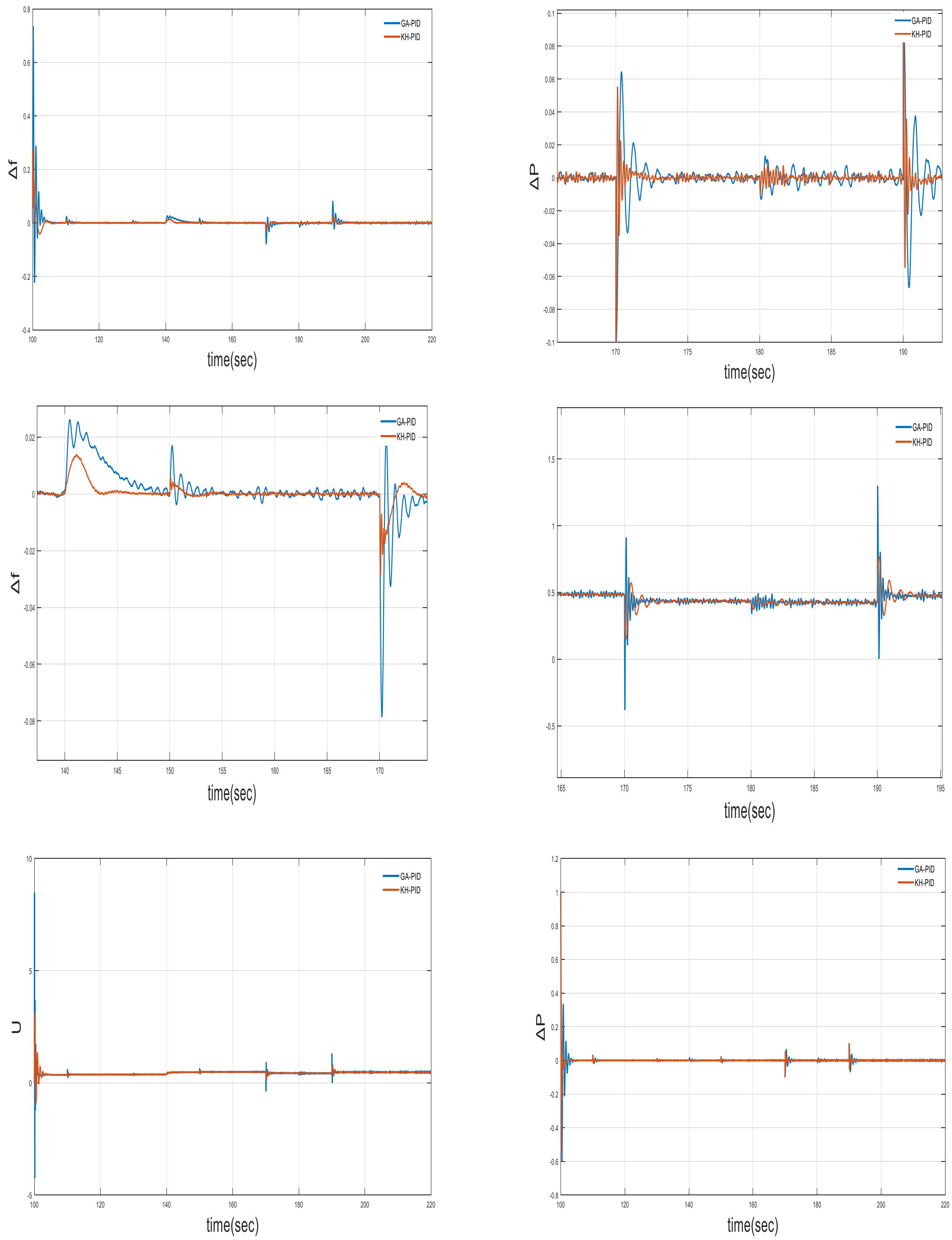

Figure 1 :Frequency deviation and power deviation of the Microgrid with control signal using the best obtained PID controllers [135].

The stochastic model of the generated power and load

Small random fluctuations and critical deviation of solar power generation, wind power generation and load demand strength can be expressed as follow

$$P = \left(\frac{\varphi.\eta.\sqrt{\beta}(1 - G(s)) + \beta}{\beta}\right).\Gamma = \Gamma.\chi \tag{.15}$$

Where φ is the stochastic component of the power, P represents the wind or solar and load powers, β presents the mean value of the power, η is a constant normalizes the generated or demand powers χ constant to correspondence per unit (p.u.) level, and Γ is time-dependent switching signal with a gain causes sudden fluctuation of the average value for stochastic power [10]. For the windpower generation, the parameters are

$$\varphi \sim U(-1, 1), \quad \eta = 0.8, \beta = 10, \quad G(s) = \frac{1}{(10^4.s + 1)} \tag{.16}$$

And

$$\Gamma = 0.24h(t) - 0.04h(t - 140) \tag{.17}$$

Where $h(t)$ is the Heaviside step function.

For the solar power generation the parameters are :

$$\varphi \sim U(-1, 1), \quad \eta = 0.9, \beta = 10, \quad G(s) = \frac{1}{(10^4.s + 1)} \tag{.18}$$

And

$$\Gamma = 0.05h(t) + 0.02h(t - 180) \tag{.19}$$

For the demand load, the parameters are :

$$\varphi \sim U(-1, 1), \quad \eta = 0.8, \beta = 10, \quad G(s) = \frac{300}{(300.s + 1)} + \frac{1}{(1800.s + 1)} \tag{.20}$$

And

$$\Gamma = \frac{1}{\chi}[0.9.h(t) + 0.03.h(t - 110) + 0.03.h(t - 130)$$

$$+0.03.h(t - 150) - 0.15h(t - 170) + 0.1.h(t - 190)] \tag{.21}$$

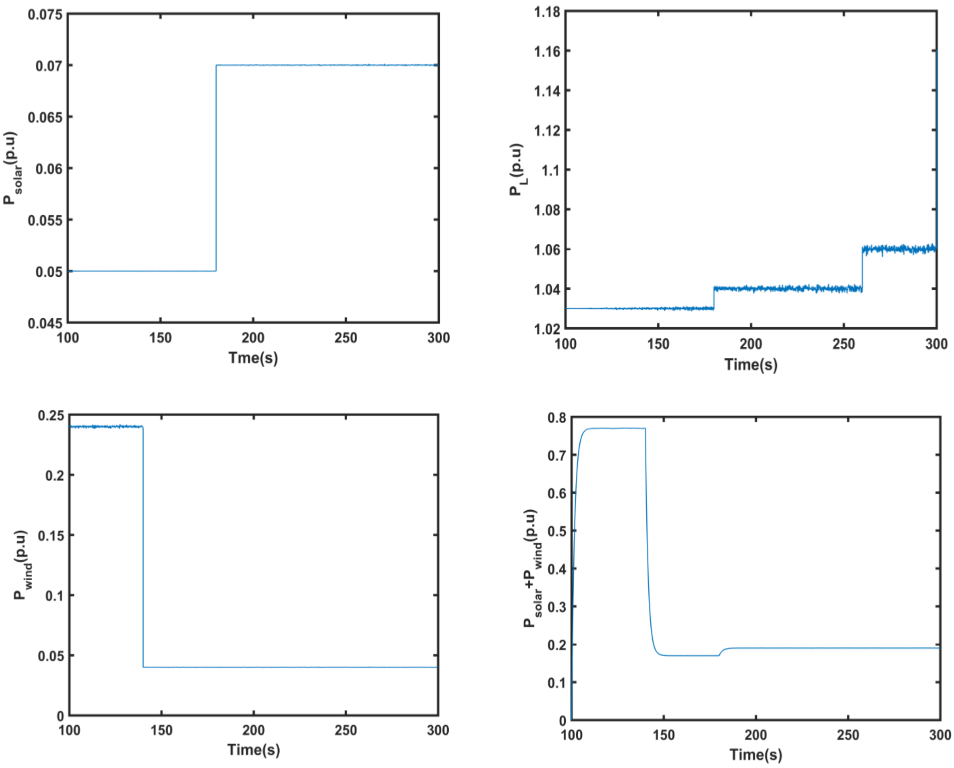

Figure 2 :Stochastic generated power from wind speed and solar radiation and load demand.

Bibliography

Bibliography

[1] Venkataramanan, Giri, and Chris Marnay. "A larger role for microgrids." IEEE power and energy magazine 6.3 (2008) : 78-82.

[2] Arra, Ankith Reddy. Modeling and stability analysis of AC and DC microgrids. PhD Dissertation. Texas Tech University, USA 2015.

[3] Su, Wencong. Microgrid modeling, planning and operation. PhD dissertation, faculty of the Virginia Polytechnic Institute and State University, USA 2009.

[4] Favuzza, Salvatore, et al. "Transition of a distribution system towards an active network. Part I : Preliminary design and scenario perspectives." 2011 International Conference on Clean Electrical Power (ICCEP). IEEE, 2011.

[5] Sen, Sachidananda, and Vishal Kumar. "Microgrid modelling : A comprehensive survey." Annual Reviews in Control (2018).

[6] Boden, Tom A., Gregg Marland, and Robert J. Andres. "Global, regional, and national fossil-fuel CO_2 emissions." Carbon Dioxide Information Analysis Center, Oak Ridge National Laboratory, US Department of Energy, Oak Ridge, Tenn., USA doi 10 (2009).

[7] Zohuri, Bahman. Hybrid energy systems : Driving reliable renewable sources of energy storage. Springer, 2017.

[8] H. Bevrani, Robust power system frequency control, Switzerland, 2nd edition, 2014.

[9] M. Regad, M. Helaimi, R. Taleb, Hossam A. Gabbar ,Ahmed M. Othman, Frequency Control of Microgrid system based Renewable Generation using Fractional PID Controller Indonesian Journal of Electrical Engineering and Computer Science Vol 19, No 2 August 2020.

[10] M. Regad, M. Helaimi, R. Taleb, Ahmed M.Othman, Hossam A. Gabbar, Frequency Control of Microgrid with Renewable Generation using PID Controller based Krill Herd Indonesian Journal of Electrical Engineering and Informatics (IJEEI) vol. 8 March 2020 .

[11] Rashid, Muhammad H., ed. Power electronics handbook. Butterworth-Heinemann,2018, Pages 725-765.

[12] Coal Facts 2006 Edition with 2005 Data, Technical Annual Report of World Coal Institute, 2006.

[13] McGlade, Christophe, and Paul Ekins. "The geographical distribution of fossil fuels unused when limiting global warming to 2 C." Nature 517.7533 (2015) : 187-190.

[14] Li, Minqi. "World energy 2017-2050 : Annual report." Department of Economics, University of Utah (2017).

[15] Department of Energy, Loan Program Office, http ://energy.gov/lpo/loan-programs-office, accessed January 20, 2015 and EIA, Direct Federal Financial Interventions and Subsidies in Fiscal Years 2010, July 2011, Table 29.

[16] De Castro, Carlos, et al. "Global wind power potential : Physical and technological limits." Energy Policy 39.10 (2011) : 6677-6682.

[17] De Castro, Carlos, et al. "Global solar electric potential : A review of their technical and sustainable limits." Renewable and Sustainable Energy Reviews 28 (2013) : 824-835.

[18] Bevrani Hassan, Masayuki Watanabe, and Yasunori Mitani. "Microgrid Control : Concepts and Classification." (2014).

[19] International Energy Outlook, Technical Report by the Energy Information Administration, Official Energy Statistics Direct Federal Financial Interventions and Subsidies in Energy in Fiscal Year 2016 April 2018.

[20] Global, British Petroleum. "BP statistical review of world energy June 2017." Relatório. Disponível em : http ://www. bp. com/en/global/corporate/energy-economics/statistical-review-of-world-energy. html (2017).

[21] Bevrani. Hassan, et al. "Intelligent frequency control in an AC microgrid : Online PSO-based fuzzy tuning approach." IEEE transactions on smart grid 3.4 (2012) : 1935-1944.

[22] Sechilariu, Manuela, and Fabrice Locment. Urban DC Microgrid : intelligent control and power flow optimization. Butterworth-Heinemann, 2016.

[23] Wang, Baochao. Intelligent control and power flow optimization of microgrid : energy management strategies. Diss. Compiègne, 2013.

[24] Palma-Behnke, R., L. Reyes, and G. Jimenez-Estevez. "Smart grid solutions for rural areas." 2012 IEEE Power and Energy Society General Meeting. IEEE, 2012.

[25] Katiraei, Farid, and Mohammad Reza Iravani. "Power management strategies for a microgrid with multiple distributed generation units." IEEE transactions on power systems 21.4 (2006) : 1821-1831.

[26] Marei, M. I., E. F. El-Saadany, and M. M. A. Salama. "Flexible distributed generation :(FDG)." IEEE Power Engineering Society Summer Meeting,. Vol. 1. IEEE, 2002.

[27] Zamora, Ramon, and Anurag K. Srivastava. "Controls for microgrids with storage : Review, challenges, and research needs." Renewable and Sustainable Energy Reviews 14.7 (2010) : 2009-2018.

[28] Moreira, C. L., and JA Peças Lopes. "Microgrids operation and control under emergency conditions." Smart Power Grids 2011. Springer, Berlin, Heidelberg, 2012. 351-399.

[29] Sebaaly, Fadia, et al. "Sliding mode fixed frequency current controller design for grid-connected NPC inverter." IEEE Journal of Emerging and Selected Topics in Power Electronics 4.4 (2016) : 1397-1405.

[30] Zhong, Qing-Chang, and Tomas Hornik. "Cascaded currentvoltage control to improve the power quality for a grid-connected inverter with a local load." IEEE Transactions on Industrial Electronics 60.4 (2012) : 1344-1355.

[31] Gandomi, Amir Hossein, et al. "Metaheuristic algorithms in modeling and optimization." Metaheuristic applications in structures and infrastructures (2013) : 1-24.

[32] Yang, Xin-She. "Bat algorithm for multi-objective optimisation." arXiv preprint arXiv :1203.6571 (2012).

[33] Blum, Christian, and Andrea Roli. "Metaheuristics in combinatorial optimization : Overview and conceptual comparison." ACM computing surveys (CSUR) 35.3 (2003) : 268-308.

[34] Yang, Xin-She. Nature-inspired metaheuristic algorithms. Luniver press, 2010.

[35] Eberhart, Russell, and James Kennedy. "Particle swarm optimization." Proceedings of the IEEE international conference on neural networks. Vol. 4. Citeseer, 1995.

[36] Magdy, Gaber, et al. "Supplementary Frequency Control in a High-penetration Real Power System by Renewables Using SMES Application." Journal of Electrical Systems 15.4 (2019).

[37] Pandey, S.K., Mohanty, S.R., Kishor, Nanda, 2013. Nanda kishor a literature survey on loadfrequency control for conventional and distribution generation power systems.Renewable Sustainable Energy Rev. 25.

[38] Lal, Deepak Kumar, Ajit Kumar Barisal, and M. Tripathy. "Load frequency control of multi area interconnected microgrid power system using grasshopper optimization algorithm optimized fuzzy PID controller." 2018 Recent Advances on Engineering, Technology and Computational Sciences (RAETCS). IEEE, 2018.

[39] Sharma, Deepesh. "Load Frequency Control : A Literature Review " international journal of scientific & technology research volume 9, issue 02, february 2020.

[40] Bevrani, Hassan, Bruno François, and Toshifumi Ise. Microgrid dynamics and control. John Wiley & Sons, 2017.chapter Microgrids : Concept, Structure, and Operation Modes

[41] El-Hendawi, Mohamed, et al. "Control and EMS of a grid-connected microgrid with economical analysis." Energies 11.1 (2018) : 129.

[42] Bae, In-Su, and Jin-O. Kim. "Reliability evaluation of customers in a microgrid." IEEE Transactions on Power Systems 23.3 (2008) : 1416-1422.

[43] Chatterjee, Abir, Ali Keyhani, and Dhruv Kapoor. "Identification of photovoltaic source models." IEEE Transactions on Energy conversion 26.3 (2011) : 883-889.

[44] Wang, Yang, et al. "Small signal analysis of microgrid with multiple micro sources based on reduced order model in islanding operation." 2011 IEEE Power and Energy Society General Meeting. IEEE, 2011.

[45] Chouhan, Sridhar, et al. "Model based design of West Virginia Super Circuit (WVSC) microgrid system." 2017 North American Power Symposium (NAPS). IEEE, 2017.

[46] Walker, Geoff. "Evaluating MPPT converter topologies using a MATLAB PV model." Journal of Electrical & Electronics Engineering 21.1 (2001) : 49-56.

[47] Ishaque, Kashif, Zainal Salam, and Hamed Taheri. "Modeling and simulation of photovoltaic (PV) system during partial shading based on a two-diode model." Simulation Modelling Practice and Theory 19.7 (2011) : 1613-1626.

[48] M. Fuentes, G. Nofuentes, J. Aguilera, D. Talavera, and M. Castro, "Application and validation of algebraic methods to predict the behaviour of crystalline silicon PV modules in Mediterranean climates," Solar Energy, vol. 81, pp. 1396-1408, 2007.

[49] J. Hofierka and J. Kauk, "Assessment of photovoltaic potential in urban areas using open-source solar radiation tools," Renewable Energy, vol. 34, pp. 2206-2214, 2009

[50] F. Lasnier, Photovoltaic engineering handbook, Ch. 11, p. 258, CRC Press, 1990

[51] Y.T. Tan, D.S. Kirschen, N. Jenkins, A model of PV generation suitable for stability analysis, IEEE Trans. Energy Convers. 19 (4) (2004) 748755.

[52] F. González-Longatt, Model of Photovoltaic Module in MatlabTM, II CIBELEC, 2005.

[53] Tomonobu Senjyu, et al A Hybrid Power System Using Alternative Energy Facilities in Isolated Island IEEE TRANSACTIONS ON ENERGY CONVERSION, VOL. 20, NO. 2, JUNE 2005.

[54] M. Regad, M. Helaimi, R. Taleb, H. A. Gabbar, and A. M. Othman, "Fractional Order PID Control of Hybrid Power System with Renewable Generation Using

Genetic Algorithm," 2019 IEEE 7^{th} International Conference on Smart Energy Grid Engineering (SEGE), Oshawa, ON, Canada, 2019, pp. 139-144

[55] I. Pan and S. Das, Kriging based surrogate modeling for fractional order control of microgrids, Smart Grid, IEEE Transactions on, vol. 6, no. 1, pp. 3644, 2015.

[56] Mohanty, Debidasi, and Sidhartha Panda. "Fractional order based controller for frequency control of hybrid power system." 2019 IEEE International Conference on Sustainable Energy Technologies (ICSET). IEEE.

[57] LEE, Dong-Jing ; WANG, Li. Small-signal stability analysis of an autonomous hybrid renewable energy power generation/energy storage system part I : Time-domain simulations. IEEE Transactions on Energy Conversion, 2008, 23.1 : 311-320.

[58] M. R. Patel, Wind and Solar Power Systems, 1999, CRC Press.

[59] PAN, Indranil ; DAS, Saptarshi. Fractional order fuzzy control of hybrid power system with renewable generation using chaotic PSO. ISA transactions, 2016, 62 : 19-29.

[60] DAS, DulalCh, et al. Genetic algorithm based PI controller for frequency control of an autonomous hybrid generation system. Proc. International Multi conference of engineers and Computer scientists, 2011, 2.

[61] Villalva, M. G., T. G. De Siqueira, and E. Ruppert. "Voltage regulation of photovoltaic arrays : small-signal analysis and control design." IET Power Electronics 3.6 (2010) : 869-880.

[62] M. Regad et al (2019) Frequency Control in Microgrid Power System with renewable Power Generation Using PID Controller Based on Particle Swarm Optimization in conference proceeding- 3^{th} International Conference on Artificial Intelligence in Renewable Energetic Systems(IC-AIRE2019.

[63] Pandey, Shashi Kant, et al. "Frequency regulation in hybrid power systems using particle swarm optimization and linear matrix inequalities based robust controller design." International Journal of Electrical Power & Energy Systems 63 (2014) : 887-900.

[64] Ray, Prakash, Soumya Mohanty, and Nand Kishor. "Small-signal analysis of autonomous hybrid distributed generation systems in presence of ultracapacitor and tie-line operation." Journal of Electrical engineering 61.4 (2010) : 205-214.

[65] Yu, Byunggyu. "Design and experimental results of battery charging system for microgrid system." International Journal of Photoenergy 2016 (2016).

[66] Wang, Li, et al. "Analysis of a novel autonomous marine hybrid power generation/energy storage system with a high-voltage direct current link." Journal of Power Sources 185.2 (2008) : 1284-1292.

[67] DAS, DulalCh ; ROY, A. K. ; SINHA, N. GA based frequency controller for solar thermaldieselwind hybrid energy generation/energy storage system. International Journal of Electrical Power & Energy Systems, 2012, 43.1 : 262-279.

[68] Mahmoud, Magdi S., S. Azher Hussain, and Mohammad Ali Abido. "Modeling and control of microgrid : An overview." Journal of the Franklin Institute 351.5 (2014) : 2822-2859.

[69] Kumari, Naresh, and A. N. Jha. "Frequency Response Enhancement of Hybrid Power System by using PI Controller Tuned with PSO technique." International Journal of Advanced Computer Research 4.1 (2014) : 116.

[70] Singh, Vijay P., et al. "Robust H-infinity load frequency control in the hybrid distributed generation system." International journal of electrical power & energy systems 46 (2013) : 294-305.

[71] Yousef, Hassan A. Power system load frequency control : classical and adaptive fuzzy approaches. CRC Press, 2017

[72] Moutchou, Rania, Ahmed Abbou, and Ahmed vall Hemeyine. "Control of the active and reactive powers of a permanent magnet synchronous generator using singular perturbations decouplage." 2018 9^{th} International Renewable Energy Congress (IREC). IEEE, 2018.

[73] Tamee, Kreangsak, and Kaewarin Jandum. "Use of Neural Network Model for Frequency Control in Microgrid System." International Symposium on Multimedia and Communication Technology. 2015.

[74] Key Performance Assessment of Fuel Cell Based Distributed Energy Generation System in Resilient Micro Energy Grid

[75] Annamraju, Anil, and Srikanth Nandiraju. "Load Frequency Control of an Autonomous Microgrid Using Robust Fuzzy PI Controller." 2019 8^{th} International Conference on Power Systems (ICPS). IEEE, 2019.

[76] Kumar, R. Hari, and S. Ushakumari. "Biogeography based tuning of PID controllers for Load Frequency Control in microgrid." 2014 International Conference on Circuits, Power and Computing Technologies [ICCPCT-2014]. IEEE, 2014.

[77] Khalil, Ashraf, Khalid Ateea Alfaitori, and Ali Asheibi. "Modeling and control of PV/Wind Microgrid." 2016 7th international renewable energy congress (IREC). IEEE, 2016.

[78] N.EL.Y. Kouba and al Automatic Generation Control in interconnected Power System with Integration of wind power Generation using PID Based on particle Swarm optimization International Conference on Renewable Energies and Power Quality (ICREPQ14) Cordoba (Spain), 8th to 10th April, 2014.

[79] Ray, Prakash K., Soumya R. Mohanty, and Nand Kishor. "Proportionalintegral controller based small-signal analysis of hybrid distributed generation systems." Energy Conversion and Management 52.4 (2011) : 1943-1954

[80] Zhao, C., Xue, D., & Chen, Y. (2005, July) A fractional order PID tuning algorithm for a class of fractional order plants. In Mechatronics and automation, 2005 IEEE international conference (Vol. 1, pp. 216-221). IEEE

[81] TEPLJAKOV, Aleksei. Fractional-order modeling and control of dynamic systems. Springer, 2017.

[82] Swagatam Das et al Design of fractional-order $PI^{\mu}D^{\lambda}$ controllers with an improved differential Engineering Applications of Artificial Intelligence 22 (2009) 343350

[83] GUO, Cheng ; YANG, Xiaoyong. A programming of genetic algorithm in matlab7. 0. Modern applied science, 2011, 5.1 : 230

[84] MITCHELL, Melanie. An introduction to genetic algorithms. MIT press, 1998.

[85] C. Houck ETall A Genetic Algorithm for Function Optimization : A Matlab Implementation, 2008 this research was funded in part by the National Science Foundation under grant number DMI-9322834

[86] Mirzal, Andri, Shinichiro Yoshii, and Masashi Furukawa. "PID parameters optimization by using genetic algorithm." arXiv preprint arXiv :1204.0885 (2012).

[87] Sharaf, Adel M., and A. A. El-Gammal. "A novel efficient PSO-self regulating PID controller for hybrid PV-FC-diesel-battery micro grid scheme for village/resort electricity utilization." 2010 IEEE Electrical Power & Energy Conference. IEEE, 2010.

[88] Gandomi, Amir Hossein, and Amir Hossein Alavi. "Krill herd : a new bio-inspired optimization algorithm." Communications in Nonlinear Science and Numerical Simulation 17.12 (2012) : 4831-4845.

[89] Gandomi, Amir Hossein, et al. "Krill herd algorithm for optimum design of truss structures." International Journal of Bio-Inspired Computation 5.5 (2013) : 281-288.

[90] YAGHOOBI, Saber ; MOJALLALI, Hamed. Tuning of a PID controller using improved chaotic Krill Herd algorithm. Optik-International Journal for Light and Electron Optics, 2016, 127.11 : 4803-4807.

[91] Alikhani, A., Suratgar, A. A., Nouri, K., Nouredanesh, M., & Salimi, S. (2013, December). Optimal PID tuning based on Krill Herd optimization algorithm. In Control, Instrumentation, and Automation (ICCIA), 2013 3rd International Conference on (pp. 11-15). IEEE.

[92] Asaju Laaro Bolaji, Mohammed Azmi Al-Betar, Mohammed A.Awadallah, Ahamad Tajudin Khader, LaithMohammadAbualigah,Acomprehensive review : krill herd algorithm (KH) and its applications, <![CDATA[Applied Soft Computing Journal]]> (2016)

[93] Wang, Gai-Ge, et al. "Chaotic krill herd algorithm." Information Sciences 274 (2014) : 17-34.

[94] lhamrouni, Ibrahim, et al. "Modeling of Micro-grid with the consideration of total harmonic distortion analysis." Indonesian Journal of Electrical Engineering and Computer Science. vol15 2 (2019) : 581-592.

[95] Jeman, Ameerul Aiman Bin, Naeem MS Hannoon, and Ismail Misrin. "Small Signal Fault Analysis for Renewable Energy (Wind) Power System Distributed

Generation by Using MATLAB Software (Simulink)." Indonesian Journal of Electrical Engineering and Computer Science 5.3 (2017) : 401-408.

[96] Khan, M. Reyasudin Basir, et al. "Optimal grid-connected PV system for a campus microgrid." Indonesian Journal of Electrical Engineering and Computer Science 12.3 (2018) : 899-906.

[97] Haddadi, Aboutaleb. Modeling, Control, and Stability Analysis of an Islanded Microgrid. Diss. McGill University Libraries, 2015.

[98] P. J. MacVicar-Whelan, “Fuzzy sets for man-machine interaction,” Int.J. Man-Mach. Stud., vol. 8, no. 6, pp. 687697, 1976.

[99] R.-J. Wai and L.-C. Shih, “Adaptive fuzzy-neural-network design for voltage tracking control of a DCDC boost converter,” IEEE Trans. Power Electron., vol. 27, no. 4, pp. 21042115, Apr. 2012.

[100] S.-Z. He, S. Tan, F.-L. Xu, and P.-Z. Wang, “Fuzzy self-tuning of PID controllers,” Fuzzy Sets Syst., vol. 56, no. 1, pp. 3746, 1993.

[101] K. J. Åström and T. Hägglund. “The future of PID control,” Control Eng. Pract., vol. 9, no. 11, pp. 11631175, 2001.

[102] E. H. Mamdani, “Application of fuzzy algorithms for control of simple dynamic plant,” Proc. Inst. Elect. Eng., vol. 121, no. 12, pp. 15851588,Dec. 1974.

[103] Z.-Y. Zhao, M. Tomizuka, and S. Isaka, “Fuzzy gain scheduling of PID controllers,” IEEE Trans. Syst., Man Cybern., vol. 23, no. 5,pp. 13921398, Sep. 1993.

[104] Arya, Yogendra. "AGC of restructured multi-area multi-source hydrothermal power systems incorporating energy storage units via optimal fractional-order fuzzy PID controller." Neural Computing and Applications 31.3 (2019) : 851-872.

[105] Pan, Indranil, and Saptarshi Das. "Fractional order AGC for distributed energy resources using robust optimization." IEEE transactions on smart grid 7.5 (2015) : 2175-2186.

[106] Pan, Indranil, and Saptarshi Das. "Fractional-order load-frequency control of interconnected power systems using chaotic multi-objective optimization." Applied Soft Computing 29 (2015) : 328-344.

[107] Zamani, Majid, et al. "Design of a fractional order PID controller for an AVR using particle swarm optimization." Control Engineering Practice 17.12 (2009) : 1380-1387.

[108] Singh, Amandeep, and Sathans Suhag. "Frequency regulation in an AC microgrid interconnected with thermal system employing multiverse-optimised fractional order-PID controller." International Journal of Sustainable Energy (2019) : 1-13.

[109] De Souza Ribeiro, Luiz Antonio, et al. Isolated micro-grids with renewable hybrid generation : The case of Lençóiland. IEEE Transactions on sustainable energy, 2011, 2.1 : 1-11

[110] Annamraju, Anil, and Srikanth Nandiraju. "Robust frequency control in a renewable penetrated power system : an adaptive fractional order-fuzzy approach." Protection and Control of Modern Power Systems 4.1 (2019) : 16.

[111] Gheisarnejad, Meysam, and Mohammad Hassan Khooban. "Design an optimal fuzzy fractional proportional integral derivative controller with derivative filter for load frequency control in power systems." Transactions of the Institute of Measurement and Control 41.9 (2019) : 2563-2581.

[112] Delassi, A., S. Arif, and L. Mokrani. "Comparison between PID, Fractional PID and Fuzzy PID for Load Frequency Control Problem." International Conference on Information Processing and Electrical Engineering ICIPEE14 November. Vol. 24. No. 25. 2014.

[113] Iruthayarajan, M. W., & Baskar, S. (2009). Evolutionary algorithms based design of multivariable PID controller. Expert Systems with applications, 36(5), 9159-9167

[114] Pourmousavi, S. Ali, and M. Hashem Nehrir. "Introducing dynamic demand response in the LFC model." IEEE Transactions on Power Systems 29.4 (2014) : 1562-1572.

[115] Pappachen, Abhijith, and A. Peer Fathima. "Critical research areas on load frequency control issues in a deregulated power system : A state-of-the-art-of-review." Renewable and Sustainable Energy Reviews 72 (2017) : 163-177.

[116] Soleimani, Koosha, and Jalil Mazloum. "Designing a GA-based robust controller for load frequency control (LFC)." Engineering, Technology & Applied Science Research 8.2 (2018) : 2633-2639.

[117] Kouba, Nour EL Yakine, et al. "Optimal load frequency control in interconnected power system using PID controller based on particle swarm optimization." 2014 International Conference on Electrical Sciences and Technologies in Maghreb (CISTEM). IEEE, 2014.

[118] N. R. Babu and L. C. Saikia, "Load Frequency Control of a Multi-area System Incorporating Dish-Stirling Solar Thermal System and Coyote Optimized PI minus DF Controller," 2020 IEEE International Conference on Power Electronics, Smart Grid and Renewable Energy (PESGRE2020), Cochin, India, 2020, pp. 1-6, doi : 10.1109/PESGRE45664.2020.9070654.

[119] Patel, Vivek, Dipayan Guha, and Shubhi Purwar. "Frequency regulation of an islanded microgrid using integral sliding mode control." 2019 8th International Conference on Power Systems (ICPS). IEEE, 2019.

[120] Dash, Sambit. "Load Frequency Control of Solar PV and Solar Thermal Integrated Micro grid using Narma-L2 Controller." arXiv preprint arXiv :2004.05776 (2020).

[121] Debnath, Manoj K., et al. "Artificial neural network tuned PID controller for LFC investigation including distributed generation." International Journal of Numerical Modelling : Electronic Networks, Devices and Fields : e2740.

[122] Bhongade, S., and Vishnu Prasad Parmar. "Jaya Algorithm-Based Optimized Automatic Generation Control Scheme for Interconnected Solar-Thermal Power System." IUP Journal of Electrical and Electronics Engineering 13.1 (2020) : 29-41.

[123] Bevrani, Hassan, and Takashi Hiyama. Intelligent automatic generation control. CRC press, 2017.

[124] Babu, Naladi Ram, et al. "Multi-area AGC System Incorporating GTPP and Coyote Optimized PI Minus DN Controller." Computing Algorithms with Applications in Engineering. Springer, Singapore, 2020. 349-360.

[125] Singh, Ashish Kumar, et al. "Load Frequency Control of Single Area Hybrid Power System Using Fuzzy-PID (FPID) Controller." 2019 IEEE Students Conference on Engineering and Systems (SCES). IEEE, 2019.

[126] Bhadoria, Vikas Singh, et al. "Firefly Algorithm for Frequency Controller of Autonomous Hybrid Energy System." 2019 2^{nd} International Conference on Power Energy, Environment and Intelligent Control (PEEIC). IEEE, 2019.

[127] Rajan, Rijo, and Francis M. Fernandez. "Impact of Increased Penetration of Photovoltaic Sources on Small-Signal Stability of Hybrid and Multi-area Power Systems." 2019 Innovations in Power and Advanced Computing Technologies (i-PACT). Vol. 1. IEEE, 2019.

[128] Singh, Kavita. "Primary frequency regulation of a microgrid by deloaded tidal turbines." Soft Computing (2020) : 1-19.

[129] Rabeh, Reda, M. Ferfra, and Ahmed Ezbakhe. "Secondary Frequency Control of an Islanded Microgrid by Combined GA-TLBO Algorithm." 2019 8^{th} International Conference on Systems and Control (ICSC). IEEE, 2019.

[130] Concepci ťon A. Monje, YangQuan Chen, Blas Vinagre, Dingyĺu Xue and Vincente Fileu. Fractional Order Controls - Fundamentals and Applications. Springer-Verlag London, Advances in Industrial Control series, (Invited book project, to be published in 2009).

[131] Dingyu Xue, YangQuan Chen and Derek Atherton. Linear Feedbac Control - Analysis and Design with Matlab. SIAM Press, 2007,ISBN : 978-0-898716-38-2. (348 pages) Chapter-8 : Fractional-order Controller - An Introduction.

[132] Chunna Zhao. Research on Analyse and Design Methods of Fractional Order System. PhD thesis, Northeastern University, China, 2006.

[133] Concepci ťon Alicia Monje Micharet. Design Methods of Fractional Order Controllers for Industrial Applications. PhD thesis, University of Extremadura, Spain, 2006.

[134] A. Oustaloup, P. Melchoir, P. Lanusse, C. Cois, and F. Dancla. The CRONE toolbox for Matlab. In Proceedings of the 11th IEEE International Symposium on Computer Aided Control System Design- CACSD, Anchorage, USA, September 2000b.

[135] Regad, Mohamed, et al. "Control of hybrid power system based renewable energy generations using PID controller." Int J Pow Elec & Dri Syst 11.4 (2020) : 1775-1784